2009

LIPID SIGNALING IN BRAIN AGING AND ALZHEIMER'S DISEASE: PHARMACOLOGICALLY TARGETING CHOLESTEROL SYNTHESIS, TRANSPORT AND METABOLISM

James Lucas Searcy
University of Kentucky, Luke.Searcy@uky.edu

ABSTRACT OF DISSERATION

JAMES LUCAS SEARCY

THE GRADUATE SCHOOL
UNIVERSITY OF KENTUCKY
2009

LIPID SIGNALING IN BRAIN AGING AND ALZHEIMER'S DISEASE: PHARMACOLOGICALLY TARGETING CHOLESTEROL SYNTHESIS, TRANSPORT AND METABOLISM

ABSTRACT OF DISSERATION

A dissertation submitted in partial fulfillment of the
requirements for the degree of Doctor of Philosophy in the
College of Medicine
at the University of Kentucky

By
James Lucas Searcy

Lexington, KY

Director: Dr. Nada Porter, Associate Professor of Pharmacology

2009

ABSTRACT OF DISSERATION

LIPID SIGNALING IN BRAIN AGING AND ALZHEIMER'S DISEASE: PHARMACOLOGICALLY TARGETING CHOLESTEROL SYNTHESIS, TRANSPORT AND METABOLISM

The role cholesterol plays in the brain has long been underappreciated even though the brain contains a disproportionately high percentage of body cholesterol. Recent studies have found a link between the dysregulation of lipid metabolism and the risk of acquiring Alzheimer's disease (AD) as well as a predisposition to cognitive decline. The goal of these studies was to elucidate the possible role lipid metabolism plays in pathological and normal brain aging by pharmacologically manipulating lipid metabolism and determining effects on key hippocampal biomarkers of AD and age-related cognitive decline. One series of experiments used an agonist (TO901317) to the liver X receptor (LXR) in two transgenic AD mouse models. Chronic LXR activation reduced AD associated pathology and improved cognitive performance in AD mouse models. However, long-term potentiation (LTP) was not enhanced and peripheral side effects were observed. In another series of experiments the effects of chronically inhibiting cholesterol synthesis on cognitive aging in rats was determined. Animals were treated with either of two commonly prescribed statins, simvastatin or atorvastatin. Simvastatin, the more lipophilic statin, increased LTP and reduced the duration of the afterhyperpolarization (AHP). In addition, simvastatin upregulated key genes of the cholesterol synthesis pathway in the hippocampus as revealed by microarray analyses, but was associated with impaired performance in the Morris Water Maze, a hippocampal dependent task. Atorvastatin, a less lipophilic statin, reduced the AHP, but did not affect LTP or cognitive performance. Atorvastatin modulated a very different set of genes and reduced brain cholesterol more than simvastatin. These results suggest that manipulation of cholesterol metabolism selectively modulates key aspects of AD and brain aging.

Key Words: cholesterol, brain aging, Alzheimer's disease, liver x receptor, statins

James Lucas Searcy

September 18, 2009

LIPID SIGNALING IN BRAIN AGING AND ALZHEIMER'S DISEASE: PHARMACOLOGICALLY TARGETING CHOLESTEROL SYNTHESIS, TRANSPORT AND METABOLISM

By

James Lucas Searcy

Dr. Nada Porter

Director of Dissertation

Dr. Robert Hadley

Director of Graduate Studies

09-18-2009

RULES FOR THE USE OF DISSERTATIONS

Unpublished dissertations submitted for the Doctor's degree and deposited in the University of Kentucky Library are as a rule open for inspection, but are to be used only with due regard to the rights of the authors. Bibliographical references may be noted, but quotations or summaries of parts may be published only with the permission of the author, and with the usual scholarly acknowledgments.

Extensive copying or publication of the dissertation in whole or in part also requires the consent of the Dean of the Graduate School of the University of Kentucky.

A library that borrows this dissertation for use by its patrons is expected to secure the signature of each user.

Name	Date

DISSERTATION

JAMES LUCAS SEARCY

The Graduate School
University of Kentucky
2009

LIPID SIGNALING IN BRAIN AGING AND ALZHEIMER'S DISEASE: PHARMACOLOGICALLY TARGETING CHOLESTEROL SYNTHESIS, TRANSPORT AND METABOLISM

DISSERATION

A dissertation submitted in partial fulfillment of the
requirements for the degree of Doctor of Philosophy in the
College of Medicine
at the University of Kentucky

By
James Lucas Searcy

Lexington, KY

Director: Dr. Nada Porter, Associate Professor of Pharmacology

2009

ACKNOWLEDGEMENTS

"No man is an island, entire of itself" J*ohn Donne (1572-1631).* The number of people who made this work possible is many. I cannot possibly list all those individuals who made this dissertation a reality. Of course, some contributed more than others and in varied ways. To those who loved me and supported me along the way, I say thank you. To those who shared their expertise, guidance and mentorship, I am eternally grateful.

I must acknowledge though that the completion of a dissertation is more than just creating a written work. It is a tangible representation of the continuing growth and formation of a person. This growth begins at birth, and continues throughout one's lifetime as they seek knowledge and understanding. With luck, we are able to stick around long enough even to grow wise. But wisdom is not acquired alone. Every personal encounter has the potential to shape us, whether it is seemingly insignificant or monumental in nature. In that sense we are connected very much to our world, and we are chapters in a much larger book whose story cannot be told without the presence of those around us to help us, to guide us and to support us. I thank all those who I have encountered thus far who have shaped me and formed me and helped me grow.

TABLE OF CONTENTS

Acknowledgements iii
List of Tables ix
List of Figures xi
List of Files xiv
Chapter One: Introduction 1
Rationale 1
Cholesterol: Structure and Origin 5
The General Nature of Cholesterol of the Nervous System 8
Regulation of Brain Cholesterol Levels. 9
Removal of Excess Brain Cholesterol. 10
Cholesterol Transport in the CNS 11
Disruption of Cholesterol Synthesis: In the CNS and Periphery 13
Cholesterol and the Aging Brain 17
The Hippocampus and Memory 19
Alzheimer's Disease Progression and Treatment 20
AD and the Cholesterol Connection 22
Liver X Receptors (LXR): Master Metabolic Regulators 24
LXR in Brain Aging and AD 27
Chapter 2: Materials and Methods 29
Introduction 29
Animal Models of Alzheimer's Disease 29
Triple transgenic model:. 30
Double-transgenic model: 30
The Fischer 344 (F344) as a Model of Normal Aging 31
The Morris Water Maze (MWM) and Cognitive Assessment 32
Rationale 32
MWM General Apparatus and Protocol 34
Active Avoidance (AA) as a Learning and Memory Paradigm 36
Rationale 36

AA General Protocol 37
Contextual Fear Conditioning (CFC) as an Assessment of Spatial Memory 38
Rationale 38
CFC General Protocol 38
Long-Term Potentiation (LTP), Memory and the Aging Hippocampus 40
Rationale 40
LTP General Protocol 42
Afterhyperpolarization (AHP) and the Aging Hippocampus 44
Rationale 44
AHP General Protocol 45
Microarray Analysis of Hippocampal Tissue 46
Rationale, Strengths and Pitfalls 46
General Protocol 46
ELISA for the Assessment of Amyloid Beta (Aβ) Levels 48
Rationale 48
Soluble Aβ Extraction 48
Insoluble Aβ Extraction 48
Assay 48
Tissue Histology 49
Oil Red O 49
Aß Pathology 50
Chapter 3: Effects of TO901317, an LXR Agonist, in a Triple Transgenic Mouse Model of AD 51
Introduction 51
Materials and Methods 53
Animals 53
Medicated Diets 53
One-way Active Avoidance 54
Blood Collection and Tissue Isolation 54
Serum Analysis 55
Liver Histology 55

Microarrays 55
CA1 Aβ Load 56
Soluble and Insoluble Aβ Levels 56
Correlation Between Hippocampal Aβ load and Cortical Aβ Levels in TO9-treated Animals 57
Slice Preparation and Extracellular Recording 57
Statistical Note 58
Results 58
Body Weights and Food Consumption 58
Active Avoidance 58
Long-term potentiation 61
Heart Weights 63
Liver Histology 63
Serum Analysis 64
Immunohistochemical Assessment of Aβ Load in the CA1 of the Hippocampus 65
Soluble and Insoluble Aβ in Cortical Tissue 65
Relationship between hippocampal Aβ load and cortical Aβ Levels 67
Microarray Analysis 69
Discussion 74
Effects on Behavior and LTP. 74
Effects on Amyloid. 75
Peripheral Side Effects. 76
Chapter 4: Assessing TO901317 dose effects on the periphery and LXR gene targets 78
Introduction 78
Materials and Methods 79
Animals and Diets 79
Tissue Collection 80
Liver Histology 80
Microarrays 81
Results 81
Animal Weights and Food Consumption 81

Liver Pathology 81
Cardiac Pathology 82
Microarrays 85
Discussion 87
Chapter 5: The Effects of Chronic LXR Activation in a 2xtg-AD Mouse Model 88
Introduction 88
Material and Methods 89
Animals 89
Medicated Diets 89
Contextual Fear Conditioning 90
Tissue Collection 92
Liver Histology 92
Blood Collection and Serum Analysis 92
Soluble and Insoluble Amyloid Beta Levels 93
Microarray Analysis 93
Results 94
Animal Weights 94
Food Consumption 96
Contextual Fear Conditioning 96
Serum Analysis 100
Liver Pathology 104
Heart Pathology 107
Soluble Aβ Levels 108
Microarray Analysis 109
Discussion 123
Effect on Aβ Levels. 123
Effect on Behavior. 123
Effect of Alzheimer's Disease Transgenes on Hippocampal Gene Expression. 124
General Effect of LXR Activation on Hippocampal Gene Expression in Wild-type and 2xTg Mice. 125
Peripheral Effects. 126

Summary of LXR Activation in Transgenic AD Models.. 126
Chapter Six: Short-term and Long-term Statin Treatment in mid-aged F344 Rats 128
Introduction 128
Materials and Methods 130
Animals and Diets: Short-term Treatment 130
Electrophysiological Recording: Short-term Treatment 130
Long term potentiation. 130
Afterhyperpolarization:. 131
Animals and Diets: Long-term Treatment 132
Behavioral Characterization: 133
Tissue Collection 134
Serum Analysis 134
Microarray Analysis 135
Brain Cholesterol Measurements 135
Results 136
Animal Weights and Food Consumption: Short-term Treatment 136
LTP Recording: Short-term Treatment 136
AHP Recording: Short-term Treatment 138
Peripheral Measurements: Long-term Treatment 139
Locomotor Assessment 142
Learning and Memory Assessment 142
Brain Cholesterol Levels 147
Microarray Analysis 148
Discussion 150
Long-Term Statins and Reductions in Brain Cholesterol. 150
Effects on LTP. 151
Effects on Behavior. 152
Statin Effects in Humans.. 153
Overall Conclusions 159
References 158
Vita 178

LIST OF TABLES

Table 3.1, Blood serum analysis of organ function in 3xTg-AD mice treated with control vehicle or TO9 for three months.....64

Table 3.2, Blood serum metabolic panel in 3xTg-AD mice treated with control or TO9 for three months.....65

Table 3.3, Top twenty genes with the lowest p-values significantly upregulated in the hippocampi of 3xTG-AD mice treated for 3 months with TO901317.....70

Table 3.4, Top twenty genes with the lowest p-values significantly downregulated in the hippocampi of 3xTG-AD mice treated for 3 months with TO901317.....71

Table 3.5, DAVID functional analysis of genes significantly upregulated in hippocampi of 3xTG-AD mice treated for 3 months with TO901317.....72

Table 3.6, DAVID functional analysis of genes significantly downregulated inhippocampi of 3xTG-AD mice treated for 3 months with T0901317.....73

Table 4.1, Diet formulations for the respective treatment group.....79

Table 5.1, Mean food consumption.....96

Table 5.2A, Serum analysis of pre-determined metabolic markers.....101

Table 5.2B, Serum Analysis of pre-determined metabolic markers.....101

Table 5.3, Expression patterns and numbers of significantly modulated genes as a function of genotype and drug dose.....110

Table 5.4, Top twenty genes with the lowest p-values significantly upregulated in 2xTg-AD mice.....114

Table 5.5, Top twenty genes with the lowest p-values significantly downregulated in 2xTg-AD mice.....115

Table 5.6, Top twenty genes with the lowest p-values significantly upregulated in linear fashion in both WT and TG mice treated with TO for six months.....116

Table 5.7, Top twenty genes with the lowest p-values significantly downregulated in a linear fashion in both WT and TG mice treated with TO for six months.....117

Table 5.8, DAVID functional analysis of significantly modulated genes categorized by expression patterns..... 118- 119

Table 5.9, DAVID functional analysis of genes significantly upregulated in hippocampi of 2xTG-AD mice treated for 6 months with TO901317 121

Table 5.10, DAVID functional analysis of genes significantly downregulated in hippocampi of 2xTG-AD mice treated for 6 months with TO90137 122

Table 6.1, Blood serum analysis after 9 months of statin treatment.....141

Table 6.2, Microarray analysis – number of genes found to be significantly modulated by 9 months of statin treatment.....148

Table 6.3, DAVID functional analysis – functional pathways significantly modulated by 9 months of simvastatin treatment 149

Table 6.4, DAVID functional analysis – functional pathways significantly modulated by 9 months of atorvastatin treatment.....149

LIST OF FIGURES

Figure 1.1, Chemical structure of cholesterol and cholesteryl esters 6

Figure 1.2, Cholesterol synthesis pathway 7

Figure 1.3, Liver X Receptor gene targets.....27

Figure 2.1, Schematic of contextual fear conditioning protocol.....40

Figure 2.2, Electrode placement within the hippocampal slice preparation.....44

Figure 3.1, Learning and memory assessment in 3xTg-AD mice treated for three month with TO9137 using one-way active avoidance.....60

Figure 3.2, Long-term potentiation recorded from the CA1 region of the hippocampus of 3xTg-AD mice treated for three months with TO901317 62

Figure 3.3, Assessment of potential cardiotoxicity and hepatotoxicity 63

Figure 3.4, Comparison of Aβ levels in the hippocampus and cortex of TO9-treated 3xTgAD mice.....66

Figure 3.5, Relationship between WO2-detected Aβ within the CA1 region of the hippocampi and ELISA detected soluble and insoluble Aβ levels in the cortices of 3xTg-AD mice treated with TO901317.....68

Figure 4.1, Liver weights of mice treated for three months with 5 or 20 mg/kg/day or either TO9 or the combination treatment of TO9 + FO (10mg/day) 82

Figure 4.2, Heart weights of mice treated for three months with 5 or 20 mg/kg/day or either TO9 or the combination treatment of TO9 + FO (10mg/day) 83

Figure 4.3, Gomori trichrome staining of cardiac tissue from mice treated with control or 20 mg/kg TO diet.....84

Figure 4.4, Mean signal intensities of known LXR targets 86

Figure 5.1, Schematic of contextual fear conditioning protocol.....91

Figure 5.2, Mean percent monthly change in body weight.....95

Figure 5.3, Mean percent freezing of mice from the different treatment groups over the course of the CFC sessions 98

Figure 5.4, Proportion of time spent freezing for all groups within the contextual environment 24 hours after final CS-UCS pairing 99

Figure 5.5, Serum panel assessing normal organ function 102

Figure 5.6, Serum panel assessing lipid and glucose metabolism 103

Figure 5.7, Dose-dependent changes in liver weights of both WT and TG animals treated with 5 mg/kg or 20 mg/kg TO9 104

Figure 5.8, Representative digital images of livers taken from WT and TG mice treated with 5 mg/kg or 20 mg/kg TO9 105

Figure 5.9, Liver histology of livers from WT and TG mice treated with 5 mg/kg or 20 mg/kg TO9.....106

Figure 5.10, Genotype and drug effects on heart weight of 2xTg-AD mice 107

Figure 5.11, Soluble Aβ levels in the cortices of WT and TG mice treated with control, 5 mg/kg TO and 20 mg/kg TO for six months.....108

Figure 5.12, Divergent gene expression patterns in TG versus WT mice 111

Figure 5.13, Linear gene expression patterns shared by both TG and WT mice treated with 5 mg/kg or 20 mg/kg TO9 112

Figure 5.14, Gene expression patterns shared by both TG and WT mice treated with 5 mg/kg or 20 mg/kg TO9 113

Figure 5.15, Gene expression patterns of all genes upregulated or downregulated by 5mg/kg or 20mg/kg TO 120

Figure 5.16, Speculative model of the role of chronic LXR activation in the AD brain.127

Figure 6.1, Long-term potentiation recorded in the CA1 region of the hippocampus in mid-aged rats treated for 1-2 months with statins.....137

Figure 6.2, AHP measurements in the CA1 region of the hippocampus in mid-aged rats treated for 1-2 months with statins.....138

Figure 6.3, AHP measurement in the CA1 region of the hippocampus in mid-aged rats treated for 1-2 months with statins.....139

Figure 6.4, Monthly mean body weights and average daily food consumption of rats treated for 9 months with statins.....140

Figure 6.5, Key serum lipid markers in rats treated for 9 months with statins.....141

Figure 6.6, Locomotor assessment after 9 months of statin treatment using the rotorod task.....142

Figure 6.7, MWM - Visual acuity and training assessment in rats treated for 9 months with statins.....144

Figure 6.8, MWM – Memory retention during probe session in rats treated for 9 months with statins.....146

Figure 6.9, Quantitative analysis of cholesterol levels in cortical tissue from rats treated with statins for 9 month using LC-MS.....147

Figure 6.10, Simvastatin regulation of isoprenoids synthesis.....152

Figure 6.11, GFAP staining in the stratum radiatum of rats treated for nine months with atorvastatin or simvastatin.....155

Figure 6.12, CNPase staining in the stratum radiatum of rats treated for nine months with atorvastatin or simvastatin.....156

Figure 6.13, The specific effect of simvastatin on specific genes within the context of the cholesterol biosynthetic pathway.....157

Figure 6.14, Speculative model of the effects of long-term statin treatment on the aging Brain.....158

LIST OF FILES

File 3.1 Name: 3xtg-AD-TO_microarray_supplemental_table

Supplemental Tables\3xtg-AD-TO_microarray_supplemental_table.pdf

Format: PDF

Size: 1406 KB

File 4.1 Name: TO_and_FO_microarray_supplemental_table

Supplemental Tables\TO_and_FO_microarray_supplemental_table.pdf

Format: PDF

Size: 611 KB

File 5.1 Name: 2xtg-AD-TO_microarray_supplemntal_table

Supplemental Tables\2xtg-AD-TO_microarray_supplemental_table.pdf

Format: PDF

Size: 1835 KB

Figure 6.1 Name: Long-term_Statin_microarray_supplement_table

Supplemental Tables\Long-term_Statin_microarray_supplement_table.pdf

Format: PDF

Size: 611 KB

Chapter One: Introduction

Rationale

As the brain ages various changes occur, some of which may increase the propensity to develop Alzheimer's disease (AD). Further, it is likely that many cellular and molecular alterations are in fact shared in both normal and pathological aging, and understandably, these alterations correlate with cognitive decline present in both states. Recently, focus has been drawn to the role lipids, specifically cholesterol, play in both aging and AD. This attention is overdue, given the disproportionate amount of cholesterol that is concentrated in the central nervous system. Given the importance of cholesterol in the brain, dysregulation of cholesterol metabolism may be detrimental to normal cognitive function and may play a role in the etiology of AD.

Most of the cholesterol in the brain is concentrated in myelin (Barztokis et al. 2004), which makes up the white matter. In both humans and monkeys, there is a decrease in white matter as the brain ages, most of this being attributed to a reduction in myelin (Peters et al. 2009). Cholesterol levels also seem to increase in the exofacial layer of cellular membranes in mice, which leads to the loss of fluidity (Igbavboa et al., 1996), which if occurring in the synapse may cause a "hardening of the synapse", therefore effecting synaptic communication.

Whether high or low cholesterol serum levels are detrimental or beneficial to brain function is still unclear. Recent epidemiological results suggest that low levels of serum cholesterol in the elderly (>65 years of age) is actually a frailty marker, and is indicative of increased chances of experiencing cognitive decline (van den Kommer et al., 2009). Yet, high cholesterol at midlife is associated with impaired cognitive function several decades later (Solomon et al., 2007; Solomon et al., 2009). Thus, as with most biological processes, either too little or too much is not optimal. In addition, the studies in humans also indicate that progressive changes in cholesterol requirements with age may alter brain cholesterol dynamics and homeostasis.

The first links between cholesterol and AD pathology were observed more than a decade ago, when it was observed that non-demented patients with cardiovascular disease and hypercholesterolemia, had significantly greater numbers of senile plaques in their

brains, one of the pathological hallmarks of the disease (Sparks et al., 1996). This suggested that peripheral cholesterol levels may be having a direct effect on the brain. In fact, high cholesterol diets can induce the formation of greater numbers of senile plaques in the brains of rabbits (Sparks et al. 1995). In humans, high peripheral levels of cholesterol have been associated with increased risk of AD; conversely, using drugs that lower serum cholesterol levels are thought to reduce AD risk (Jick et al., 2000; Wolozin et al., 2000; Pappolla et al., 2003; Wolozin et al., 2007). Similarly, in mouse models of AD, cholesterol-lowering drugs have been shown to reduce AD-associated pathology (Refolo et al., 2001; Petanceska et al., 2002).

Rodent animal models have great utility in studies of brain aging. Many of the same changes occurring in humans are also experienced by aging animals or can be modeled through genetic manipulation. Thus, some common changes believed to underlie normal aging include increased inflammation, glial reactivity, and decreased mitochondrial function (Norris et al., 2005; Wyss-Coray, 2006; Gibson et al., 2008). In studies of AD, aspects of the pathology are modeled in transgenic mice that are engineered to carry those familial mutations that cause amyloidogenesis (Oddo et al., 2003; Jankowsky et al., 2004). Therefore, many insights can be gleaned from studying aging changes in animals, in particular how therapeutic interventions can be used to attenuate or ameliorate these alterations in brain function.

An issue increasingly recognized as being a critical factor in studies of aging is determining when the aging process begins to occur. In rat models, a temporal decline in cognition begins at midlife, at approximately 12 months of age, as measured by performance in the Morris water maze, a spatial memory paradigm (Blalock et al., 2003). This is the same time point in which electrophysiological biomarkers of brain aging also begin to emerge (Gant et al., 2006; Lynch et al., 2006). This reflects cognitive changes that occur at approximately the same time in humans (midlife) as well (Park et al., 2002).

Microarray studies in rats have revealed alterations in lipid metabolism that coincide with cognitive decline at midlife (Rowe et al. 2007, Kadish et al. 2009). Many genes involved in lipid catabolism, cholesterol trafficking and myelinogenesis were found to be upregulated. This coincides with increased staining of SOAT1 within the hippocampus of aging animals, indicating upregulation of processes involved in

cholesterol esterification and cholesterol storage. Cholesterol levels within the normal brain are tightly controlled and most of this is in the form of free cholesterol (Dietschy 2009). Therefore, a shift toward esterification and storage marks a divergence in metabolism.

One interpretation of the age-related change in hippocampal gene expression across the lifespan is that it points to a more generalized shift occurring in metabolism as the brain ages. Genes involved in lipid and protein catabolism, as well as lysosomal activity, are upregulated at midlife, pointing toward an increase in the endocytosis of materials from the extracellular space (Kadish et al. 2009). In addition to these gene pathways, a parallel increase in expression of genes involved in immune responses is seen (Blalock et al., 2003; McGeer and McGeer, 2004). Along with the signals for increased myelinogenesis, these may act together to degrade and remyelinate axons, a process known to continue throughout aging (Peters, 2009). The degeneration of myelin may result in increased extracellular debris, especially if it is a result of inflammatory degradation via activated microglia. Endocytosis of the myelin debris may cause a shift in the brain to utilize more free fatty acids and amino acids as its major fuel source. Given the high concentration of cholesterol in myelin, degradation of myelin would also lead to an increased uptake of free cholesterol, leading to cellular excess within astrocytes of the brain. This is corroborated by the increase in the cholesterol acyltransferase, SOAT, as mentioned above, which esterifies cholesterol thus enabling it for storage within vesicles. Because cholesterol levels in the brain are so finely regulated, any excess in levels directly affects cholesterol synthesis, degradation and efflux (Dietschy, 2009).

As excess cholesterol accumulates in the cell, turnover increases, and cholesterol is catabolized to 24-S-hydroxycholesterol, an endogenous ligand of the liver X receptor (LXR). LXR regulates mechanisms directly involved with the efflux of cholesterol out of the cell. This is accomplished by driving the expression of a number of cholesterol trafficking genes including Apoe (Apolipoprotein E) and the transcription factor Srebp (sterol regulatory element binding transcription factor), similar to that seen in aging brain (Repa et al., 2002; Repa and Mangelsdorf, 2002). The beta isoform of LXR has also been found to upregulated in the aging brain (Rowe et al., 2007). The upregulation of this key

regulator of cholesterol efflux as well as genes involved in cholesterol trafficking suggest a potential compensatory reaction to excess cholesterol in the cell.

If these phenomena observed in the aging brain are compensatory in some way, pharmacological approaches that could increase cholesterol removal from the cell or decrease synthesis may help maintain an appropriate brain cholesterol concentration. In support of this notion are studies showing that potent LXR agonists that drive cholesterol efflux from cells reduce Aβ pathologies and improve memory (Koldamova et al. 2007, Jiang et al. 2008).

These observations suggest that cholesterol dysregulation may underlie some of the cognitive deficits present as a function of age and AD. Yet, very little is known about cholesterol dysregulation in the brain. Much of our knowledge about cholesterol's role in AD as well as normal aging is circumstantial in nature and very speculative. Given the increasing evidence pointing to cholesterol dysregulation as an important factor, answers to the following questions appear to be especially important: *Does cholesterol dysregulation play a role in AD and brain aging? Is part of the dysregulation attributed to excess cholesterol in the brain? Is it possible to pharmacologically intervene by targeting cholesterol metabolism through increasing cholesterol trafficking or directly inhibiting its synthesis? Are the observed brain aging changes compensatory?*

The goal of this dissertation has been to elucidate the role lipid metabolism plays in normal and pathological brain aging. This goal has been driven by two main hypotheses: 1). Chronically activating the liver X receptor (LXR), which in turn drives the expression of genes involved in cholesterol metabolism, transport, and efflux will reduce pathology and cognitive deficits associated with Alzheimer's disease (AD) as modeled in mice, and 2). Chronically inhibiting cholesterol synthesis in mid-aged rats, when many signs of aging begin to appear, will attenuate the appearance of cognitive deficits and associated electrophysiological correlates later in life.

To test the first hypothesis, a potent LXR agonist was administered chronically to two different transgenic AD mouse models, which were then assessed using a multidisciplinary approach including memory paradigms, electrophysiological measures, brain pathology assessment, and extensive microarray analysis. To test the second

hypothesis, we chronically treated mid-aged Fischer 344 rats with two different HMG-CoA reductase inhibitors (statins) and used similar techniques as above.

The following literature review presents pertinent background information on various topics relevant to the work presented as well as justification for why this type of research is necessary. The novel findings presented subsequently have implications in both the treatment of AD and the aging population as well, especially in the large part of the populace that currently take statins to reduce the risk of heart attack and stroke.

Cholesterol: Structure and Origin

Cholesterol is essential for life as it provides integrity to plasma membranes due to the rigidity inherent to its molecular structure. Perhaps surprising to most is that dietary cholesterol is not essential in order to have adequate amounts within the tissues of our bodies. Every cell has the capacity to make as much cholesterol as it needs and the body has various mechanisms to deal with levels that may not be optimal. Yet, hypercholesterolemia is still present in a large section of the population. The CDC reports that approximately 20% and 50% of the population have cholesterol levels greater than 240mg/dL and 200mg/dL, respectively (www.cdc.gov). This is attributed to either genetic variations leading to an increased synthesis or, the excess intake of lipid-rich dietary sources, with dietary factors playing a greater role. It is no surprise then that prescribing drugs to treat dyslipidemia is common practice around the world.

Cholesterol, as alluded to above, has two distinct origins, endogenous and exogenous. The central regulatory organ for both pools is the liver. Ingested cholesterol, as well as triacylglycerols (TAG), are absorbed in the intestine and are shuttled to the liver by chylomicrons containing Apolipoprotein B (ApoB), Apolipoprotein E (ApoE), and Apolipoprotein C-II. Upon reaching the plasma, some of the triglycerides associated with the chylomicrons are converted to free fatty acids by extracellular lipases. The remaining TAG as well as cholesterol is then delivered to the liver. Excess lipids are either stored or disbursed about the body. Various mechanisms are in place for the transport of both TAGs and cholesterol to extrahepatic tissues. The majority of TAGs are shuttled from the liver to peripheral tissues by very low-density lipoproteins (VLDL), whereas cholesterol is predominantly shuttled by low-density lipoproteins (LDL). The

cholesterol contained within LDL is both free and in the form of cholesteryl esters (CE), formed via an action of acyl-CoA-cholesterol acyl transferase (ACAT) that transfers a fatty acid onto the cholesterol making it more hydrophobic, and typically less toxic to the cell.

Besides cholesterol and CE, the LDL is also composed of ApoB, which allow for their absorption into cells via the large family of LDL receptors (LDLR). After binding to LDLR, the complex is endocytosed and digested by lysosomes within cells and broken down into its components, which include amino acids, CE and free cholesterol. Cholesterol, specifically, is able to then participate in the regulation of cholesterol synthesis pathways in extrahepatic tissues (Goldstein and Brown, 2009).

Endogenous cholesterol is synthesized in the liver and in extrahepatic tissues, from acetyl Co-A (much like other lipids), yet the structure of cholesterol is quite different from other lipids that typically contain long chain fatty acids (Figure 1.1). Cholesterol consists of a nucleus of four fused rings that create a relatively planar and, thus, rigid structure. The molecule has a polar moiety at C3, which gives it its amphipathic nature. These characteristics make it perfectly suitable to provide structural integrity to membranes.

The cholesterol synthesis pathway (Figure 1.2) is quite complex and involves a great many enzymes that produce a whole range of different metabolites that act to regulate the pathway itself. Many of these metabolites act as precursors to a variety of other isoprenoid molecules that play important roles in the prenylation of many small G-proteins. Cholesterol also plays the role of precursor molecule in that it is further processed to produce steroid hormones, essential vitamins as well as bile acids that allow for the digestion of dietary lipids. Figure 1.2 shows some of the major reaction products within the cholesterol synthesis pathway including key enzymes involved in their catalysis.

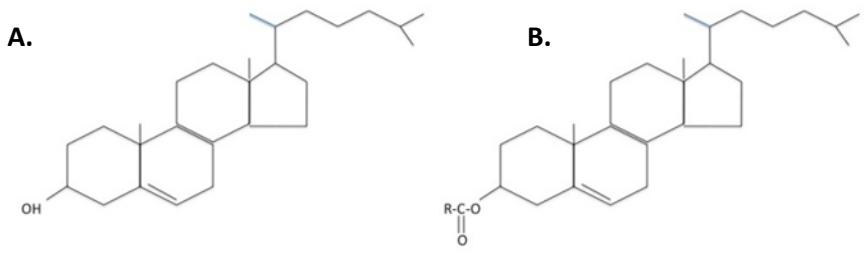

Figure 1.1: Chemical structure of cholesterol and cholesteryl. A. Cholesterol is composed of four fused rings which make up its non-polar, hydrophobic body. A hydroxyl group is bonded to C3 and acts to create a polar head giving the molecule its amphipathic nature. B. Cholesteryl esters have their hydroxyl group replaced by a fatty acid making the molecule more hydrophobic and typically less toxic to the cell.

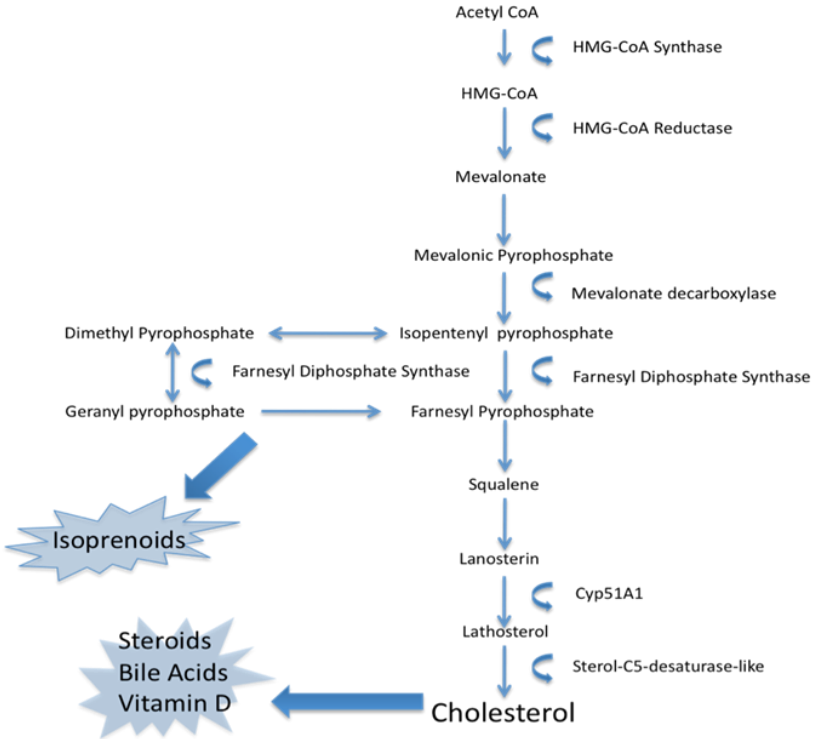

Figure 1.2: Cholesterol synthesis pathway. Key molecules within the cholesterol synthesis pathway are represented along with several enzymes that produce them. Acetyl-CoA is quickly converted to HmG-CoA by HmG-CoA synthase. The action of the next enzyme in the pathway, HmG-CoA reductase, is considered rate-limiting. HmG-CoA reductase inhibitors, commonly known as statins, act to inhibit the actions of this enzyme, which leads to the subsequent reduction of several reaction products. Besides cholesterol, several other essential molecules are created as a result of this pathway including the production of isoprenoids from cholesterol precursors. Finally, further cholesterol modification leads to the production of steroid hormones, essential vitamins and bile acids.

The General Nature of Cholesterol of the Nervous System

The brain comprises 25% of the body's total cholesterol pool, but is only 2% of the body's total weight and essentially all the cholesterol that is found in the brain is synthesized there (Dietschy and Turley, 2001; Dietschy, 2009). Brain cholesterol is at a concentration of 15-20 g/kg of tissue weight, is mostly unesterified and predominantly concentrated within the myelin that serves to insulate neuronal axons and, thus, increase the efficiency of their electrical signaling. Unlike in other tissues, brain cholesterol has a slow turnover rate, with a flux rate of only 0.9% of that normally seen across the entire body, which translates into a half-life of 4-6 months in the rat brain and 6-12 months in a human (Dietschy and Turley, 2004; Vance et al., 2005; Vaya and Schipper, 2007). It is important to note that that total flux rates of cholesterol in humans, primates, and rodents differ considerably, with rodents having a much higher metabolic rate and thus a faster turnover rate of cholesterol. Given that various animal models are used in the study of cognition it is important to consider these differences since the effects of specific drugs that modulate or directly inhibit metabolic processes involved in cholesterol synthesis and transport may differ given the length and dose of treatment with various animal species. What remains true for all of these mammals is that, considering the rate of peripheral cholesterol catabolism, the turnover rate of cholesterol in the brain is still disproportionately low (Dietschy and Turley, 2001, 2004).

As briefly mentioned above, the cholesterol that is incorporated into the plasma membranes of neurons and glia is produced *de novo* within the brain (Dietschy and Turley, 2001) and its level is tightly controlled. Even in models of peripheral nerve regeneration, the cholesterol utilized for the regeneration of damaged sciatic nerves is synthesized locally. There is a direct correlation between the rate of cholesterol synthesis and the accumulation of cholesterol within the regenerating nerve (Jurevics et al., 1998) and this synthesis is independent of dietary cholesterol (Jurevics and Morell, 1994). Similar to damaged sciatic nerves, exogenous cholesterol has little to no effect on the brain. Isotopically labeled exogenous cholesterol does not enter the brain during development, and the accumulation of sterols during this time closely correlates with their synthesis (Jurevics and Morell, 1995). Levels of myelin basic protein and cerebroside also correlate with cholesterol synthesis and accumulation, suggesting a

sophisticated level of coordination of mechanisms involved in lipid and protein formation during myelination, remeylination and axonal outgrowth.

Regulation of Brain Cholesterol Levels. Cholesterol levels in the brain are tightly regulated, and even during hypercholesterolemic conditions when plasma cholesterol levels are high, brain cholesterol levels are not altered (Edmond et al., 1991), unlike peripheral tissues which often display lipid accumulation. Cholesterol in the periphery is typically transported via lipoproteins and is endocytosed by cells upon binding to LDLR. There is no strong evidence to support that this type of transport occurs across the blood brain barrier. Mice lacking LDLR show no difference in brain cholesterol levels and studies in sheep show no detectable uptake of LDL from the periphery to the brain (Osono et al., 1995; Turley et al., 1996). There also seem to be few molecules that are rate-limiting and capable of significantly altering cholesterol levels in the brain, apart from perhaps a complete inhibition of HMG-CoA reductase. Various knockout mice lacking specific proteins that play vital roles in cholesterol metabolism in the periphery (ABCA1, ApoE, ApoA1, LDLR, and SRB1, Cyp46a) show little change in overall cholesterol levels within the brain. However, the absence of certain molecules can lead to changes in cholesterol synthesis rates. For instance, mice lacking the cytochrome p450 Cyp46a, also known as cholesterol 24-hydroxylase, show a reduction in synthesis. Cyp46a is almost exclusively found in the brain and produces the primary metabolite of brain cholesterol, 24(S)-hydroxycholesterol (24-OH-Chol), an oxysterol. Thus, Cyp46a is involved directly in cholesterol turnover. Reductions in cholesterol breakdown (e.g., with inhibition of Cyp46a) are accompanied by reductions in brain cholesterol synthesis (Lund et al., 2003) and, therefore, cholesterol levels are maintained (Quan et al., 2003). Together, these findings suggest a series of finely regulated feedback pathways controlling overall cholesterol levels in the CNS.

Interestingly though, mice lacking the Niemann-Pick disease, Type C1 (Npc1) gene show significant decreases in CNS cholesterol synthesis as well as overall concentrations within tissues. People with Niemann-Pick disease Type C1 have lower levels of the protein leading to a decreased ability to process cholesterol as it is endocytosed, leading to endosomal accumulation of cholesterol. NPC1 is associated with progressive neurodegeneration ending in adolescent mortality. Histological examination

shows an accumulation of cholesterol and other lipids in late endosomes of peripheral tissues (Ikonen and Hölttä-Vuori, 2004), whereas in the brain, cholesterol accumulation is absent while demyelination and neuronal death are both observed (Higashi et al., 1993; Takikita et al., 2004).

Removal of Excess Brain Cholesterol. Yet cholesterol levels can become excessive in the brain. Free cholesterol, if allowed to accumulate, is toxic to cells because of its amphipathic nature (Dietschy 2009). Unlike other tissues, the mechanism by which cholesterol is removed in the brain differs somewhat because of the presence of the blood brain barrier (BBB). As briefly discussed above, much of the excess cholesterol must first be converted to an oxysterol by Cyp46 before it is able to exit through the BBB. This enzyme is highly expressed in the brain relative to other regions of the body with higher levels of expression in the cerebrum and specifically in neurons (Dietschy and Turley, 2001; Lund et al., 2003; Xie et al., 2003; Vance et al., 2005). Much of Cyp46's synthesis occurs early in life during the formation of axons and their myelination (Vance et al., 2005). Given the high level of Cyp46 expression in the brain, it would stand to reason that the amount of 24(S)-hydroxycholesterol (24-OH-Chol), the oxysterol metabolite of the enzyme's activity, would be higher in the brain than any other tissue of the body. This is in fact the case with the absolute concentration of this metabolite observed to be 3.8-4.8ng/mg in the cerebellum and 8.6-15.1 ng/mg in the cerebrum. This accounts for 80% of the body's total pool of 24-OH-Chol (Lutjohann et al., 1996). The 24-OH-Chol has a flux rate of 6.4 ±1.8 mg/24hrs across the brain. This mirrors the rate of uptake of this metabolite by the liver at 7.6 mg/24 hours, again confirming that production of this particular metabolite takes place predominantly in the brain (Bjorkhem et al., 1998). Cholesterol can also be removed to a much lesser extent by apolipoproteins that are transported to the CSF (Pitas et al., 1987b; Pitas et al., 1987a; Vaya and Schipper, 2007). The transport and efflux of cholesterol is discussed further below.

Whereas 24-OH-Chol mostly moves unidirectionally from the brain to the plasma, other oxysterols enter into the brain from circulating plasma, perhaps acting as signaling molecules from the periphery. 27-OH-Chol is one oxysterol able to flux across the BBB from the plasma and is later metabolized to 7α-hydroxyl-3-oxo-4 cholestenoic

acid, which is then fluxed back out of the brain (Heverin et al., 2005; Meaney et al., 2007). Given that 27-OH-Chol does not remain in the brain, but is in fact metabolized for removal may suggest that the brain is able to utilize the molecule to sense peripheral levels of oxysterols.

24-OH-Chol itself plays a vital role in the cholesterol homeostasis of neurons in that high levels of this particular metabolite can actually attenuate the expression of enzymes critical in the production of cholesterol by activating the liver x receptor (LXR), for which it is a ligand (Wang et al., 2008). A more detailed discussion of the role of LXR will follow, but briefly LXR activation leads to the expression of a whole host of genes, involved in reverse cholesterol efflux as well as enzymes that participate in various aspects of lipid metabolism.

Cholesterol Transport in the CNS

Most of what is known about cholesterol transport comes from studies in the periphery. As briefly reviewed above, peripheral transport of cholesterol involves the movement of cholesterol along with other lipid species within lipoprotein particles like high-density lipoproteins (HDL), very low density lipoproteins (VLDL) and low-density lipoproteins (LDL) (Goldstein and Brown, 2009). Various apolipoproteins associate with these lipoproteins that carry cholesterol from the GI to peripheral tissues or from peripheral tissues to the liver in a process known as reverse cholesterol transport, referring to the movement of cholesterol from peripheral tissues to the liver. These lipoprotein/apolipoprotein complexes associate with receptors in the large LDLR family allowing for the endocytosis of the lipid molecules in the respective tissue. Cholesterol transport in the brain, though not dependent on outside sources, still occurs and utilizes similar mechanisms to move cholesterol and other lipids throughout the CNS. ApoE along with ApoA1 are thought to be the major apolipoproteins expressed in the CNS (Rebeck et al., 2006) and are contained within HDL-like lipoproteins. These nascent lipoproteins are produced by astrocytes, are discoidal in shape and are generally lipid-poor when first released from the cell indicating their readiness to collect cholesterol from other tissues (LaDu et al., 1998).

ApoE is the most studied CNS apolipoprotein due to its role in Alzheimer's disease as well as stroke and ischemic events (Poirier, 1996; Horsburgh et al., 1999;

McColl et al., 2007). There are three different ApoE isoforms found in the human population, differing only in presence or absence of one or two amino acids (ApoEε2: Cys-112, 158; ApoEε3: Cys-112, Arg-158; ApoEε4: Arg-112, Arg-158) at specific locations (Rebeck et al., 1998). The CNS highly expresses ApoE and several different LDLR family members are found on the surface of both neurons and astrocytes ApoE will bind to LDLR, VLDR, low density-related protein (LRP) and apolipoprotein receptor 2 (APOER2) (Rebeck et al., 2006). There is evidence that cholesterol may be recycled, as well, under conditions of damage by being gathered by apolipoproteins and redistributed to cellular membranes. The large number of lipoprotein receptors in the brain, most likely allow for a redundancy in the recycling pathway in case of an interruption (Dietschy and Turley, 2001), and facilitates scavenging of free cholesterol from the intercellular space.

The HDL-like lipoproteins, secreted from astrocytes, are in a different state from those found in the CSF, suggesting that perhaps the HDL-like particles derived from astrocytes may act to shuttle cholesterol within the CNS (LaDu et al., 1998; Rebeck et al., 1998). ApoE is physically associated with astrocytes, especially those below the pia mater and along large blood vessels and less so with neurons and microglia (Boyles et al., 1985). The formation of synapses and neurite outgrowth are promoted by ApoE-associated cholesterol from surrounding astrocytes (Mauch et al., 2001). The utilization of ApoE molecules may help to explain how axons of sympathetic neurons that do not synthesize cholesterol themselves, are able to incorporate cholesterol within their membranes, especially during periods of elongation (Vance et al., 1994; de Chaves et al., 1997).

As indicated above, axonal growth and elongation are dependent on the synthesis and the proper transport and allocation of cholesterol. In cultured neurons, blocking synthesis via an HMG-CoA reductase inhibitor stopped axonal elongation after only 2.7 days (Pfrieger, 2003a). This growth was rescued though with the addition of either mevalonic acid or an exogenous source of cholesterol, namely lipidated lipoproteins. But neurons in culture are in early stages of development relatively speaking, and mature neurons *in vivo* act much differently and are more intimately associated with surrounding glia. It has been suggested that neurons, in a proposed attempt to conserve energy,

outsources cholesterol synthesis to astrocytes (Pfrieger, 2003b). The amount of cholesterol needed later in life is not as great as during development (Bjorkhem and Meaney, 2004) at which time a neuron supplies most of its own cholesterol. As the neurons mature, the rate of synthesis drops and the axon terminus would be more dependent on cholesterol supplied from neighboring astrocytes (Pfrieger, 2003a). The needed cholesterol would be most likely delivered by apolipoproteins like ApoE.

Disruption of Cholesterol Synthesis: In the CNS and Periphery

The rate-limiting step in the production of cholesterol is the enzymatic activity of HMG-CoA reductase. The enzyme is regulated by cholesterol itself, with high levels triggering mechanisms that suppress synthesis and reduce cholesterol levels. The feedback is dependent on the products of the mevalonic pathways as opposed to actual regulation by cholesterol itself (Kita et al., 1980; Corsini et al., 1995). These products lead to actions resulting in the binding of HMG-CoA reductase to insulting induced gene 1 (INSIG1) and INSIG2 leading to its degradation, reduction of sterol regulatory element-binding protein (SREBP) activity, and revving up LXR activation which in turn increases the production of bile acids, the last step in reverse cholesterol transport (Goldstein and Brown, 1990; Corsini et al., 1995; Dietschy, 2009).

Cholesterol synthesis can be pharmacologically inhibited by blocking HMG-CoA reductase activity, typically with the use of a class of drugs collectively called statins. Statins were originally derived from fungal metabolites that competitively inhibit HMG-CoA reductase (Endo et al., 1976). The earliest statins, compactin (mevastatin) and mevinolin (lovastatin) have K_i of 10^{-9}M, indicating an affinity to the enzyme in the nanomolar range, which is 10^4-10^5 times greater than the affinity of the endogenous substrate (HMG-CoA) which binds at the 30 uM range (Corsini et al., 1995). The statin inhibits the enzyme by mimicking HMG-CoA via its lactone segment and blocking enzyme activity by directly binding within the substrate binding pocket (Schachter, 2005).

These early statins were able to lower serum cholesterol levels in a number of mammals. Surprisingly, the statins are unable to reduce serum cholesterol levels in rats (Endo, 1988) which should be noted given the data that will be presented below. To compensate for the potent inhibition of HMG-CoA reductase, there is a 200 fold increase

in reductase protein within a few hours of exposure (Liscum et al., 1983; Goldstein and Brown, 1990). Long-term effects of statins in rodents have not been thoroughly elucidated. Statin use increases the expression of LDLR on hepatocytes leading to a reduction in circulating LDL levels. They also increase HDL and decrease triglycerides. The original targets for statins were peripheral, in that they were intended to block cholesterol synthesis in the liver, which then increases the clearance of LDL from the plasma and thus act to help prevent atherosclerosis.

Given the importance of cholesterol in the brain and the role that statins play in reducing synthesis and quantities in the periphery, it is no wonder that there were questions to whether statins could in fact get across the BBB and whether or not the presence of the compound would confer an effect on the CNS. The effects of specific statins on the CNS are potentially dependent on their unique chemical structures which in turn determine their relative lipophilicity. Two commonly prescribed statins that are taken in two distinct forms are simvastatin and atorvastatin. The maximal dose for both in humans for LDL reduction is 80 mg/day. Simvastatin is thought to be brain penetrant whereas atorvastatin is not (Wood, 1999). The difference in lipophilicity is due in part to the chemical attributes of different functional groups of the respective drugs. Simvastatin, a modified version of lovastatin, which is a direct fungal derivative, is delivered in its lactone form, whereas atorvastatin, a completely synthetic statin, is delivered in its acid form (Hamelin and Turgeon, 1998; Schachter, 2005). Both are metabolized by Cyp3a4 and have a rather low bioavailability at 5 and 12%, respectively, when taken orally. The lactone form of simvastatin must first be hydrolyzed into its acid form, before it can actively inhibit HMG-CoA reductase, by a non-specific carboxyesterase in a reversible reaction (Tubic-Grozdanis et al., 2008). The lactone form of simvastatin has been found in circulating plasma and is three times more lipophilic than its acid form (Hamelin and Turgeon, 1998; Schachter, 2005). Atorvastatin's bioavailability, already rather low, can actually be reduced further when taken with food (Lennernas, 2003). The C_{max} (the maximum concentration of the drug in plasma after its administration) for Simvastatin and Atorvastatin are 10-34 ng/ml and 27-66 ng/ml respectively (Corsini et al., 1999).

Studies using BBB models utilizing bovine brain capillary endothelial cells (BCEC) found that the lactone form of simvastatin and lovastatin are much more

permeable then the their acid forms. Simvastatin had a permeability coefficient of 4.76 in the lactone form, whereas it only showed a coefficient of 0.193 in the acid form. The acid form is able to cross the BCEC model though, and appeared to do so in a passive from, most likely via a monocarboxylic acid carrier that requires no energy (Tsuji et al., 1993; Saheki et al., 1994). Given that simvastatin is taken in the lactone form, and the lactone form is found within the plasma, it would stand to reason that simvastatin would be more likely to enter the CNS than would a statin that is delivered in an acid form and is generally less lipophilic.

There is evidence that statins are able to reduce cholesterol synthesis in the brain, but very little to indicate that such a reduction does anything to overall cholesterol levels in the CNS. In a rather short-term study, 10 days of treatment in mice with simvastatin was unable to reduce cholesterol levels in the striatum as measured with GC/MS (Selley, 2005). Yet, longer studies also fail to show any real effect on cholesterol levels. After four weeks of high-dose treatment with both pravastatin and simvastatin, two distinctly different statins in regards to their lipophilicty, cholesterol synthesis was be reduced in the brains of guinea pigs, but there was not a significant effect on cholesterol levels. Pravastatin is considered hydrophilic and is thought to be unable to pass through the BBB, yet it still had an effect on cholesterol synthesis despite a perceived inability to pass through the BBB (Lutjohann et al., 2004). This particular effect of statins on cholesterol synthesis in the brain was corroborated in a later study in which very high doses of simvastatin (100 mg/kg) given to mice for approximately one month again showed no effect on cholesterol levels or the major cholesterol metabolite 24S-OH-CHOL in whole brain homogenates, but again, decreased cholesterol synthesis (Mok et al., 2006).

Though reports in the current literature of pharmacologically reducing cholesterol levels in the CNS are rare, benefits of using drugs that target cholesterol synthesis within the brain may have benefits independent of grossly reducing overall levels, and there is ample evidence that statins are able to confer positive effects in the CNS. In several studies involving traumatic brain injury (TBI), statins were found to beneficial in reducing TBI-associated deficits. Both simvastatin and atorvastatin are able to improve performance on the rotorod paradigm after TBI as well as reduce hippocampal degeneration and improve cerebral blood flow (Wang et al., 2007). Atorvastatin and

simvastatin are also able to improve performance on the Morris water maze in rodents (Lu et al., 2007; Wang et al., 2007). In another study with a shorter term of treatment, simvastatin improved rotorod performance in TBI animals as well as lowered mRNA levels of toll-like receptor 4 (TLR4), nuclear factor kappa-light-chain-enhancer of activated B cells (NF-κB), interleukin 1β (IL-1β), tumor necrosis factor –alpha (TNFα), interleukin-6 (IL6) and ICAM around the area of injury, concurrent with an overall reduction in the NF-κB activity (Chen et al.). Statins, It would seem, are able to ameliorate potentially harmful immune reactions, and the role of statins as immunomodulators is well documented (Kwak et al., 2000; Lindberg et al., 2005; Selley, 2005; Clarke et al., 2008; Aoki et al., 2009; Li et al., 2009). But its benefits go beyond reducing the deleterious effects of inflammation in TBI, statins may also be able to increase neurogenesis and reduce neuronal death following TBI (Lu et al., 2007).

Not all observed statin-induced effects in the brain are positive or consistent. There are several studies that indicate that statins may actually be deleterious to the CNS. Klopfleisch and colleagues (2008) found that inhibition of cholesterol synthesis in mature oligodendrocytes *in vitro* can actually cause the retraction of processes due to the disruption of Ras and Rho signaling that is dependent on the isoprenoids produced upstream of cholesterol in the mevalonic pathway. These metabolites are essential for the proper targeting of Ras and Rho to the membrane, which are integral in process elongation. This disruption in normal oligodendrocyte functioning also delays remyelination after cuprizone treatment *in vivo* (Klopfleisch et al., 2008). The effect seen on oligodendrocyte process retraction in this study depended on the lipophilicity of the statin, in that lovastatin induced process retraction whereas pravastatin, a much less lipophilic statin was unable to do so. Another study contradicts this when it was reported that the hydrophilic pravastatin retarded neurite growth of axons in neuronal culture (de Chaves et al., 1997). In both instances though the retraction could be rescued with co-treatment of mevalonic acid or with the isoprenoid analogs farnesol and geranyl-geraniol, but not with cholesterol, confirming that the effect in both was most likely due to a lack of prenylation capability as opposed to an overall change in lipid dynamics of the membrane (Miron et al., 2007). Isoprenoids like farnesylpyrophosphate and geranylgeranylpyrophosphate are needed for the prenylation for a whole host of small

GTPases. These include Rho and Ras, which without proper prenylation accumulate in the cytoplasm (Liao and Laufs, 2005). These GTPases play major roles in neuron growth and elongation(Cijiang He et al., 2006). Therefore, it is not clear how disruption of cholesterol synthesis would affect myelination. Firstly, the retraction of oligodendrocytic processes via inhibition of the synthesis of isoprenoids can inhibit proper myelination of axons. Secondly, the inhibition of neural outgrowth via the same mechanism would reduce the number axons available to myelinate. Thirdly, reduction of cholesterol itself would reduce materials needed to actually myelinate axons.

The effects of potentially induced cholesterol depletion in the brain should not be completely dismissed. Changes in cholesterol dynamics of the plasma membrane can modulate the activity of signaling molecules found within the lipid bilayer, specifically those associated with cholesterol rich lipid rafts. For instance, simvastatin protected against NMDA-induced neuronal excitotoxicity by reducing the number of NMDA receptors that are actually associated with lipid rafts without actually modulating the number of total receptors in a membrane fraction. In this case, isoprenoids do not seem to involved (Ponce et al., 2008), and the change in the fluid dynamics of the lipid rafts may affect the efficiency of NMDA receptor activity. Another study suggested, but failed to provide strong mechanistic support, that chronic simvastatin treatment could actually act like an NMDA receptor antagonist as well (Wang et al., 2009a).

Cholesterol and the Aging Brain

Cholesterol in the CNS is not static, and is subject to regular turnover; therefore dysregulation of cholesterol metabolism could potentially confer detrimental effects on normal neuronal function and participate in cognitive decline. The lipid bilayer is normally asymmetrical in its distribution of various phospholipids and cholesterol, which contributes to the fluidity of exofacial and cytofacial leaflets of the membrane (Wood et al., 2002). In mice, the exofacial leaflet gains cholesterol over its lifetime and the leaflets become less asymmetrical, which leads to a loss in fluidity (Igbavboa et al., 1996). The decrease in fluidity and the increase in cholesterol in the outer leaflet of the cell membrane could be due to a decreased capacity to efflux cholesterol. In ApoE knockout mice, the exofacial leaflet is much more concentrated in cholesterol than age-matched animals (Igbavboa et al., 1997) and as mice age, brain ApoE expression actually

increases (Masliah et al., 1996), suggesting that perhaps the brain is compensating for the disproportionate amount of cholesterol in the exofacial leaflet.

An age-dependent effect on the level of 24-OH-Chol exists in blood plasma. The levels appear to decrease over the lifetime of an individual, comparing the first decade of life to the sixth. This is most likely attributed to the fact that synthesis at earlier stages of development is much greater due to the need for cholesterol during axonal growth (Lutjohann et al., 1996). When myelin production decreases as neural networks are established, the need for cholesterol is not as great, and therefore synthesis, and the process by which cholesterol is metabolized can be reduced. In fact, 24-OH-Chol levels have been reported to decrease in the hippocampal regions of elderly subjects, leading the researchers to conclude that cholesterol synthesis is decreasing, while overall cholesterol levels in the brain remain stable (Thelen et al., 2006). This suggests that cholesterol turnover is reduced in parallel with the reduction in synthesis, very similar to the phenomenon seen in Cyp46a KO mice which show a reduction in cholesterol synthesis as a way to compensate for the absence of the Cyp46a, which is mainly responsible for the metabolism of cholesterol to 24-OH-Chol.

Evidence suggests that a metabolic shift in cholesterol metabolism takes place at mid-life. Studies carried out in rats have shown that a whole host of genes begin to be expressed differently as a part of normal aging starting at mid-age, marking a shift in expression patterns. A significantly disproportionate number of these are involved in cholesterol metabolism (Blalock et al., 2003; Rowe et al., 2007; Kadish et al., 2009). Several of these genes are positively correlated with cognitive impairment including ApoE and the sterol regulatory element-binding transcription factor (Srebf1) (Kadish et al., 2009).

Cholesterol is involved in determining the permeability characteristics of cellular membranes, and this point is vitally important when considering the role membrane potentials play in neuronal signaling. Myelin has a greater amount of cholesterol than most of the plasma membrane and it plays a key role in lowering the capacitance of axons, allowing for rapid salutatory conduction (Bartzokis et al., 2004; Dietschy and Turley, 2004). As the brain ages, the extent of myelination decreases with respect to the total length of myelinated fiber in the neocortex, which is reduced by 40-50 %

(Pakkenberg et al., 2003). Thus, dysregulation in cholesterol metabolism over the lifespan could impact myelin, compromising its integrity, and promoting degeneration and related pathologies. In fact, those axons myelinated later in life are thinner and less thickly sheathed in myelin, and these regions of the brain are those first affected by AD pathologies (Bartzokis, 2004). The demyelination and abnormalities in white matter have been implicated in both brain aging (Chia et al., 1983; Guttmann et al., 1998; Bartzokis et al., 2001) and Alzheimer disease as well (Roher et al., 2002; Bartzokis et al., 2003; Bartzokis et al., 2004; Chalmers et al., 2005; Bartzokis et al., 2007).

One must also not exclude the role vascular events may play in cognitive decline, even though these may be beyond the scope for this work, cholesterol levels are major risk factors in the development of atherosclerosis, and subsequently the possibility of having a heart attack or stroke. The risk for developing atherosclerosis and suffering from a stroke increases with age, as vasculature accumulates lipid-laden plaques (Allen and Bayraktutan, 2008). The brain itself is extremely vascularized, and thus cholesterol dysregulation seen in aging vasculature is potentially mirrored in the brain. Occlusion of small capillary beds throughout the brain would result in small areas of hypoxia, which can lead to cell death in areas deprived of normal blood flow (Thomas et al., 2002). These "mini-strokes" over time can be visualized as hyperintensities on MRI brain scans, and over time the recurrence of these events may lead to an underappreciated level of damage with serious cognitive effects. Many see these hyperintensities as part of normal aging, but the effects of these are not well studied.

The Hippocampus and Memory

One of the most studied individuals in science was a man known by the initials HM. In order to attenuate debilitating intractable seizures in the 1950s, HM underwent surgery to remove a posterior portion of the temporal lobe, which in turn destroyed approximately two-thirds of his hippocampus (Scoville and Milner, 1957) after which he was unable to form any new memories for the remainder of his life. Without the hippocampus, we humans along with the majority of our mammalian relatives are unable to acquire new memories or engage in spatial memory (deToledo-Morrell et al., 1988). As in the case of HM, older memories acquired before a lesion are undisturbed, negating the notion that the hippocampus is where memories are archived, but rather where

memories are reinforced and acquired, as will be discussed below, most likely through the strengthening of synaptic connections. As we age or develop certain neurodegenerative diseases, our ability to acquire new memories becomes impaired. It is no surprise then that loss of synaptic plasticity is the hippocampus during aging is highly associated with this impairment and is very similar to deficits seen with hippocampal ablation (deToledo-Morrell et al., 1988). Animal models for both aging and Alzheimer's disease that attempt to replicate this phenomenon of age-related cognitive decline are discussed in more detail below.

Alzheimer's Disease Progression and Treatment

Alzheimer's disease is the most common form of dementia and was first described by Dr. Alois Alzheimer in the early part of the 20th century. It is a progressive neurodegenerative disease considered to be fatal. The most prominent symptom early in the disease is the loss of episodic or declarative memory with latter symptoms including problems speaking, loss of executive functions, and changes in personality and behavior. Because of the rate at which the population is aging along with the duration of the disease, AD is becoming a major global health concern. AD exerts a considerable burden on the healthcare industry as well as on the financial stability of the nations of the world with the cost of treating and caring for AD patients costing over 100 billion dollars a year (Fillit and Hill, 2005; Sanders and Morano, 2008).

Most cases of AD are sporadic with the majority of cases occurring after the age of sixty-five. Age is the greatest risk factor for acquiring AD, with further increased risk in older individuals that carry the ApoE4 allele. Familial forms of early-onset AD do exist and are typically caused by the presence of an autosomal dominant mutations in the amyloid precursor protein (APP), presenilin 1 (PSEN1) or presenilin 2 (PSEN2) genes (Shepherd et al., 2009) all of which increase the production of amyloid beta (Aβ).

AD is associated with two specific pathological hallmarks, often referred to as plaques and tangles, both of which must be present for proper post-mortem diagnosis. The symptoms of the disease tend to follow the pathological changes that occur in the brain as the disease progresses, which include the formation of these senile plaques and neurofibrillary tangles (Davis et al., 1999), leading to cell death throughout various brain regions. These senile plaques are composed of deposits of amyloid beta peptides,

activated glia associated with increased inflammatory responses and degenerating neurons (Dickson, 1997). Neurofibrillary tangles are composed of hyperphosphorylated tau proteins (tau being the protein that makes up the microtubules of the cytoskeleton) which form paired helical filaments (Shepherd et al., 2009). Human pathology is correlated with the progression of observed cognitive deficits, as seen when Braak staging is compared with scores on the Mini-Mental State Examination (Nelson et al., 2009). Yet, it is important to note that there is evidence of gross pathology in the absence of cognitive deficits (Davis et al., 1999).

Some of the first noticeable symptoms of AD are the effects seen in short-term memory or the acquisition of new memories. This is often referred to as forgetfulness or general confusion about the placement of objects, the recall of words, or recollection of events occurring only minutes to hours before. One of the first areas of the brain affected by AD is the hippocampus with symptoms mirroring the functions of those regions sequentially affected by AD's pathological progression (Smith, 2002). As the disease progresses and more regions begin to atrophy, the severity of the symptoms increase until one is completely demented and is only a mere shell of who they used to be. The progression from mild-memory loss at early stages of the disease, often referred to as mild-cognitive impairment, to the final stages of the disease can span nearly a decade (Burns and Iliffe, 2009).

There are very few FDA-approved treatments, the most prominent of which attempt to increase the availability of the neurotransmitter acetylcholine or reduce excitotoxicity by antagonizing NMDA receptors (Scarpini et al., 2003). Such drugs do not target the cause of the disease, and therefore will always lack in their long-term efficacy. The development of therapeutics for AD has proven challenging because the actual cause of the disease remains elusive and with every hypothesized cause there is a corresponding targeted therapeutic. Given that the most quoted hypothesis for the cause of AD is the amyloid cascade hypothesis, it is no wonder that a great many drugs under development target Aβ either directly or indirectly by targeting those proteins involved in its processing. Yet there are other therapeutics under investigation including NSAIDS, fish oil, antioxidants and various currently used drugs that may confer pleiotropic effects that may prevent the onset or at least attenuate the progression of AD (Hull et al., 2006).

AD and the Cholesterol Connection

One of the major risk factors for Alzheimer's disease, besides age, is carrying the ApoE epsilon 4 allele (ApoEε4). As mentioned above, ApoE is a vital component in the movement of cholesterol within the brain (Wolozin, 2004). Transgenic mice (PDAPP) that express the human ApoEε4 gene have increased levels of Aβ42 at an earlier age and greater deposition of Aβ later in life. At the same time, these animals show reduced levels of ApoE in the CSF. These findings suggest the possibility that ApoE4 carriers have reduced ApoE levels in the CSF and that increasing levels of ApoE may help reduce Aβ (Bales et al., 2009) which in a lipidated state aids in its degradation (Jiang et al., 2008). It is also hypothesized that ApoE4 contributes to poor transport of cholesterol in the brain and, thus, reduced capability of lowering Aβ levels (Refolo et al., 2000).

It has been observed that individuals with AD pathology have higher serum levels of total cholesterol as well as LDL (Lesser et al., 2009). Epidemiological data has shown that statins as well as other lipid lowering drug may reduce the risk of developing dementia (Jick et al., 2000; Wolozin et al., 2000; Rockwood et al., 2002; Rodriguez et al., 2002; Sparks et al., 2006; Wolozin et al., 2007; Sparks et al., 2008; Haag et al., 2009), however there are instances where statins were reported to have no effect (Rea et al., 2005; Arvanitakis et al., 2008). It has also been found that AD patients have a significantly higher level of 24-OH-Chol in their plasma than healthy volunteers (Lutjohann et al., 2000; Papassotiropoulos et al., 2000) suggestive of a dysregulation in cholesterol metabolism in the AD brain. The elevated 24-OH-Chol may provide a biomarker of early stage AD only, given that the levels of 24-OH-Chol are reduced in late-stage AD patients because fewer neurons are capable of catabolizing cholesterol (Abildayeva et al., 2006).

Interestingly, it would not appear that it is as simple as "high cholesterol is bad, low cholesterol is good" in the context of predicting cognitive functioning later in life. In the elderly (defined as patients over 65), low serum cholesterol levels are actually negatively associated with cognition, and when coupled with carrying ApoEε4, the rate of cognitive decline is actually increased (van den Kommer et al., 2009). Yet, at midlife, high serum cholesterol actually increases the risk of AD and vascular dementia later in

life (Solomon et al., 2009), which creates a bit of a conundrum as far as trying to determine what therapy to provide as well as how long to provide it.

Amyloid precursor protein (APP) is the major protein implicated in AD pathology. Its aberrant processing, folding, and aggregation is what some believe is the culprit behind the development of the disease. Cholesterol plays a part in the processing of this particular protein. Animals that are fed a diet containing high levels of cholesterol tend to develop more AD pathology (Sparks et al., 1994; Sparks et al., 2002; Pappolla et al., 2003). Hypercholesterolemia may actually lead to cholesterol enrichment of microdomains within the cell membrane, favoring APP cleavage, and subsequent increased Aβ production via γ-secretases located within these domains (Refolo et al., 2000). A popular hypothesis explaining the effects of cholesterol and APP processing considers the important role cholesterol plays in membrane fluidity. APP can be potentially processed by three different secretases, α, β, and γ. The sequence in which these proteases act on the APP determines whether or not the toxic form of Aβ is formed. Alpha secretase cleavage forms the APPsα fragment and precludes Aβ formation. It is thought that high levels of cholesterol would favor the cleavage of the APP by the beta and gamma secretases, which would produce the Aβ40 or Aβ42 peptides, which are thought to be responsible for AD pathology (Golde and Eckman, 2001; Wolozin, 2001).

One mustn't forget that the most common risk factor for acquiring AD is age. As mice age, the lipid dynamics of neuronal membranes change and the fluidity of the exofacial layer of the membrane decreases. As mentioned, this is most likely attributable to the twofold increase in cholesterol levels within the exofacial layer of the membrane (Igbavboa et al., 1996; Wood et al., 2002; Rojo et al., 2006). Furthermore, high cholesterol can accelerate AD pathology in a transgenic mouse model (Refolo et al., 2000) and its depletion can inhibit Aβ production (Simons et al., 1998). Polymorphisms in the Cyp46 gene, which encodes the enzyme responsible for the majority of cholesterol turnover in the brain are also associated with greater levels of Aβ accumulation in human brain tissue and an increase risk of developing AD (Papassotiropoulos et al., 2003). This suggests that by lowering cholesterol or impeding its synthesis one could reduce Aβ levels and reduce the risk of AD. Both of these have been shown (Fassbender et al., 2001; Kojro et al., 2001; Refolo et al., 2001; Schneider et al., 2006).

Liver X Receptors (LXR): Master Metabolic Regulators

LXR may be considered as a master regulator of metabolism in the body because of its diverse ability to regulate the crosstalk between a number of signaling pathways that include lipid metabolism, insulin signaling as well as immune responses. Given its diverse role, it has been the subject of various studies in hopes to exploit its regulatory nature in the context of various disease models to both better understand the disease as well as find potential therapies. Perhaps LXR's largest role is in lipid metabolism, and several components of cholesterol metabolism share a common denominator in the LXR, which includes regulatory aspects of its transport and efflux. This transcription factor, as we will see, also plays an important role in lipogenesis as well as in glucose control. Pharmacological manipulations of LXR have implications in treating a large list of diseases associated with cholesterol dysregulation, specifically atherosclerosis and AD.

LXR is a member of the nuclear receptor superfamily. LXRs exist in two isoforms, LXR-α and LXR-β. Both isoforms heterodimerize in an obligatory fashion with the retinoic acid receptor (RXR) (Apfel et al., 1994; Teboul et al., 1995; Willy et al., 1995; Janowski et al., 1996). The LXR-α isoform is predominately expressed in the liver, intestines, and adipose tissue, whereas LXR-β is considered more ubiquitous and is the more active of the two in the brain (Janowski et al., 1996); yet, the gene targets of both isoforms overlap considerably, and one can potentially compensate for the loss of the other (Zelcer and Tontonoz, 2006).

The endogenous ligands of LXR are various oxysterols, including 27-hydroxycholesterol, 24(S),25-epoxcholesterol and 24(S)-Hydroxycholesterol, which is the major activating species in the brain (Hu et al., 2003; Tontonoz and Mangelsdorf, 2003). LXR can be pharmacologically activated with at least two known agonists, T0901317 and GW3965, with T0901317 having a much more robust effect on the receptor's targets (Albers et al., 2006). The GW3965 compound is considered by some to be a partial agonist because it can only achieve 37% activation of LXR-α and 62% of LXR-β when compared to T0901317 treatment (Albers et al., 2006). This also suggests that GW3965 has a slight preference for LXR-β, which has implications for its effect on peripheral organs like the liver.

The classical pathway for the receptor's activation involves binding of the ligand, subsequent release of the co-repressors NCoR and SMRT and binding of co-activators that enhance expression (Hu et al., 2003; Zelcer and Tontonoz, 2006). Those genes targeted by LXR contain an LXR binding element. These elements are direct repeats of the sequence AGGTCA separated by four nucleotides (Janowski et al., 1996).

The LXRs, as noted above, are regulators of cholesterol homeostasis and their target genes are directly involved in cholesterol metabolism (Schultz et al., 2000; Venkateswaran et al., 2000; Zhang et al., 2001; Cao et al., 2002; Joseph et al., 2002a; Whitney et al., 2002; Liang et al., 2004; Ulven et al., 2004; Karten et al., 2006) as well as genes involved in the synthesis of both fatty acids and bile acids (BA) (Ulven et al., 2005; Watanabe et al., 2005). The first LXR gene target discovered was cholesterol 7-alpha hydroxylase (CYP7a1), a rate-limiting enzyme in the production of BA (Peet et al., 1998). A summary of LXR gene targets is shown below (Figure 1.3).

LXR activation leads to an upregulation of major fatty acid synthesis genes as well as to an increase in plasma triglyceride levels. Much of this is attributed to its upregulation of SREBP1 (Schultz et al., 2000), which shares some of LXR's other gene targets including ApoE (Ulven et al., 2004), ApoA-1, a variety of ATP binding cassettes (e.g. ABCA1, ABCG1), fatty acid synthase (FAS), phospholipids transfer protein (PLTP), and lipoprotein lipase (Peet et al., 1998; Naik et al., 2006).

In the periphery, apart from it integral role in the lipogenesis, LXR is responsible for reverse cholesterol transport (RCT) and acts as a sensor of excess dietary cholesterol. When LXR is absent in mice, cholesterol accumulates due to a decrease in one of it targets, CYP7a1, disrupting the main pathway by which cholesterol is removed from the body (Zelcer and Tontonoz, 2006).

As mentioned above, LXR upregulates the expression of ATP-binding cassettes like ABCA1 and ABCG1 transmembrane transporters which facilitate the lipidation of lipid-poor apolipoproteins within HDL complexes allowing shuttling of cholesterol back to the liver to be degraded into BA (Brooks-Wilson et al., 1999). Macrophages are integral in the removal of cholesterol from blood vessels, and the dysregulation of this process can lead to atherosclerosis. LXR is highly expressed in macrophages and foam cells within atherosclerotic lesions (Watanabe et al., 2005). These macrophages are

involved in the movement of cholesterol out of the macrophages to HDL particles. It follows that LXR activation can inhibit the development of atherosclerosis in mice (Dean et al., 2001; Joseph et al., 2002b) given its role in upregulating the genes that facilitate RCT.

LXR activation leads to the upregulation of a host of genes involved in lipid synthesis, specifically triglycerides. Given that the production of lipids is dependent on available materials, it is not surprising that LXR helps regulate the crosstalk between carbohydrate availability and the production of triglycerides. The expression of insulin-sensitive glucose transporter 4 (GLUT4) in adipocytes is dependent on LXR-α, which is downregulated in diabetic patients who have become insulin-resistant (Dalen et al., 2003). The increase in GLUT4 on the surface of adipocytes allows for the production of triglycerides in the adipose tissue as a result of an increase in glucose uptake, providing further evidence of LXR's role as a glucose sensor engaged in the upregulation of lipogenic processes (Mitro et al., 2007). In hyperinsulinemic mice (db/db mice), hypertryglyeridemia and the accumulation of triglycerides in the liver was greatly increased when they were treated with an LXR agonist (Chisholm et al., 2003). There is also evidence that LXR can act on pancreatic beta cells to increase the insulin levels, which would further lead to an increase in triglyceride formation (Efanov et al., 2004).

LXR is also known to be anti-inflammatory in macrophages where their activation leads to inhibition of NF-κB dependent signaling (Zelcer and Tontonoz, 2006). This includes the inhibition of classic inflammatory-associated genes after insult with lipopolysaccharide (LPS) in macrophages, including the inhibition of inducible nitric oxide (iNOS), cycloxygenase (COX), and interleukin six (IL-6). LXR activation also reduces the inflammatory response in the aorta of atherosclerotic mice (Joseph et al., 2003). The ability of LXR to reduce inflammation has been shown in glial cultures as well, where GW3965 inhibits the normal inflammatory response associated with a fibrillar Aβ insult as well as promote its phagocytosis in microglia (Zelcer et al., 2007).

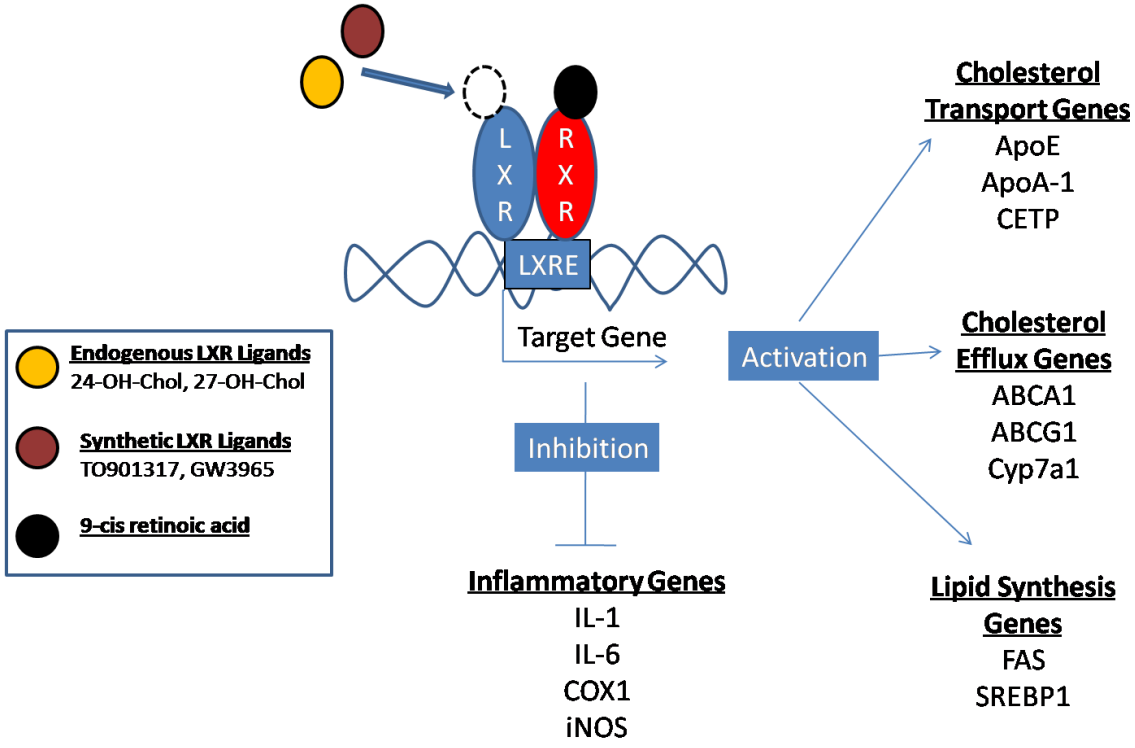

Figure 1.3: Liver X Receptor gene targets: Upon heterodimerizing with RXR and binding to a ligand either endogenous or synthetic, LXR activation leads to the upregulation and downregualtion of genes involved in various metabolic and non-metabolic pathway, specifically in the upregulation of genes involved in lipid metabolism and the downregulation of classically associated inflammatory genes.

LXR in Brain Aging and AD

Given the many links between cholesterol metabolism and AD, and knowing that the LXRs are intimately involved in several facets of lipid metabolism it may not be surprising that pharmacological modulation of the LXR pathway has been implicated in the reduction of biomarkers associated with AD pathology. Endogenous oxysterols (Janowski et al., 1996) including 24(S)-OH-Chol, the major cholesterol metabolite of the brain, bind to LXRs. Activation of LXR is directly involved in the upregulation of key proteins associated with AD as well as being involved in cholesterol metabolism and transport including apolipoprotein E and several ATP binding cassettes (Teboul et al.,

1995; Schultz et al., 2000; Zhang et al., 2001; Cao et al., 2002; Whitney et al., 2002; Liang et al., 2004; Ulven et al., 2004; Zelcer and Tontonoz, 2006). As mentioned, the oxysterol 24-OH-Chol is elevated in the plasma of AD patients and has been suggested as being an AD biomarker (Lutjohann et al., 1996; Lutjohann et al., 2000; Papassotiropoulos et al., 2000; Lutjohann and von Bergmann, 2003). Evidence of alterations with aging include the recent observation by our lab that LXR-β is significantly upregulated in the hippocampus of aged male F344 rats (Rowe et al., 2007). Furthermore, SREBP as well as ApoE are upregulated in rats at midlife as part of shift in metabolism, both of which are direct targets of LXR activity (Kadish et al. 2009). The cause and effect relationship between aging and in increase in LXR and its targets are not full understood and these results indicate either a compensatory role of LXR in the aged brain or perhaps a deleterious outcome of increased levels of cholesterol metabolites

Most of the research targeting LXR with synthetic agonists has shown it to be more beneficial in nature. Some studies find that LXR activation reduces Aβ processing and/or levels in both *in vitro* and *in vivo* models along with associated cognitive deficits (Sun et al., 2003; Koldamova et al., 2005; Burns et al., 2006; Riddell et al., 2007; Zelcer et al., 2007). The mechanism behind this reduction in Aβ is not well understood, but may be due to an increase in ApoE and ABCA1 along with an increase in cholesterol transport mechanisms within the brain (Pfrieger, 2003b; Hirsch-Reinshagen et al., 2004; Wahrle et al., 2005; Abildayeva et al., 2006; Bjorkhem, 2006). For instance, Burns and colleagues found that in an *in vitro* system, Aβ levels were reduced with LXR activation and ABCA1 upregulation, but only if there was a cholesterol efflux acceptor (ApoA1) available in the media along with ABCA1(Burns et al., 2006). Without ABCA1, Aβ was not reduced (Wahrle et al., 2005). Therefore, a direct link between the expression and function of both ABCA1 and the apolipoproteins seems to exist and that the co-expression of both is essential to confer benefits. Furthermore, a potential mechanism explaining the ability to reduce Aβ through LXR activation has been somewhat elucidated in that lipidated ApoE, driven by a LXR agonist, is able to subsequently promote the proteolysis degradation of Aβ through facilitating the endocytosis of Aβ into microglia or making the Aβ available for extracellular enzymatic degradation (Jiang et al., 2008).

Chapter 2: Materials and Methods

Introduction

Described below are the general materials and methods used throughout the six experiments discussed within this document. They include not only descriptions of the protocols used, but also the rationale for their use. The protocols are generalized and are not identical across all the experiments due the use of different models and experimental designs. Therefore, a separate description of the materials and methods used in a particular study is included within its respective chapter.

Animal Models of Alzheimer's Disease

There exist today a great and varied number of mouse models of AD. Typically, the models exploit the expression of a select gene or set of genes that act to induce some pathological characteristic of the disease state. AD pathology is marked by the presence of dense senile plaques created from the deposition of Aβ, created from the proteolytic cleavage of amyloid precursor proteins (APP) (Jankowsky et al., 2004), as well as neurofibrillary tangles composed of hyperphosphorylated Tau protein (Selkoe, 2001). The most commonly used AD models overexpress gene mutations that are found in familial forms of AD. These include the gene variants of APP and presenilin 1 (PS1), both of which are associated with the overproduction of Aβ. APP is cleaved by a series of enzymes to create a number of different Aβ species. PS1 is a γ-secretase that is integral in the formation of Aβ. Mutations in PS1 as well as the protein on which it acts, APP, are known to lead to familial forms of AD and result in the overproduction of Aβ (Citron et al., 1992; Cai et al., 1993; Haass et al., 1994; Rogaev et al., 1995; Sherrington et al., 1995; Jankowsky et al., 2002; Jankowsky et al., 2004).

Juxtaposed to the experimental models of AD which genetically manipulate specific genes is that fact that very few cases of AD are known to be directly caused by a specific gene (Morrissette et al., 2009). Most cases of AD are sporadic without any concrete indication of causality and not familial in origin. Nonetheless, despite the earlier onset of the familial form, sporadic and familial AD are usually pathologically indistinguishable (Selkoe, 2001). Given this similarity, it is believed that the use of experimental models of familial AD may provide insight into the sporadic form of the disease, as well.

Triple transgenic model: The triple-transgenic model (3xTg) of AD appears to be an ideal model in that it presents with both pathological hallmarks required for diagnosis in the post-mortem brain, plaques and tangles, and does so in a relatively quick manner. The mouse was developed by Frank LaFerla and colleagues in 2003 at the University of California, Irvine and has been characterized by that lab and its collaborators. The mouse was created by microinjecting two independent transgenes (human APP_{swe} and tau_{P301L}) into embryos harvested from $PS1_{M146V}$knockin mice (Oddo et al., 2003). The first pathological manifestations in the mice is intraneuronal Aβ appearing between 3-4 months of age which appears to be oligomeric (Oddo et al., 2006). Extracellular Aβ is not seen until around 12 months of age.

In this model, Aβ formation precedes tangle formation and an antibody vaccine toward oligomeric Aβ clears both forms of pathology, suggesting a causative role of Aβ in tangle formation (Oddo et al., 2006). Synaptic plasticity is also impaired in the animals as they age, determined by measuring EPSPs in the CA1 region of the hippocampus. Synaptic deficits correlate with sequential increases in Aβ accumulation (Oddo et al., 2003), and are indicative of decreased ability to form memories. Thus, in these animals, the reduction in synaptic plasticity correlates with cognitive deficits, specifically in hippocampal-dependent spatial memory as measured by the Morris water maze (MWM) and passive avoidance tasks (Billings et al., 2005).

Double-transgenic model: Various versions of the "double transgenic mouse" model (2xTg) exist, but the model used in the present studies makes use of the overexpression of both the APP_{swe} and $PS1_{\Delta 9}$ genes. These mice were originally created by crossing a mouse carrying the APP_{swe} mutation with a mouse carrying the $PS1_{\Delta 9}$ mutation (Borchelt et al., 1996). Later a line was created through the co-injection of both transgenes which co-segregated making the production of progeny more efficient (Jankowsky et al., 2001). The mouse strain used in the experiment described below is of the original type and was created by crossing founder mice expressing either APP_{swe} or the $PS1_{\Delta 9}$ mutation. Mice expressing both transgenes were then backcrossed to C57Bl6 mice for 10 generations to create a congenic strain.

Models co-expressing these mutations present with accelerated Aβ deposition with observable deposits at 6 months of age with the majority of deposits located in the

frontal and entorhinal cortices and the hippocampus with deposition continuing to worsen as the mouse ages (Gordon et al., 2002; Jankowsky et al., 2004; Savonenko et al., 2005). This accelerated processing is due to the co-expression of both the delta-9 PS1 mutation along with the APP_{swe} mutation, whereas animals expressing only one of these fail to present with Aβ deposition at this same rate (Borchelt et al., 1997).

Behavioral characterization of this model shows that anxiety levels are not significantly higher when compared to age-matched controls (Reiserer et al., 2007). There is an age-dependent effect on episodic memory deficits, which correlate with Aβ accumulation (Savonenko et al., 2005). Similarly, mice co-expressing both transgenes also show impairments in a version of the Barnes maze and show less of an impairment in reference memory but rather a deficit in learning flexibility (Reiserer et al., 2007). Lalonde and colleagues have shown that spatial memory deficits do exist though (Lalonde et al., 2005). Furthermore, other mouse models of AD, specifically those that express only human mutations of APP without expressing the mutant form of PSEN1 show performance deficits in contextual fear conditioning (Comery et al., 2005; Jiang et al., 2008), another behavioral paradigm that assesses contextual memory.

Given that this particular 2xTg model presents with Aβ pathology and behavioral deficits, it appears to be an appropriate model for therapeutic intervention studies to examine potential attenuation of both pathology and related cognitive deficits.

The Fischer 344 (F344) as a Model of Normal Aging

A commonly used rodent model of aging is the F344, a rat model used by various aging research groups over the past two decades (Barnes et al., 1987; Barnes et al., 1990; Barnes et al., 2000; Gant et al., 2006; Rowe et al., 2007; Brewer et al., 2009; Kadish et al., 2009). As seen in human aging (Park et al., 2002), deficits in memory can be detected in F344 rats with the Morris water maze (MWM) starting around mid-age and continue to worsen with increasing age (Shukitt-Hale et al., 1998; Bizon et al., 2009). Much of the work done by members of our research group has been carried out in F344s, including electrophysiological studies, behavioral studies and microarray studies (Landfield and Lynch, 1977; Landfield et al., 1978; Landfield and Pitler, 1984; Gant et al., 2006; Rowe et al., 2007; Brewer et al., 2009; Kadish et al., 2009). Given the amount

of data amassed with this particular model, it is only reasonable that the aging studies described here would include the use of this model so that appropriate comparisons can be made to both previously observed deficits seen in various behavioral paradigms as well as changes in gene expression as measured with microarray technology.

The Morris Water Maze (MWM) and Cognitive Assessment

Rationale

The Morris water maze has become the gold standard for assessing learning and memory deficits in rodents and is used extensively in models of aging and neurodegenerative disease. It has been 25 years since the water maze was first described as a spatial memory paradigm by Dr. Richard Morris at the University of St. Andrews (Morris, 1981). It was developed to study spatial localization in rats and forces the animal to use its surrounding visualized environment to navigate (Brandeis et al., 1989). The aquatic context of the environment also allows for assessment of spatial memory even if locomotor deficiencies exist. Essentially, an animal in the maze must use distal, extramaze cues to orient themselves within a pool filled with water and then locate a fixed platform hidden just beneath the surface of the water (Morris et al., 1982; Vorhees and Williams, 2006). Navigation is dependent on these distal visual cues and precludes a repeated pattern of movement implying a strategy that would use muscle memory (Sutherland et al., 1983; D'Hooge and De Deyn, 2001). The spatial navigation within the maze is not entirely hippocampal dependent, but performance in the hidden-platform MWM is severely impaired when the hippocampus is lesioned providing support for the role of the hippocampus in spatial memory (Morris et al., 1982; Morris et al., 1986). Interestingly, blocking long-term potentiation (LTP), considered by some to underlie hippocampal-dependent learning, impairs performance in the MWM similar to that seen with hippocampal lesions (Morris et al., 1986).

During the training phase of the MWM, when animals are taught how to perform the task, the aged animals show slower acquisition during the first few days of training. However, by the end of this period, several days later, the aged animals perform as well as younger animals. Thus, the aged animals "learn" the task, but at a slower rate. The "memory" part of the task comes during the "probe trial" after the acquisition phase.

During the probe trial, the submerged platform is removed, and various measures are taken to assess recall. Aged animals typically show impaired performance on the probe trial (Rapp et al., 1987). Age-related deficits observed in spatial memory also resemble those seen in animals with damage in hippocampal circuitry (Bizon et al., 2009), suggesting that the impaired ability of aged animals to perform as well as younger animals could be due to deleterious changes occurring in the hippocampus with aging.

When assessing the cognitive ability of older animals in the MWM, other various age-related deficits that could potentially confound the observed behavior must also be considered. Visualization of the distal extramaze cues is an integral part of orienting in the maze, and the animal's visual acuity must be at a level that will allow them to see the spatial cues. Dr. Morris originally described performing a cue task (Morris, 1981; Morris et al., 1982) to assess the ability of the animal to see a conspicuous platform that was placed in various locations in the maze to assure that the animal would be able to be trained on the task. Similarly, training the animal to find a marked platform while being placed in different quadrants over the course of training assures that the animal has an appropriate level of visual acuity but also understands the point of the task, which is to find a submerged platform to escape from swimming.

When assessing aging differences in cognition it is also important to consider differences in locomotor ability of the animals. A commonly used outcome measure for the MWM is latency to the platform during training. Older animals tend to have reduced swim speed making this measurement problematic in assessing cognitive differences (Gallagher et al., 1993). A better measurement is length to platform during training sessions, which is not dependent on swim speed. This may not be as an important consideration when determining differences between groups of the same age, where differences in swim speed itself could be an interesting outcome measure in experiments involving drug intervention.

As mentioned above, the probe sessions are important in assessing memory and are usually executed by placing an animal in the pool after the platform has been removed and allowing the animal to freely swim for 60-90 seconds. The animal displays recall if it uses the extramaze cues to orient to the quadrant where the platform was previously located and spends more time in the quadrant trying to locate the platform in

order to escape. Various measurements are used to analyze performance during a probe session, including: latency/path length to goal, number of platform crossings, percent time in goal quadrant and cumulative distance to platform. It has been found that in aging animals cumulative distance, thus proximity to the area in which the platform was located during previous training sessions, is a better assessment of whether or not the animal is using reference memory to locate the platform as opposed to an alternative search pattern that would allow the animal to cross the platform area with an inflated success rate. Such a search pattern may produce reduced latency and path length measures (Gallagher and Nicolle, 1993).

The percent time spent in a particular quadrant also allows for determining whether the animal is spending more time looking for the platform in the goal quadrant, suggesting the use of spatial memory to locate the platform. Even though the free swim probe session lasts 60-90 seconds, it is common to assess only the first 30 seconds given that animals will often determine that the platform is not in its normal location and then begin searching throughout the pool (Vorhees and Williams, 2006), therefore skewing data in a way that does not represent the animal's initial behavior upon introduction into the maze.

MWM General Apparatus and Protocol

The pool is a galvanized metal water tub 183 cm in diameter and 60 cm high. It is enclosed within black curtains that produce a semi-dark environment within the testing room. The bottom and inward facing sides of the pool are painted black to provide contrast for the video camera system and facilitate the tracking of the albino rats used in this study. Three large contrasting spatial cues hang from three of the four surrounding walls and are lit by LED rope lights that wrap around the pool itself as well as LED lights that project a beam of light onto the cues. This allows for visualization of the spatial cues and provides contrast needed for the Videomex tracking system and accompanying water maze software (Columbus Instruments). Illumination in the pool area is verified with a lux meter to ensure it is at a in a visible range for F344 rats. The pool is filled with water (25±1C°) to a height sufficient enough to submerge a 15 cm diameter platform (by 2 cm of water.

Prior to the training phase, cue training takes place to verify the eyesight by the rats. During cue training, a conspicuous cue is suspended from the ceiling and hangs approximately 12 inches above the submerged platform marking its location. Aged animals are often unable to pull themselves on top of the platform, so the platform was submerged during cue training to aid the rats. Cue training lasts for three days with each rat given three trials a day. A trial consists of 60 seconds to find the platform, 30 seconds to acclimate to the surrounding while on the platform, and 120 seconds within a holding cage heated by a heat lamp before being reintroduced to the maze. On day one, animals were introduced to the maze in the same quadrant for every trial. On subsequent days, the animal was introduced in different quadrants every trial, rotating the drop spot in a clockwise fashion.

Seventy-two hours after the last cue-training trial, the training phase commenced with the animals trained in a similar manner as described above, but with the suspended cue removed. Throughout the training sessions (3 trials/session/day) we rotated the drop spot within the day, and subsequently rotated the first drop spot of the day on following days in the same clockwise fashion in order to ensure that the rat was using the spatial cues for orientation within the maze instead of an alternative search pattern.

Twenty-four hours after the last day of training the platform was removed from the maze and animals given 60 seconds to swim freely while being monitored by the tracking system. The probe session provides a variety of different measurements to assess memory. These include: latency to goal, path length to goal, number of goal crossings, proximity to goal, percent time spent in goal quadrant and number of goal quadrant entries. The goal is defined as the extended annulus of the platform equaling 2.8 times its original area.

Active Avoidance (AA) as a Learning and Memory Paradigm

Rationale

The active avoidance learning paradigm has been used to assess learning for many decades, but has been overshadowed by the MWM which has proliferated as the task of choice when assessing spatial memory. It is also an assessment of hippocampal dependent spatial memory in rats, and given the potential pitfalls of behavioral experiments, it is often useful to have additional behavioral methods to assess memory within a cohort. Also, mice are notoriously, if not more anecdotally, difficult to assess in the MWM, thus the active avoidance learning task may, therefore, be useful as an alternative task to assess cognitive deficits associated with aging and related dementias in mice.

The essential premise of the task is to train an animal to actively avoid an unconditioned stimulus (US), a footshock, by remembering the context in which it was shocked during the training sessions. The task employs a light/dark dual chamber or shuttle box. During training, the animal is placed in the dark side of the shuttle box, which is innately preferred by nocturnal rodents, and a light footshock applied. Historically the footshock is preceded by a conditioned stimulus (CS) such as a tone or buzzer, but in the studies to be described we have not included this, forcing the animal instead to use the contextual space that surrounds it to remember that a shock occurred in the dark side of the chamber. Following a shock, animals typically move to the other, lit side of the shuttle box (the side it doesn't innately prefer). The animal learns to move to the light side of the shuttle box in order to avoid a shock. Performance can be measured through the analysis of latency to escape the chamber on subsequent sessions, as well as the number of avoidances in a given training session.

Given the role of the hippocampus in spatial memory, it is important to ascertain whether or not active avoidance learning is in fact hippocampal dependent. Classically this is done by lesioning the hippocampus and determining whether performance on the behavioral task is impaired. Olten and Issacson (1968) found that surgical ablation of the hippocampus results in poorer performance than sham control animals. Furthermore, they found that one-way active avoidance, used in the present experiments, appeared to be more hippocampal dependent than the related two-way active avoidance paradigm (Olton

and Isaacson, 1968b). Similarly, kainite depletion of neurons within the hippocampus can also lead to impairment (Munoz and Grossman, 1981) along with intrahippocampal injections of the muscarinic antagonist scopolamine (Brito and Brito, 1990). Even though it is thought that a simple, paired CS, such as a buzzer, that elicits a learned response is partially amygdalar as well as hippocampal-dependent(Anagnostaras et al., 2001), making the task more stringent by removing any CS besides the spatial context should only strengthen the role the hippocampus plays in this particular paradigm.

AA General Protocol

Slight differences exist in the protocols used for specific experiments described below, but the general method for all remains very similar. Changes made were typically introduced to improve data acquisition or to remove potential confounds. The standard protocol includes introducing the animals to the behavior room for twenty minutes prior to the start of training. Animals are placed behind a divider in the room blocking any view of the apparatus. Soft music is playing in the room to block extraneous noise.

The apparatus itself consisted of a dual-chambered shuttle box with an electrifiable wire grid floor hooked to a scrambler. One chamber was masked with black tape and kept very dark, while the other was lit by an overhead lamp. The two chambers were divided by a guillotine door. The grid floor in the dark chamber was set to deliver a footshock of 0.8 mA for 25 seconds.

Animals were trained over the course of one week with one training session per day, which included three separate trials divided by a one-minute inter-trial interval. Animals were placed in the dark side of the chamber facing away from the door. Following a 4-5 second delay, the footshock was applied. This typically induced a rapid exit to the light side of the chamber in which no shock was applied. Time to escape the chamber was recorded for each trial and avoidances were noted, with an avoidance being defined as exiting the chamber before the footshock begins. After approximately 4 training sessions a probe session took place 24 hours after the final training session. During this probe session, the animals were placed in the dark side of the chamber for 30 seconds; however, no footshock was applied. The latency to escape was measured.

Contextual Fear Conditioning (CFC) as an Assessment of Spatial Memory

Rationale

Pavlovian conditioning is the elicitation of a response via a CS, such as a tone, by pairing the tone with an US such as a footshock over several sessions, and is the basis for many rodent-based behavioral paradigms. The response is typically an innate behavior such as freezing, in the case of rodents, when faced with a perceived danger, a natural defense mechanism to avoid being seen by a predator (Bolles, 1970). In the absence of a CS, it is possible to induce such freezing behavior in specific contexts when paired with an US. Under these conditions, two brain regions are believed to play a role in triggering this behavior, namely the amygdala and the hippocampus. Lesions to the amygdala seem to completely block freezing behavior in both a cued environment where a CS is present as well as a contextual environment where a CS is not present, indicating the amygdale as being critical in the formation of US associated memory (Phillips and LeDoux, 1992), whereas hippocampal lesions only interfere with contextual-elicited freezing (R. J. Blanchard and D. C. Blanchard, 1969; D. C. Blanchard and R. J. Blanchard, 1972; S. Maren and M. S. Fanselow, 1997) suggesting that both regions are involved in fear conditioning, but the hippocampus appears preferential to conditioning involving the recollection of the environment in which an aversive event took place. Furthermore, hippocampal lesions made one day after training also block contextual fear conditioned responses, while leaving tone-elicited freezing intact (Kim and Fanselow, 1992; Maren and Fanselow, 1997).

Given the role the hippocampus plays in contextual fear conditioning, researchers have used this particular paradigm to assess hippocampal dependent cognitive deficits in various animal models of AD. These models typically show impairment on this task (Corcoran et al., 2002; Dineley et al., 2002; Comery et al., 2005; Jiang et al., 2008).

CFC General Protocol

Figure 2.1 outlines the sequence for the general CFC protocol used in experiments described below. Animals were first introduced into an environment that will be referred to as the contextual environment in which the animal eventually receives an unpleasant shock. The contextual environment is defined as one half of a two-chamber shuttle box

with a wire-grid electrifiable floor. The door to the other side of the chamber was closed. Three of the walls of the contextual environment were covered by aluminum and a large and prominent black and white cue was placed on the back wall of the chamber. The front wall, facing the observers, was partially visible to allow for visual scoring of behavior. A lamp was placed directly overhead a clear Plexiglas door and the room lights were off. The chamber was wiped clean with ethanol between each animal.

The animal is placed in the contextual environment and monitored for 2 min to determine the baseline behavior (Figure 2.1). Following baseline observation, the animal is exposed to an audible conditioned stimulus (CS) for twenty-two seconds. During the final two seconds of the CS, the animal receives a 2-second footshock, the unconditioned stimulus (US). This sequence is then repeated once so that the animal receives only two footshocks in the contextual environment during the whole training component of the CFC paradigm.

Twenty-four hours after the CS/UCS pairing, the animal is placed back into the contextual environment and observed for 5 minutes by two observers. Freezing behavior is defined as the lack of any movement other than that associated with respiration. Approximately 1-2 hours after completion of behavioral observations within the contextual environment, the animals are placed in a novel environment that differed substantially from the contextual environment consisting of a cylindrical glass chamber with a metal bottom and lid. The chamber was washed with 4% acetic acid between animals to reduce olfactory cues.

Incidences of disagreement between the observers were removed from statistical consideration. Freezing behavior within the contextual environment was calculated by subtracting out the baseline behavior in the same environment (pre-UCS) from the freezing behavior observed 24 hours later post-UCS.

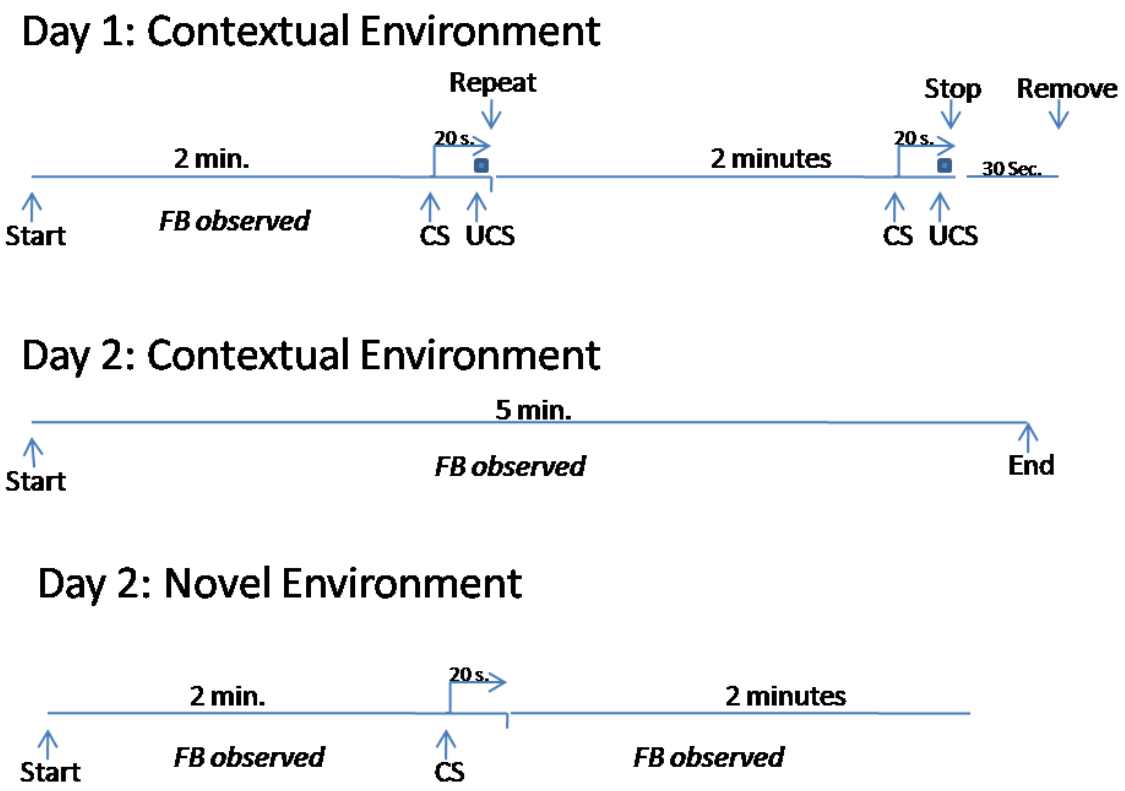

Figure 2.1: Schematic of contextual fear conditioning protocol. On day 1, the animals experiences two CS-UCS pairings within the contextual environment. Twenty-four hours later the animals is returned to the same contextual environment as is observed for freezing behavior for five minutes minus the CS. Later in the day, the mouse is placed in a novel environment and observed for freezing behavior befor and after the CS.

Long-Term Potentiation (LTP), Memory and the Aging Hippocampus

Rationale

LTP is considered an essential mechanism underlying learning and memory formation in the hippocampus and other brain regions. Age-related changes in LTP induction and maintenance are believed to contribute to a decrease in cognitive acuity. When synapses are repetitively stimulated, the communication between the neurons within those synapses is strengthened. This enhancement can last for hours to days. It was first reported by Lomo in 1966 who described a long-lasting potentiated response that could be evoked in the dentate gyrus if the perforant path leading to the dentate was

stimulated initially with several conditioning stimuli (Lynch, 2004). In initial reports it was referred to as frequency potentiation but is now known as long-term potentiation or LTP. LTP can thus be measured to determine synaptic plasticity and changes in the post-synaptic potential. LTP is most commonly measured in the hippocampus (Malenka and Nicoll, 1999), but can be elicited in other brain areas, as well. As mentioned, specific agents that block hippocampal LTP, impair the ability of animals to perform on the MWM suggesting that LTP may play a role in spatial memory.

LTP is also often induced in experimental settings with a stimulus rhythm called a theta burst, which mimics the frequency (~7 Hz) observed in animals during exploratory behavior (Bland et al., 1980; Larson et al., 1986). This theta frequency brain activity is thought to facilitate the formation of memories of the surrounding environs. It has also been found that interventions that improve LTP, improve memory and that a phenomenon much like LTP is observed after the acquisition of a novel experience (Geinisman et al., 1995).

Because LTP is implicated in learning and memory, researchers soon began examining whether LTP is affected by the aging process. Some of the first studies showed little effect of aging on LTP. Landfield and Lynch (1977) looked for impairments in LTP and found that potentiation in hippocampal slices from older animals was not different than that recorded in slices from young animals, despite impaired memory retention in the older animals (Landfield and Lynch, 1977). However, they did find that impairment did present itself in the inability of aged rats to develop latter processes of potentiation within the context of a biphasic pattern of potentiation (potentiation was induced, depressed and then potentiated a second time). Aged animals were less able to develop the second phase of this pattern and also showed more prominent exhaustion of the synapses after prolonged stimulation (Landfield et al., 1978). While recording LTP *in vivo*, Barnes later found that LTP decayed more quickly in the dentate gyrus, with the EPSPs in aged animals declining at a faster rate in the older compared to younger cohort even though the same level of potentiation was achieved as observed by Landfield and Lynch *in vitro* (1977). This faster decay was correlated with poorer spatial memory on the circle maze as well (Barnes, 1979), further providing support for a connection between sustained LTP and memory, and also suggesting that

memory retention or the lack thereof my be affected by increased rate of LTP decay. Differences in LTP in aged animals may, in fact, be due to their inability to maintain LTP over the long-term (Geinisman et al., 1995; Bach et al., 1999). This was reiterated in a study looking at aged mice in which hippocampal slices from older mice were not able to maintain late-LTP, which is cAMP-dependent, and these deficits were correlated with performance on the circular maze much like Barnes' aged rats (Barnes, 2003).

A few reports in the literature suggest that inducing LTP is harder in the aged brain. Aged rats seem to require more intense stimulation at the presynaptic neuron to induce LTP, in a sense making it more difficult to induce LTP (Landfield and Pitler, 1984; Moyer et al., 1992; Moyer and Disterhoft, 1994; Geinisman et al., 1995), which could be likened to speaking more loudly to a person hard of hearing. The age-associated deficits observed in LTP recordings may be due to calcium signaling, which is known to be dysregulated in aging animals (Landfield et al., 1989; Thibault et al., 1995; Campbell et al., 1996). Calcium plays a role in LTP induction and can be blocked with a calcium chelator (Lynch et al., 1983).

LTP General Protocol

There are a large number of protocols used to induce and record LTP in the hippocampus and include both *in vivo* and *in vitro* methods. The LTP measurements described here are all *in vitro* recordings done within sections of the hippocampus. Hippocampal slices are prepared as previously described (Thibault et al., 1995), but briefly, animals are deeply anesthetized with CO_2 and then quickly decapitated. The brains are rapidly removed and placed in ice-cold artificial cerebral spinal fluid (aCSF). The cerebellum is removed and the hemispheres are divided by a razor blade. Extraneous cortical tissue is typically kept for further analysis. The hippocampus is removed from the respective hemispheres that are kept cold with a frequent bath of ice-cold ACSF of the following constituents (in mM): 114 NaCl, 3 KCl, 10 Glucose, 1.25 KH_2PO_4, 26 $NaHCO_3$, 8 MgCl, and 0.1 Ca_2Cl. Hippocampal tissue is mounted and transversely sectioned in ice-cold ACSF by a Vibratome 3000 (TPI, Saint Louis, MO) to a thickness of 400 microns. Slices were then transferred to a recording chamber with wells containing oxygenated recording CSF (RCSF) containing (in mM): 114 NaCl, 3 KCl, 10

Glucose, 1.25 KH_2PO_4, 26 $NaHCO_3$, 2.5 Ca_2Cl and 1.3 MgCl. RCSF was kept at 32° C with O_2 perfusion of the closed interface chamber throughout the two-hour acclimation and recording periods.

A twisted, bipolar, Teflon-coated stainless steel stimulating electrode was placed perpendicular to the slice in the Schaeffer collaterals. A sharp glass recording electrode (3-15 MΩ) was pulled from borosilicate glass capillaries (World Precision Instruments, Sarasota, FL), using a P80 pipette puller (Sutter Instruments, Novato, CA), is filled with ACSF and positioned in the stratum radiatum as shown in Figure 2.2.

Data was acquired using Clampex Software and analyzed using Clampfit 10.2 (Molecular Devices). Current outputs (I/O) were recorded during stepwise increases in voltage at the stimulating electrode separated by 10-second intervals. The stimulation intensity needed to elicit a fEPSP (field EPSP) that was 50% of the maximum uncontaminated fEPSP was noted and utilized throughout.

Baseline fEPSPs were subsequently recorded for 60 sweeps every 20 seconds for 20 minutes using the same stimulation intensity determined by the I/O and used in PPF. LTP was induced with a single 1-second 100 Hz tetanus in murine slices and with a theta burst stimulation consisting of 10 pulses of 4 bursts each at 100 Hz every 200 ms for 2 seconds in rat hippocampal preps. fEPSPs were recorded for 30 minutes post-LTP induction with the same parameters used during baseline for a total of 90 sweeps every 20 seconds. The I/O and PPF protocols were then repeated.

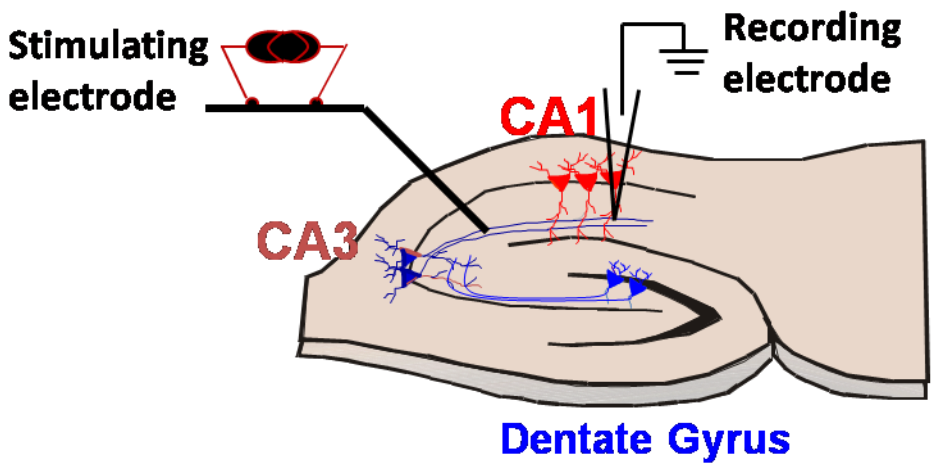

Figure 2.2: Electrode placement within the hippocampal slice preparation. The twisted, bipolar stimulating electrode is placed within the Schaffer collateral axons running from the CA3 region to the CA1 region of the hippocampus. The recording electrode is placed in the stratum radiatum among the apical dendrites of the CA1 pyramidal neurons where it records the field excitatory post-synaptic potentials.

Afterhyperpolarization (AHP) and the Aging Hippocampus

Rationale

The AHP is a post-synaptic property of neuronal membranes that occurs following a burst of action potential. The effect of the AHP is to decrease the ability of incoming stimuli to depolarize the membrane to threshold potential. The amplitude and duration of afterhyperpolarizations induced in the CA1 region of the hippocampus are increased in aged animals and is attributed to a dysregulation in Ca^{2+} (Landfield and Pitler, 1984; Landfield et al., 1989; Campbell et al., 1996). An increase in its size would make the membrane less excitable, or at least less efficient in its capacity to fire as readily as a young neuron. Some forms of hippocampal-dependent learning are impaired in aged animals, and the AHP is associated with cognitive processes, specifically hippocampal-dependent eye-blink conditioning (Disterhoft et al., 1986; Moyer et al., 1990; Power et al., 1997). Larger AHPs are found F344 rats that are impaired in the MWM (Tombaugh et al., 2005). Given this, measuring the AHP within the CA1 region of the hippocampus has become a standard electrophysiological measure and biomarker of brain aging as well as age-related neurodegenerative diseases such as AD (Disterhoft and Oh, 2006).

AHP General Protocol

AHP measurements were graciously done my Mr. Tristano Pancani, a graduate student under the mentorship of Dr. Olivier Thibault. Hippocampal slices were prepared in the same manner described above for LTP recordings. Briefly, animals were anesthetized in CO_2 chamber prior to decapitation, hippocampi removed and transversally sliced using a Vibratome to obtain 350 μm thick slices in ice cold low-calcium artificial cerebrospinal fluid (ACSF) containing (in mM): 128 NaCl, 1.25 KH_2PO_4, 10 Glucose, 26 $NaHCO_3$, 3 KCl, 0.1 $CaCl_2$, 2 $MgCl_2$. Slices were then transferred in an interface-type chamber and maintained in oxygenated (95% O_2, 5% CO_2) high-calcium ACSF containing 2mM $CaCl_2$, at 32^oC for at least 2hrs to allow recovery of the tissue. At the time of the experiment each hippocampal slice was placed in a recording chamber (RC22C, Warner Instruments, Co., Hamden, CT) maintaining a continuous flow of oxygenated ACSF pre-heated at 32°C using a TC2Bip/HPRE2 in line heating system (Cell Micro Controls, Northfolk, VA). This setup was mounted in a Nikon E660E inverted microscope. Cells were impaled with a sharp microelectrode (tip resistance~110 ± 24 MΩ), filled with 2M $KMeSO_4$ and 10mM HEPES pH 7.4. All experiments were performed in current clamp mode with bridge balance compensation and capacitance neutralization. Signals were digitized at 2 kHz and low-pass filtered at 1 kHz. Recordings of membrane input resistance (IR) were obtained approximately 5 min after impalement measuring the steady hyperpolarization obtained injecting 200 pA hyperpolarizing current with an Axoclamp 2B amplifier (Axon instruments) for 800 ms while holding the cell at -70mV. To generate an afterhyperpolarization (AHP) cells were held at -65 mV (baseline) and depolarized with a 100 ms current pulse in order to generate three Na^+ action potentials (APs) delivered through the intracellular electrode. AHPs were elicited every 30s and at least 6 AHPs were averaged per each cell. Medium AHP (mAHP) represents the peak hyperpolarization reached after the end of the depolarizing stimulus, slow AHP (sAHP) represents the hyperpolarization 800 ms after the end of the stimulus and the AHP duration was measured from the end of the depolarizing step until return to baseline. Neurons with input resistance < 50MΩ, holding current > 500pA and AP height < 0mV, were excluded from in this study. Data were acquired using pClamp 8.0 (Axon Instruments) software through a Digidata 1320A, A/D

converter (Axon Instrument) while mAHP, sAHP as well as duration of AHPs were calculated using Calmpfit software (Axon Instruments).

Microarray Analysis of Hippocampal Tissue

Rationale, Strengths and Pitfalls

Microarray technology is a very powerful tool for studying complex processes at the gene level. A single chip allows the researcher to explore the intricacies of gene expression in very specific ways. The experiments described below utilize this technology in the context of chronic drug treatment, and gene expression analysis is performed on tissue taken from the hippocampal region of the brain. This type of analysis has been used successfully before in experiments assessing gene expression patterns combined with behavioral correlates (Blalock et al., 2003; Rowe et al., 2007; Kadish et al., 2009). These types of studies allow one to assess gene expression patterns that are unique to different stages of the aging hippocampus (Blalock et al., 2005), and thus allow one to determine whether or not certain drug interventions are able to affect such patterns, and potentially ameliorate those deficits associated with said patterns. Yet there are some disadvantages of this technology cannot be ignored. The GeneChips used here have the capability to detect over 35,000 genes and, thus, an exceptionally large number of genes must be detected as being significantly changed in order for the data set to be meaningful. This in return means that the dataset produced is potentially unwieldy in its magnitude. Analysis of the data can be cumbersome and time-consuming. This forces the researcher to narrow their focus on certain expression patterns that help explain other collected data or mine the data to better answer the question at hand. The strength is that the data can also be used to create more hypotheses driven research that will better elucidate the results observed as well as give a much broader and realistic view of how complex and interconnected signaling pathways truly are.

General Protocol

Using the same techniques used to prepare hippocampal slices for electrophysiological recording described above, the hippocampus is removed and processed as described previously (Blalock et al., 2003; Rowe et al., 2007; Kadish et al., 2009). Briefly, RNA is extracted from hippocampal tissue with Trizol and is precipitated

with ethanol, reconstituted in RNAse-free water, and quantified and checked for RNA integrity with an Agilent 2100 bioanalyzer. RNA was processed to generate biotin-labeled cRNA following the standard protocol in the Affymetrix expression analysis technical manual, of which 20 µg of labeled-cRNA was then applied to a full genome rat (230v2.0) or mouse (430v2.0) GeneChip (Affymetrix) for hybridization (one chip per animal). Scanned microarray images were analyzed using the Microarray Suite 5.0 (MAS5; Affymetrix) algorithm. I have tried to ensure that the number of animals used for each experiment exceeds a minimum of eight per group with the exception of the pilot study described in chapter five. This allows for more relevant representation of the expression pattern seen in the animals when exposed to a given treatment.

Statistical methods used are similar to those previously described (Blalock et al., 2003). Data are prepared for analysis with extensive outlier removal techniques to remove repeats as well as unannotated genes along with filtering by presence and absence calls as well as probe set grade. Genes determined to be present and annotated and meeting pre-determined criteria were analyzed for significant differences with a one-way or two-way ANOVA depending on the specific experimental design. The statistics used for a given experiment will be discussed in more detail in their respective chapters.

DAVID (Database for Annotation, Visualization, and Integrated Discovery) functional analysis was completed on genes that were found to be significantly modulated. Gene accession numbers were uploaded into DAVID (http://david.abcc.ncifcrf.gov/), web-based software to determine functional pathways that are overrepresented by the gene list provided (Dennis et al. 2003). The functional pathways are listed in table format with pathway description, number of genes found representing the pathway, and the EASE score (p-value). The EASE score is a modified Fisher exact p-value and describes the enrichment of the pathway and the likelihood of finding said number of genes given the number of genes associated with a pathway as well as the number of genes detected with the GeneChip.

ELISA for the Assessment of Amyloid Beta (Aβ) Levels

Rationale

In order to determine the levels of detergent-soluble and insoluble levels of Aβ in the cortices of the transgenic models used in these studies, a well characterized serial extraction method was used to extract Aβ from the tissue. Subsequently, the total amount of Aβ in the respective fractions was measured using a two-site sandwich ELISA (Murphy et al., 2007).

Soluble Aβ Extraction

The materials used for these assays were graciously provided by Dr. M. Paul Murphy and Ms. Tina Beckett kindly assisted. Frozen cortical tissue was first placed in either RIPA buffer (50 mM Tris-HCL, 150 mM NaCl, 1% Triton X-100, 0.5% Deoxycholate, 0.1% SDS) or SDS (2% SDS in water alone) with a 1X complete protease inhibitor to create a concentration of 0.1mg/uL and then homogenized with a polytron. Five hundred microliters of the homogenate was then aliquoted to a microcentrifuge tubes and centrifugated at 100,000xg for one hour. The supernatant was collected and the remaining pellet was reserved at -80° C for formic acid extraction.

Insoluble Aβ Extraction

Reserved pellets from the previous extraction were sonicated in 70% formic acid (FA) and centrifugated at 100,000xg for 1 hour. The supernatant was stored at -80° C until later use. Upon thawing the FA samples were neutralized by 1:20 dilution in TP buffer (1M Tris base, 0.5 M Na_2HPO_4).

Assay

All samples were diluted for sandwich ELISA in AC buffer [0.02 M sodium phosphate buffer (pH 7.0), 0.4 M NaCl, 2 mM EDTA, 0.4% Block Ace (Serotec), 0.2% BSA, 0.05% CHAPS, and 0.05% NaN_3]. Sandwich ELISAs for total Aβ levels for both the detergent soluble fraction along with the FA soluble fraction utilized capture antibody Ab9 (human Aβ1-16) and detection antibody 4G8 (human Aβ17-24). In short, 384-well plates were coated with capture antibody in PBS overnight at 4°C. Plates were then washed with 1X PBS and blocked with SYNBLOCK (Serotec) for two hours at room temperature (RT) after which the plate was allowed to dry. Standards and samples were

then loaded into the well in duplicates or triplicates and incubated overnight at 4°C. Plates were then washed with 1X PBST (PBS + Tween 20) followed by 1X PBS. Biotinylated 4G8 (4G8-BIO) was added and allowed to incubate for 4 hours at RT. The 4G8-BIO was detected with neutravidin-HRP incubated at RT for two hours. The plate was developed with TMB developing solution and stopped with 6% o-phosphoric acid and read with a Vector plate reader. Data were then corrected for dilution factors and is presented as either fmol or pmol per milligram of tissue.

Tissue Histology

Various histological methods were used throughout. These include staining for neutral lipids (oil red O), collagen (Gomori trichrome), and amyloid beta (WO2 ab). These methods are described briefly here.

Oil Red O

This particular stain of lipids was developed decades ago (McVean et al., 1965), but is still used to detect lipids within frozen tissue, and specifically as way to detect lipid accumulation in the liver (Fiorini et al., 2004). This stain is considered an efficient method by which to assess the extent of steatosis induced by chronic treatment with an LXR agonist.

Flash frozen livers were sectioned (10 μm) on glass slides and stored at -80°C. At a later time, the tissue was thawed and allowed to air dry for 30 minutes, fixed in ice-cold 10% formalin for 5 minutes and washed three times in distilled water.

Sections were stained with oil red O stain via two different vehicles. Certain sections were placed in 100% propylene glycol, stained in 5% oil red O stain in 100% propylene glycol (Sigma Aldrich) for 8 minutes at 60°C, and subsequently placed in 85% propylene glycol. Slides were rinsed in distilled water and counterstained with hematoxylin and subsequently mounted with an aqueous mounting media.

Other sections were stained with oil red O stain that had been prepared in 100% isopropyl alcohol and the sections were processed with the MicroProbe System (Fisher Scientific). This allowed for more intense staining as well as improved the efficiency of the staining process. In short, the liver sections were first thawed and washed twice with PBS. The tissue was fixed in 10% formalin for 15 minutes at room temperature (RT) and subsequently rinsed with 60% isopropyl alcohol. The sections were then stained with oil

red O for 30 minutes at RT. Sections were again rinsed with 60% isopropyl alcohol twice, washed twice with distilled water and counterstained with hematoxylin for 30 seconds, after which the slides were rinsed again with distilled water and mounted with a warmed glycerol gelatin.

Aß Pathology

Aβ pathology was visualized in the CA1 region of the hippocampus with immunohistochemistry (IHC) utilizing the monoclonal WO2 antibody that binds the N-terminal (human Aβ2-8) region of human Aβ and is used to detect all forms of human Aβ (Miles et al., 2008). Such studies provide information on the total Aβ load within specific regions of the brain. Given that the deposition of is a key pathological hallmark of AD, changes in total Aβ load allow for the assessment of potential benefits of therapeutic interventions.

The actual histology was done by a collaborator, Dr. Inga Kadish, at the University of Alabama, Birmingham, and her methods are referenced here (Wang et al., 2003; van Groen and Kadish, 2005). Depending on the study, rats or mice were deeply anesthetized with intraperitoneal pentobarbital and intracardial perfusion performed with ice cold saline. The brains were removed and placed in cold 4% paraformaldehyde for at least two hours or overnight and then transferred to a 30% sucrose solution for 24 hours or until they sank to the bottom of the container in which they were stored. The brains were then placed in an antifreeze solution (15% sucrose, 30% ethylene glycol) and kept at -20°C. Frozen brains were shipped to the University of Alabama and sectioned on a freezing microtome to a thickness of 35 microns and stained with WO2 and detected with biotinylated goat anti-mouse and later visualized with ExtrAvidin and Ni-enhanced DAB.

The Aβ densities were measured as described (J. Wang et al., 2003; T. van Groen and I. Kadish, 2005). A photomicrograph of the CA1 region of the hippocampus was digitized with a digital camera and converted to grayscale using Paintshop Pro 7. The area of the CA1 region that was stained by WO2 was measured in several sections of the region using the ScionImage (NIH) program. The data are presented as mean densities from the measured sections within a single section.

Chapter 3: Effects of TO901317, an LXR Agonist, in a Triple Transgenic Mouse Model of AD

Introduction

There is good reason to consider the roles that lipids, especially cholesterol, play in the brain. The brain contains nearly 25% of the entire cholesterol pool within the body, while only making up 2% of the total body weight. Most, if not all of this cholesterol is made *de novo* (Dietschy and Turley, 2001) and its turnover is thought to be very slow, most of which is attributed to its catabolism by Cyp46 to 24-OH-Chol, which readily diffuses out of the brain (Bjorkhem et al., 1997). Cholesterol efflux to Apolipoprotein E (ApoE) may also plays a role in the transport of cholesterol out of the brain (Wahrle et al., 2004). Dysregulation in cholesterol metabolism, specifically during aging, could potentially have a negative effect on neuronal function.

Much more attention has been turned to the role of lipid metabolism in the brain given that epidemiological data suggests that lipid-lowering drugs may confer some benefit in lowering one's risk of acquiring AD (Jick et al., 2000; Wolozin, 2004; Wolozin et al., 2004; Rea et al., 2005; Sparks et al., 2006; Wolozin et al., 2006; Arvanitakis et al., 2008; Haag et al., 2009). Hypercholesterolemia is correlated with an increased risk of presenting with AD-related pathology (Kuo et al., 1998; Pappolla et al., 2003) and increased dietary cholesterol leads to an increase in amyloid-β (Aβ) levels in specific breeds of rabbits and transgenic mouse models (Refolo et al., 2000; Sparks et al., 2000). Cholesterol levels within the plasma membranes are thought to influence Aβ processing, with higher cholesterol levels leading to increased production (Xiong et al., 2008) and lower cholesterol levels leading to a reduced rates of amyloidogenic processing (Bodovitz and Klein, 1996; Simons et al., 1998; Kojro et al., 2001) perhaps due to modulations in γ-secretase activity within cholesterol enriched microdomains (Wahrle et al., 2002). A major risk factor for AD is carrying the ApoE ε4 allele which leads to the production of an ApoE isoform that is not as efficient in binding and transporting Aβ (Corder et al., 1993; Strittmatter et al., 1993; LaDu et al., 1994; LaDu et al., 1995). Cholesterol is also thought to accumulate around senile plaques found in the brains of human AD patients as well as transgenic mouse models (Mori et al., 2001) and therefore

may play a role in AD pathology itself. These plaques are often associated with ApoE as well (Huang, 2006), which may be playing a role to remove both cholesterol and Aβ.

Microarray data obtained from studies in aged rats show that expression levels of certain genes intimately involved in cholesterol metabolism change around mid-age (approximately 12 months of age). These include LXR itself and as well as some of its target genes, including SREBP and ApoE (Rowe et al., 2007; Kadish et al., 2009). Currently there is not a clear understanding as to why such an upregulation in this pathway is occurring. One could argue that such an upregulation is a compensatory measure to deal with changes in lipid dynamics. Alternatively, such an upregulation could be contributing to correlated cognitive decline. Understanding the role LXRs are playing in this capacity could be key in elucidating the more complex role overall cholesterol metabolism may be playing in AD.

LXRs themselves are nuclear receptors that bind to endogenous oxysterols (cholesterol metabolites), (Janowski et al., 1996) including 24(S)-OH-Chol, the major brain cholesterol metabolite, which, perhaps coincidentally, are elevated in the plasma of AD patients (Lutjohann et al., 1996; Lutjohann et al., 2000; Papassotiropoulos et al., 2000; Lutjohann and von Bergmann, 2003). Upon LXR activation, key proteins involved in cholesterol metabolism and transport including ApoE and several ATP binding cassettes such as ABCA1 (Teboul et al., 1995; Schultz et al., 2000; Zhang et al., 2001; Cao et al., 2002; Whitney et al., 2002; Liang et al., 2004; Ulven et al., 2004; Zelcer and Tontonoz, 2006) are upregulated. The LXR gene target ABCA1, specifically, is involved in cholesterol efflux trough the lipidation of apolipoproteins (Lawn et al., 1999) and is thought to be essential in the lipidation of ApoE, considered by some to be integral in the efflux of amyloid-β (Aβ) (Hirsch-Reinshagen et al., 2004; Hirsch-Reinshagen et al., 2005; Wahrle et al., 2005).

LXR activation has been shown to reduce Aβ processing and/or levels in both *in vitro* and *in vivo* models, along with associated cognitive deficits (Sun et al., 2003; Koldamova et al., 2005; Burns et al., 2006; Riddell et al., 2007; Zelcer et al., 2007). The mechanism behind this reduction in Aβ as well as the improvement in cognition is not well understood, but has been attributed to its ability to increase ApoE and ABCA1,

which in turn increases efflux of both cholesterol and Aβ (Pfrieger, 2003b; Hirsch-Reinshagen et al., 2004; Wahrle et al., 2005; Abildayeva et al., 2006; Bjorkhem, 2006).

Taking into consideration the role that LXR appears to play in AD etiology and pathology, we tested the hypothesis that chronically activating LXR with a potent agonist, TO901317, can attenuate some of the deleterious pathologies and associated cognitive decline in a unique mouse model of AD that presents with both pathological hallmarks of the disease, plaques and tangles, the triple transgenic model (3xTg) of AD (APP_{SWE}, PS1M146V, and Tau_{P301L}). Pathology in this model progresses with the development of intracellular accumulation of Aβ, subsequent aggregation in extracellular plaques, and eventual appearance of tangles. It has been shown that the temporal progression of said pathologies correlates with a mirrored decline in the cognitive abilities of these animals (Billings et al., 2005; Oddo et al., 2006).

Materials and Methods

Animals

Experiments were conducted in compliance with the institutional guidelines of the Animal Care and Use Committee at the University of Kentucky. Ten month-old female triple transgenic mice expressing APP_{SWE}, PS1M146V, and Tau_{P301L} (3xTg-AD) were maintained in a 10 hour dark and 14 hour light cycle in groups of three or four. Animal weights and food consumption were recorded every Monday, Wednesday and Friday throughout the study. Food consumption was determined from the difference in the amount of food remaining in a respective cage following its earlier allotment divided by the number of days between feedings and the number of animals in the cage. This was considered an approximated average daily food intake per animal per day.

Medicated Diets

Two different diets were created and formulated using the AIN-93G purified diet from Harlan Teklad as the base diet. The mice were divided into treatment groups and fed the following diets: control diet (CON) consisting of the AIN-93G only (n=15) or TO901317 diet (TO9) formulated at 400 mg of active compound per kilogram of chow (n=13). The intended dose of T09 for the study was 50 mg/kg body weight, but the calculated dose, based on average food consumption for the treatment groups was

approximately 33 mg/kg body weight and was determined using the daily average food intake, the concentration of drug in the diet, and the average weight of the mice in the group.

One-way Active Avoidance

The one-way active avoidance paradigm, a hippocampal-dependent memory task (Olton and Isaacson, 1968a; Munoz and Grossman, 1981), was used to assess cognitive ability of the mice. Mice were trained in a dual chambered, light/dark, one-way active-avoidance box with an electrifiable wire-grid bottom (Med Associates, VT). Mice were acclimated to the dimly lit training room for twenty minutes with soft music playing to mask sounds in the room before each session. On day one, the mice were acclimated to the box for a total of 120 seconds during which time they roamed freely. Baseline activity was recorded, including time spent in each chamber to determine chamber preference.

Mice were then trained on the task with three trials per session for a total of four sessions over three days. During a single trial the mice were introduced to the dark side of the box and given 4 seconds to exit to the benign, lighted side before a 0.8 mA, 25-second foot shock was introduced. A guillotine door between the chambers was dropped upon proper exit. Time to exit was recorded. The mouse was removed from the light chamber and immediately placed in a holding cage for one minute until subsequent trials. Day one of training consisted of one morning session. Day two of training consisted of a morning and an afternoon session and day 4 consisted of one morning session. Chamber preference is presented as time (seconds) spent in one of two chamber choices over a two-minute interval and compared across the groups with a 2-way ANOVA. Training data is presented as mean number of avoidance/animal/session. Count data was first transformed by taking its square root and then averaged across treatment groups. Mean transformed counts were compared with a repeated measure two-way ANOVA.

Blood Collection and Tissue Isolation

Eight of the mice from each treatment group were anesthetized with an intraperitoneal (i.p.) injection of phenobarbital at a dose of 100 mg/kg and transcardially perfused with 0.9% PBS. Blood was collected via cardiac puncture from the right ventricle immediately prior to perfusion. Mice were then decapitated via guillotine. Brains were removed, and bisected with one hemisphere flash frozen in liquid nitrogen

and reserved for immunoassays. The hearts and livers were also harvested. Hearts were weighed and normalized to body weight (mg/g). Hearts and livers were flash frozen in liquid nitrogen.

Serum Analysis

Collected blood was centrifugated at 3,000 rpm for 10 minutes in BD Microtainer Tubes to separate out plasma. Plasma was aliquoted into centrifuge tubes and stored at -20°C until analysis. Serum samples were analyzed by the Comparative Pathology Laboratory at the University of California, Davis by a Roche COBAS Mira Plus Chemistry Analyzer. Values were averaged across the groups and compared with a one-way ANOVA.

Liver Histology

To determine the extent of lipid accumulation in the liver of drug treated mice, oil red O staining was used. Flash frozen livers were sectioned (10 μm) on glass slides and stored at -80°C. At a later time, the tissue was thawed and allowed to air dry for 30 minutes, fixed in ice-cold 10% formalin for 5 minutes and then washed three times in distilled water. Sections were placed in 100% propylene glycol and then stained in filtered 5% oil red o stain in propylene glycol (Sigma Aldrich) for 8 minutes at 60°C, and subsequently placed in 85% propylene glycol. Slides were rinsed in distilled water and counterstained with hematoxylin.

Microarrays

Hippocampi were microdissected from one hemisphere (n=8/group) and placed in tubes on dry ice with RNA subsequently extracted using TRIzol reagent and precipitated with ethanol, reconstituted in RNAase-free water, and quantified and checked for RNA integrity with Agilent 2100 bioanalyzer RNA was then hybridized to an Affymetrix GeneChip Mouse Genome 430v2 array. Scanned microarray images were analyzed using the MicroarraySuite 5.0 (MAS5; Affymetrix) algorithm. Probe set annotations were downloaded from Affymetrix. Data were analyzed with a one-way ANOVA. Genes with $p<0.05$ were compared with a t-test. Data were further analyzed through the use of the Ingenuity Pathway Analysis (Ingenuity® Systems, www.ingenuity.com).

DAVID (Database for Annotation, Visualization, and Integrated Discovery) functional analysis was completed on genes that were found to be significantly modulated. Gene accession numbers were uploaded into DAVID (http://david.abcc.ncifcrf.gov/), web-based software to determine functional pathways that are overrepresented by the gene list provided (Dennis et al. 2003). The functional pathways are listed in table format with pathway description, number of genes found representing the pathway, and the EASE score (p-value). The EASE score is a modified Fisher exact p-value and describes the enrichment of the pathway and the likelihood of finding said number of genes given the number of genes associated with a pathway as well as the number of genes detected with the genechip.

CA1 Aβ Load

Eight brain hemispheres of mice from each of the treatment groups were removed after saline perfusion, flash frozen and later thawed and placed in 4% paraformaldehyde for two hours at which point the hemispheres were placed in a 30% sucrose solution for 24 hours and then placed in an antifreeze solution (15% sucrose, 30% ethylene glycol) until sectioning. Brains were sectioned 35 microns thick on a freezing microtome and immunohistochemically stained with WO2 that recognizes the Aβ peptide (Miles et al., 2008). Amyloid beta densities were measured as previously described (van Groen and Kadish, 2005).

Soluble and Insoluble Aβ Levels

Fifty to one hundred milligrams of tissue from 7-8 cortices of mice from each treatment group were placed in enough (radio-immunoprecipitation assay) (RIPA) buffer to create equal concentrations of 0.1 mg/uL of tissue. Tissue was then homogenized by a polytron set at medium speed. Five hundred microliters of the homogenate was aliquoted to microcentrifuge tubes and centrifuged at 100,000 x g for one hour. The supernatant was collected and the remaining pellet was reserved for formic acid (FA) extraction.

The pellet was sonicated in 70% FA for 30 second at 0.5 second pulses. The homogenate was then centrifugated at 100,000 g for one hour. The aqueous layer was collected and stored at -80°C until further use.

RIPA and FA samples were thawed on ice and vortexed well to mix. FA samples were neutralized with 1:20 dilution in TPB. Sandwich ELISA was conducted using Ab9

and 4G8 antibodies and detected with neutravidin-HRP and read with a Victor plate reader. Data are presented as the log transformation of fmol/mg tissue.

Correlation Between Hippocampal Aβ load and Cortical Aβ Levels in TO9-treated Animals

Mean densities of Aβ staining within the CA1 region of the hippocampus were plotted along with either the soluble or insoluble cortical Aβ levels from the same mice. Regression analysis was completed. A line was fitted to the plotted data and the R-squared value and p-value were generated. Further correlation analysis was completed to obtain the Pearson r value. Data are presented with the best-fit line along with its 95% confidence band.

Slice Preparation and Extracellular Recording

Five to seven mice (n=7 Control, n=5 T0901317) from each treatment group were anesthetized in a CO2 filled chamber before rapid decapitation. Brains were quickly removed and placed in a bath of oxygenated artificial cerebral spinal fluid (ACSF) of the following constituents (in mM): 114 NaCl, 3 KCl, 10 Glucose, 1.25 KH_2PO_4, 26 $NaHCO_3$, 8 MgCl, and 0.1 Ca_2Cl. Hippocampi were transversely sectioned with a Vibratome 3000 yielding 350 μm slices. Slices were transferred to a recording chamber wells containing oxygenated recording CSF (RCSF) of the following constituents (in mM): 114 NaCl, 3 KCl, 10 Glucose, 1.25 KH_2PO_4, 26 $NaHCO_3$, 2.5 Ca_2Cl and 1.3 MgCl. RCSF was kept at 32° C with O_2 perfusion of the closed interface chamber throughout the two-hour acclimation and recording periods.

A twisted, bipolar Teflon coated stainless steel stimulating electrode was placed perpendicular to the slice in the Schaeffer collaterals, while the sharp glass recording electrode (3-15 MΩ) was positioned in the stratum radiatum. The slice was stimulated manually, approximately once every 20 seconds for ten minutes with 0.1 volts to acclimate the slice. Current outputs (I/O) were recorded during stepwise increases in voltage at the stimulating electrode to determine maximum output. Baseline fEPSPs were recorded for 20 minutes with voltage needed empirically determined to elicit 50% of the maximum output as determined by I/O. LTP was induced with a 1.0 second train of 100 Hz. fEPSPs were recorded for 30 minutes post-LTP induction with the same parameters used during baseline.

Statistical Note

All results are represented as the mean + SEM. The one-way ANOVA was used throughout this study, except where noted due to the nature of the original experimental design which included a third treatment group (which received the anti-diabetes drug, pioglitazone). The data collected from this subset of animals are not included in this description as it did not test specifically the hypothesis of interest for this dissertation. The data from all three groups are to be presented together in a manuscript designed for publication. (In its entirety, the study was designed with the three treatment groups (control, TO9, pioglitazone), and was an attempt to take advantage of a one-time opportunity to test key hypotheses and questions related to AD in a limited number of 3xTg animals made available to us.)

Results

Body Weights and Food Consumption

At the end of three months of treatment, the average percent change in body weights between the control and TO9-treated groups were significantly different as determined by a 2-way repeated measure ANOVA (mean percent change: CON +20.46 % ± 6.06 % ; TO9: -1.34% ± 4.29%). Thus, over the course of the study, only the control vehicle-treated animals gained weight while the TO9-treated mice essentially maintained their initial weights. Despite the lack of change in body weight in the TO9-treated animals, there was no significant difference in food consumption over the course of the study between groups (mean grams of food/mouse/day: CON 2.79 ± 0.54; TO9 2.48 ± 0.3).

Active Avoidance

Each mouse was given 120 seconds to freely explore the dark and light chambers of the active-avoidance shuttle box (Figure 3.1A). Both groups showed a significant preference for the dark side of the chamber [mean time (seconds): Dark 72.4 ± 2.3, Light 47.8 ± 2.3; 2-way ANOVA; $p<0.0001$; $F_{(2,76)}= 54.83$]. However, there was no significant difference between groups with respect to the mean time spent in the dark chamber [mean time (seconds): CON: 74.4 ± 4.5; TO9: 74.1 ± 5.5] (Figure 3.1A), nor in the mean number of crossings from light to dark (CON: 7.6 ± 0.9; TO9: 4.4 ± 1.3) or in the mean

time (seconds) to first crossing (CON: 20.9 ± 5.6; TO9: 9.3 ± 2.8) indicating no differences in chamber preference.

The animals were trained over a course of four sessions over three days, with three trials per session, to avoid an impending footshock in the dark side of the chamber. The number of avoidances during a session was recorded for each animal. The number of times the mouse avoided (the count) was transformed by taking the square root of the count and averaging the transformed data across the group to allow for statistical analysis with a 2-way ANOVA. There was an overall effect of time on learning in the AA paradigm (Figure 3.1B) as well as a trend toward an effect of TO9 on learning as measured by the mean number of times the TO9-treated mice actively avoided the dark chamber over the four training sessions (2-way repeated measures ANOVA; $p = 0.0832$; $F_{(3,75)}=3.256$).

A.

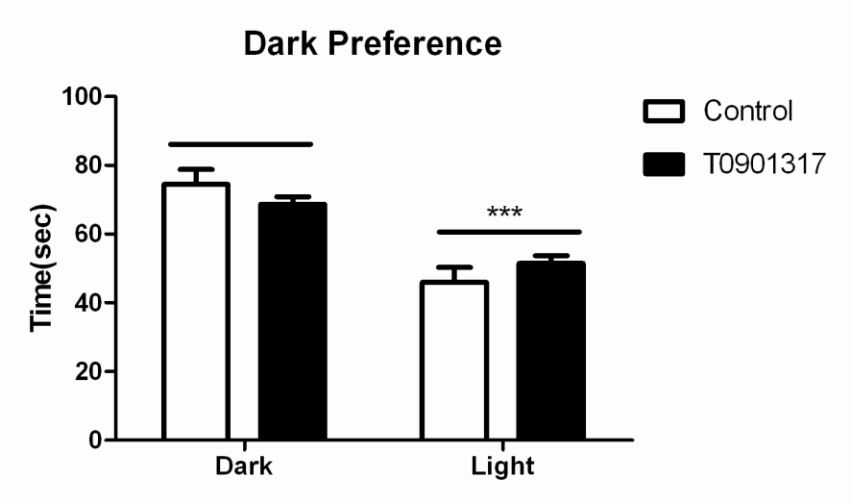

B.

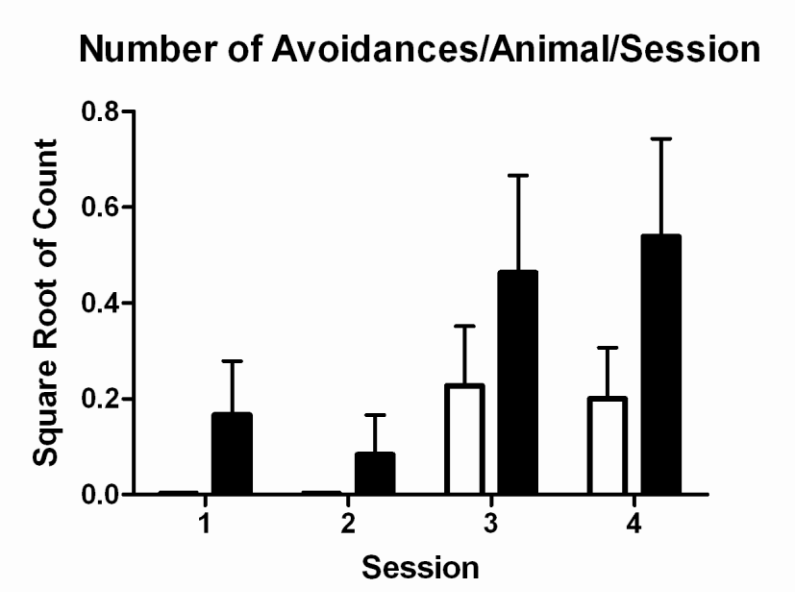

Figure 3.1: Learning and memory assessment in 3xTg-AD mice treated for three months with TO901317 using one-way active avoidance: A. There was a significant difference in the preference for the dark side of the chamber for both groups [CON (n=15) & TO9 (n=11);*** $p<0.0001$; $F_{(2,76)}= 54.83$; 2-way ANOVA], but there was no significant difference between the level of preference between groups. **B.** Treatment with TO9 (n=11) showed a trend toward increased learning ability across the training sessions as compared to controls (n=15) [repeated measures 2-way ANOVA; $F_{(3,75)}=3.256$; $p=0.0832$].

Long-term potentiation

Baseline fEPSPs were recorded within the CA1 region of the hippocampus for twenty minutes prior to LTP induction from 1-3 slices taken from 3 TO9- treated animals and 5 control animals. There was no significant difference in the mean amplitudes of the fEPSPs across all treatment groups [mean amplitudes (mV): CON 1.46 ± 0.16; TO9 1.18 ± 0.19; one-way ANOVA]. LTP was induced with a single 1-second train at 100 Hz within the CA1 region of the hippocampus. CON and TO9 animals showed no significant change in the slope of the fEPSP during the first three minutes following the induction [post-tetanic potentiation (PTP)] of LTP. Neither group maintained LTP over the course of the 30 minute after induction and TO9-treated animals actually dropped below baseline levels and had significantly lower fEPSP slopes than the control group (% baseline fEPSP slope.: CON 98.78 ± 3.44 & TO9 88.02 ± 1.13; by one-way ANOVA and Newman-Keuls *post-hoc* ($p<0.05$).

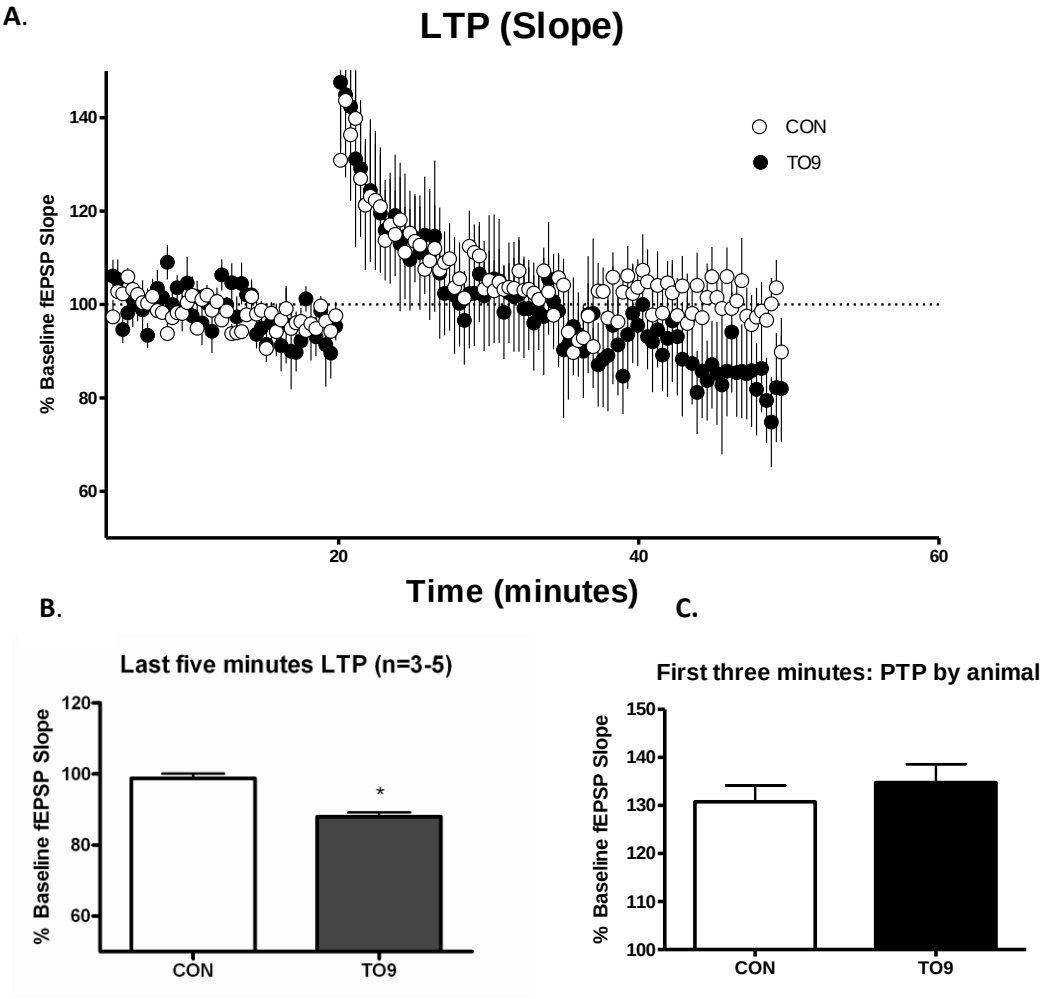

Figure 3.2:Long-term potentiation recorded from the CA1 region of the hippocampus of 3xTg-AD mice treated for three months with TO91317. A. Neither CON-treated (n=5) or TO9-treated animals (n=3) were able to sustain LTP for thirty minutes after a 1 second, 100 Hz tetanus stimulation. **B.** There was not a significant difference in the induction of LTP (post-tetanic potentiation (PTP) between the groups). **C.** During the last five minutes of recording post-tetanus, TO9-treated mice showed a significant reduction in the slopes of the fEPSP as compared to CON, with TO9 animals actually dropping below the mean baseline (one-way ANOVA; Newman-Keuls post

Heart Weights

The hearts of the animals were weighed upon removal from the chest cavity. Hearts were visibly larger in the TO9-treated mice. Because of the difference in body weight between groups, heart weight was normalized to body weight. TO9 caused a significant increase in heart weight (mg heart weight/g body weight: CON 3.24 ± 0.17; TO9 5.67 ± 0.19; one-way ANOVA, and Tukey *post-hoc; $p<0.05$*).

Liver Histology

Qualitative analysis of oil-red O staining in the livers of the 3xTg-AD mice demonstrated heavy lipid staining in the livers of TO9-treated mice, indicative of steatosis of the liver. Figure 3.3B and C show representative histological liver sections stained with oil-red O. TO9 treatment resulted in large red-stained vacuoles which were largely absent in the livers of the control vehicle-treated mice.

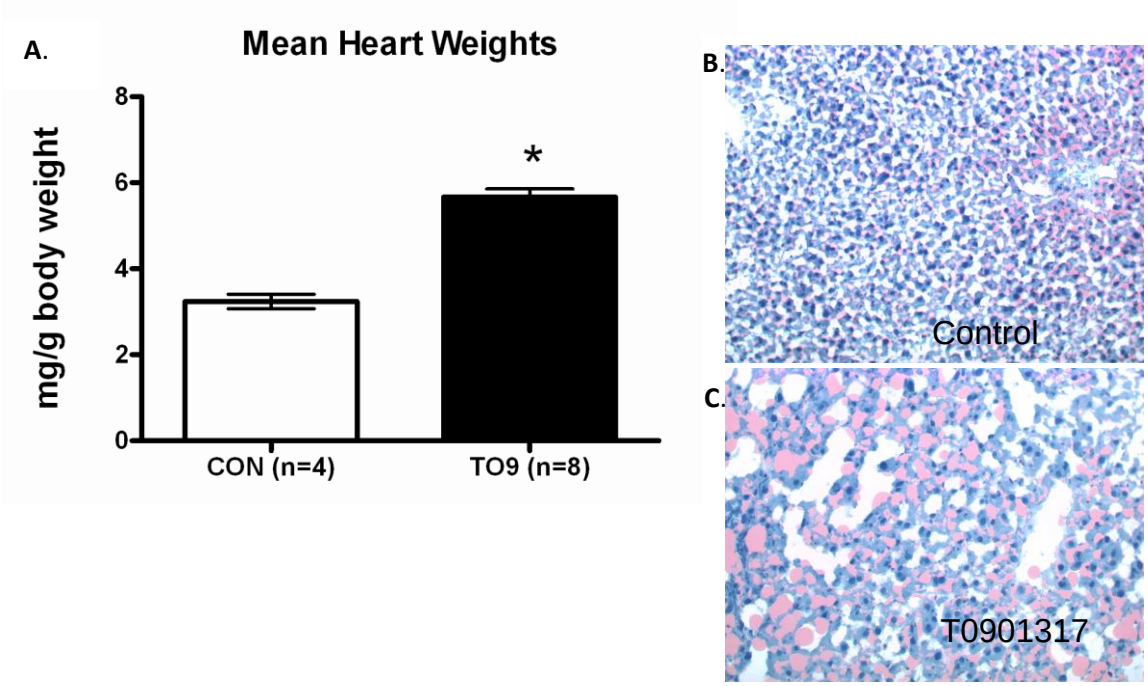

Figure 3.3: Assessment of potential cardiotoxicity and hepatotoxicity. A. TO9 significantly increased the heart weights of mice after three months of treatment (one-way ANOVA, Tukey *post hoc* *p<0.05). **B & C.** Representative liver images of oil-red-O staining of liver tissue. TO9-treated mice (C) appeared to have larger, more lipid-laden livers as compared to CON livers (B) as determined with oil red O stain.

Serum Analysis

A full chemistry panel was completed on the serum from animals of both treatment groups (Tables 3.1 and 3.2). Three of ten serum markers measured showed significant deviations between treatments. TO9-treated animals had significant increases in calcium, glucose and uric acid as compared to CON vehicle-treated groups. The combination of elevated calcium along with uric acid in humans has been found to be associated with the formation of kidney stones and may be a sign of hypertension (Tisler et al., 2002). The elevated glucose suggests that the TO9 treatment likely exacerbated a pre-existing hyperglycemia in these mice.

Table 3.1: Blood serum analysis of organ function in 3xTg-AD mice treated with control vehicle or TO9 for three months: Values are reported as mean values ± S.E. Values indicated with an asterisk were found to be significantly different by a one-way ANOVA and Student Newman-Keuls *post-hoc*;**p<0.01, *p<0.05. Serum marker abbreviations: BUN: blood/urea nitrogen: ALT: alanine transaminase: CK: creatinine kinase.

	Ca2+ ion homeostasis	BUN kidney function	ALT liver function	CK muscle function	Uric Acid kidney function
	mg/dL	**mg/dL**	**U/L**	**U/L**	**mg/dL**
CON ***(n=15)***	9.26 ± 0.39	26.43 ± 4.29	93.07 ± 27.95	799.4 ± 192.73	1.74 ± 0.24
TO9 ***(n=11)***	****10.88 ± 0.41**	23 ± 1.95	98.18 ± 12.2	1289 ± 295.71	***3.625 ± 0.80**

Table 3.2: Blood serum metabolic panel in 3xTg-AD mice treated with control or TO9 for three months. There was no significant difference in lipid levels between groups. TO9 did have significantly increased glucose levels. Values indicated with an asterisk were found to be significantly different. (one-way ANOVA; Sudent Newman-Keuls *post hoc*; **p<0.01).

	CHOL	HDL	LDL	TAG	GLUC
	mg/dL	**mg/dL**	**mg/dL**	**mg/dL**	**mg/dL**
CON (n=15)	113.9 ± 13.4	63.61 ± 7.9	11.31 ± 1.46	101.8 ± 19.4	167.4 ± 19.23
TO9 (n=11)	142.98 ± 4.95	70.92 ± 6.04	11.93 ± 1.28	99.47 ± 10.66	****316.56± 7.27**

Immunohistochemical Assessment of Aβ Load in the CA1 of the Hippocampus

WO-2 Staining of CA1: WO-2 staining (antibodies directed toward human Aβ2-8) revealed both intracellular and extracellular Aβ deposition in this model (Figure 3.4B and C). TO9-treated animals showed a significant reduction in the levels of Aβ in the CA1 region of the hippocampus. Average Aβ densities in control vehicle- and TO9- treated animals were 100.3 ± 3.19 and 80.25 ± 6.80, respectively; (one-way ANOVA and Tukey *post hoc*;p<0.05). Surprisingly, a reduction in Aβ within the CA1 region did not confer a positive effect on LTP, as determined also from measures within the CA1 from the contralateral hippocampus of the same animals.

Soluble and Insoluble Aβ in Cortical Tissue

Cortical tissue was saved and used to measure soluble and insoluble Aβ levels. Similar to the effects seen on Aβ load in the CA1, TO9 significantly reduced the levels of soluble Aβ in the RIPA-isolated fraction from homogenates of cortical tissue in 3xTg mice by ~28% (CON 0.943 ± 0.047; TO9 0.6745 ± 0.102; one-way ANOVA and Tukey *post-hoc*; p<0.05). Interestingly, there was no significant difference in insoluble levels between the groups, suggesting that the reduction in Aβ load observed by WO-2 staining (Figures 3.4A, B and C) likely reflects reduction in soluble, intracellular Aβ.

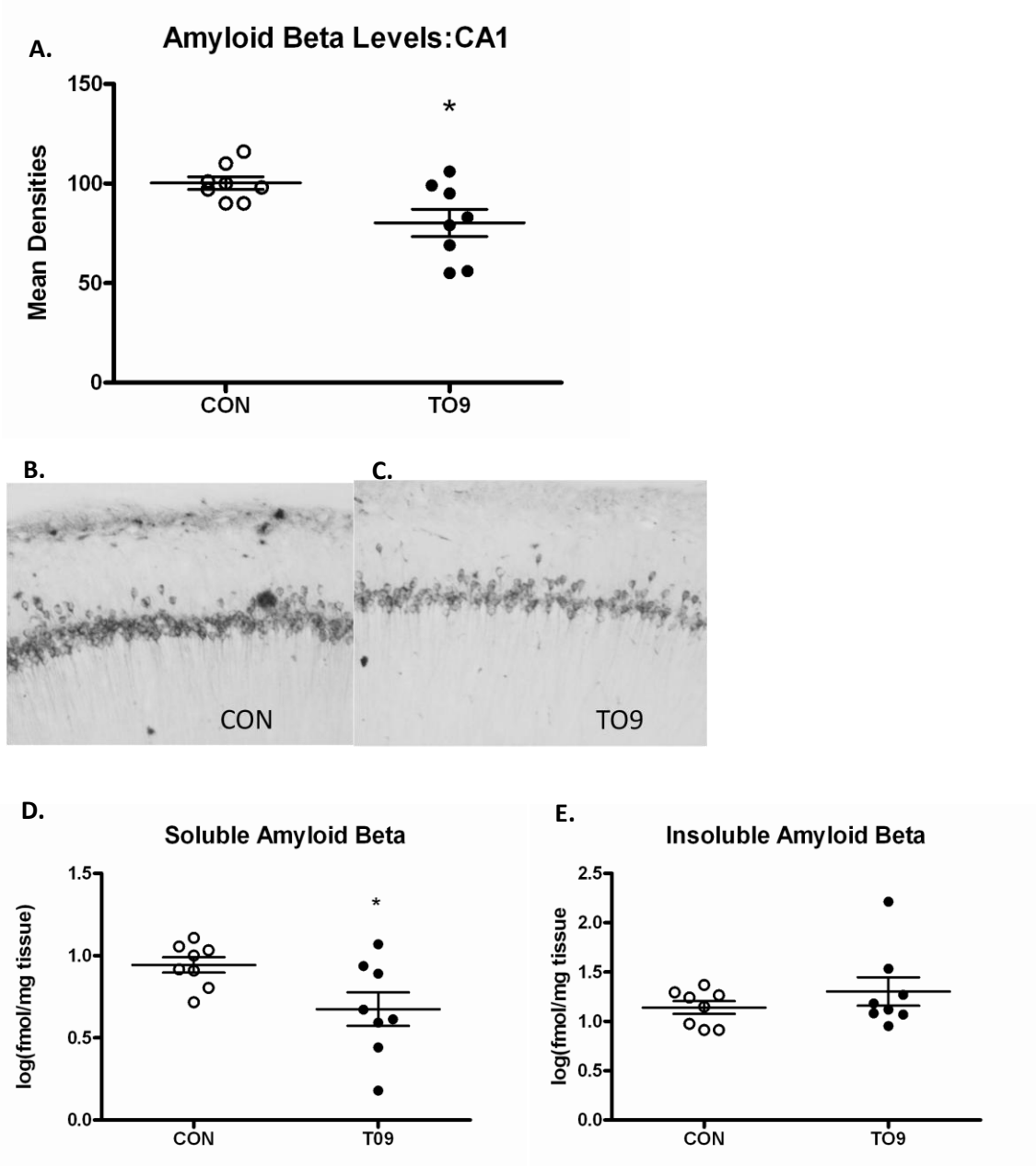

Figure 3.4: Comparison of Aβ levels in the hippocampus and cortex of TO9-treated 3xTg-AD mice. A. TO9 significantly reduced the WO2 staining in the CA1 region of the hippocampus as compared to controls: *n=8/group*, one-way ANOVA and Tukey *post-hoc;* * $p<0.05$. **B and C**. Representative photomicrographs showing WO-2 staining of the CA1 cell body layer. **D and E.** ELISA results indicate that TO9 significantly reduced soluble Aβ in the cortex (one-way ANOVA, Tukey *post-hoc* *$p<0.05$), but not insoluble levels.

Relationship between hippocampal Aβ load and cortical Aβ Levels

We further evaluated the relationship between WO-2 staining in the hippocampus and levels of soluble and insoluble Aβ in the cortex. As shown in Figure 3.4A, cortical levels of soluble Aβ levels were significantly correlated (Figure 3.5A) with Aβ density measures in the CA1 region of the respective TO9-treated mice where the slope of the regression line significantly deviated from zero and positively correlated (R^2=0.6496, F=11.12, Pearson r = 0.8060, $p<0.05$). There was a trend toward a positive correlation with the insoluble Aβ levels as well; however, this was not significant. (Figure 3.5B R^2=0.4824, F = 4.661, Pearson r = 0.6946, p=0.08).

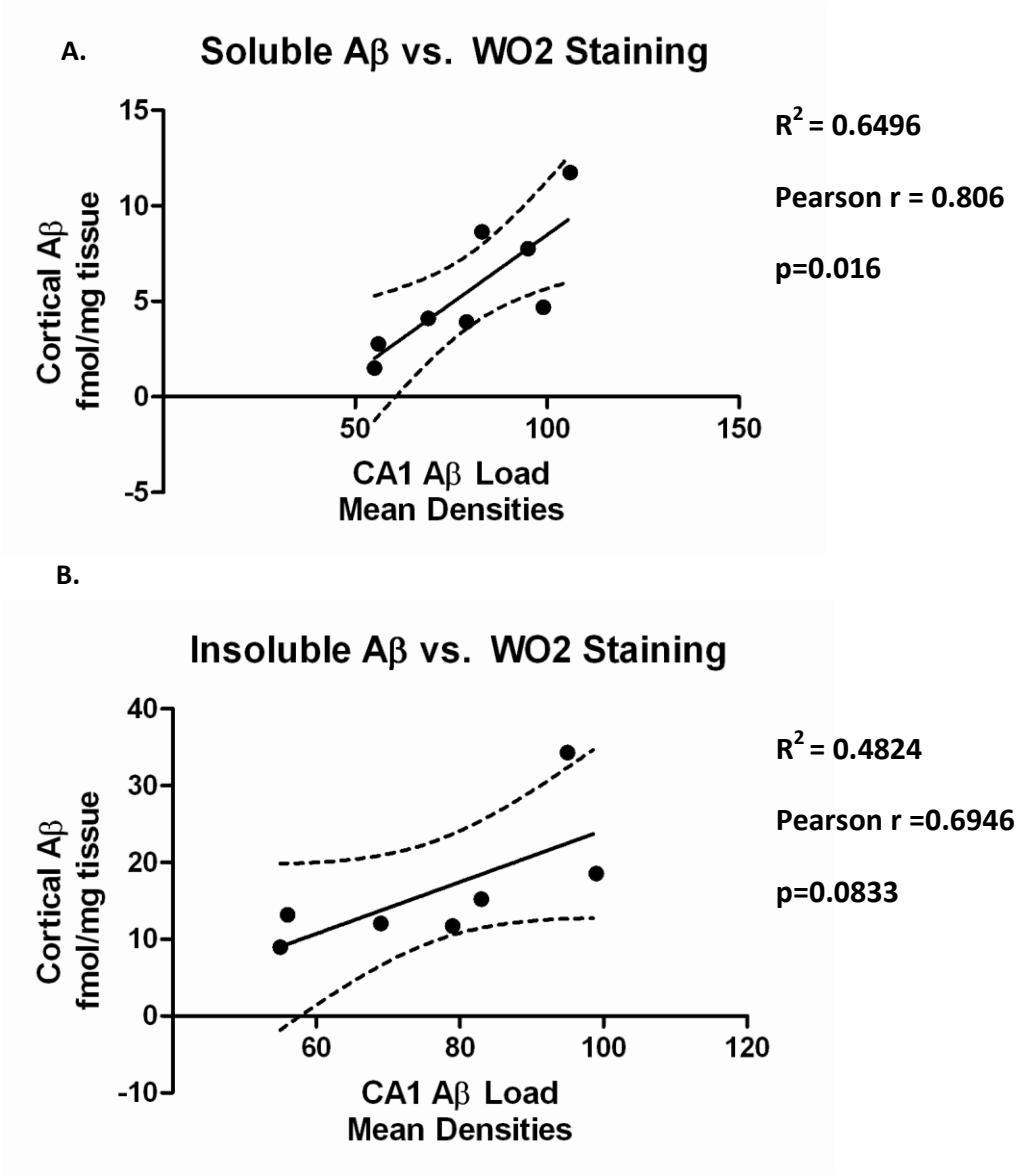

Figure 3.5: Relationship between WO2 detected Aβ load within the CA1 region of the hippocampi and ELISA detected soluble and insoluble Aβ levels in the cortices of 3xTg-AD mice treated with TO901317 (n=7-8). A. There was a significant positive correlation between Aβ load and soluble Aβ levels (R^2=0.6496, F=11.12, Pearson r = 0.8060, $p<0.05$). **B.** A nonsignificant trend toward a positive correlation between Aβ load and insoluble Aβ levels was observed (R^2=0.4824, F=4.661, Pearson r = 0.6946, p=0.08).

Microarray Analysis

TO9 treatment upregulated 1272 genes and downregulated 1403 genes as compared to controls (one-way ANOVA; t-test post-hoc). Lists of significantly modulated genes along with there p-values as determined by ANOVA were uploaded to Ingenuity Pathway web-based software for further analysis *(data not shown)*. Tables 3.3 and 3.4 list the top 20 genes most significantly upregulated or downregulated by TO9 treatment. The genes are organized in order of ascending p-value. Supplemental tables of all those genes can be found linked here: Supplemental Tables\3xtg-AD-TO_microarray_supplemental_table.pdf

DAVID functional analysis revealed a number of functional pathways overrepresented by genes that were found to be significantly modulated by three months of TO901317 treatment. These pathways are organized into two tables of upregulated and downregulated pathways. The functional pathways are listed in order of ascending p-value. Not all functional pathways are listed to avoid redundancy. Pathways were filtered by the number of represented molecules (5-35) and p-value (<0.05). Lists were further truncated by removing pathways subsumed by more extensively represented pathways within a given cluster.

Table 3.3: Top twenty genes with the lowest p-values significantly upregulated in the hippocampi of 3xTG-AD mice treated for 3 months with TO901317. Twenty genes found to be significantly upregulated in 3xTg-AD mice after three months of treatment with the LXR agonist TO901317 and organized in order of ascending p-value.

Symbol	Title
Rpl35a	ribosomal protein L35a
Mid1ip1	Mid1 interacting protein 1 (gastrulation specific G12-like (zebrafish)
Fasn	fatty acid synthase
Abca1	ATP-binding cassette, sub-family A (ABC1), member 1
Btf3l4	basic transcription factor 3-like 4
Scd2	stearoyl-Coenzyme A desaturase 2
Scd1	stearoyl-Coenzyme A desaturase 1
Apoe	apolipoprotein E
Srebf1	sterol regulatory element binding factor 1
Mfsd4	major facilitator superfamily domain containing 4
Abcg1	ATP-binding cassette, sub-family G (WHITE), member 1
Nipsnap1	4-nitrophenylphosphatase domain and non-neuronal SNAP25-like
Slc35b3	solute carrier family 35, member B3
Gpc5	glypican 5
Pnpt1	polyribonucleotide nucleotidyltransferase 1
Slc2a4	solute carrier family 2 (facilitated glucose transporter), member 4
Synpo2	synaptopodin 2
Reps1	RalBP1 associated Eps domain containing protein
Mfsd2	major facilitator superfamily domain containing 2
Mboat5	membrane bound O-acyltransferase domain containing 5

Table 3.4: Top twenty genes with the lowest p-values significantly downregulated in the hippocampi of 3xTG-AD mice treated for 3 months with TO901317. Twenty genes found to be significantly downregulated in 3xTg-AD mice after three months of treatment with the LXR agonist TO901317 and organized in order of ascending p-value.

Symbol	Title
Acn9	ACN9 homolog (S. cerevisiae)
Spred1	sprouty protein with EVH-1 domain 1, related sequence
Ddef1	development and differentiation enhancing
Setd7	SET domain containing (lysine methyltransferase) 7
Zmym1	zinc finger, MYM domain containing 1
Ascc3	activating signal cointegrator 1 complex subunit 3
Stard3	START domain containing 3
Dcamkl1	doublecortin and calcium/calmodulin-dependent protein kinase-like 1
Frmd5	FERM domain containing 5
Bxdc2	brix domain containing 2
EG622320	predicted gene, EG622320
Foxk2	forkhead box K2
Mrps15	mitochondrial ribosomal protein S15
Trfp	Trf (TATA binding protein-related factor)-proximal protein homolog (Drosophila)
Nfya	nuclear transcription factor-Y alpha
Mrp63	mitochondrial ribosomal protein 63
Stat1	signal transducer and activator of transcription 1
Tns1	tensin 1
Tnfrsf25	tumor necrosis factor receptor superfamily, member 25
Tloc1	translocation protein 1

Table 3.5: DAVID functional analysis of genes significantly upregulated in hippocampi of 3xTG-AD mice treated for 3 months with TO901317. Functional pathways are listed in order of ascending p-value.

Functional Pathways Upregulated	#	p-value
Protein Biosynthesis *(Genes encoding ribosomal proteins and eukaryotic translation initiation factors)*	33	2.83E-07
Oxidative Phosphorylation *(Various isoforms of ATP synthase, Cytochrome c oxidase, ATPase, NADH dehydrogenase, Succinate dehydrogenase)*	28	4.68E-04
mTOR Signaling Pathway *(Pyruvate dehydrogenase kinase, Protein phosphatase 2, Regulatory subunit)*	8	0.0025
Signaling Pathway-G-Protein Families *(Mitogen activated protein kinase kinase 1, Calmodulin 1, Guanine nucleotide binding protein, Alpha q polypeptide, Protein kinase, Mitogen activated kinase 3)*	8	0.0052
Ubiquitin *(Ubiquitin-like protein 5, ubiquitin-like 5, Ubiquitin C, Ubiquitin B)*	10	0.0153
Proteasome *(Proteasome (prosome, macropain) subunit, alpha type 3, Proteasome (prosome, macropain) 26S subunit, ATPase 2, Proteasome (prosome, macropain) subunit, beta type 3)*	12	0.0167
Regulation of Growth *(Angiotensinogen (serpin peptidase inhibitor, clade A, member 8), Insulin-like growth factor-binding protein 5 precursor, Mitochondrial glycerol-3-phosphate acyltransferase)*	19	0.0183
Protein Targeting *(Solute carrier family 1 (glial high affinity glutamate transporter), Member 3, Malonyl-CoA decarboxylase, Erbb2 interacting protein)*	30	0.0192
Secretory Pathway *(SNAP-associated protein, RAB3A, member RAS oncogene family, ERGIC and golgi 3, Myosin heavy chain 10, non-muscle,synaptotagmin-like 3, Synapsin II)*	29	0.0203
Fatty Acid Biosynthesis *(Fatty acid synthase, Stearoyl-Coenzyme A desaturase 1, Stearoyl-Coenzyme A desaturase 2, Protein kinase, AMP-activated, gamma 1 non-catalytic subunit, Fatty acid desaturase 1)*	10	0.0351
Copper Binding Protein *(Amyloid beta (A4) precursor protein, Cytochrome c oxidase, Subunit XVII assembly protein homolog (yeast), Amyloid beta (A4) precursor-like protein 1, Superoxide dismutase 1, Soluble)*	9	0.0351
Acyltransferase Activity *(Fatty acid synthase, Nuclear receptor coactivator 1, CREB binding protein, Acetyl-Coenzyme A acetyltransferase 1, Diacylglycerol O-acyltransferase 2, Mitochondrial glycerol-3-phosphate acyltransferase)*	21	0.0404
Transmission of Nerve Impulse/Cell-Cell Signaling *(Apolipoprotein E, Synaptic vesicle glycoprotein 2 a, Monoamine oxidase A, Neurotrophin 3, Acetylcholinesterase, Glutamate receptor, ionotropic, AMPA2 (alpha 2), Myelin basic protein, Synaptophysin)*	29	0.0489

Table 3.6: DAVID functional analysis of genes significantly downregulated in hippocampi of 3xTG-AD mice treated for 3 months with TO901317. Functional pathways are listed in order of ascending p-value.

Downregulated	#	P-value
Steroid metabolism *(Lecithin-cholesterol acyltransferase, Sterol O-acyltransferase 1, 7-dehydrocholesterol reductase, 24-dehydrocholesterol reductase, **c**ytochrome P450, family 51, 3-hydroxy-3-methylglutaryl-Coenzyme A synthase 1)*	21	0.002488
Protein transporter activity *(Synaptosomal-associated protein 23, Sortilin 1, Syntaxin 4A (placental), Syntaxin-11, Synaptosomal-associated protein)*	27	0.002689
Membrane lipid metabolism *(Phospholipase A2, group IVA (cytosolic, calcium-dependent), UDP galactosyltransferase 8A, Phospholipase C, delta 4, Phospholipase A2, activating protein)*	22	0.003244
Regulation of Wnt receptor signaling pathway *(Axin1, Axin2, Dickkopf homolog 3 (Xenopus laevis))*	6	0.006246
Toll-like receptor signaling pathway *(Phosphatidylinositol 3-kinase catalytic delta polypeptide, Toll-like receptor 2, mitogen-activated protein kinase 11, Phosphatidylinositol 3- kinase, regulatory subunit, polypeptide 1 (p85 alpha), Toll-like receptor 3 , Phosphatidylinositol 3-kinase, catalytic, alpha polypeptide)*	13	0.012962
Cadherin-like *(Mulitple protocadherins: beta 3 and alpha 2, 3, 4, 5, 8)*	15	0.016753
Intramolecular oxidoreductase activity *(Prostaglandin E synthase 3 (cytosolic), Isopentenyl-diphosphate delta isomerase)*	9	0.018979
Unfolded protein binding *(Heat shock protein 1B, Calnexin, Calreticulin, dnaj(hsp40) homolog, suppression of tumorigenicity 13, chaperonin subunit 4)*	23	0.04002
I-kappaB kinase/NF-kappaB cascade (*traf family member associated nf-kappa b activator, interleukin-1 receptor associated kinase 2, smad nuclear interacting protein 1)*	7	0.043463

Discussion

The present study explored the effects of a three month chronic treatment with a potent LXR agonist in the 3xTg model of Alzheimer's disease. We hypothesized that TO901317 would improve cognition and reduce hallmark AD pathologies in the 3xTg-AD mouse model based on its ability to alter cholesterol metabolism and studies showing that LXR agonists may have positive effects in other murine models of AD (Sun et al., 2003; Koldamova et al., 2005; Jiang et al., 2008).

Effects on Behavior and LTP. In our behavioral analyses, we found that there was a nonsignificant trend toward improved performance during the learning phase of the active avoidance paradigm, during which TO-treated 3xTg mice appeared to perform better than controls over four training sessions (Figure 3.1). This trend, however, was not observed during the probe session when memory was assessed, and there were no detectable differences between the treatment groups *(data not shown).*

Consistent with a previous report, we also found that LTP was severely impaired in 3xTg-AD mice, as demonstrated by the amount of LTP recorded from control slices (Oddo et al., 2003). TO901317 treatment had no effect during the first 20-25 minutes of post-tetanus recording of LTP. However, during the final phase of recording, slices from TO901317 treated mice were unable to sustain LTP, and actually dropped below baseline (Figure 3.2). Thus, treatment with the LXR agonist appeared to exacerbate the deficits already present in LTP. The microarray results provide some support for the notion that LTP may be modulated by the LXR agonist in such a way that would have been detrimental to maintaining LTP. For example, one of the strongest downregulated gene pathways as identified by the DAVID functional analysis (Huang da et al., 2009) was the category of *protein transporter activity*, which includes numerous proteins involved in promoting the exocytosis of synaptic vesicles mediating neurotransmitter release. *Membrane lipid metabolism*, and specifically the expression of phospholipase C (PLC), was downregulated; this reduction could, in turn, reduce IP3 signaling and the release of Ca2+ from the endoplasmic reticulum store and inhibit synaptic activity. The gene coding for the mGluR4 subtype of glutamate receptors was reduced with LXR and mGluR4 knockout mice are characterized by synaptic deficits (Pekhletski et al., 1996). Additional genes involved in LTP and shown to be modulated by LXR activation in the

present study include calcineurin, PKA and CREB. Calcineurin gene expression was increased and the constitutive activation of calcineurin has been linked to LTP deficits (Mansuy et al., 1998). Finally, the expression of PKA and CREB, two of the most important positive regulators of LTP, was reduced by LXR treatment (Lee and Silva, 2009).

Effects on Amyloid. Findings consistent with published effects of LXR activation include the reduction in Aβ (Koldamova et al., 2005; Jiang et al., 2008). TO was able to significantly reduce Aβ load within the CA1 region of the hippocampus as measured by IHC, as well as significantly reduce the levels of soluble Aβ in cortical tissue from these animals (Figure 3.4). While there may have been a trend ($p=0.08$) toward a reduction in the insoluble form of Aβ, this was nonsignificant. Most of the Aβ visualized with IHC staining with WO2 revealed intracellular deposition, which was reduced with TO treatment. Circumstantially one could conclude then that the intracellular Aβ was soluble Aβ given that the hippocampal Aβ load was significantly correlated with the soluble Aβ levels. A potential mechanism by which LXR agonist treatment reduced Aβ is by increasing the expression of the family of ABC transporters, which are ATP-dependent and responsible for causing efflux of a number of cellular constituents, including lipids and sterols. Such an effect on ABCA1 has been described following LXR agonist treatment both *in vitro* and *in vivo* (Koldamova et al., 2003; 2005). Alternatively, LXR may reduce Aβ by increasing the ApoE, which facilitates the clearance of soluble Aβ from the brain (Jiang et al., 2008). The microarray results in the present studies provide support for both of these mechanisms and show that the expression of both ABCA1 and ApoE were significantly increased in the hippocampus following chronic treatment with the LXR agonist. In fact, both of these were among the top 20 most significant genes found to be upregulated by treatment with the TO compound (Table 3.3). Furthermore, the microarray results confirmed and validated our method of incorporating the drug into the animals' food; these gene expression results indicate that sufficient concentrations of the drug were capable of reaching the brain and driving the expression of known LXR targets in the brain.

Peripheral Side Effects. Despite the potential benefits associated with a reduction in brain Aβ levels, serious peripheral side effects with chronic TO treatment were identified in the present study (Figure 3.3). The livers and hearts of TO-treated animals were significantly larger than control mice and an Ingenuity Pathway Analysis (IPA) of the microarray results, which can identify toxic pathways activated by treatments or conditions, corroborated our findings. In fact, the IPA analysis showed that some gene pathways targeted by the LXR agonist in the brain are associated with cardiac and liver toxicity in the periphery (e.g., cardiac and liver hypertrophy). Histology of the livers showed that the likely cause of the hypertrophied liver is a buildup of lipids in the liver. This could be due to the excessive upregulation of genes involved in lipogenesis driven by chronic LXR activation. For example, these genes are represented by the *fatty acid synthesis* and *acyltransferase activity* categories identified by the DAVID functional analysis (Table 3.5).

In addition, blood serum analyses revealed that uric acid and calcium levels were significantly different than controls, suggesting potential kidney dysfunction and ion dysregulation. Glucose levels were also significantly increased as compared to control indicative of hyperglycemia and potentially diabetes in these animals. This could be attributed to the steatite liver. While this is only speculation, a recent human study demonstrated that intrahepatic fat rather than visceral fat is more predictive of the symptoms of metabolic syndrome, including hyperglycemia (Fabbrini et al., 2009). Unlike previous studies done for shorter periods of time, lipid levels were not significantly changed, perhaps indicating a certain homeostasis after longer periods on the drug.

The results of this study opened up several more questions and issues, answers to which appeared to be critical in order to fully understand the role of the LXR pathway in the brain. The mouse model had a great deal of variation, especially in weights, suggesting that the strain is not well established and may have a significant level of divergence within it. The peripheral side effects also led to questions of appropriate dosage. The dose selected was based on a study in the literature which had used a dose of 50 mg/kg/day administered by gavage for 11 days (Koldamova et al., 2005). The present study was originally designed to deliver that dose, but over the course of the

study it was observed that the mice were not eating as much as anticipated; the calculated dose based on food consumption revealed an actual dose of 33mg/kg/day. The studies in the following chapters addressed the question of whether a lower dose could be found that could confer the positive effects of the drug without associated peripheral side effects.

Chapter 4: Assessing TO901317 dose effects on the periphery and LXR gene targets

Introduction

After treating 3xTg-AD mice with TO901317 (TO) for three months, additional studies were undertaken to determine whether lower doses could mitigate some of the side effects seen with treatment at the initial dose of 50 mg/kg/day (actual dosage calculated based on food ingestion was estimated to be ~33mg/kg/day). These side effects (discussed in Chapter 3) included increased heart weight, steatosis of the liver, hyperglycemia and reduced body weight as compared to control animals. Given our continued interest in the role LXR activity plays in AD, it was necessary to determine a dosage that would activate key target pathways without inducing side effects. There seemed to be benefits of the drug that included a reduction in AD pathology and a trend toward improved learning in the 3xTg AD model; these effects, if attainable, could potentially outweigh some of the side effects, especially if substantially minimized. Therefore, a study was initiated in which mice were treated with different doses of the LXR agonist TO901317 (TO9) for the same duration (3 months) and some of the same outcome measures were assessed as in the previous study.

Certain groups were also concomitantly treated with fish oil (FO), given evidence suggesting that FO, at higher doses, can protect against steatosis of the liver (Davidson, 2006). This has been shown to be the case in experiments involving the treatment of mice with induced hepatitis with purified eicospentaenoic acid, an omega-3 fatty acid constituent of fish oil. Such treatment suppresses the accumulation of fat within hepatic tissues, supposedly through the inhibition of SREBP, a transcription factor associated with the upregulation of genes directly involved in fatty acid synthesis (Kajikawa et al., 2009b, a).

Thus, the present study was undertaken to determine whether lower doses of the LXR agonist, TO901317, could potentially confer beneficial effects while reducing risk for peripheral side effects. As discussed above, some groups received concomitant treatment with FO as an alternative strategy to reduce residual risk associated with the TO compound. The results of this study proved to be quite helpful in determining doses that were later used in long-term treatment study in a double transgenic model (2xTg) of AD, which will be discussed in Chapter 5. The experiment also allowed us to

demonstrate that we could detect dose-dependent effects on gene expression with microarray technology in a very sensitive and quantitative way.

Materials and Methods

Animals and Diets

Twenty-eight 7 month old female B6129sv mice, a hybrid strain of the C57BL/6J strain and the 129/SvJ, considered to be the closest non-littermate controls to the 3xTg-AD mice, were used. Mice were maintained in a 10 hour dark and 14 hour light cycle in groups of three or four. Animal weights and food consumption were recorded every Monday, Wednesday and Friday throughout the study. Food consumption was determined from the difference in the amount of food remaining in a respective cage following its earlier allotment divided by the number of days between feedings and the number of animals in the cage. This was considered the approximated average daily food intake per animal per day.

Six different diets were created all within the context of the AIN-93G diet from Harlan Teklad. The animals were divided as evenly as possible by body weight and were given the following diets:

Table 4.1: Diet formulations for the respective treatment groups.

Treatment Group	n	Diet Formulation
Control	4	AIN-93G Diet (Harlan Teklad)
FO	4	10 mg/day Fish Oil (2:1 EPA:DHA)
5mg/kg TO9	5	5 mg/kg TO901317 per day
5mg/kg TO9 + FO	5	5 mg/kg TO901317 per day + 10 mg/day Fish Oil
20mg/kg TO9	5	20 mg/kg TO901317 per day + 10 mg/day Fish Oil
20mg/kg TO9 + FO	5	20 mg/kg TO901317 per day + 10 mg/day Fish Oil

TO9 was purchased from Cayman Chemicals (Ann Arbor, MI). Fish Oil was provided by Zone Labs (Boston, MA). Diets were manufactured by Harlan Teklad (Madison, WI) per the researcher's formulation. Mice were treated with the respective diets for 3 months.

Tissue Collection

All mice were anesthetized with CO2 and were subsequently decapitated via guillotine. Brains were bisected out, with one hemisphere flash frozen in liquid nitrogen and reserved for later assays; the other hemisphere was used for microarray analysis. The hearts and livers were harvested. Both were weighed and normalized to body weight (mg/g). Hearts and livers were then flash frozen in liquid nitrogen.

Liver Histology

To determine the extent of lipid accumulation in the liver of drug treated mice, oil red O staining was performed. Flash frozen livers were sectioned (10 μm) on glass slides and stored at -80°C. At a later time, the tissue was thawed and allowed to air dry for 30 minutes, fixed in ice-cold 10% formalin for 5 minutes and then washed three times in distilled water. Sections were placed in 100% propylene glycol, stained in 5% oil red O stain (Sigma Aldrich) for 8 minutes at 60°C, and subsequently placed in 85% propylene glycol. Slides were rinsed in distilled water and counterstained with hematoxylin.

Cardiac Histology: Flash frozen hearts were sectioned with a cryostat onto glass slides. Tissue was later fixed with acetone for 10 minutes and subsequently incubated with Bouin solution for 1 hour at 56°C. Sections were then rinsed with dH_2O until clear. Sections were stained with Weigert hematoxylin for 10 minutes and again rinsed with dH_2O followed by staining with Gomori Trichrome stain for 15 minutes. Sections were differentiated with Acetic acid for 2 minutes at RT and washed with serially with ethanol and dH_2O and then coverslipped with Permount (Fisher Scientific).

Microarrays

Microarray analysis was completed on three of the six treatment groups, control, 5 mg/kg TO9 and 20 mg/kg TO9. Hippocampi were microdissected from the remaining unfrozen hemispheres and placed on ice with RNA subsequently extracted using TRIzol reagent and precipitated with ethanol, reconstituted in RNAase-free water, and quantified and checked for RNA integrity with Agilent 2100 bioanalyzer RNA was then hybridized to an Affymetrix GeneChip Mouse Genome 430v2 array. Scanned microarray images were analyzed using the MicroarraySuite 5.0 (MAS5; Affymetrix) algorithm. Probe set annotations were downloaded from Affymetrix. Data were analyzed with a one-way ANOVA.

Results

Animal Weights and Food Consumption

The mean monthly weights of the respective treatment groups did not significantly differ over the course of the study *(data not shown)*. All groups significantly increased in weight over time, but there was no difference between groups in a given month (2-way ANOVA). There was also no difference in average food consumption over the course of the study. Food consumption data confirmed that the intended doses of TO9 were delivered.

Liver Pathology

TO9 treatment significantly increased liver weight in a dose-dependent manner. However, only the higher dose of 20 mg/kg/day resulted in a significant elevation with liver weight increasing by almost 3-fold (one way ANOVA; Tukey *post hoc*; $p<0.01$). Co-treatment with FO was not able to mitigate the increase in liver weight.

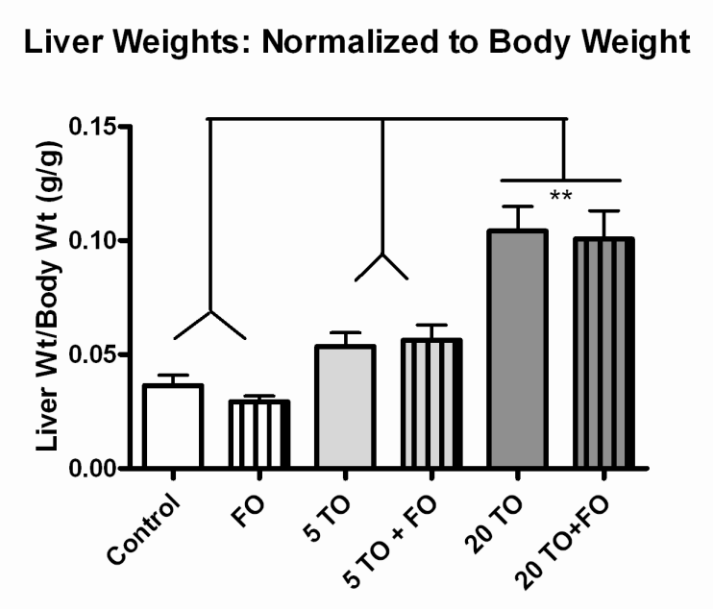

Figure 4.1: Liver weights of mice treated for three months with 5 or 20 mg/kg/day of either TO9 or the combination treatment of TO9 + FO (10mg/day). There was a significant difference in the weights of livers from the 20mg/kg TO9 & 20m/kg TO9+FO treated mice as compared to all other groups (one-way ANOVA; Tukey *post hoc* **$p<0.01$); *(n=4-5 group).*

Cardiac Pathology

Animals receiving the 20mg/kg daily dose of TO9 had significantly higher heart weights (Figure 4.2) but only compared to mice that received only FO. Tri-chrome staining of the hearts from mice in the 20 mg/kg TO9 and 20 mg/kg TO9 + FO groups showed the presence of collagen staining, indicative of cardiac fibrosis. The blue stained collagen is indicated with arrows in Figure 4.3B.

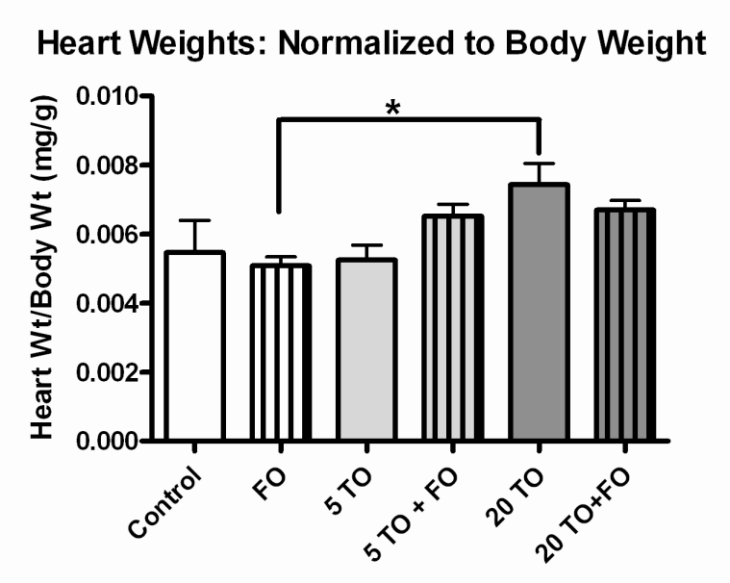

Figure 4.2: Heart weights of mice treated for three months with 5 or 20 mg/kg/day of either TO9 or the combination treatment of TO9 + FO (10mg/day). Heart weights were normalized to body weight. There was a significant difference in the heart weights of the 20mg/kg TO and the FO treated mice as compared to all other groups (one-way ANOVA, Tukey *post hoc* *$p<0.05$).

A.

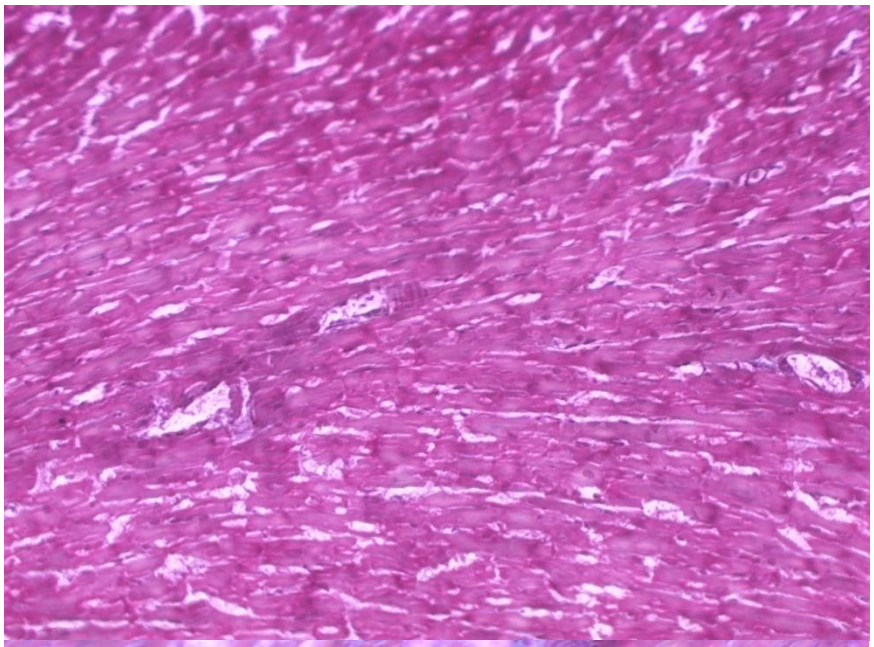

B.

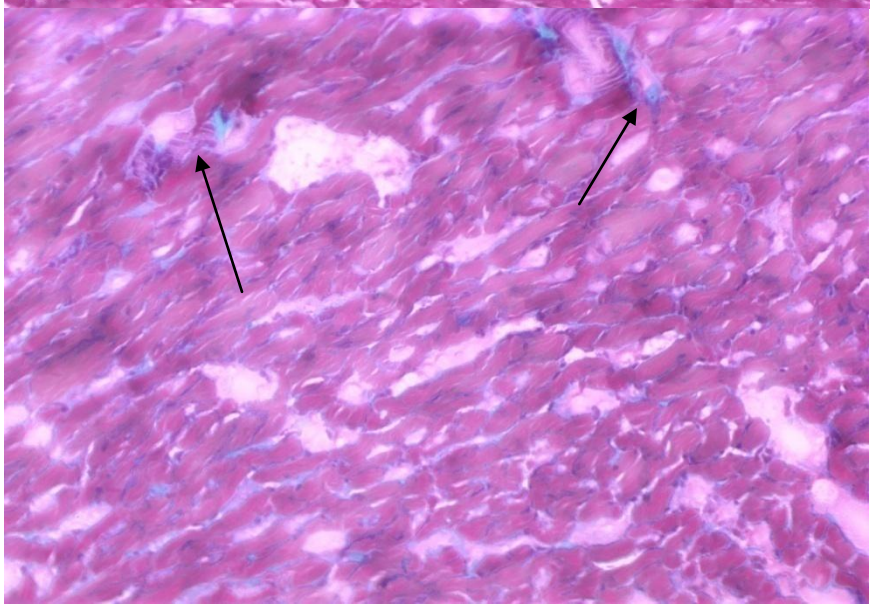

Figure 4.3: Gomori trichrome staining of cardiac tissue from mice treated with control or the 20 mg/kg TO diet. A. Representative image (20X) of cardiac tissue from a control mouse shows confluency of cardiomyocytes and lack of blue collagen staining. **B.** Representative image (20X) of cardiac tissue from a mouse fed the 20mg/kg TO diet shows the presence of blue collagen staining (indicated by arrows) along with changes in cell morphology which are largely absent in control animals.

Microarrays

Microarray analysis was completed on three of the six treatment groups: control (n=4), 5 mg/kg TO9 (n=5) and 20 mg/kg TO9 (n=5). Analysis revealed a dose-dependent effect on the mean signal-intensities of known LXR targets identified from literature searches. These included ABCA1, ABCG1, ApoC1, ApoD, SREBP and SCD1 (Figure 4.4). Other known targets, specifically those associated with the peripheral side effects of liver steatosis and fatty acid synthesis, were significantly affected only by 20 mg/kg TO9 (FASn and FADS2). These targets are shown in Figure 4.4. Significance was determined using a one-way ANOVA and Tukey's *post hoc* ($p<0.05$). Links to supplemental tables of all genes found to be significantly modulated can be found linked here: Supplemental Tables\TO9_and_FO_microarray_supplemental_table.pdf.

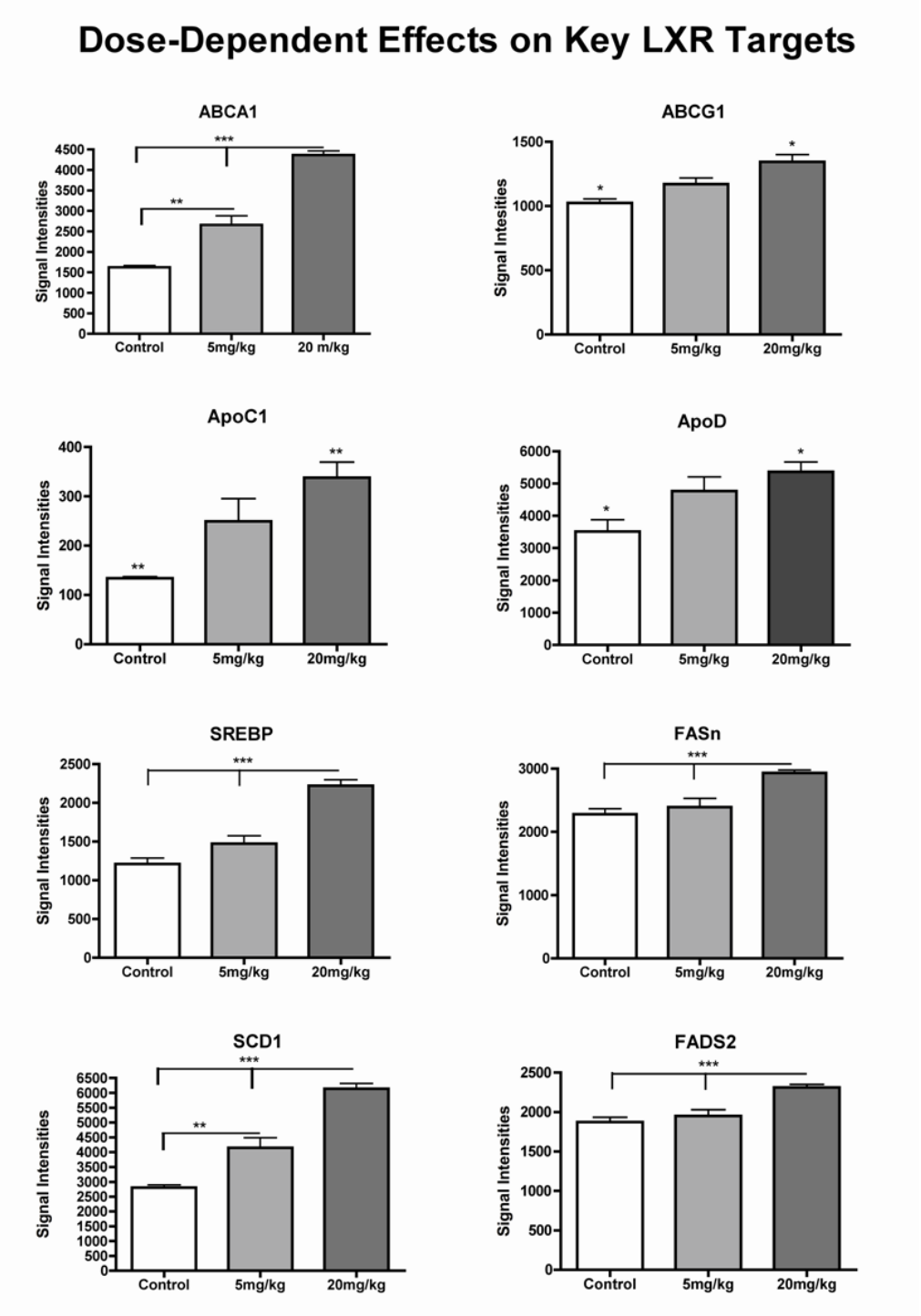

Figure 4.4: Mean signal intensities of known LXR targets. These known LXR target genes show a dose-dependent upregulation of the gene expression as measured by microarray and analyzed with a one-way ANOVA (n=4-5**)**; Tukey *post hoc* (*=p<0.05, **=p<0.01. ***=p<0.001).

Discussion

The lower dose daily dose of 5 mg/kg of the TO9 compound did not have as severe of an effect on the liver and heart weight as did the higher dose of 20 mg/kg (Figures 4.1 and 4.2). The lower dose was also able to significantly increase the gene expression of several key LXR targets including those associated with the beneficial effects of the compound (e.g., ABCA1 and various apolipoproteins). Although the lower dose increased expression of several known LXR targets, not all known LXR targets were altered (e.g., ApoE). Thus, whether this lower dose confers the same level of benefit as seen in the previous study (50mg/kg/day to 3xTg AD mice), specifically in reducing AD related pathologies, remains to be determined. It should be noted that the addition of fish oil (FO) to the treatments was unable to attenuate the liver hypertrophy observed at the higher TO9 dose of 20 mg/kg, although it may have slightly reduced cardiac hypertrophy (Figures 4.1 and 4.2).

An interesting aspect of the present study was that several known targets of LXR were modulated in a dose-dependent manner within the hippocampus. Again, this experiment is a proof of principle demonstration that the drug, included in the food, can exert dose-dependent effects in the brain. Secondly, it shows that microarray technology is very sensitive and can reliably detect changes in gene expression in response to different levels (e.g., doses) of treatment, which goes beyond simple directional analysis (e.g., up or down expression). Thus, microarray analyses can be used to determine the magnitude of the effect of pharmacological intervention on specific pathways.

Chapter 5: The Effects of Chronic LXR Activation in a 2xtg-AD Mouse Model

Introduction

We previously described the effects of chronic treatment with the potent liver X receptor (LXR) agonist TO901317 (TO9) in the 3xTg mouse model of Alzheimer's disease (AD). In addition, we examined the effects of additional doses of the TO9 compound in a separate group of mice (hybrid strain of the C57BL/6J strain and the 129/SvJ) considered to be the closest non-littermate controls to the 3xTg-AD mice (Chapters 3 and 4). In the 3xTg model, TO9 reduced Aβ pathology with minimal effects on learning and memory or LTP. The triple-transgenic animals used in the study first described in chapter 3 present with early intracellular Aβ accumulation and have marked cognitive deficits. TO9 was able to lower the Aβ load within the CA1 region of the hippocampus as well as significantly reduce the soluble Aβ levels within the cortical tissue. This appeared to translate into improved learning in the one-way active avoidance learning paradigm, a hippocampal dependent task. Yet there were substantial peripheral side effects which included steatosis of the liver as well as cardiac hypertrophy. To address these issues, a second study was carried out in which two different doses of the TO9 compound were used a low dose (5mg/kg/mouse/day) and a high dose (20mg/kg/mouse/day).

The experiment described in chapter four found that the lower dose of TO9 did not significantly increase the liver weights of the mice as compared to animals fed either a control diet or a diet supplemented with fish oil. This was also true of heart weight. Furthermore, the low dose was able to upregulate known LXR targets thought to be responsible for benefits observed. Yet this low dose did not upregulate these genes at the same level as did the high dose of TO9 nor was it able to significantly upregulate all those genes that the high dose was able to upregulate, therefore introducing some uncertainty about whether or not the low dose could upregulate genes that were actually required to confer the compound's benefits but were yet unknown. But the side effects observed with the high dose TO9 cannot be ignored, so the utilization of this dose in future long-term treatment studies carries certain risk.

It was decided then to carry out a third experiment involving six months of treatment with both doses in a double transgenic model of AD (2xTg-AD). There were

concerns about the 3xTg-AD mouse line, in that there was unresolved variability within the strain that could potentially confound long-term treatment results. There were also issues about its availability; therefore it was more reasonable to carry out the experiment described below in a more stable and established mouse model of AD.

Material and Methods

Animals

Experiments were conducted in compliance with the institutional guidelines of the Animal Care and Use Committee at the University of Kentucky. Five to six-month old male wild-type (n=31) and hemizygous (n=30) congenic AD mice (B6.Cg-Tg(APPswe, PSEN1dE9)85Dbo/J) were purchased from Jackson Laboratories (stock number 315864) and maintained in a 10 hour dark and 14 hour light cycle. Animal weights and food consumption were recorded throughout the study. Food consumption is considered to be an approximated average in that the food consumed is averaged for 2-3 days across the entire population of a given cage.

Medicated Diets

All diets were purchased from Harlan Teklad (Madison, WI). The AIN-93G diet was used as the base formulation into which the T0901317 (TO9) compound (Cayman Chemical, Ann Arbor, MI) was added. Based on our previous studies we knew the approximate amount of food a mouse eats, which in our hands is approximately 3 grams of food per day. Based on this figure, three diets were formulated, two of which were to deliver the following doses of TO9: control diet (AIN-93G only), 5 mg/kg/body weight diet (AIN-93G + 45 mg TO9 per kg of diet), and 20 mg/kg/body weight diet (AIN-93G + 200 mg TO9 per kg of diet). Intense heat associated with autoclaving along with irradiation was avoided to insure that the chemical structures of the incorporated compounds were not compromised. The 31 wild-type and 29 hemizygous mice were divided as equally as possible based on weight and fed one of the three diets creating six groups of nine to eleven mice. The mice were allowed water and the respective diets *ad libitum* for 7 months. The groups were as follows: WT-CON (n=11), TG-CON (n=9), WT-5mg/kg (n=10), TG-5mg/kg (n=10), WT-20mg/kg (n=10) and TG-20mg/kg (n=10).

Contextual Fear Conditioning

Conditioning took place in one half of a shuttle box with an electrifiable grid floor in a darkened training room lit only by a single lamp approximately one foot above the chamber. Two of the walls as well as the ceiling of the chamber consisted of clear Plexiglas with the front wall covered halfway with red tape to allow for observation and the back wall covered by a black and white contrasting plus sign. The guillotine door to the neighboring chamber was closed to prevent escape from an unavoidable shock. The surrounding environment was kept as silent as possible. The novel environment consisted of a clear glass cylinder 7 inches high and 8 inches in diameter with a galvanized steel lid and bottom. The novel environment apparatus was placed in the opposite corner of the room in which previous training took place under normal room lights.

Animals were trained and observed over two consecutive days. On day one animals were brought into a dark training room individually. Each animal was placed in the chamber for two minutes to freely explore. The animals' freezing behavior was observed during the initial introduction to the chamber with freezing behavior defined as the lack of all voluntary movement. At the end of two minutes a 22-second audible conditioned stimulus (CS) started (a clicking sound at 4 Hz). During the last two seconds of the CS, a 1.5 mA footshock was initiated. The entire session was then repeated once, followed by a 30 second interval after which the animal was removed from the training room. The chamber was wiped with ethanol between each animal.

Twenty-four hours later the animals were reintroduced into the context in which they were shocked the previous day and freezing behavior was again observed by two observers using 10 second time samplings for five minutes. The animal was then removed from the training room. Approximately one hour after the last animal was observed in the contextual environment, the animals were introduced into the novel environment in a lit training room. Animals were given 2 minutes of free exploration during which time freezing behavior was observed. After 2 minutes the CS was played for 22 seconds and freezing behavior was again observed for 2 minutes. The novel environment was swabbed with 1% acetic acid between animals to avoid olfactory

associations with the contextual environment. A schematic of the CFC paradigm is found below in Figure 5.1.

Contextual freezing behavior was determined by subtracting out percent freezing behavior in the contextual environment prior to footshock from percent freezing behavior in the same contextual environment 24 hours post-footshock. Proportions of time spent freezing in the contextual environment for the respective treatment groups were transformed by taking its arcsin and then analyzed with 2-way ANOVA.

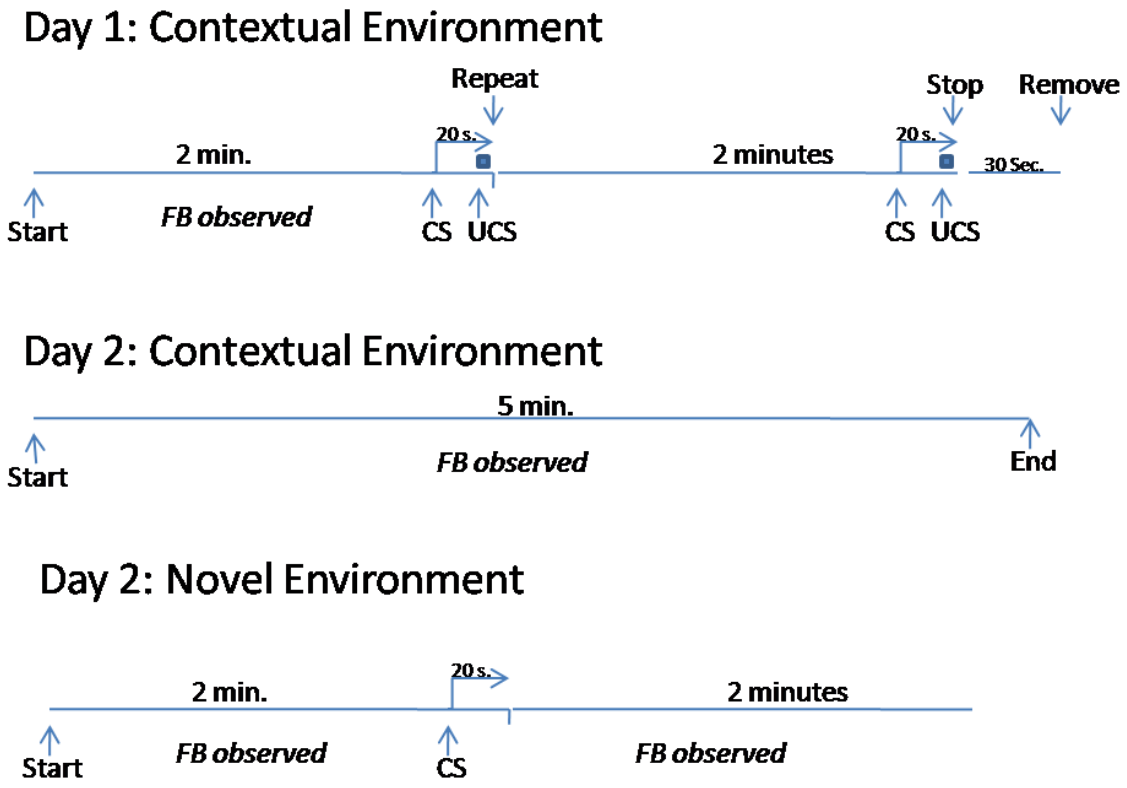

Figure 5.1: Schematic of contextual fear conditioning protocol. On day 1, the animal experiences two CS-UCS pairings within the contextual environment. Twenty-four hours later the animal is returned to the same contextual environment and freezing behavior is measured for five minutes minus the CS. Later in the day, the mouse is placed in a novel environment and observed for freezing behavior before and after the CS.

Tissue Collection

Animals were anesthetized with pentobarbital (150 mg/kg) and transcardially perfused with 0.9% cold saline. Blood was collected via heart puncture prior to perfusion. Animals were then decapitated and brains were quickly removed and placed in ice-cold artificial cerebral spinal fluid and were subsequently bisected. The right hemisphere was placed in cold 4% paraformaldehyde. The hippocampus was dissected out of the remaining left hemisphere and was snap frozen in RNAse free tubes embedded in dry ice. The livers and hearts of the animals were dissected out post-perfusion and weighed. Tissue weights were normalized to body weight. Digital photographs were taken of the livers for qualitative comparisons of gross changes in liver morphology.

Liver Histology

Frozen liver sections were first thawed and washed twice with PBS. Tissue was fixed in 10% formalin for 15 minutes at room temperature (RT) and subsequently rinsed with 60% isopropyl alcohol. The section were then stained with oil red O in 100% isopropyl alcohol for 30 minutes at RT. Sections were again rinsed with 60% isopropyl alcohol twice, then washed twice with distilled water twice and then counterstained with hematoxylin for 30 seconds, after which the slides were rinsed again with distilled water and mounted with a warmed glycerol gelatin.

Blood Collection and Serum Analysis

Blood was collected via cardiac puncture from the right atrium immediately prior to perfusion. Collected blood was centrifugated at 3,000 rpm for 10 minutes in BD Microtainer Tubes to separate out plasma. Plasma was aliquoted into centrifuge tubes and stored at -20°C until analysis. Serum samples were analyzed by the Comparative Pathology Laboratory at the University of California, Davis by a Roche COBAS Mira Plus Chemistry Analyzer. Values for each animal were averaged across the treatment group respective of genotype and statistically analyzed with a 2-way ANOVA and Bonferroni *post-hoc* multiple comparison test.

Soluble and Insoluble Amyloid Beta Levels

RIPA Extraction: Fifty to one hundred milligrams of cortical tissue from each of the mice were placed in enough SDS buffer to create equal concentrations of 0.1 mg/uL of tissue. Tissue was then homogenized with a polytron set at medium speed. Five hundred microliters of the homogenate was aliquoted to microcentrifuge tubes and centrifuged at 100,000 g for thirty minutes. The supernatant was collected and the remaining pellet was reserved for formic acid (FA) extraction.

Formic Acid Extraction: Pellet was sonicated in 70% FA for 10 second at 0.5 second pulses. The homogenate was then centrifugated at 100,000 g for one hour. The aqueous layer was collected and stored at -80°C until further use.

ELISA: SDS and FA fractions were thawed on ice and vortexed well to mix. FA samples were neutralized with 1:20 dilution in TP-buffer. Sandwich ELISA was conducted using Ab9 and 4G8 antibodies and detected with neutravidin-HRP and read with a Victor plate reader. Data was normalized for dilution and is presented at pmol/g wet tissue.

Microarray Analysis

Using techniques used to prepare hippocampal slices for electrophysiological recording described above and as previously described (Thibault et al., 1995), after the animals are anesthetized and blood was collected the animal was decapitated with a guillotine. The brains were rapidly removed and placed in ice-cold artificial cerebral spinal fluid. The cerebellum was removed and the brain was divided by a razor blade into left and right hemispheres. The hippocampus was removed from the left hemisphere and processed as described previously (Blalock et al., 2003; Rowe et al., 2007; Kadish et al., 2009). Briefly, RNA was extracted from hippocampal tissue with Trizol to and is precipitated with ethanol, reconstituted in RNAse-free water, and quantified and checked for RNA integrity with an Agilent 2100 bioanalyzer. RNA was processed to generate biotin-labeled cRNA following the standard protocol in the Affymetrix expression analysis technical manual, of which 20 µg of labeled-cRNA was then applied to a full mouse genome GeneChip 430v2.0 (Affymetrix) for hybridization (one chip per animal). Scanned microarray images were analyzed using the Microarray Suite 5.0 (MAS5; Affymetrix) algorithm.

Statistical methods used are similar to those described previously (Blalock et al., 2003). Data is prepared for analysis with extensive outlier removal techniques to remove repeats as well as unannotated genes. Genes determined to be present were analyzed for significant differences with a 2-way ANOVA.

DAVID functional analysis was completed on genes that were found to be significantly modulated. Gene accession numbers were uploaded into DAVID (http://david.abcc.ncifcrf.gov/), a web-based software to determine functional pathways that are overrepresented by the gene list provided. The functional pathways are listed in table format with pathway descriptions, number of genes found within the pathway, and the p-value describing the likelihood of finding that many genes with respect to the number of known genes in the pathway along with the number of genes detected with the genechip.

Results

Animal Weights

There was a significant effect of drug ($F_{(5,35)} = 27.7$) and time ($F_{(7,35)} = 10.5$) on the extent of weight change over the course of the eight months of treatment ($p<0.001$; 2-way ANOVA). All the mice gained weight over the course of the study, but mice fed the 20mg/kg TO diet had a significantly reduced change in body weight as compared to both controls (Bonferroni *post hoc;* $p<0.001$) from the time the diet was first introduced (Figure 5.2).

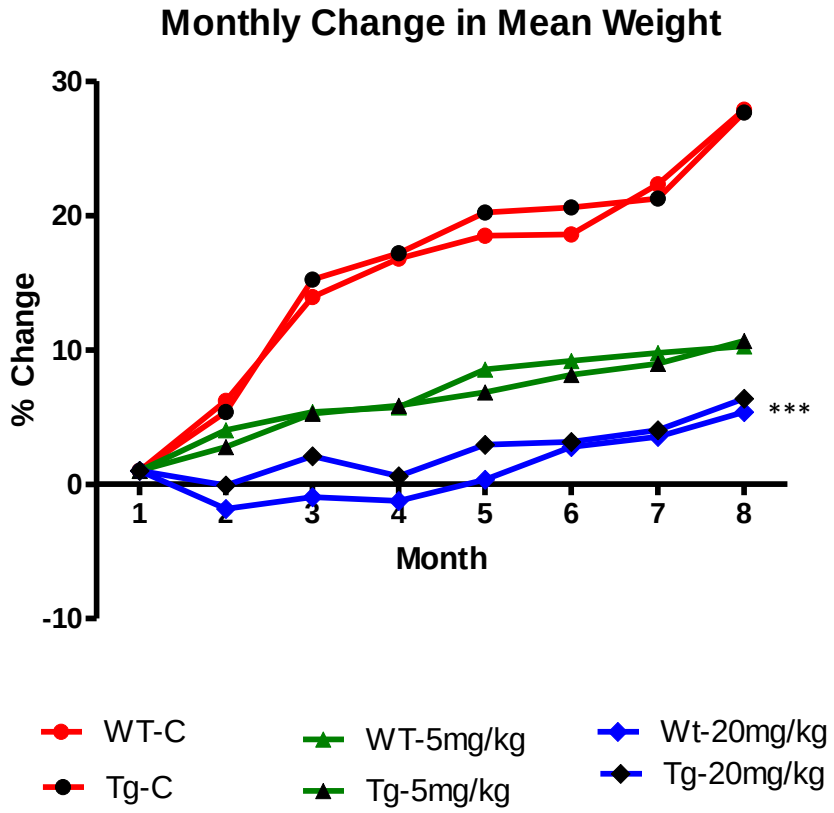

Figure 5.2: Mean percent monthly change in body weight. The mean animal weights for each treatment group (n=9-11/group) were obtained for each week and then averaged over a given month. Mean monthly weights were then compared to the mean weight of the respective treatment group during month one and are presented here as percent change for each groups mean starting weight. There was a positive change in weight for all six groups. TO treatment had a dose-dependent effect on the magnitude of this change over the course of treatment with the 20mg/kg fed animals showing a significant lack of weight gain at the end of the study (2-way ANOVA, Bonferroni *post hoc;* ***$p<0.001$).

Food Consumption

As was seen in previous studies with this particular compound, there was not a significant difference in the daily food intake averaged for each week across the course of the study (Table 5.1) with mean daily consumption ranging between 2.7 and 3.1 g/mouse/day.

Table 5.1: Mean food consumption. All mice were allotted 5 grams of food per day per mouse. The food was placed in a cage of 1-4 mice. Remaining food was measured and divided by the number of mice in a cage and by the number of days since the time they were last fed. This number is considered an approximate average. Average daily food intake for each mouse was averaged for a given week and then averaged over the course of the study. There was not a significant difference in the average daily food intake for any of the groups.

Group	WT-Control (n=11)	TG-Control (n=9)	WT-5mg/kg (n=10)	TG-5mg/kg (n=10)	WT-20mg/kg (n=10)	Tg-20mg/kg (n=10)
g/day Mean±SE	2.9 ± 0.05	2.8 ±0.03	2.97 ± 0.04	2.7 ± 0.04	2.9± 0.04	3.1 ± 0.03

Contextual Fear Conditioning

Figure 5.3 shows the percent freezing within the individual sessions of the CFC paradigm. There was a marked difference in the freezing behavior between the WT and TG animals, indicating memory deficits in the transgenic animals.

Freezing behavior was observed and measured 24 hours after the last conditioning session within the same environment that a footshock was delivered before to measure memory recall of the spatial context (Figure 5.4). Data are represented as the arc sin transformation of the proportion of time spent freezing during a five minute interval. There was a significant effect of drug ($F_{(2,54)}$=9.0; $p<0.001$) and genotype ($F_{(1,54)}$=11.14; $p<0.01$) on freezing behavior (2-way ANOVA). WT animals spent a significantly greater amount of time freezing in the contextual environment when compared to TG animals

and TO treatment increased freezing behavior in all groups. The 20mg/kg TO-treated WT mice spent a significantly greater amount of time freezing than the CON-treated WT mice ($p<0.05$; Bonferroni post hoc). Within the TG mouse cohort, only the 20 mg/kg TO-treated animals showed significantly increased freezing behavior that both the CON- and 5mg/kg TO9-treated TG animals ($p<0.05$; Bonferroni post hoc).

A.

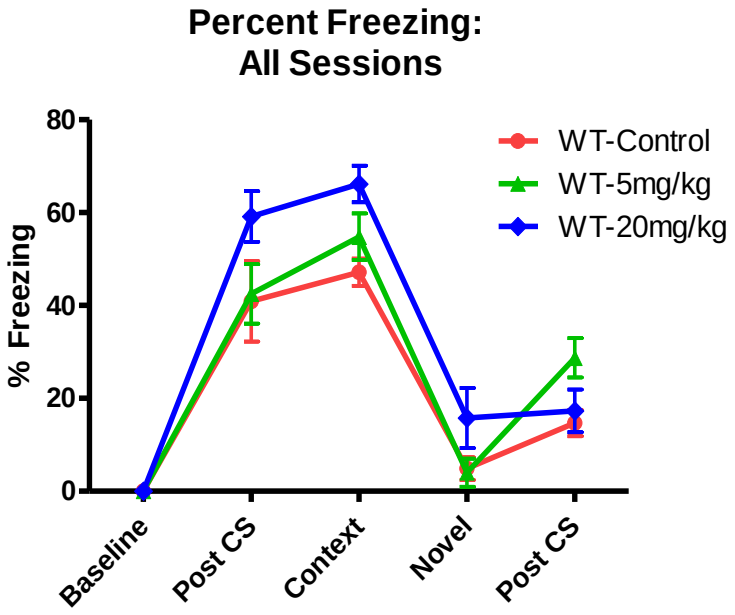

B.

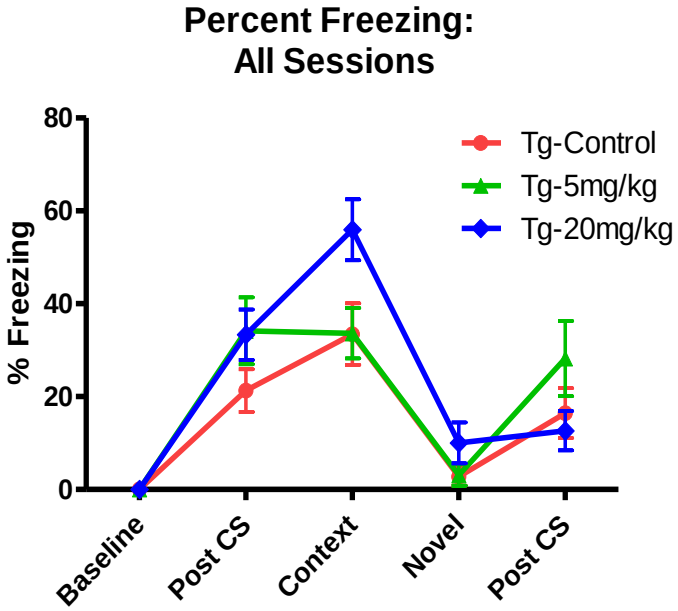

Figure 5.3: Mean percent freezing of mice from the different treatment groups over the course of the CFC sessions. Freezing behavior was absent during baseline observations (n=9-11/group). Freezing behavior increases dramatically after the first CS/UCS pairing for the WT animals and remained high 24 hours later in the contextual environment, with the highest freezing behavior seen in WT-20mg/kg TO9. Only Tg-20mg/kg TO9 mice appear to exhibit a similar level of response within the contextual environment as did the WT. Freezing behavior within the novel environment was low for both WT and TG animals.

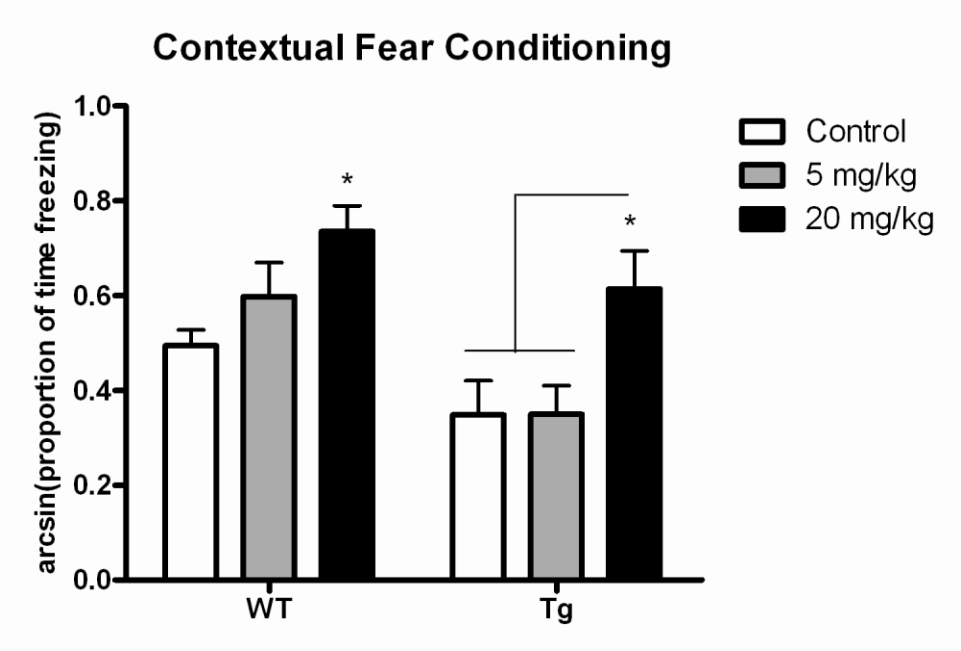

Figure 5.4: Proportion of time spent freezing for all groups within the contextual environment 24 hours after final CS-UCS pairing. (n=9-11/group) There were both significant effects of drug ($F_{(2,54)}$ = 9.0; $p<0.001$) and genotype ($F_{(1,54)}$=11.14;$p<0.01$) on the amount of time spent freezing in the contextual environment (2-way ANOVA). WT animals showed a dose-dependent increase in freezing behavior with 20mg/kg significantly increasing freezing behavior as compared to WT-Controls (Bonferroni *post hoc*; *$p<0.05$). High doses of TO9 were able to increase freezing behavior in the TG-20mg/kg mice, which froze more than both TG-Con and TG-5mg/kg TO9 groups (Bonferroni *post hoc*; $p<0.05$) within the same context.

Serum Analysis

An extensive blood serum analysis was completed on the serum from all of the animals in the study. Data revealed not only dramatic treatment effects on specific serum markers, but also genotype differences. Mean values for all the respective treatment groups can be found in Table 5.2A and Table 5.2B. These values are represented in a graphical form as well in order to facilitate a clearer understanding of the effects of both genotype and drug on individual biomarkers. Table 5.2A shows blood markers used to determine normal organ function while Table 5.2B lists metabolic markers.

There was a significant effect of genotype and drug on the levels of alanine transaminase (ALT) with higher levels seen in the TG animals and with TO9 treatment. Cholesterol levels were found to be significantly higher in TG as compared to WT animals treated with either CON or 5mg/kg TO9 diets. The 20 mg/kg TO9 diet significantly increased cholesterol levels as compared to both CON and 5 mg/kg TO9 treated groups irrespective of genotype. HDL levels were significantly reduced by both 5 and 20 mg/kg TO9 doses. LDL levels were significantly higher in CON-treated TG animals as compared to WT and were significantly increased in both genotypes with either TO9 dose. Triglyceride levels were significantly reduced with 5mg/kg TO9 in both genotypes, but with higher doses there was a significant divergence, with TG animals showing increased triglyceride levels with 20 mg/kg TO9. Glucose levels were significantly increased by TO9 in a dose-dependent fashion.

Tables 5.2A & 5.2B: Serum analysis of pre-determined metabolic markers: Pre-determined serum biomarkers were measured for all animals within the study. Values are presented as means across 9-11 animals per treatment group ± SE and were compared with 2-way ANOVA and Bonferroni multiple comparison test. Levels of significance are indicated on the following graphs. **A.** *Normal organ function*. Biomarkers indicating normal organ function indicate potentially problematic peripheral drug effects of high TO9 doses**. B.** *Metabolic markers*. Key metabolic biomarkers show significant effects of TO9 on lipid and glucose metabolism.

A.

	ALT U/L	BUN mg/dL	CK U/L	Ca^{2+} mg/dl	Creatinine mg/dl
WT	42.3 ± 12.5	28.5 ± 1.1	407.8 ± 68.3	9.8 ± 0.1	0.2 ± 0.0
TG	63.7 ± 10.9	30.2 ± 1.4	407.8 ± 68.3	9.9 ± 0.2	0.2 ± 0.0
WT-5mg/kg TO	75.0 ± 6.8	27.1 ± 0.9	1865.0 ± 579.9	10.2 ± 0.3	0.2 ± 0.0
Tg-5mg/kg TO	142.4 ± 25.7	26.7 ± 1.4	1235.3 ± 275.3	10.4 ± 0.3	0.2 ± 0.0
WT-20mg/kg TO	131.7 ± 16.3	28.0 ± 1.4	594.4 ± 124.2	10.8 ± 0.5	0.2 ± 0.0
Tg-20mg/kg TO	209.3 ± 54.4	30.5 ± 1.3	1216.9 ± 406.2	10.2 ± 0.2	0.2 ± 0.0

B.

	Cholesterol mg/dL	HDL mg/dL	LDL mg/dL	Triglycerides mg/dL	Glucose mg/dl
WT	166.5 ± 11.6	146.8 ± 12.4	31.7 ± 4.0	38.5 ± 7.8	257.6 ± 27.4
TG	209.4 ± 6.9	172.8 ± 10.8	45.8 ± 3.2	29.5 ± 6.5	254.3 ± 30.6
WT-5mg/kg TO	169.8 ± 6.2	112.2 ± 8.6	44.3 ± 4.3	12.6 ± 1.0	349.1 ± 43.8
Tg-5mg/kg TO	196.1 ± 9.1	130.6 ± 13.9	55.1 ± 4.8	14.8 ± 0.9	351.0 ± 32.2
WT-20mg/kg TO	230.7 ± 11.7	98.3 ± 4.0	81.3 ± 4.6	16.5 ± 1.8	453.6 ± 41.5
Tg-20mg/kg TO	239.5 ± 11.1	107.9 ± 13.2	92.3 ± 7.7	32.0 ± 7.6	426.7 ± 30.6

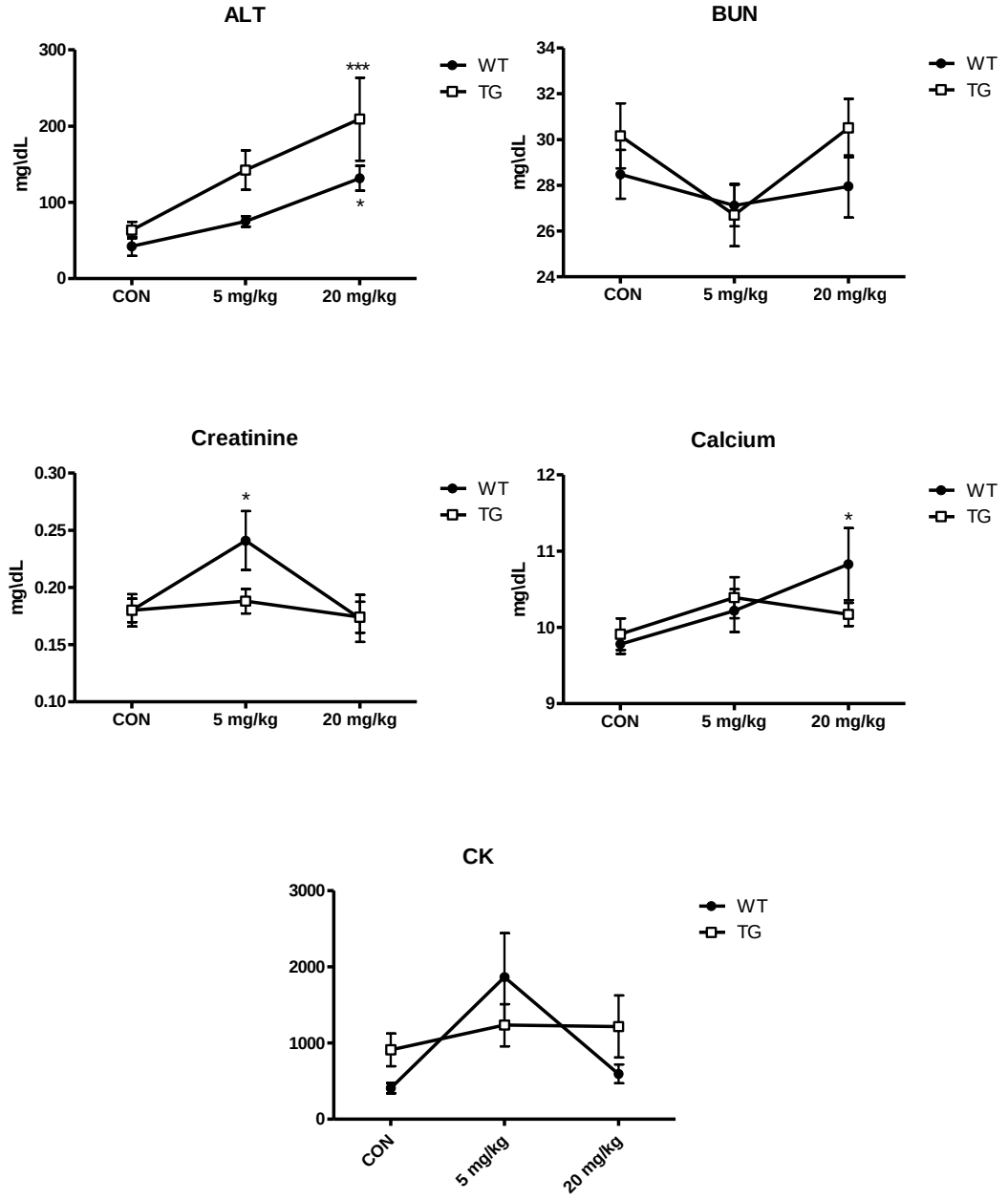

Figure 5.5: Serum panel assessing normal organ functions. Panel of serum biomarkers indicating potential changes in normal functioning in key organs associated with drug metabolism and system homeostasis (n=9-11/group). High doses of TO9 lead to a significant increase in ALT levels, indicative of liver damage. BUN levels remained similar for all groups indicative of proper kidney function. CK levels did appear to climb with higher dosage suggesting that muscle damage, including cardiac damage may be present. Significance was determined with a 2-way ANOVA and Bonferroni *post hoc test* (***$p<0.001$, *$p<0.05$).

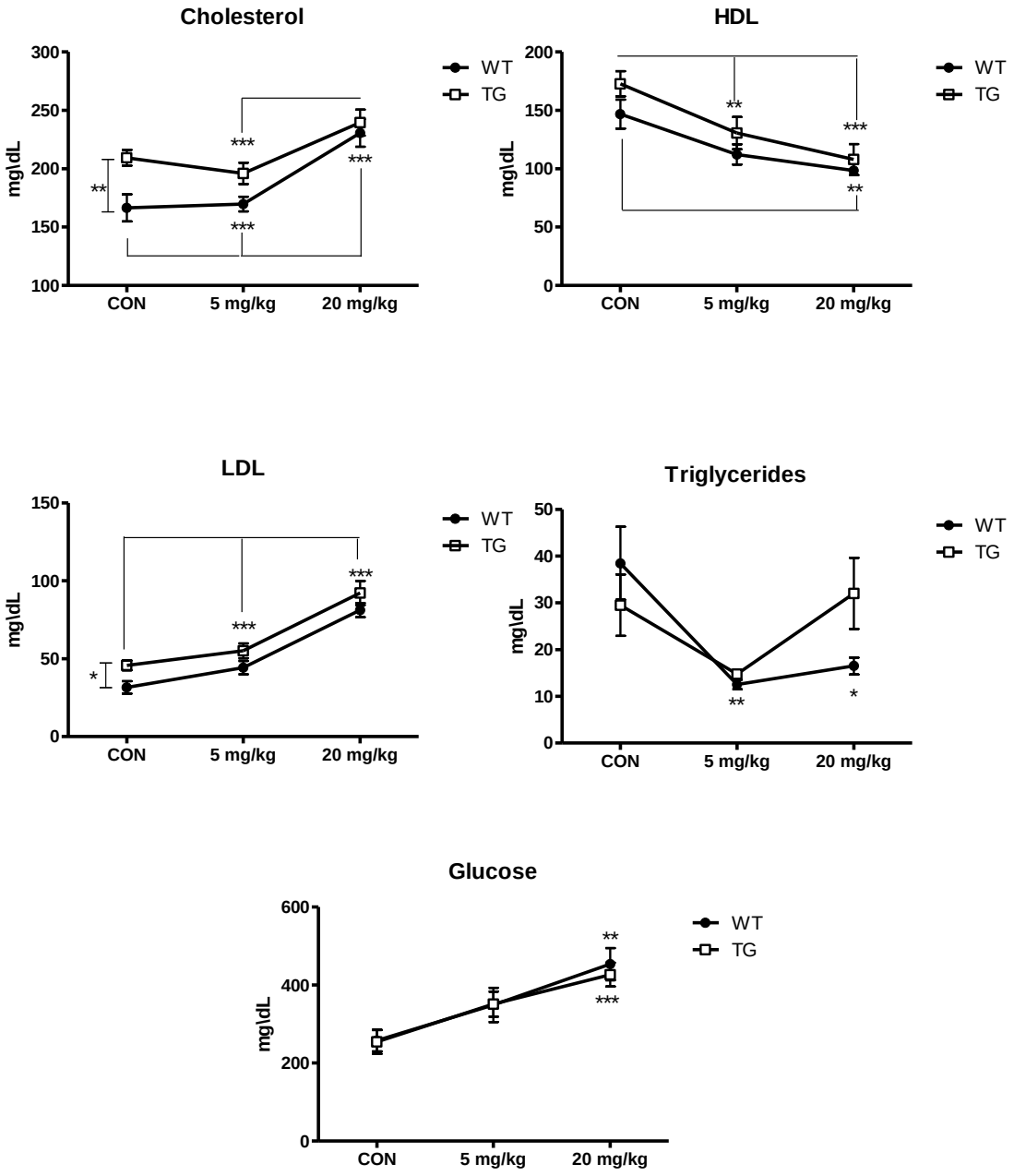

Figure 5.6: Serum panel assessing lipid and glucose metabolism. Standard lipid and glucose measurements from serum of WT and 2xTg–AD mice treated with control, 5 mg/kg TO9 or 20 mg/kg TO9 for 6 months (n=9-11/group). Higher doses of TO9 conferred the greater effect on various lipid levels, with cholesterol levels significantly increased by 20mg/kg TO9. This was accompanied by an increase in LDL levels and a reduction in HDL levels. Significance was determine with a 2-way ANOVA and Bonferroni *post hoc test* (*p<0.05, **p<0.01, ***p<0.001).

Liver Pathology

Liver weights were normalized to body weight and were found to be significantly increased in a dose-dependent fashion without any effect of genotype (Figure 5.4). Low and high doses of TO9 increased liver weight by 2 and 3 times the respective controls (2-way ANOVA; Bonferroni *post hoc;* $p<0.001$).

Figure 5.5 shows representative digital images of livers from TG and WT mice treated with control, 5mg/kg TO9 or 20mg/kg TO9. There was a gross morphological change in the size and coloration of the livers that seemed to mirror the dose-dependent effects on liver weights. Mice treated with both low and high doses of TO9 displayed extensive liver hypertrophy.

Figure 5.6 shows oil red O staining of liver sections taken from the livers pictured in Figure 5.5. Hypertrophy of the livers appears to be directly associated with the concurrent accumulation of neutral lipids in large vacuoles within the hepatic tissue.

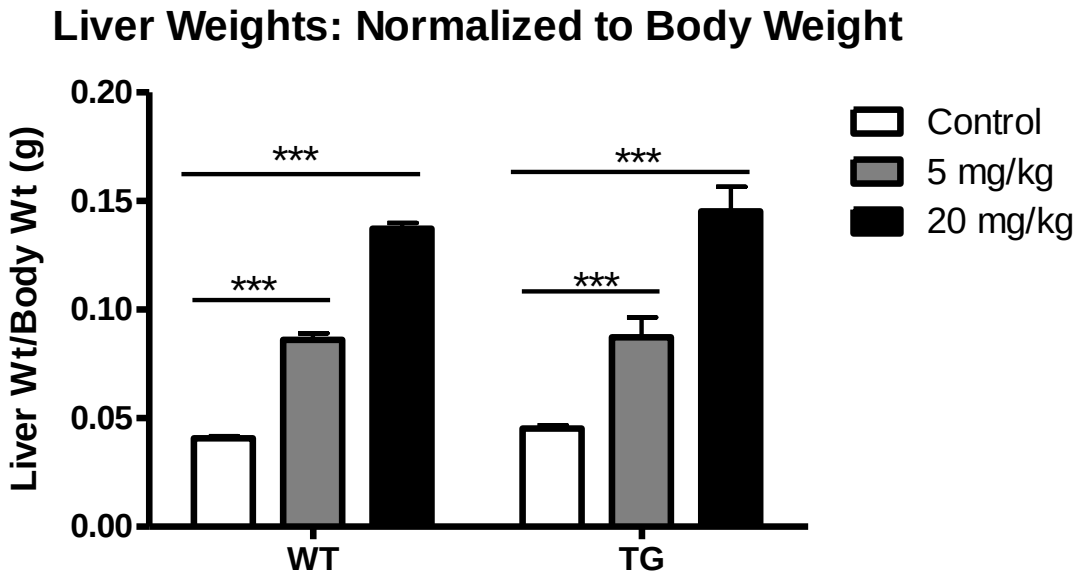

Figure 5.7: Dose-dependent changes in liver weights of both WT and TG treated with 5 mg/kg or 20 mg/kg TO9. There was a significant effect of drug on the weights of the livers treated with either control diet, 5 mg/kg TO diet or 20 mg/kg TO diet for six months (n=9-11/group). The 5 mg/kg TO diet and the 20 mg/kg TO diet increased the weights of the livers by 2 and 3 fold, respectively (2-way ANOVA; Bonferroni *post hoc*; *** $p<0.001$).

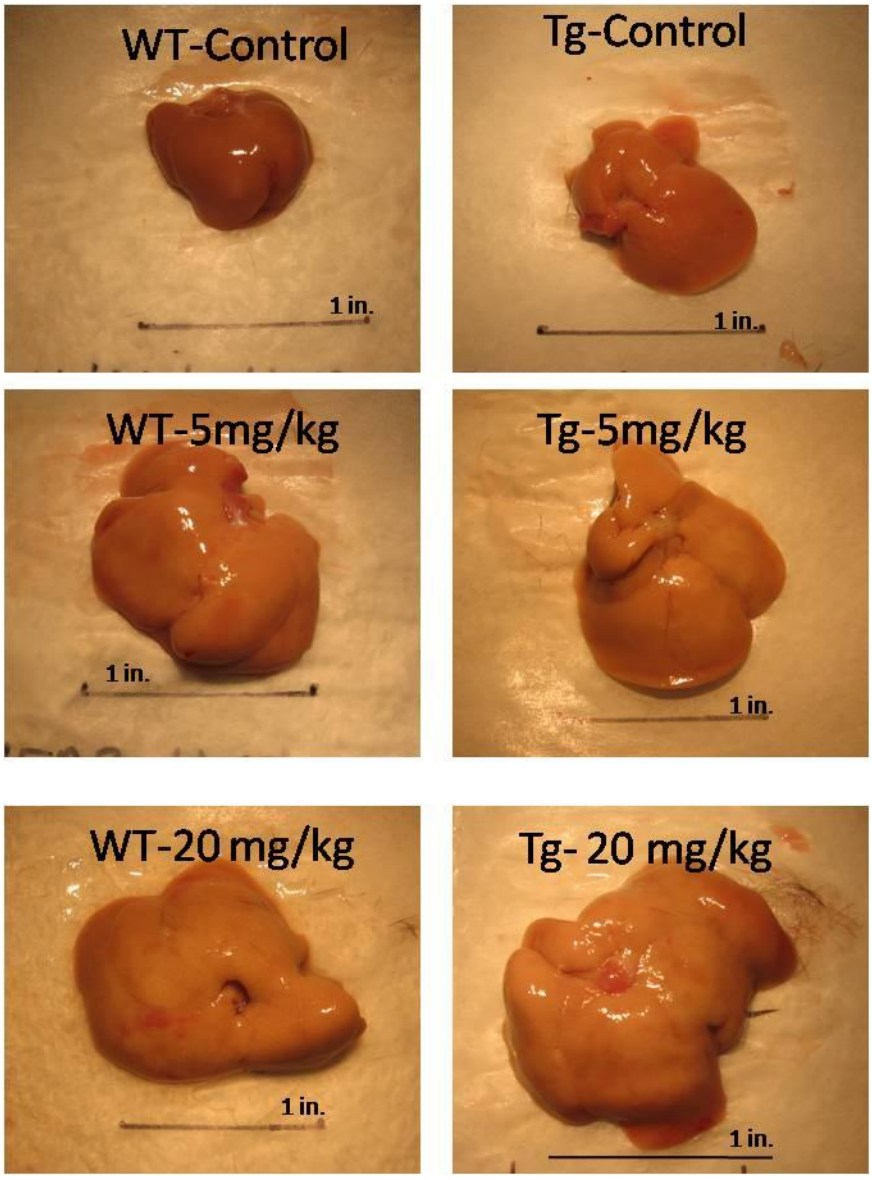

Figure 5.8: Representative digital images of livers taken from WT and TG mice treated with 5 mg/kg or 20 mg/kg TO9. Gross morphological changes in liver size appeared to be dose dependent. The gross changes in size correspond to changes in weights.

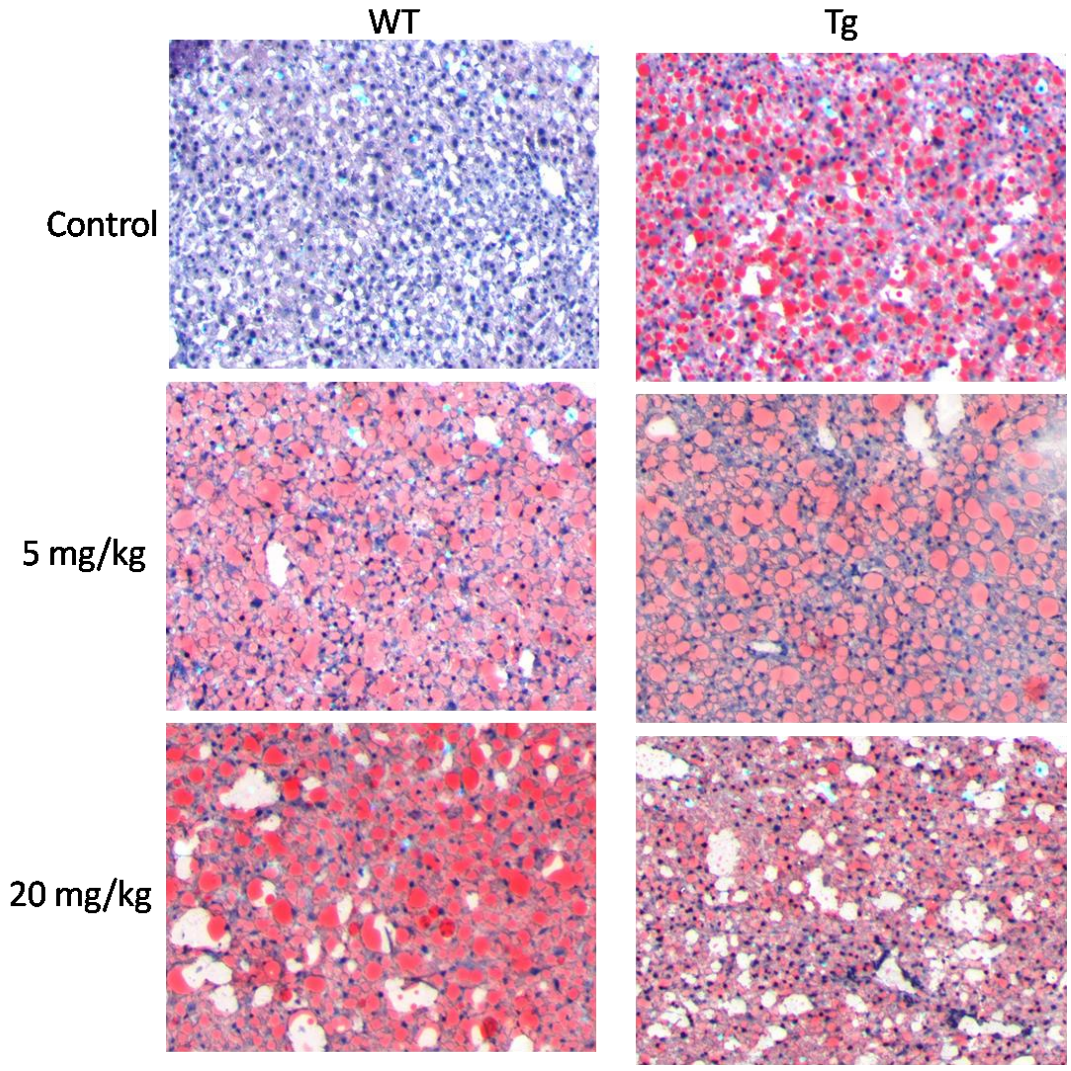

Figure 5.9: Liver histology from WT and TG mice treated with 5mg/kg or 20 mg/kg TO9. Oil red O staining of liver sections from WT and TG mice treated with 5mg/kg or 20mg/kg TO9 showed increased staining as compared to WT-Control. Lipid staining appeared to be higher in Tg-control animals indicating steatosis of liver as a result of the transgene. Greater lipid staining in the TG-Control animals did not translate to significant difference in liver weight.

Heart Pathology

Heart weights were significantly increased as a result of TO9 treatment ($p<0.0001$). There was also a significant effect of genotype on heart weight ($p=0.0386$) but there was no significant interaction effect as determined by 2-way ANOVA. In WT animals, both 5mg/kg TO9 and 20mg/kg TO9 significantly increased the heart weights (Bonferroni *post hoc*; $p<0.01$), but only the 20mg/kg TO9 significantly increased the heart weight in TG animals (Bonferroni *post hoc*; $p<0.001$).

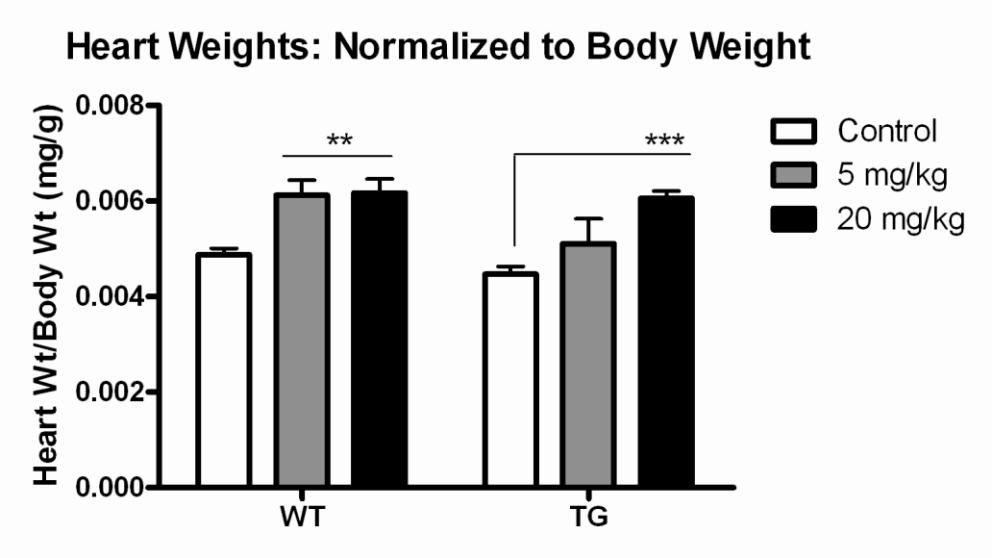

Figure 5.10: Genotype and drug effects on heart weight of 2xTg-AD mice. There was a significant effect of drug ($F_{(2,54)} = 12.3$; $p<0.0001$) on heart weight as well as an effect of genotype ($F_{(2,54)} = 4.9$; $p<0.05$), though there was not a significant interaction **(**n=9-11/group; 2-way ANOVA). Both doses of TO9 significantly increased heart weights of WT mice while only the 20mg/kg TO9 dose increased the heart weights of TG mice (Bonferroni *post hoc;***$p<0.01$ ***$p<0.001$).

Soluble Aβ Levels

As expected there was a significant difference in the soluble Aβ levels between the WT animals that do not express the transgenes and the TG animals that do (2-way ANOVA). Within the context of the transgenic animals, the 20mg/kg TO9 dose was able to significantly lower levels of soluble Aβ in the cortices of the mice as compared to both CON-treated (Bonferroni *post hoc*; $p<0.01$) and 5mg/kg TO9-treated animals (Bonferroni *post hoc*; $p<0.05$) in what appears to be a stepwise, dose-dependent decrease in soluble Aβ levels. There was no effect of drug on insoluble levels (data not shown).

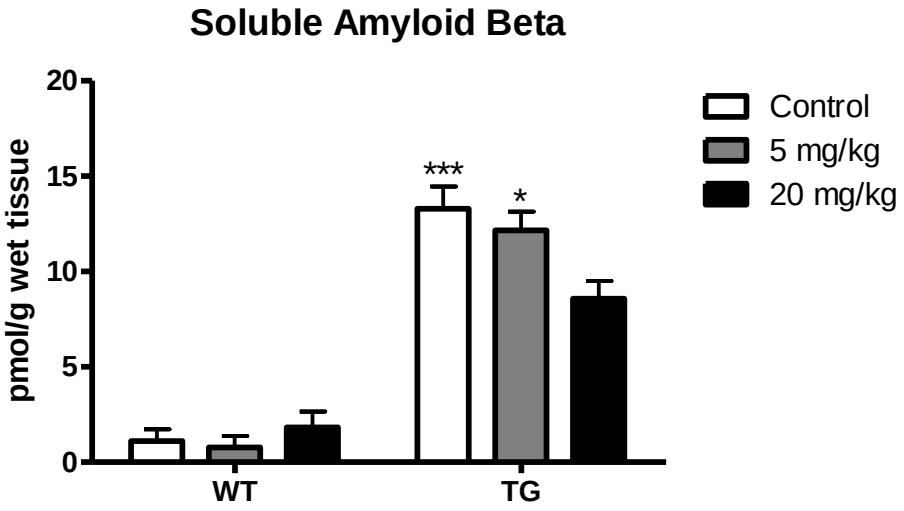

Figure 5.11: Soluble Aβ levels in the cortices of WT and Tg mice treated with control, 5mg/kg TO and 20mg/kg TO for six months. As expected, a difference in Aβ levels was seen between WT and TG animals with very low levels found in the WT (n=9-11/group; $F_{(2,53)} = 206.3$; $p<0.0001$; 2-way ANOVA). In 2xTg AD mice, The LXR agonist, TO9, reduced soluble Aβ in a dose dependent manner [2-way ANOVA ;Bonferroni *post hoc;* *$p<0.05$ (20mg/kg vs. 5mg/kg) and **$p<0.01$ (20mg/kg vs. Control)].

Microarray Analysis

Data were first filtered as being present or absent. Only probe sets with a grade of A were kept for further analysis and repeated probe sets were filtered. There were a total of 15011 genes found to meet these criteria. Two-way ANOVA analysis revealed only significant effects of genotype and drug whereas there was no overall interaction effect with FDRs as follows: Genotype = 0.36, Drug = 0.33, Interaction = 2.028 . Genes were further filtered by median FDR (0.02) producing a list of 12,372 genes. The 1825 genes that were found to be significantly modulated at a p-value of 0.05 fit specific expression patterns. These patterns and the number of respective genes represented by those patterns can be found in Table 5.3. Graphical representations of those patterns are shown in Figures 5.12-5.14. Tables 5.4-5.7 list the top twenty genes that are found to be either divergent in WT versus 2xTg mice or share the same linear pattern in respect to the upregulation and downregulation of specific genes. Supplemental tables listing all genes within the respective categories listed in Table 5.3 have been linked here: Supplemental Tables\2xtg-AD-TO_microarray_supplemental_table.pdf.

DAVID functional analysis of genes categorized by patterns described in Table 5.3 was completed as well. A selection of functional pathways can be found listed in Table 5.8. These functional pathways were generated by all genes that fit the same pattern of the top twenty genes shown in Tables 5.4-5.7. Patterns shown were selected based on their low p-value, their molecule representation, or their relevance to neurodegenerative disease. Not all functional pathways are listed due to redundancies of molecules within similar pathways. Pathways are listed in order of ascending p-value, where the p-value was determined by the likelihood of finding the number of known genes within the given pathway from the provided list. Lists were further truncated by removing pathways subsumed by more extensively represented pathways within a given cluster.

To further explore the effect of the drug on functional pathways, genes represented graphically in Figure 5.13 and 5.14 were collapsed into two groups: upregulated by drug and downregulated by drug and is presented graphically in Figure 5.15. A second DAVID analysis was completed on this set of genes. Pathways most

overly represented by the genes within this list are listed in Tables 5.9 and 5.10 along with select genes within a given pathway.

Table 5.3: Expression patterns and number of significantly modulated genes as a function of genotype and drug dose. There was a significant effect of drug and genotype on gene expression levels as determined by 2-way ANOVA ($p<0.05$; Median FDR= 0.02).Standardized signal intensities of significantly modulated genes followed particular expression patterns. These patterns are listed above along with the number of genes within each respective pattern.

Directional Description	Number of Sig. Genes
Divergent Genes Upregulated in TG	**571**
Divergent Genes Downregulated in TG	**364**
Linearly Increased by TO9 in WT and TG	**234**
Linearly Decreased by TO9 in WT and TG	**173**
Upregulated by 5 mg/kg & 20 mg/kg TO9	**127**
Downregulated by 5mg/kg & 20 mg/kg TO9	**131**
Upregulated by 20 mg/kg TO9 only	**97**
Downregulated by 20 mg/kg TO9 only	**57**
Upregulated by 5mg/kg TO9 only	**45**
Downregulated by 5 mg/kg TO9 only	**26**
Total Modulated Genes	**1825**

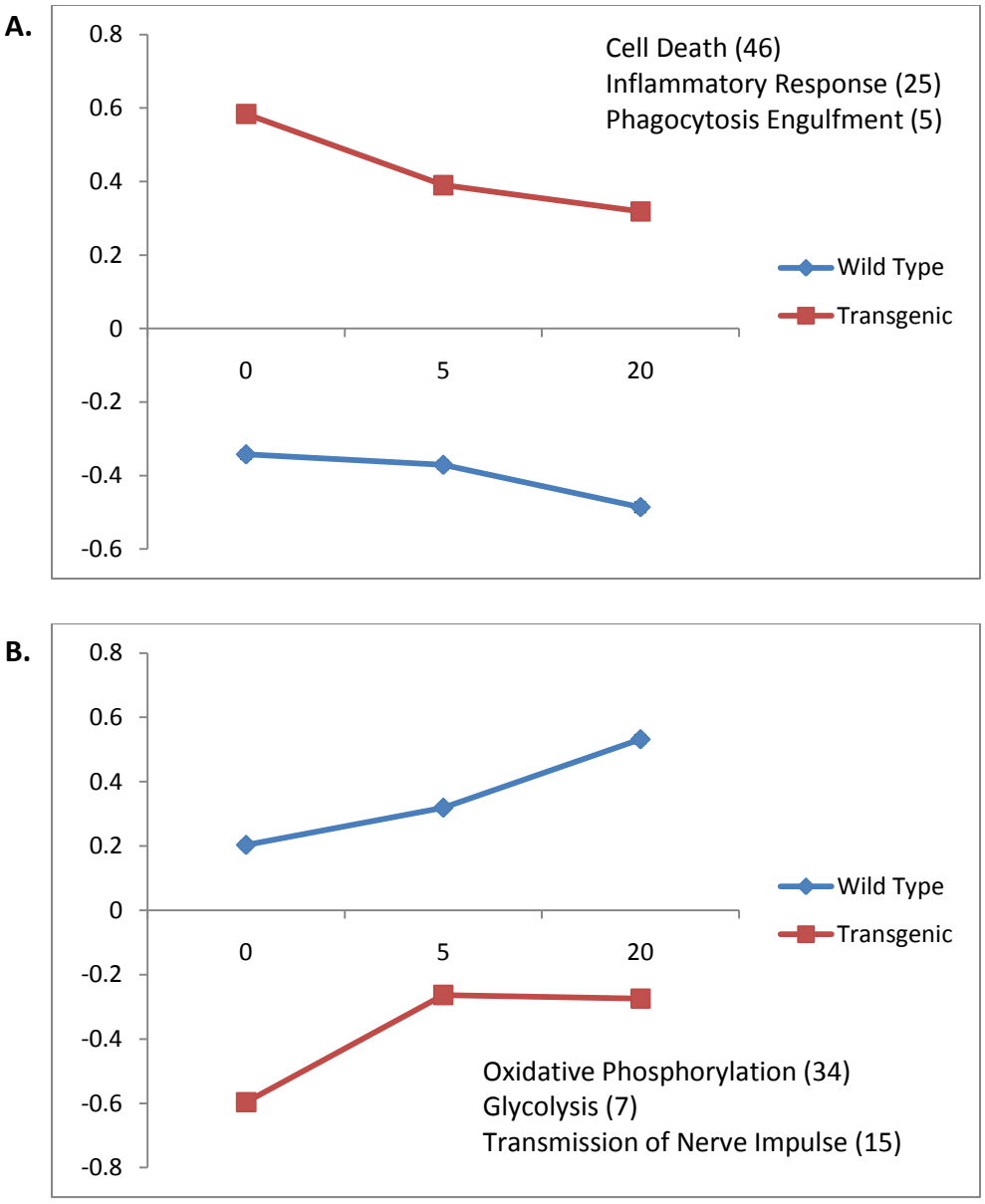

Figure 5.12: Divergent gene expression patterns in TG versus WT mice. A. A total of 571 genes were found to be upregulated in TG (TG) animals versus WT mice and (**B**) 364 genes were downregulated as an effect of the transgene being present. Select functional pathways and represented gene numbers are shown with their respective pattern of expression.

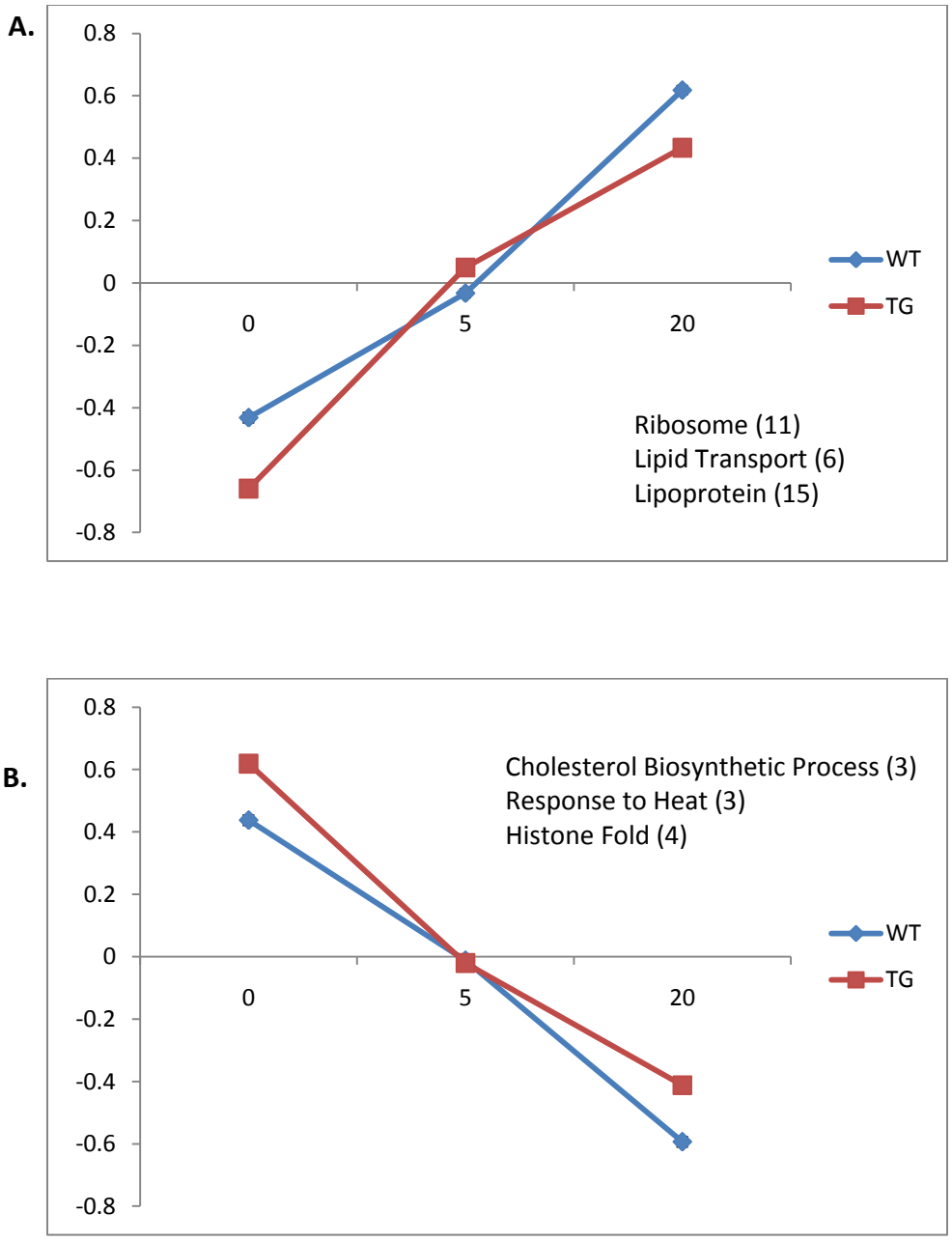

Figure 5.13: Linear gene expression patterns shared by both TG and WT mice treated with either 5 mg/kg and 20 mg/kg TO9. A. A total of 234 genes were found to be upregulated in a linear fashion as a function of drug dose in both WT and TG mice and (**B**) 173 genes were linearly downregulated as a function of dose. Select functional pathways and represented gene numbers are shown with their respective pattern of expression.

A.

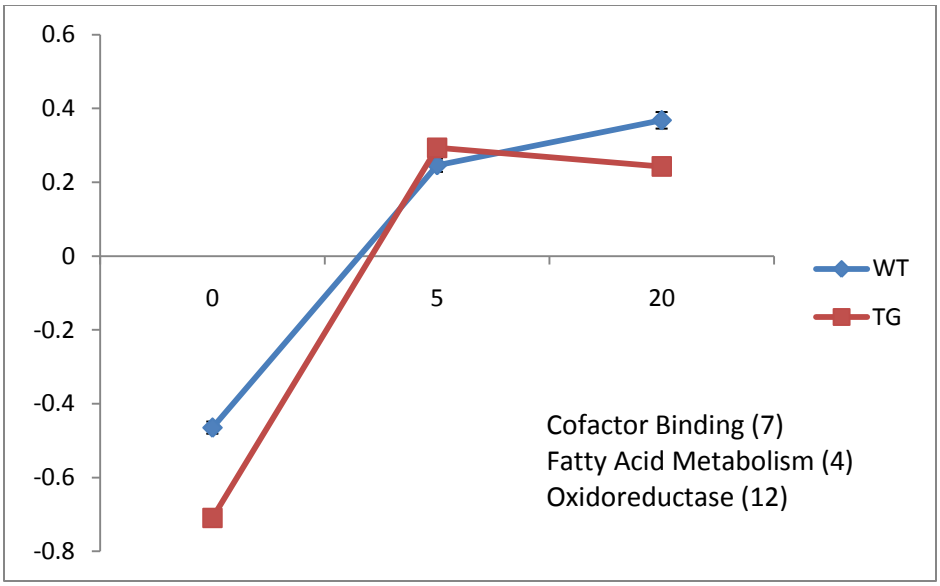

B.

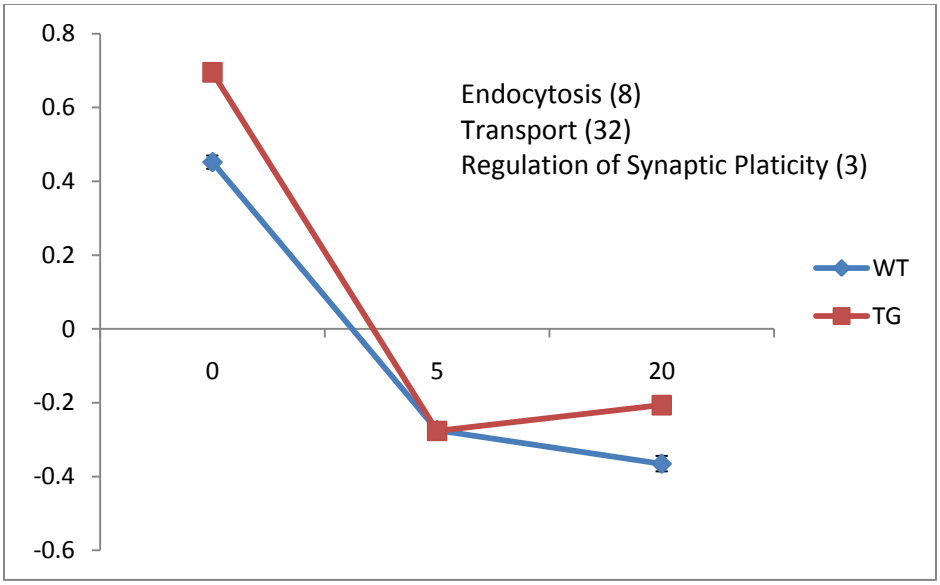

Figure 5.14: Gene expression patterns shared in both TG and WT mice treated with either 5 mg/kg TO9 or 20 mg/kg TO9. **A.** A total of 127 genes were found to be upregulated in similar magnitude with either drug dose in both WT and TG mice (**B**) while 131 genes were downregulated by either dose. Select functional pathways and represented gene numbers are shown with their respective pattern of expression. Select functional pathways and represented gene numbers are shown with their respective pattern of expression.

Table 5.4: Top twenty genes with the lowest p-values significantly upregulated in 2xTg-AD mice. Twenty genes found to be significantly upregulated in 2xTg-AD mice as compared to WT mice.

Symbol	Title
Ccl6	chemokine (C-C motif) ligand 6
Clec7a	C-type lectin domain family 7, member a
Gp49a	glycoprotein 49 A
Cd68	CD68 antigen
Mpeg1	macrophage expressed gene 1
Lyz2	lysozyme 2
Cd14	CD14 antigen
Ccl3	chemokine (C-C motif) ligand 3
Itgb2	integrin beta 2
Ctsd	cathepsin D
AU020206	expressed sequence AU020206
Trem2	triggering receptor expressed on myeloid cells 2
C1qc	complement component 1, q subcomponent, C chain
Cd53	CD53 antigen
C1qa	complement component 1, q subcomponent, alpha polypeptide
Plek	pleckstrin
Rnase4	ribonuclease, RNase A family 4
Slc11a1	solute carrier family 11 (proton-coupled divalent metal ion transporters), member 1
C3ar1	complement component 3a receptor 1
Fcer1g	Fc receptor, IgE, high affinity I, gamma polypeptide

Table 5.5: Top twenty genes with the lowest p-values significantly downregulated in 2xTg-AD mice. Twenty genes found to be significantly upregulated in 2xTg-AD mice as compared to WT mice.

Symbol	Title
Arpp21	cyclic AMP-regulated phosphoprotein, 21
Sst	somatostatin
Crhbp	corticotropin releasing hormone binding protein
B3gat3	beta-1,3-glucuronyltransferase 3 (glucuronosyltransferase I)
Cox5a	cytochrome c oxidase, subunit Va
Stx6	syntaxin 6
Dennd5a	DENN/MADD domain containing 5A
Gabra1	gamma-aminobutyric acid (GABA-A) receptor, subunit alpha 1
Pvalb	parvalbumin
Fam81a	family with sequence similarity 81, member A
Vgf	VGF nerve growth factor inducible
Ccl27a	chemokine (C-C motif) ligand 27A
Trak2	trafficking protein, kinesin binding 2
Car2	carbonic anhydrase 2
Stmn4	stathmin-like 4
Ahcyl1	S-adenosylhomocysteine hydrolase-like 1
Ndufb9	NADH dehydrogenase (ubiquinone) 1 beta subcomplex, 9
Zcrb1	zinc finger CCHC-type and RNA binding motif 1
Tmem59l	transmembrane protein 59-like
Npy	neuropeptide Y

Table 5.6: Top twenty genes with the lowest p-values significantly upregulated in a linear fashion in both WT and TG mice treated with TO9 for six months.

Twenty genes found to be significantly upregulated in a linear fashion.

Symbol	Title
Abca1	ATP-binding cassette, sub-family A (ABC1), member 1
Mid1ip1	Mid1 interacting protein 1 (gastrulation specific G12-like (zebrafish))
Scd1	stearoyl-Coenzyme A desaturase 1
Srebf1	sterol regulatory element binding transcription factor 1
Scd2	stearoyl-Coenzyme A desaturase 2
Apod	apolipoprotein D
Apoc1	apolipoprotein C-I
Lpcat3	lysophosphatidylcholine acyltransferase 3
Abcg1	ATP-binding cassette, sub-family G (WHITE), member 1
Acsl1	acyl-CoA synthetase long-chain family member 1
Mfsd2	major facilitator superfamily domain containing 2
Fads2	fatty acid desaturase 2
Prom1	prominin 1
Ggt1	gamma-glutamyltransferase 1
Apoe	apolipoprotein E
Col9a1	collagen, type IX, alpha 1
Tgm2	transglutaminase 2, C polypeptide
Trim35	tripartite motif-containing 35
Col4a3bp	collagen, type IV, alpha 3 (Goodpasture antigen) binding protein
Agt	angiotensinogen (serpin peptidase inhibitor, clade A, member 8)

Table 5.7: Top twenty genes with the lowest p-values significantly downregulated in a linear fashion in both WT and TG mice treated with TO for six months. Twenty genes found to be significantly downregulated in a linear fashion.

Symbol	Title
Idi1	isopentenyl-diphosphate delta isomerase
S100b	S100 protein, beta polypeptide, neural
Cyp51	cytochrome P450, family 51
Egfl6	EGF-like-domain, multiple 6
Dmp1	dentin matrix protein 1
Mkks	McKusick-Kaufman syndrome protein
Aldh1a1	aldehyde dehydrogenase family 1, subfamily A1
Apc	adenomatosis polyposis coli
Sacm1l	SAC1 (suppressor of actin mutations 1, homolog)-like (S. cerevisiae)
Hist2h3c2	histone cluster 2, H3c2
Lap3	leucine aminopeptidase 3
Mmgt1	membrane magnesium transporter 1
Sbk1	SH3-binding kinase 1
Epha6	Eph receptor A6
Jhdm1d	jumonji C domain-containing histone demethylase 1 homolog D (S. cerevisiae)
Kctd21	potassium channel tetramerisation domain containing 21
Nudt5	nudix (nucleoside diphosphate linked moiety X)-type motif 5
Sc5d	sterol-C5-desaturase (fungal ERG3, delta-5-desaturase) homolog (S. cerevisae)
Nipa1	non imprinted in Prader-Willi/Angelman syndrome 1 homolog (human)
Ppp2r5c	protein phosphatase 2, regulatory subunit B (B56), gamma isoform

Table 5.8. DAVID functional analysis of signficanlty modulated genes categorized by expression patterns. Tables **5.4A-D** list select biological pathways modulated by the presence of a the transgene or the TO compound at both the 5 mg/kg dose and the 20 mg/ kg dose. Pathway listings include the number of genes within the pathway and the significance level (p-value) based on the likelikhood of finding such a number of genes within a pathway by chance based on the original gene list provided in relation to the number of genes associated with a particular functional pathway *(continued on page 119).*

A.

Functional Pathway: Increased in TG	Gene Count	p-value
Inflammatory Response	25	$1.72x10^{-8}$
Locomotory Behavior	24	$1.01x10^{-6}$
Lytic Vacuole	23	$2.52x10^{-6}$
Phagocytosis Engulfment	5	0.002638
Zymogen	16	$3.67x10^{-5}$
Cell Death	46	0.0018
Natural killer mediated cytotoxicity	17	$4.53x10^{-5}$
Proteolysis	37	0.007718
Cytokine-cytokine receptor interaction	20	0.000685
Leukocyte differentiation	15	0.001012
Transmembrane receptor activity	42	$6.84x10^{-5}$
Regulation of apoptosis	30	0.012
Cytokine production	11	0.002398

(Continued on the following page)

B.

Functional Pathway: Decreased in TG	Gene Count	p-value
Oxidative Phosphorylation	34	5.04×10^{-22}
NADH dehydrogenase activity	11	1.13×10^{-7}
Mitochondrial envelope	31	5.94×10^{-10}
Glycolysis	7	0.001348
Neuron projection	12	0.001603
Transmission of nerve impulse	15	0.008375

C.

Functional Pathway: Linear Increase	Gene Count	p-value
Ribosome	11	2.96×10^{-6}
Lipid transport	6	0.0076
Cellular lipid metabolic process	17	0.0114
Lipoprotein	15	0.0289
Cellular carbohydrate metabolic process	11	0.00949

D.

Functional Pathway: Linear Decrease	Gene Count	p-value
Cholesterol biosynthetic process	3	0.04
Response to stress	16	0.012
Response to heat	3	0.031
EGF, extracellular	4	0.0233
Histone fold	4	0.006471

A.

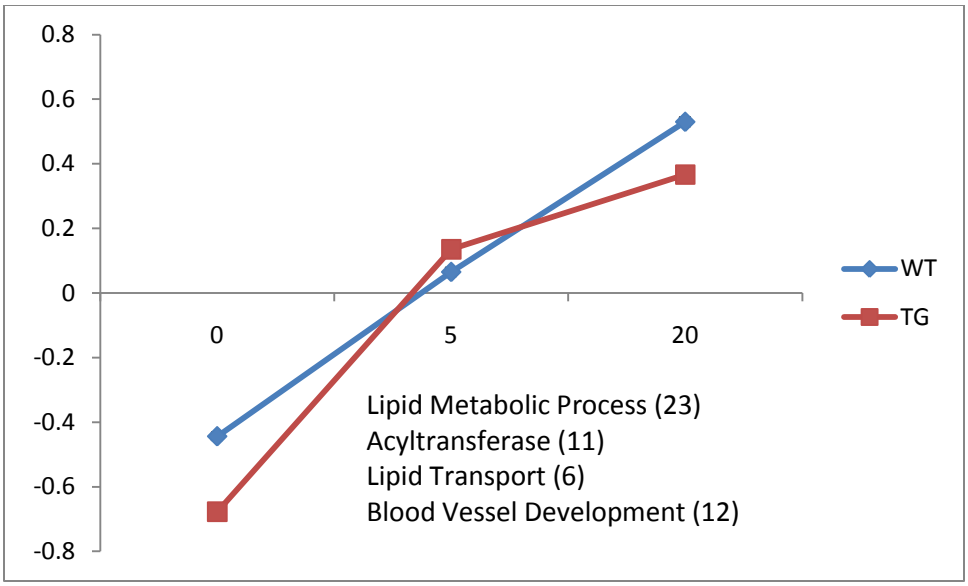

B.

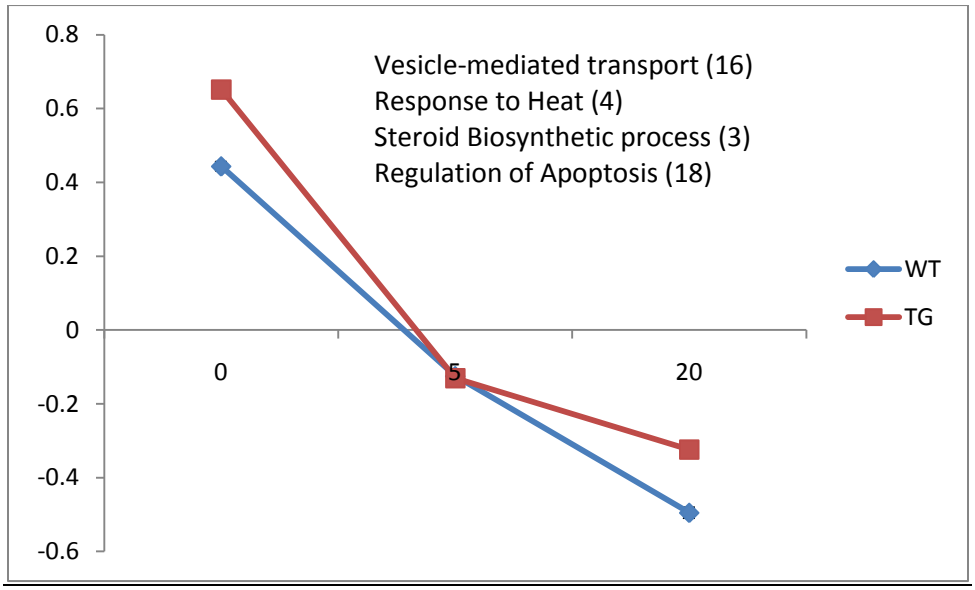

Figure 5.15: Gene expression patterns of all genes upregulated or downregulated by 5mg/kg or 20mg/kg TO9. A. Genes linearly increased and genes upregulated equally by both doeses were collapsed into a single list 361 gene upregulated by drug. **B.** Genes linearly decreased and genes downregulated equally by both doeses were collapsed into a single list 304 gene downregulated by drug. Select functional pathways and represented gene numbers are shown with their respective pattern of expression.

Table 5.9: DAVID functional analysis of genes significantly upregulated in hippocampi of 2xTG-AD mice treated for 6 months with TO901317. Functional pathways are listed with the number of genes representing the pathway .

Upregulated with LXR Agonist in 2xTg Mice	#	p-value
Lipid metabolic process *(apolipoprotein E, fatty acid synthase, ATP binding cassette A1,sterol regulatory element binding trasnscription factor, Stearoyl-Coenzyme A desaturase 1 & 2, Fatty Acid desaturase 1 & 2, Angiotensinogen, acetyl-Coenzyme A carboxylase alpha, hydroxyacyl-Coenzyme A dehydrogenase)*	23	0.046776
Acyltransferase activity (*diacylglycerol O-acyltransferase 2, gamma-glutamyltransferase, glycerol-3-phosphate acyltransferase, acetyl-Coenzyme A acetyltransferase)*	11	0.007341
Ribonucleoprotein complex biogenesis and assembly *(eukaryotic translation initiation factor 5, ribosomal RNA processing 1 hom**olog, ribosomal protein L7, s**plicing factor **argini**ne/serine rich-5, nucleolar protein 5A)*	17	0.000164
Oxidoreductase activity, acting on the CH-OH group of donors, NAD or NADP as acceptor *(malic enzyme 2 & 3, glyoxylate reductase, carbonyl reductase 1)*	8	0.008294
Lipid transport *(apolipoprotein E, ATP binding cassette G1, Apolipoprotein C1, Apolipoprotein D)*	6	0.040288
G-protein-coupled receptor binding *(endothelin 1, neuron specific gene family member 2, chemokine ligand 12)*	6	0.006645
Blood vessel development *(endothelin 1, leukocyte cell derived chemotaxin, endoglin, ras homolog gene family member B, endomucin)*	12	0.024426
Cellular carbohydrate catabolic process *(pyruvate kinase, phosphofructokinase, glucosamine, glucose phosphate isomerase)*	7	0.004799

Table 5.10: DAVID functional analysis of genes significantly downregulated in hippocampi of 2xTG-AD mice treated for 6 months with TO901317. Functional pathways are listed with the number of genes representing the pathway.

Downregulated with LXR agonist in 2xTg mice	#	p-value
Vesicle-mediated transport *(low density lipoprotein receptor-related protein 4, huntingtin interacting protein 1, exocyst complex component 3, caveolin 1, clathrin interactor 1, synaptojanin 1, synaptojanin 1 binding protein)*	16	0.048263
Response to heat *(heat shock protein 1B, heat shock protein 1, crystallin alpha b)*	4	0.013912
Regulation of hydrolase activity *(cytochrome c somatic, 24-dehydroxycholesterol reductase, regulator of calcineurin 1)*	9	0.011042
Inactivation of MAPK activity	3	0.019186
Steroid biosynthetic process *(7-dehydroxycholesterol reductase, 24-dehydroxycholesterol reductase, sterol-C5-desaturase, cytochrome p450 family 51, isopentenyl-diphosphate delta isomerase)*	6	0.011667
Regulation of apoptosis *(superoxide dismutase, 2, cytochrome c somatic, S100 protein beta polypeptide, neuroblastoma ras oncogene, scinderin, fibroblast growth factor receptor 3, cell division cycle and apoptosis regulator 1)*	18	0.0066
Nucleosome *(multiple histone clusters)*	5	0.004384
Regulation of synaptic plasticity *(glutamate receptor-ionotropic, myosin VI)*	4	0.0224
Regulation of MAPKKK cascade	3	0.044766
Regulation of protein metabolic process	12	0.011776

Discussion

The liver X receptor (LXR) is a key regulator of lipid metabolism in the brain and has been shown to be altered with brain aging (Rowe et al., 2007; Kadish et al., 2009). Further, many of its gene targets, including ApoE and the ABCA1, have been implicated in Alzheimer's disease (AD)-related pathology. The present study was undertaken to test the hypothesis that chronically activating LXR, which drives the expression of genes involved in cholesterol metabolism and transport, will reduce pathology and cognitive deficits associated with AD. We used the APP_{swe} and $PS1_{\Delta 9\ double}$ transgenic mouse model (2xTg) of AD originally created by crossing a mouse carrying the APP_{swe} mutation with a mouse carrying the $PS1_{\Delta 9}$ mutation (Borchelt et al., 1996). The 2xTg model presents with accelerated Aβ deposition with observable deposits at 6 months of age (Gordon et al., 2002; Jankowsky et al., 2004; Savonenko et al., 2005). Thus, chronic treatment with the LXR agonist was initiated at this critical point.

Effect on Aβ Levels. Similar to what was observed in the 3xTg model of AD (Chapter 3), we found that soluble levels of Aβ were reduced. Further, this reduction was dose-dependent as TO9 reduced levels by ~12% and 40% at the 5 mg/kg and 20mg/kg doses, respectively (Figure 5.10). Additional analyses will be required to determine Aβ deposition within specific brain regions including the hippocampus. Nevertheless, because soluble Aβ levels correlated with Aβ load (measured by staining with the WO-2 antibody and IHC) in the 3xTg model (Figure 3.5), we can infer a similar reduction in total Aβ load in the 2xTg model, as well.

Effect on Behavior. Another goal of the present study was to determine whether treatment with an LXR agonist could reduce associated cognitive deficits in an animal model of AD. In the 3xTg animals treated for three months with TO9, there was a trend toward improved learning on the active avoidance learning and memory paradigm in the absence of any significant effect on memory. In the present study we chose the contextual fear conditioning paradigm, another common behavioral task used to assess hippocampal dependent memory in various AD mouse models (Comery et al., 2005; Jiang et al., 2008). Animals receive a brief footshock paired with a conditioned stimulus (i.e., tone or clicking sound) within a specific context or environment. Memory for the

context in which the footshock is delivered is measured as freezing behavior when the animal is exposed to the same contextual environment 24 hours later. Freezing behavior is also observed within a novel environment, serving as a measure of context discrimination. Twenty-four hours after being shocked, freezing behavior was significantly increased in both wild-type and transgenic mice within the contextual environment, although overall freezing behavior appeared to be somewhat less in the 2x-Tg as compared to their wild-type counterparts. Chronic TO9 treatment at the higher dose of 20mg/kg significantly increased freezing behavior above that observed in both control and 5mg/kg TO treated animals irrespective of genotype (Figure 5.3). Discrimination between the contextual and novel environments was demonstrated by low freezing behavior within the novel environment in both genotypic groups. Furthermore, when the conditioned stimulus was played in the novel environment, freezing behavior increased slightly, but not to the extent observed previously in the original context.

Together, these results indicate that activation of the LXR pathway can improve contextual memory. Our results are similar to those recently reported in another AD model, the Tg2576 mouse (hAPPswe), where mice were treated with a LXR agonist for a much shorter duration (5 days) and at 5 months of age, prior to significant Aβ deposition (Jiang et a., 2008). Interestingly, memory was improved only in Tg2576 mice and not the wild-type counterparts. In contrast, we observed an effect in both wild-type and transgenic animals suggesting that LXR activation may have a more generalized effect on memory that is also independent of reductions in soluble Aβ (Figure 5.10).

Effect of Alzheimer's Disease Transgenes on Hippocampal Gene Expression. The microarray results indicated that a total of 935 genes were divergently expressed between wild-type and 2xTg mice, indicating a strong effect of the transgenes on hippocampal gene expression (Figure 5.11). The presence of both the APP_{swe} mutation and the $PS1_{\Delta 9}$ mutations led to a substantial upregulation of genes involved in immune response. Inflammatory responses are prominent in the brains of AD patients and are thought to be in response to the accumulation of Aβ in the brain (Golde, 2002; Wyss-Coray, 2006), thus the 2xTg model appears to recapitulate this aspect of the disease. DAVID functional analyses suggested a generalized inflammatory state in the 2xTg model as the following functional pathways were all significantly upregulated including *inflammatory response,*

cytokine-cytokine receptor interaction, *cytokine production*, and *natural killer mediated cytotoxicity*. Accompanying the upregulation in inflammatory pathways was the upregulation of gene pathways involved in cell death including *regulation of apoptosis*. Perhaps exacerbating inflammation/cell death, were key cellular pathways that were downregulated and included *glycolysis* and *oxidative phosphorylation*, suggesting impaired mitochondrial bioenergetics. These results are consistent with studies showing reduced brain metabolism in AD and impaired mitochondrial dysfunction, with AD neurons characterized by fewer normally functioning mitochondria (Wang et al., 2009b). Other gene pathways downregulated include *neuron projection* and *transmission of nerve impulse* suggestive of impaired synaptic function in the 2xTg mice.

General Effect of LXR Activation on Hippocampal Gene Expression in Wild-type and 2xTg Mice. A total of 361 genes were upregulated at both doses of the LXR agonist in both wild-type and 2xTg mice (234 of these were increased in a linear or dose dependent fashion – Table 5.3). The most significant upregulated pathways were *lipid metabolic process* and *acyltransferase activity*, representing pathways also identified in the prior 3xTg study. Another upregulated pathway included *ribonucleoprotein complex biogenesis and assembly*, a pathway very similar to *protein biosynthesis* (also identified in the 3xTg study). Genes within these categories are involved in ribosomal assembly and protein translation. A novel pathway not identified in the prior 3xTg study was *blood vessel development*. Apart from upregulating similar functional pathways, multiple well-established LXR gene targets consistently upregulated throughout these studies include ApoE, ABCA1, SREBF, FASN, ApoD, ApoC1, ACAT, ABCG1, FADS2, SCD1, and MBP.

A total of 304 genes were downregulated at both doses of the LXR agonist in both wild-type and 2xTg mice (173 of these were decreased in a linear or dose dependent fashion – Table 5.3). Some of the gene pathways significantly downregulated by chronic TO9 included *vesicle-mediated transport, steroid biosynthetic process,* and *regulation of apoptosis*. Unlike the 3xTg study, where one of the major functional pathways downregulated was *TOLL-like receptor signaling pathway*, there appeared to be a lack of effect on inflammatory processes. Perhaps the LXR-mediated anti-inflammatory effect is dose-dependent and was not observed here because of the lower doses used.

Peripheral Effects. The results above need to be viewed within the context of the significant liver and cardiac pathology which include cardiac and liver hypertrophy (Figures 5.4 through 5.7), most likely due to lipid accumulation within these tissues. Notable serum markers also altered by treatment with the LXR agonist included ALT (indicative of liver damage), glucose (likely due to hepatic steatosis), and unfavorable alterations in total cholesterol, LDL and HDL levels at the higher 20mg/kg dose of the TO compound. Thus, while there may be several CNS-related benefits associated with LXR activation, particularly for neurodegenerative conditions such as AD, the significant peripheral side effects will likely limit its use in the clinical setting.

Summary of LXR Activation in Transgenic AD Models. Below is a speculative model that attempts to synthesize results from the three previously described studies in which LXR agonists were given chronically in two AD different AD mouse models. The key component within the pathway is the upregulation of various aspects of lipid metabolism, including cholesterol synthesis and transport, which in turn has downstream effects that include the modulation of key genes involved in synaptic plasticity, apoptosis and the reduction of Aβ pathology. Questions about the role of LXR on integral aspects of memory remain. There is a disconnect between the reduced ability to maintain LTP and perceived improvement in memory. At the same time, we see improvements in contextual memory absent of any correlated reductions in AD-associated pathology.

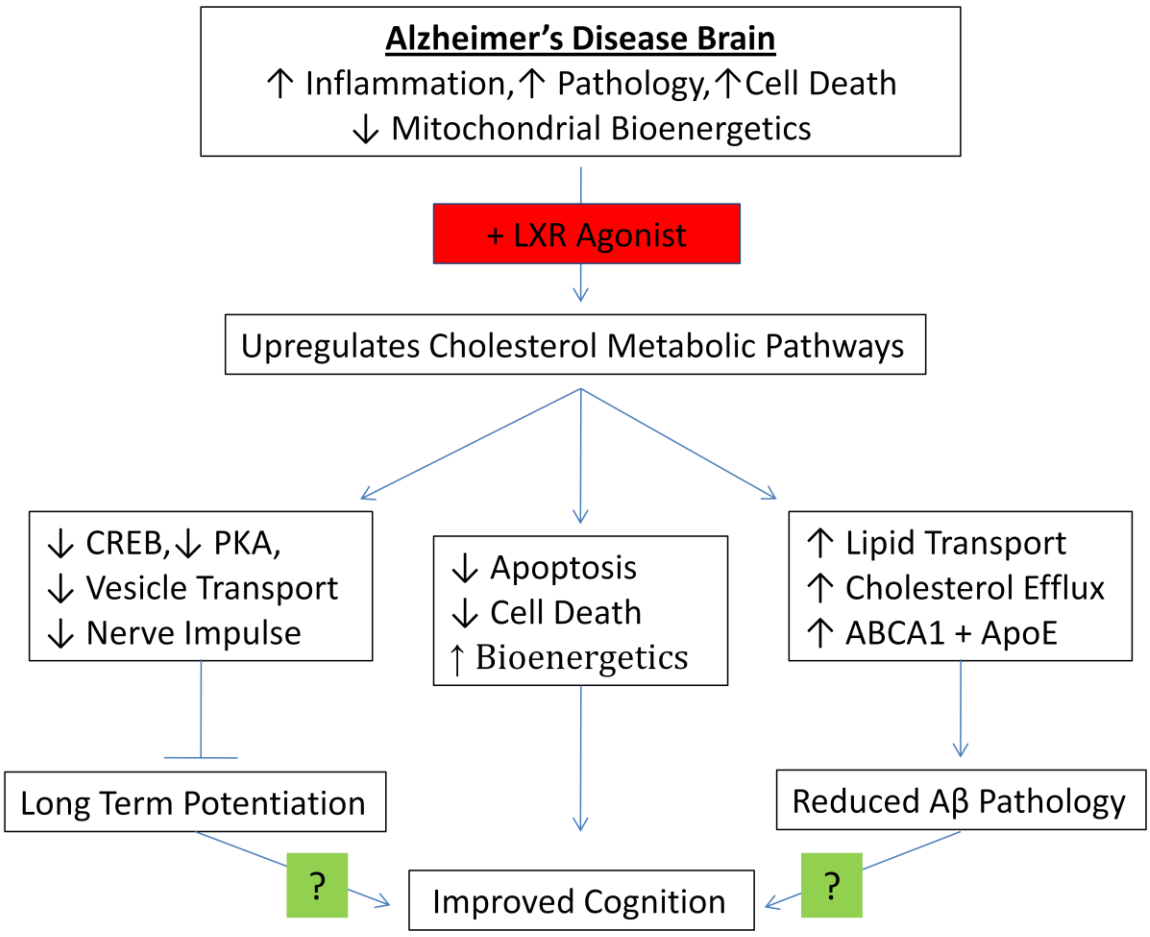

Figure 5.16: Speculative model of the role of chronic LXR activation role in the AD brain. This model attempts to integrate key findings in studies involving the long-term treatment of AD mouse models with a potent LXR agonist. The central component to this pathway is the upregulation of cholesterol metabolic pathways, which in turn leads to changes in gene expression patterns that may explain measured changes in synaptic plasticity, cognition and pathology.

Chapter Six: Short-term and Long-term Statin Treatment in mid-aged F344 Rats

Introduction

As reiterated throughout this document, the brain is one of the largest pools of cholesterol in the entire body, with 25% of the total cholesterol contained within its tissues. Most, if not all, of this cholesterol is made *de novo* by neurons and glia, whose cholesterol content is affected little by extracerebral levels (Andersson et al., 1990; Edmond et al., 1991; Jurevics and Morell, 1995; Dietschy and Turley, 2001). Most of this cholesterol is contained within myelin sheaths that encase axons. Therefore, dysregulation in cholesterol metabolism over the lifespan may have greater impact on myelin than other brain components, making it more susceptible to degeneration and related pathologies. In fact, those axons myelinated later in life are thinner and less thickly sheathed in myelin. These regions of the brain are first affected by AD pathologies (Bartzokis, 2004). The demyelination and abnormalities in white matter have been implicated in both brain aging (Chia et al., 1983; Guttmann et al., 1998; Bartzokis et al., 2001) and AD as well (Roher et al., 2002; Bartzokis et al., 2003; Bartzokis et al., 2004; Chalmers et al., 2005; Bartzokis et al., 2007).

Further corroborating this notion of potential metabolic dysregulation leading to age-associated impairments are links between dyslipidemia and the risk of acquiring dementia (Notkola et al., 1998; Yaffe et al., 2002; Pappolla et al., 2003). Recently, it was shown that high cholesterol levels at midlife increase the risk of AD and vascular dementia later in life (Solomon et al., 2009), yet in the elderly (>65 years of age), lower cholesterol levels may actually predict cognitive decline (van den Kommer et al., 2009).

Lipid metabolism also seems to make a shift in midlife, at the time when cognitive deficits begin to first emerge. Studies carried out in rats have shown that a whole host of genes begin to be expressed differently as a part of normal aging starting at this critical time point. A significantly disproportionate number of these are involved specifically in cholesterol metabolism (Rowe et al., 2007; Kadish et al., 2009). Several of these genes are also positively correlated with cognitive impairment, including ApoE and

the sterol regulatory element-binding transcription factor (Srebf1) (Kadish et al., 2009). Given this shift in lipid metabolism, and the potential emergence of metabolic dysregulation, it is of great interest to pharmacologically intervene in very targeted ways to prevent or ameliorate those deficits correlated with these events.

One of the most common classes of drug used to treat dyslipidemia within the periphery is the family of inhibitors of 3-hydroxy-3-methylglutaryl (HMG)-CoA reductase, or statins. These drugs act to lower total cholesterol levels by competitively inhibiting the rate limiting enzyme in its synthetic pathway (Endo et al., 1976). There have been anecdotal reports though that HMG-CoA reductase inhibitors (statins) impair short-term memory (Galatti et al., 2006). This seems juxtaposed to epidemiological data suggesting that statins may actually reduce the risk of acquiring AD (Jick et al., 2000; Wolozin et al., 2007), which is marked clinically by short-term memory deficits.

Unfortunately, there have been few studies that have directly tested the hypothesis that chronic treatment with statins improves cognition as well as electrophysiological correlates of memory formation. Those studies that have been completed are often conflicting in their results, some showing statins to be protective in various conditions including traumatic brain injury (Wu et al., 2008), drug induced amnesia (Parle and Singh, 2007) and induced inflammatory states (Clarke et al., 2008) while other studies have shown that statins can actually inhibit LTP by reducing levels of geranlygeraniol (Kotti et al., 2006), a product of the cholesterol synthesis pathway.

Because statins are so widely prescribed throughout the world, and given the inconsistencies in reported data obtained from experiments utilizing these drugs, it was of interest to explore the effects of statins within a context similar to that in which the drugs are normally prescribed: to mid-age adults. The following experiments were designed to address the role cholesterol regulation and metabolism plays in the brain as it passes through midlife into later life. Cholesterol synthesis was targeted with two of the most commonly prescribed statins, simvastatin and atorvastatin. It was hypothesized that by reducing cholesterol synthesis over the lifetime of an aging rodent model, we could attenuate deficits specific to the aging brain. More specifically, by inhibiting the synthesis of cholesterol in mid-age F344 rats, it would be possible to ameliorate age-associated deficits in long-term potentiation (LTP) and reduce the increased

afterhyperpolarization (AHP) that is observed in aged rats as well as attenuate correlated cognitive decline. Until these experiments, very few published studies have looked at the effects of long-term, chronic treatment of statins in rodents, especially focusing on statins' effects on the CNS.

Materials and Methods

Animals and Diets: Short-term Treatment

The original intended use of the rats described under the subheading, *short-term treatment,* was to study the effects of LXR activation in normal aging. Unfortunately the animals would not eat the medicated diet, and therefore this particular study had to be abandoned. These rats were then utilized in a pilot study to ensure that the F344 rats would in fact consume the statin-medicated diets. After 1-2 months of treatment, it was decided to electrophysiologically study key biomarkers of aging in the hippocampi of these mid-aged animals.

In this short-term study, 15 month-old male Fischer 344 rats were obtained from an aged rat colony and fed either a simvastatin (n=11) or atorvastatin (n=9) medicated diet formulated to deliver a daily dose of 20 mg/kg body weight of the respective statin or a control diet (n=9). Both diets were produced by Harlan Teklad (Madison, WI) using the AIN-93 G diet formulation and were available to the animals in pellet form along with water *ad libitum* for a span of 1-2 months. Animals were housed in pairs and were kept on a 12 hour light/dark cycle. Animals' weights and food consumption were monitored throughout. Animals were treated in compliance with the institutional guidelines of the Animal Care and Use Committee at the University of Kentucky. .

Electrophysiological Recording: Short-term Treatment

Long term potentiation. Nine to eleven rats from each treatment group were anesthetized in a CO2 filled chamber before rapid decapitation. Brains were quickly removed and placed in a bath of chilled oxygenated artificial cerebral spinal fluid (ACSF) of the following constituents (in mM): 114 NaCl, 3 KCl, 10 Glucose, 1.25 KH_2PO_4, 26 $NaHCO_3$, 8 MgCl, and 0.1 Ca_2Cl. Hippocampi were transversely sectioned with a Vibratome 3000 yielding 400 μm slices. Slices were transferred to a recording chamber containing oxygenated recording CSF (RCSF) of the following constituents (in mM): 114

NaCl, 3 KCl, 10 Glucose, 1.25 KH_2PO_4, 26 $NaHCO_3$, 2.5 Ca_2Cl and 1.3 MgCl. RCSF was kept at 32° C with O_2 perfusion of the closed interface chamber throughout the two-hour acclimation and recording periods.

A twisted, bipolar, Teflon-coated stainless steel stimulating electrode was placed perpendicular to the slice in the Schaeffer collaterals, while the sharp glass recording electrode (3-15 MΩ) filled with ACSF was positioned in the stratum radiatum.

Data were recorded and analyzed with Clampex and Clampfit software respectively. Current outputs (I/O) were recorded during stepwise increases in voltage at the stimulating electrode. The stimulation intensity required to elicit a fEPSP that was 50% of the maximum uncontaminated fEPSP was used for baseline recording, LTP inducing tetanus, and post titanic recordings. Prior to delivering an LTP inducing stimuli, baseline fEPSPs were subsequently recorded every 20 seconds for 20 minutes using the same stimulation intensity noted above. LTP was induced with a theta burst stimulation consisting of 10 bursts of 4 pulses each at 100 Hz every 200 ms for 2 seconds. Post-titanic FEPSPs were recorded every 20 seconds for 30 minutes after LTP was induced with the same parameters used during baseline.

Mean slopes and amplitudes of the last fifteen minutes of post-LTP recording were compared using one-way ANOVA. Slices whose baseline fEPSPs changed more than 20% during recording were omitted from the analysis.

Afterhyperpolarization: Nine to eleven rats per treatment group were sacrificed and hippocampi removed to obtain 350 μm thick slices. Slices were maintained in ice cold low-calcium artificial cerebrospinal fluid (ACSF) of the following constituents (in mM): 128 NaCl, 1.25 KH_2PO_4, 10 Glucose, 26 $NaHCO_3$, 3 KCl, 0.1 $CaCl_2$, 2 $MgCl_2$. Slices were then transferred in an interface-type chamber and maintained in oxygenated (95% O_2, 5% CO_2) high-calcium ACSF containing 2mM $CaCl_2$, at 32^{o}C for at least 2hrs to allow recovery of the tissue. Hippocampal slices were placed in a recording chamber (RC22C, Warner Instruments, Co., Hamden, CT) maintaining a continuous flow of oxygenated ACSF pre-heated at 32°C using a TC2Bip/HPRE2 in line heating system (Cell Micro Controls, Norfolk, VA). This setup was mounted in a Nikon E660E inverted microscope. Cells were impaled with sharp microelectrode, filled with 2M $KMeSO_4$ and

10mM HEPES pH 7.4 (tip resistance~110 ± 24 MΩ), pulled from borosilicate glass capillaries (World Precision Instruments, Sarasota, FL) using a P80 pipette puller (Sutter Instruments, Novato, CA). All experiments were performed in current clamp mode with bridge balance compensation and capacitance neutralization. Signals were digitized at 2 kHz and low-pass filtered at 1 kHz. Recordings of membrane input resistance (IR) were obtained approximately 5min after impalement by measuring the steady hyperpolarization obtained from injecting 200pA hyperpolarizing current with an Axoclamp 2B amplifier (Axon instruments) for 800ms while holding the cell at -70mV. To generate an afterhyperpolarization (AHP) cells were held at -65mV (baseline) and depolarized with a 100ms current pulse in order to generate three Na^+ action potentials delivered through the intracellular electrode. AHPs were elicited every 30s and at least 6 AHPs were averaged per each cell. Medium AHP (mAHP) represents the peak hyperpolarization reached after the end of the depolarizing stimulus, slow AHP (sAHP) represents the hyperpolarization 800ms after the end of the stimulus and the AHP duration was measured from the end of the depolarizing step until return to baseline. Neurons with input resistance < 50MΩ, Holding current > 500pA and APs height < 0mV, were excluded from in this study. Data were acquired using pClamp 8.0 (Axon Instruments) software through a Digidata 1320A, A/D converter (Axon Instrument) while mAHP, sAHP as well as duration of AHPs were calculated using Calmpfit software (Axon Instruments).

Animals and Diets: Long-term Treatment

Experiments were conducted in compliance with the institutional guidelines of the Animal Care and Use Committee at the University of Kentucky. Male F344 rats were purchased at 9 months of age from the NIA aged rat colony. Upon receipt the animals were acclimated to a control diet (AIN-93G from Harlan Teklad). After two weeks of acclimation, when the animals were approximately 10 months old, they were started on their respective diets eaten *ad libitum* for 9 months. Animals were given a control (n=11), simvastatin (n=11) or an atorvastatin (n=11) diet. Animals were housed two per cage in clear plastic cages with wire grid tops and maintained in a 12 hour dark and light cycle. Food consumption and animal weights were recorded throughout the study, approximately 2-3 times/week. (It should be noted that food consumption was averaged

across two animals within a single cage and should be considered an approximate average).

Medicated diets were formulated within the context of AIN-93G diet by Harlan Teklad, Madison, WI. Tablets containing 80 mg of Atorvastatin and Simvastatin were crushed with a mortar and pestle to create a fine powder. This powder was incorporated in the diet by the manufacturer at a concentration of 200mg/Kg and subsequently pelleted. Intense heat along with irradiation was avoided to insure that the chemical structures of the incorporated compounds were not compromised.

Behavioral Characterization:

The *rotorod* was used to assess motor coordination of the rats after 8-9 months of treatment. Rats were trained on the rotorod apparatus for three days prior to a final accelerated test. The training consisted of a one-minute training trial per animal per day at a constant RPM. Animals were started at 8 RPM and graduated to 10 and 12 RPM on the two subsequent training days. Animals were repositioned on the rotorod upon falling during the training sessions. The final accelerated test involved a trial in which the rotorod revolution speed accelerated from 4-40 RPM over the course of the trial. Latency to fall during the accelerated task was recorded.

The *Morris water maze* consisted of a pool (183x60cm) enclosed within black curtains that produce a semi-dark environment within the testing room. The bottom and sides of the pool had been painted black. Three large contrasting spatial cues hanging from three of the four surrounding walls are lit by LED rope lights that wrap around the pool itself as well as LED can lights surrounding the pool and projecting light upward. This allowed for visualization of the spatial cues as well as created contrast needed for the Videomex tracking system and accompanying water maze software (Columbus Instruments). The pool was filled with water (25±1°) to a height sufficient enough to submerge a hidden platform 15 centimeters in diameter by 2 cm of water.

The animals were brought into the dark testing room lit by only one red heating lamp and two monitors. During cue training, a conspicuous cue was suspended from the ceiling and hung 12 inches above the submerged platform marking its location. The

platform was submerged during cue training to aid the rats getting on to the platform. Cue training lasted for three days with each rat given three trials a day. A trial consisted of 60 seconds to find the platform, 30 seconds to acclimate to its surrounding while on the platform, and 120 seconds within a holding cage heated by a heat lamp before being reintroduced to the maze. On day one, animals were introduced to the maze via the same quadrant for every trial. On subsequent days, the animal was introduced in different quadrants every trial, rotating the drop spot in a clockwise fashion.

Seventy-two hours after the last cue-training trial, the animals were trained in a similar manner as described above, but with the suspended cue removed. Throughout the training sessions (3 trials/session/day) the drop spot was rotated within the day. The first drop spot of each day was rotated in the same clockwise fashion in order to insure that the rat was using the spatial cues for orientation within the maze. Both latencies to goal as well as path length to goal were used to determine cognitive differences between treatment groups during training.

During the MWM *probe trial*, platform was removed from the maze and animals were given 60 seconds to swim freely while being monitored. Memory was assessed using the percent of the time the animal spent in the goal quadrant during the first 30 seconds of the free swim as well as the number of times the animal entered the goal quadrant.

Tissue Collection

Animals were anesthetized with pentobarbital (60mg/kg) and transcardially perfused with 0.9% cold saline. Blood was collected via heart puncture prior to perfusion. Animals were then decapitated and brains were quickly removed and placed in ice-cold artificial cerebral spinal fluid and were subsequently bisected. The right hemisphere was placed in cold 4% paraformaldehyde. The hippocampus was dissected out of the remaining left hemisphere and was snap frozen in RNAse free tubes embedded in dry ice.

Serum Analysis

Blood was drawn via cardiac puncture and collected in Vacutainer tubes with lithium/heparin. Blood was centrifugated at 3,000 RPM at room temperature for ten

minutes to separate out plasma. Five hundred microliters of serum from each animals (n=33) were collected and stored at -20° C until shipped for analysis. Analysis was carried out by the Comparative Pathology Laboratory at the University of California, Davis by a Roche COBAS Mira Plus Chemistry Analyzer.

Microarray Analysis

Hippocampi were microdissected from the remaining unfrozen hemispheres (n=8/group) and placed on ice with RNA subsequently extracted using TRIzol reagent and precipitated with ethanol, reconstituted in RNAse-free water, and quantified and checked for RNA integrity with Agilent 2100 bioanalyzer RNA was then hybridized to an Affymetrix GeneChip Rat Genome 230-2.0 array. Scanned microarray images were analyzed using the MicroarraySuite 5.0 (MAS5; Affymetrix) algorithm. Probe set annotations were downloaded from Affymetrix. Data were analyzed with one-way ANOVA after removal of outliers and repeats.

DAVID (Database for Annotation, Visualization, and Integrated Discovery) functional analysis was completed on genes that were found to be significantly modulated. Gene accession numbers were uploaded into DAVID (http://david.abcc.ncifcrf.gov/), web-based software to determine functional pathways that are overrepresented by the gene list provided (Dennis et al. 2003). The functional pathways are listed in table format with pathway description, number of genes found representing the pathway, and the EASE score (p-value). The EASE score is a modified Fisher exact p-value and describes the enrichment of the pathway and the likelihood of finding said number of genes given the number of genes associated with a pathway as well as the number of genes detected with the genechip.

Brain Cholesterol Measurements

Cortical samples were homogenized in methanol and HCL and subsequently extracted with a methanol:chloroform extraction. The lipid layer was removed and dried under a stream of nitrogen and reconstituted in methanol. Free cholesterol measurements were done from aliquots of these samples. Other aliquots were saponified in KOH in methanol. Lipids were re-extracted, dried and reconstituted in the manner described above and these prepared samples were used to measure cholesterol esters. Samples were analyzed using Liquid Chromatography and tandem mass spectrometry with ABI-

4000 Q-TRAP hybrid triple quadrupole/iontrap mass spectrometer coupled with an Agilent 1100 liquid chromatography system. Measurements that were at were greater than two standard deviations away from the mean within a group were excluded.

Results

Animal Weights and Food Consumption: Short-term Treatment

Change in overall body weight was indistinguishable between groups over the course of treatment with a decrease in weight of less than 2% for all experimental groups. There was not a significant difference in daily food consumption across treatment cohorts within respective groups.

LTP Recording: Short-term Treatment

Long-term potentiation (LTP) was recorded in transverse slices of the hippocampus in field CA1. LTP was induced with theta burst stimulation (TBS) via a stimulating electrode placed in the stratum radiatum after 20 minutes of baseline recording (Figure 6.1A). Simvastatin (SIMVA) treated animals showed a significant increase in LTP as compared to control and atorvastatin (ATORVA)-treated animals. The slope values of the field excitatory post-synaptic potentials (fEPSP) during the last fifteen minutes of recording were significantly greater in slices prepared from SIMVA-treated animals.

There were no significant differences in the mean baseline amplitudes across the treatment groups (mean baseline amplitudes of the EPSP ± SE: CON -1.032mV ± 0.073, SIMVA -1.167 mV ± 0.09, ATORVA -0.887 mV ± 0.082; one-way ANOVA).

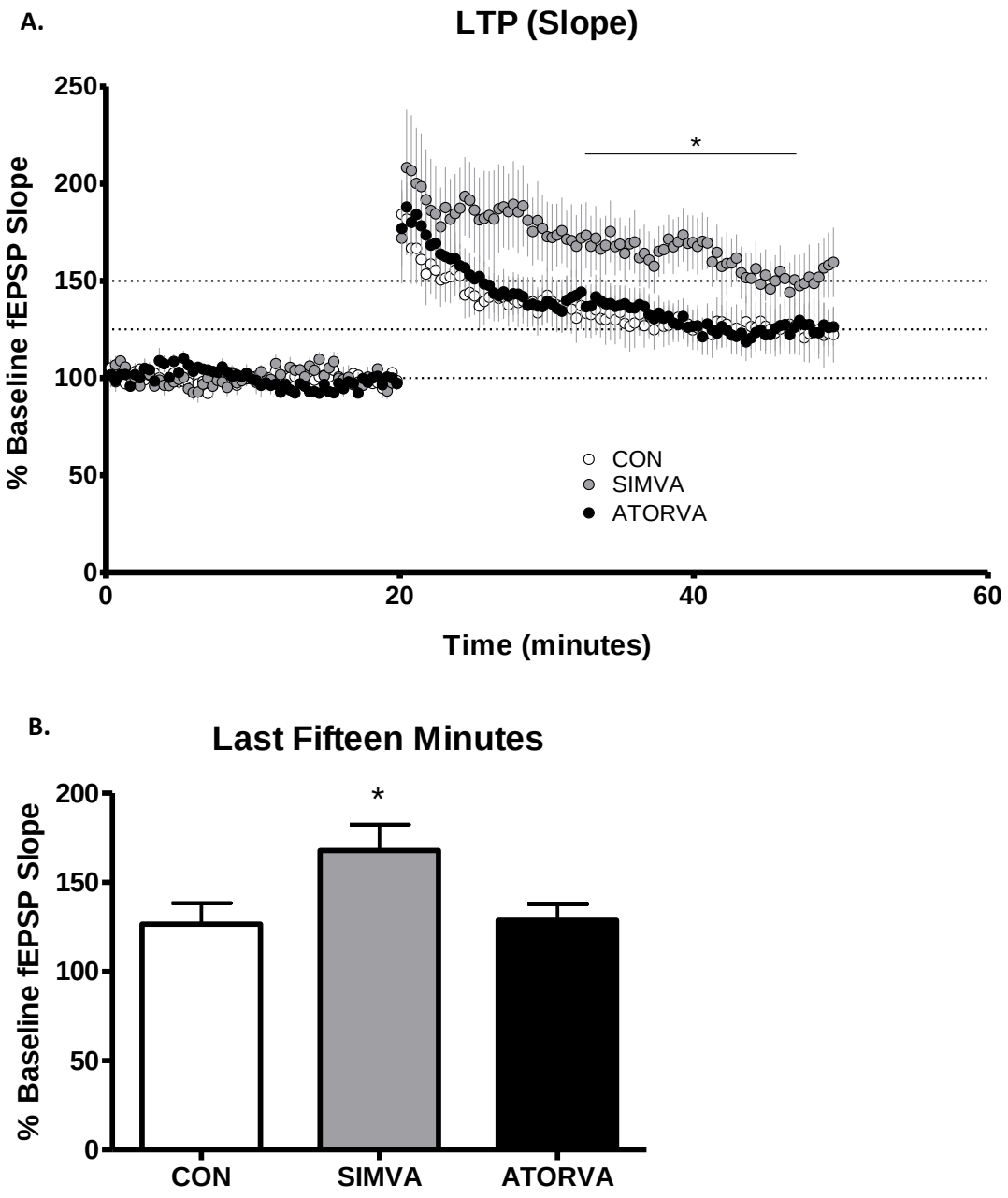

Figure 6.1: Long-term potentiation recorded in the CA1 region of the hippocampus in mid-aged F344 rats treated for 1-2 months with statins. **A.** Simvastatin significantly enhanced LTP as measured by the slopes of the EPSPs compared to both control and ATORV- treated animals(n=9-11/group). **B.** The slopes of the EPSPs during the last fifteen minutes of recording were significantly greater than the slopes of both CON and ATORVA-treated animals (one-way ANOVA, Dunnett's *post hoc* *$p<0.05$).

AHP Recording: Short-term Treatment

Figure 6.2A is a representative image of an AHP following a burst of action potentials and the points at which the respective peaks were measured. AHPs were recorded from 22-25 pyramidal hippocampal neurons per treatment group with each group consisting of 9-11 animals. The mAHP was defined as the most hyperpolarized portion of the AHP and occurred within 50 ms following the end of the depolarizing stimulus. The sAHP was measured 800 ms after the end of the stimulus. There were no significant differences in the mAHP (Figure 6.6B) and the sAHP (Figure 6.2C) between the three treatment groups. However, statin treatment did significantly reduce the duration of the AHP (Figure 6.3), by approximately 33%.

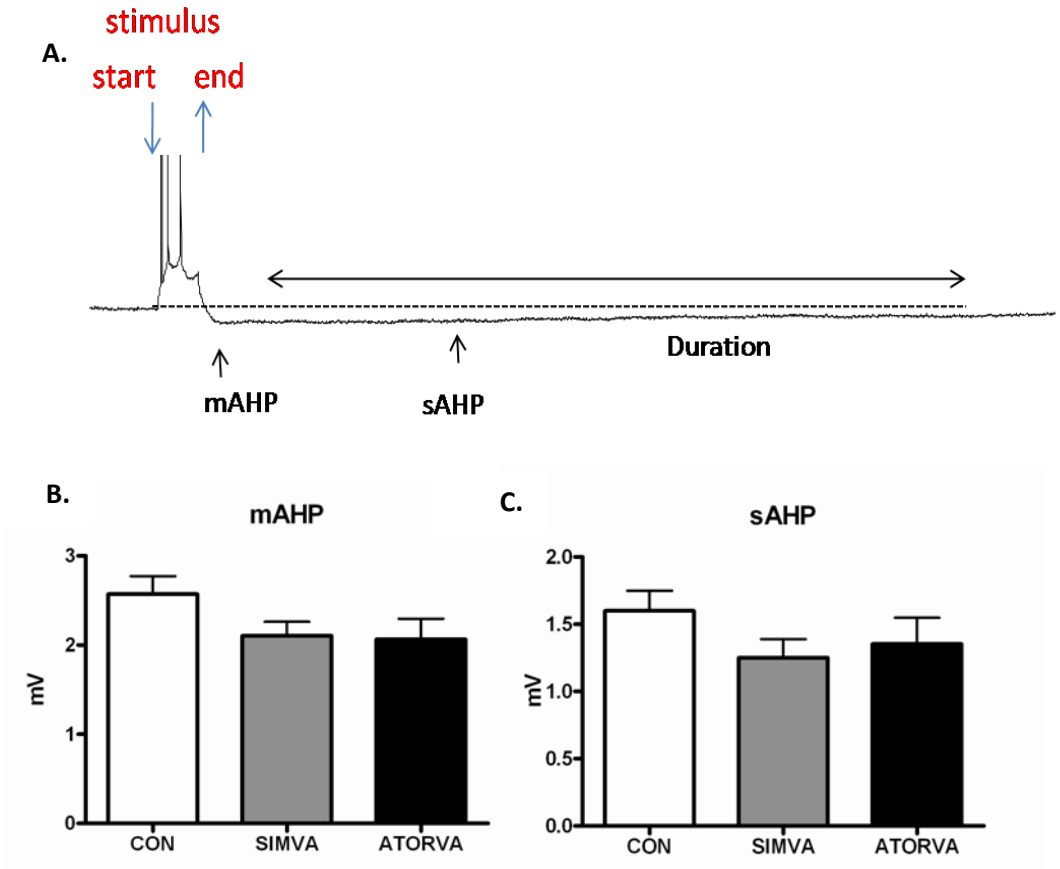

Figure 6.2: AHP measurements in the CA1 region of the hippocampus of mid-aged F344 rats treated for 1-2 months with statins. **A.** Representative image of an afterhyperpolarization showing stimulus, mAHP, sAHP and the duration of the AHP. **B&C.** No significant differences between groups were observed in regards to the peak values of the mAHP or the sAHP after depolarization (n=9-11/group: 22-25 cells/group).

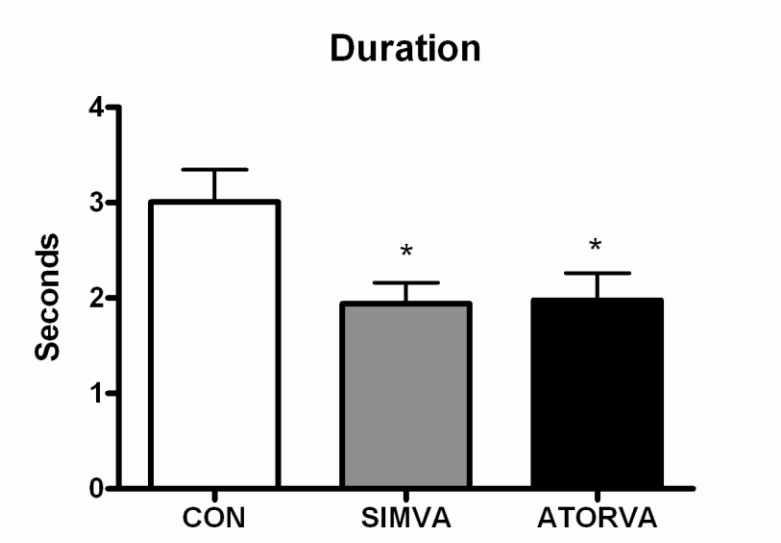

Figure 6.3: AHP measurement in the CA1 region of the hippocampus of mid-aged F344 rats treated for 1-2 months with statins. The duration of the AHP was significantly reduced by both simvastatin and atorvastatin treatment (one-way ANOVA, Tukey *post hoc* *p<0.05).

Peripheral Measurements: Long-term Treatment

There was a significant interaction effect of drug and time on body weight over the course of the study as seen in Figure 7.1A ($F=(_{18,\ 270)} = 2.0$; $p<0.01$; repeated measures 2-way ANOVA). SIMVA animals had significantly lower body weight compared to CON during the last two months of treatment (Bonferroni *post hoc*; $p<0.01$). Surprisingly, the average daily food intake did not differ significantly across the treatment groups (Figure 6.4B)

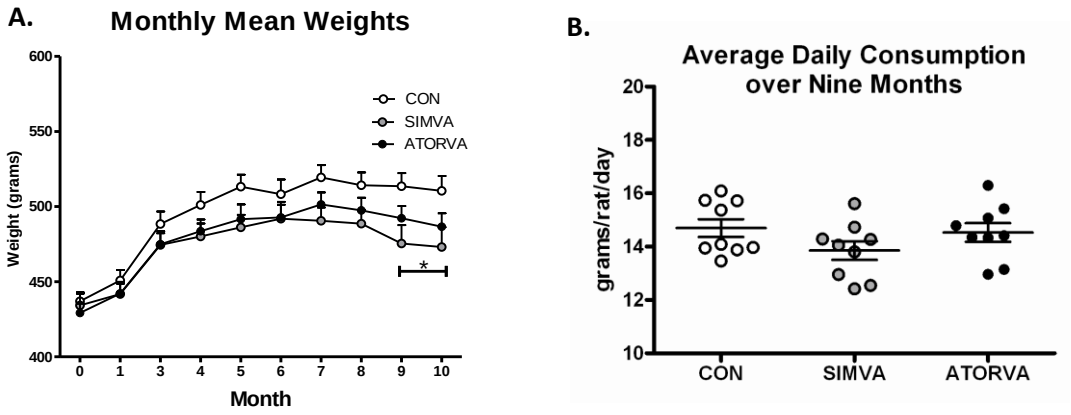

Figure 6.4: Monthly mean body weights and average daily food consumption of rats treated for 9 months with statins (n=11/group). A. Mean body weights were the same at the start of the statin treatment, but there was a significant drug effect on the groups over the course of the study. SIMVA-treated animals had significantly lower body weights than controls during the last two months of treatment (repeated measure 2-way ANOVA, Bonferroni *post hoc* *$p<0.05$). **B.** The approximated average daily food consumption was not found to be significantly different (one-way ANOVA).

An extensive blood chemistry profiles panel was determined from the serum of all the animals in the study to evaluate overall health and drug efficacy (Table 6.1). Results indicated that there was not a significant difference in the indicators of normal kidney, liver and muscle function. Unlike previous studies using statins in rats (Krause and Newton, 1995), we did see a significant reduction in total cholesterol levels with both SIMVA and ATORVA by 27% and 19% respectively compared to CON animals. SIMVA was able to significantly reduce LDL levels by 37%, whereas ATORVA lowered triglycerides by 59%. Select lipid markers affected by statin treatment are listed below in Table 6.1 and presented graphically in Figure 6.5.

Table 6.1: Blood serum analysis after 9 months of statin treatment (n=11/group). Serum levels of measured markers showed no effect of drug on key markers of normal liver, kidney and muscle function. Both SIMVA and ATORVA significantly lowered cholesterol levels by 27% and 19%, respectively. SIMVA had a greater lowering effect on LDL whereas Atorvastatin conferred a greater reduction of triglycerides. Neither SIMVA nor ATORVA affected HDL levels (one-way ANOVA; Tukey's *post hoc*; * = $p<0.05$, ** = $p<0.01$).

	ALT	BUN	CK	Ca2+	Cholesterol	Creatinine	Glucose	HDL	LDL	Triglyceride
	U/L	mg/dL	U/L	mg/dl	mg/dL	mg/dl	mg/dl	mg/dL	mg/dL	mg/dL
Control	59.3±6.2	14.8±0.4	863.2±138.6	11.3±0.04	175.7±8.8	0.4±0.01	234.1±25.1	81.9±5.1	39.3±3.8	120.8±23.7
Simva	46.4±4.5	17.1±1.0	1148.5±194.4	11.4±0.06	127.4±7.1	0.4±0.02	193.1±16.5	68.4±7.3	24.6±2.0	84.0±13.5
Atorva	49.1±3.7	16.1±0.5	1162.5±118.7	11.2±0.05	142.8±10.1	0.4±0.02	212.5±9.5	83.2±5.0	30.6±3.3	49.4±6.3
	ns	ns	ns	ns	SIMVA**,ATORVA*	ns	ns	ns	SIMVA**	ATORVA*

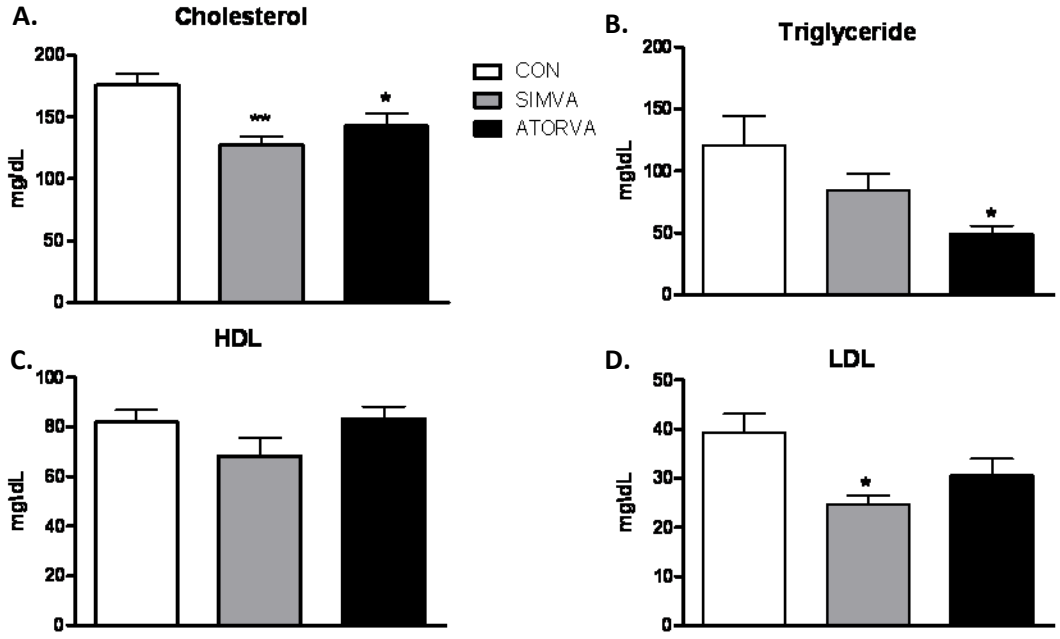

Figure 6.5: Key serum lipid markers in rats treated for 9 months with statins (n=11/group). A. Both SIMVA and ATORVA significantly lowered cholesterol levels by 27% and 19% respectively as compared to CON. **B.** ATORVA conferred a greater reduction of triglycerides than did SIMVA**. C.** Neither SIMVA nor ATORVA affected HDL levels **D.** SIMVA had a greater lowering effect on LDL (one-way ANOVA; Tukey's *post hoc* * = $p<0.05$, ** = $p<0.01$).

Locomotor Assessment

The rotorod task was used to assess potential motor impairments. It has been reported that statins may induce certain myopathies (Gotto, 2003), therefore it seemed reasonable to assess possible muscle impairments across treatment groups to determine the presence of side effects as well as to determine whether or not cofounds existed before running the animals in the MWM to assess learning and memory, given that performance in the maze could have been hindered by a lessened ability to swim. Animals performed the rotorod task similarly with no significant difference in either the capability to learn the task or in their ability to perform during the probe session suggesting that there was not a distinguishable difference in the rats in respect to locomotor activity.

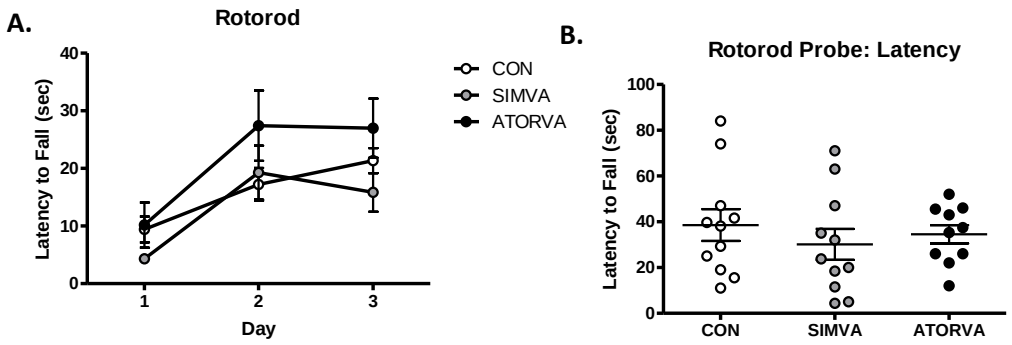

Figure 6.6: Locomotor assessment after 9 months of statin treatment using the rotorod task. There were no discernable difference between the treatment groups in their ability to learn the **(A)** rotorod task over time or their performance during the **(B)** probe session (n=11/group).

Learning and Memory Assessment

Animals were first trained to reach the platform for three days in the presence of a conspicuous cue hanging above the partially submerged platform. During cue training (Figure 6.7), there was no discernable difference between the treatment groups with respect to their ability to see the cue and find the platform suggesting that the animals had sufficient visual acuity to see the hanging spatial cues used to find the submerged platform during training sessions.

Seventy-two hours after the cue training on day 6, the groups began four days of training (3trials/day) absent the cue. There was a significant effect of SIMVA with respect to performance during the third trial of a given training session as measured by both latency and distance to the platform over the four days of training as shown in Figure 6.7B&C (repeated measure ANOVA; Fisher's PLSD *post hoc*; $p<0.05$).

During the probe session there was an effect of SIMVA treatment on performance. The percentage of time spent in the goal quadrant during the first thirty seconds of the probe free swim as well as the number of times the animals entered the goal quadrant was significantly decreased in SIMVA-treated animals compared to CON groups (Figure 6.8).

A.

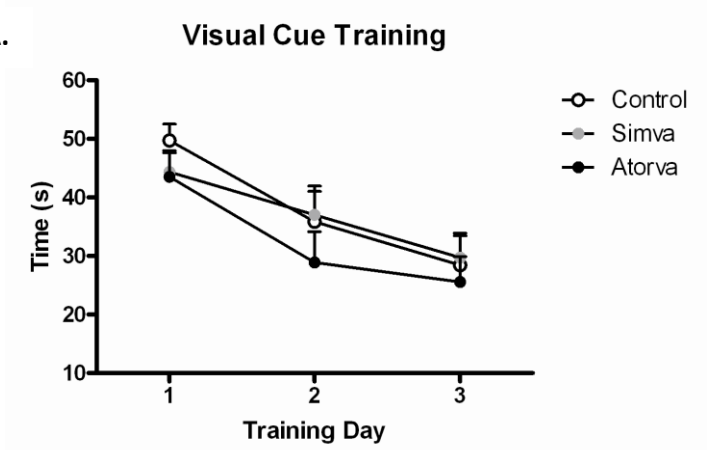
Visual Cue Training
Time (s)
60
50
40
30
20
10
1
2
3
Training Day
Control
Simva
Atorva

B.

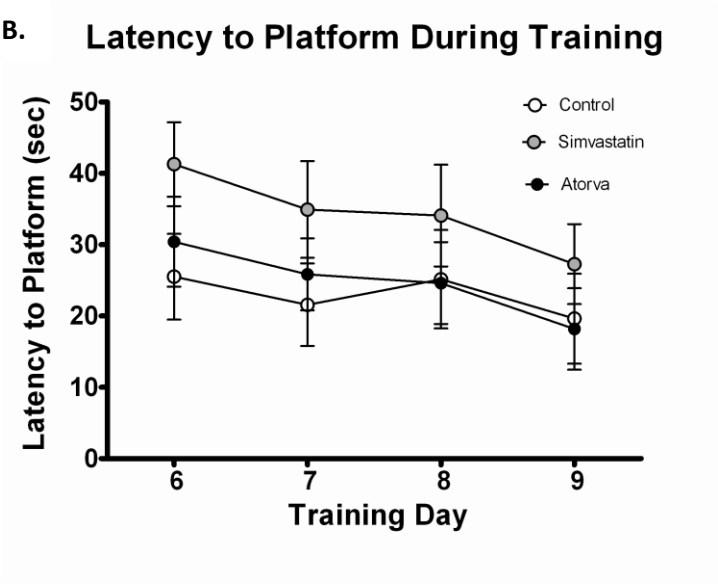
Latency to Platform During Training
Latency to Platform (sec)
50
40
30
20
10
0
6
7
8
9
Training Day
Control
Simvastatin
Atorva

C.

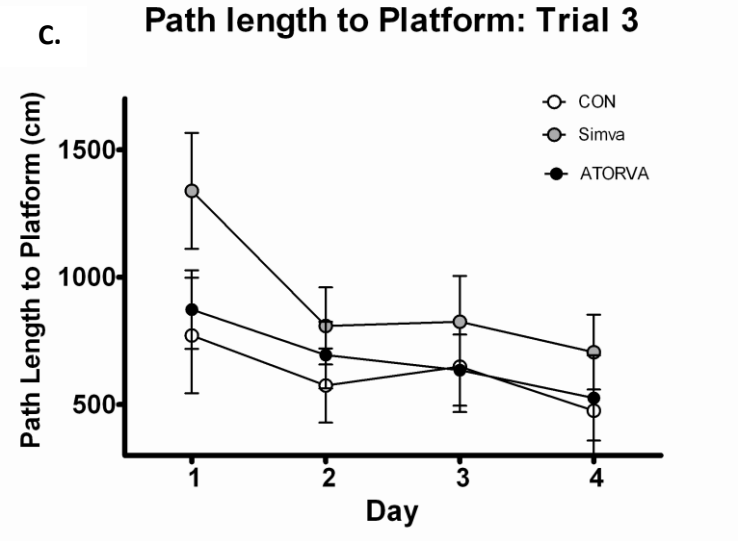
Path length to Platform: Trial 3
Path Length to Platform (cm)
1500
1000
500
1
2
3
4
Day
CON
Simva
ATORVA

Figure 6.7: MWM - Visual acuity and training assessment in rats treated for 9 months with statins. **A.** There was no significant difference between groups (n=11/group) during the three cue training sessions indicative of similar visual acuity across the three treatment groups with all animals showing a reduction in the latency to the platform over the course of cue training. **B.** SIMVA rats had a significantly greater latency to the platform during the third trial of the respective training sessions over the four days as compared to both control animals and those treated with atorvastatin ($F_{(2,84)} = 3.9$; $p<0.05$ repeated measure ANOVA, Fisher PLSD $p<0.05$). **C.** There was a SIMVA effect on the distance to the platform during the same trial (repeated measure 2-way ANOVA $F_{(2,75)} = 4.5$; $p<0.05$, Fisher PLSD $p<0.05$).

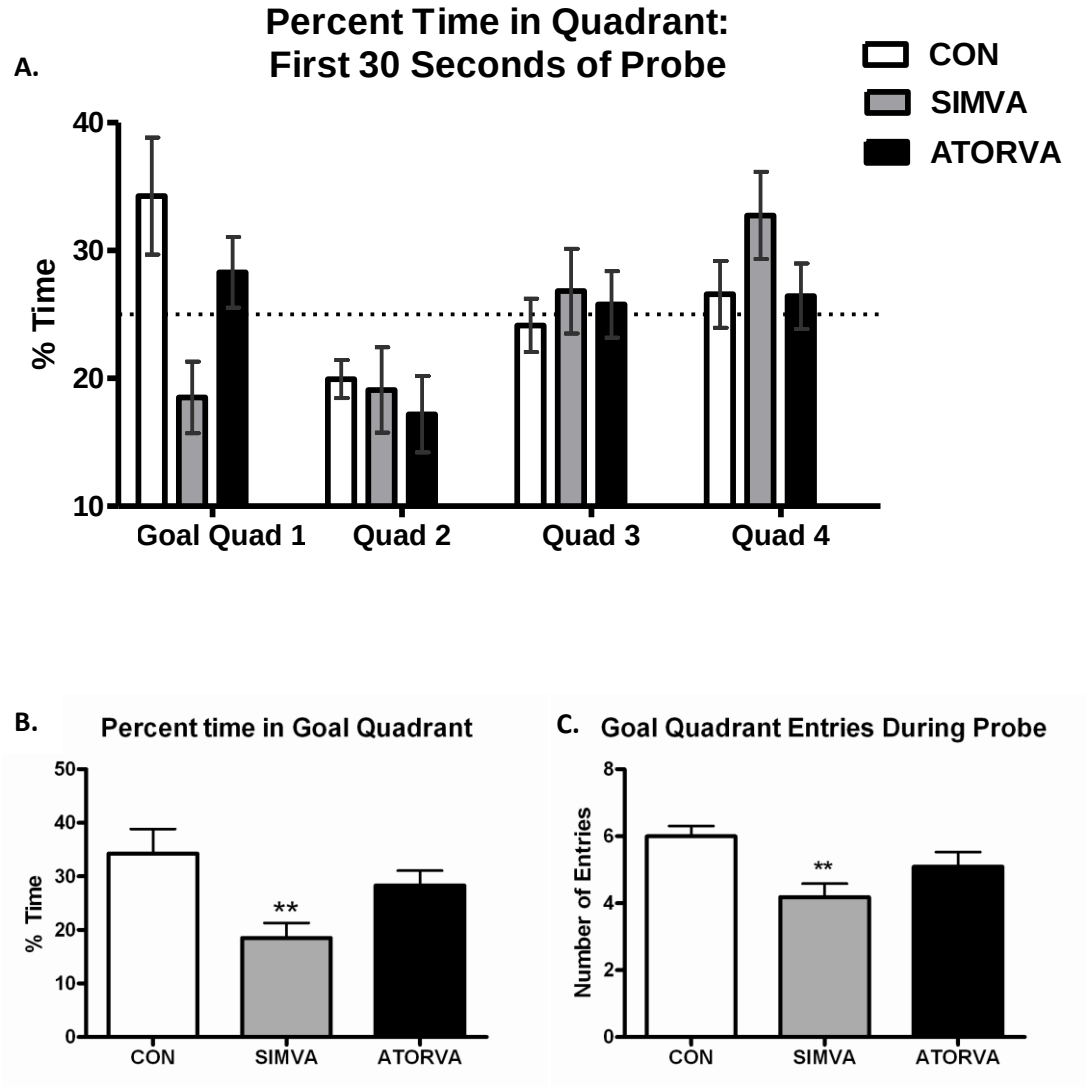

Figure 6.8: MWM - Memory retention during probe session in rats treated for 9 months with statins. **A.** Percentage of time during the first thirty seconds spent in each quadrant by the respective treatment groups (n=11/group). The dotted line is set at 25%, the percentage of time that would be spent in each quadrant by chance. **B.** SIMVA-treated animals spent a greater percentage of time during the first thirty seconds of the probe trial within the goal quadrant compared to controls (Kruskal-Wallis, Dunn's *post hoc* ** $p<0.01$). **C.** SIMVA-treated rats entered the goal quandrant significantly less than did controls during the probe (one-way ANOVA, Tukey *post hoc test* **$p<0.01$).

Brain Cholesterol Levels

Cholesterol levels were measured from cortical tissue from all the animals in the study using LC-MS. Cholesterol levels were significantly reduced after 9 months of treatment, with the majority of measured cholesterol being of the unesterified species as has been previously found (Dietschy and Turley, 2004). Cholesteryl esters species were negligible after saponification. Cholesterol was reduced by about 30% by ATORVA (Figure 6.9). The results reported here are quantitatively comparable to those levels previously reported in the literature (Dietschy and Turley, 2004). Quantities are reported at mg/gram of weight tissue.

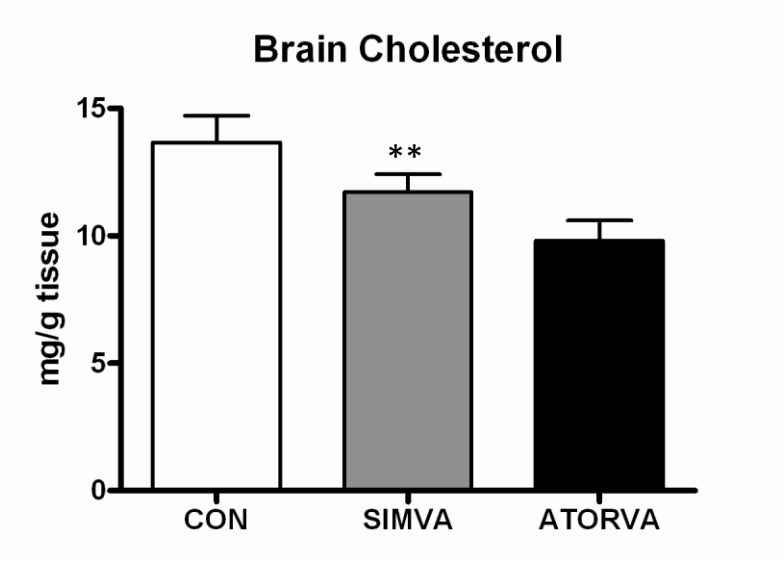

Figure 6.9: Quantitative analysis of cholesterol levels in cortical tissue from rats treated with statins for 9 months using LC-MS. There was a significant effect of drug on cholesterol levels in the brain (n=11/group; one-way ANOVA). Atorvastatin significantly reduced cholesterol levels as compared to controls (Tukey *post hoc;* **$p<0.01$).

Microarray Analysis

Long-term statin treatment with SIMVA and ATORVA upregulated 21 different genes and downregulated 31 and 25 different genes respectively. SIMVA and ATORVA mutually upregulated 23 genes and downregulated 17 genes. Supplemental tables listing all modulated genes can be found here: D:\Long-term_Statin_microarray_supplement_table.pdf.

The numbers of genes that are listed in Table 6.2 were exceptionally low and were selected based on a very stringent p-value (0.005) to insure a median false discovery rate (FDR) of 0.29. As a result, the list of functional pathways modulated by statin treatment revealed by the original DAVID analysis was similarly brief. To provide a larger pool of genes to use in a second DAVID analysis, the p-value cutoff was loosened to 0.015, which generated a gene list with a median FDR of 0.34. The pathways described in Tables 6.3-6.4 represent those pathways found to be overrepresented by those genes with a p-value of 0.015 and a median FDR of 0.34. DAVID functional analysis (Table 6.3) revealed that SIMVA and ATORVA modulated distinctly different functional pathways, with SIMVA significantly upregulating genes involved in lipid biosynthetic pathways whereas ATORVA did not.

Table 6.2: Microarray analysis – number of genes found to be significantly modulated by 9 months of statin treatment. A. Number of genes significantly upregulated and downregulated at a p-value of 0.005, median FDR of 0.29 by both SIMVA and ATORVA after 9 months of treatment.

Group	Upregulated	Downregulated
Simvastatin	21	31
Atorvastatin	21	25
Modulated by Both	23	17

Table 6.3: DAVID functional analysis – functional pathways significantly modulated by 9 months of simvastatin treatment.

Upregulated by Simvastatin	#	p-value
Sterol biosynthetic process (*cytochrome P450-51, farnesyl diphosphate farnesyl transferase 1, sterol-C4-methyl oxidase-like, mevalonate decarboxylase, 3-hydroxy-3-methylglutaryl-Coenzyme A synthase 1, farnesyl diphosphate synthetase)*	8	2.23E-09
Lipid metabolic process *(acyl-coA synthetase short-chain family member 2, hydroxyacyl-CoA dehydrogenase trifunctional protein subunit A, thyroid hormone responsive)*	11	0.001341
proteolysis *(protease 26S subunit-ATPase 5, matrix metallopeptidase 9, ubiquitin specific peptidase 36, calpain 7)*	8	0.022094
positive regulation of cellular metabolic process *(cholecystokinin, activating transcription factor 4, RAR-related orphan receptor beta)*	6	0.033624
Downregulated by Simvastatin	**#**	**p-value**
Nervous system development (fasciculation and elongation protein zeta 2, ciliary neurotrophic factor, glutamate receptor-metabotropic 5)	7	0.034699

Table 6.4: DAVID functional analysis – functional pathways significantly modulated by 9 months of atorvastatin treatment.

Upregulated by Atorvastatin	#	p-value
Intracellular organelle part/Mitochondrial Part (*sterol regulatory binding transcription factor, ATP-binding cassette, AC8, survival motor neuron, NADH dehydrogenase, mitochondrial ribosomal protein)*	20	0.001826
Calcium ion binding/voltage-gated calcium channel complex *(calcium channel-voltage dependent, L type, alpha 1C subunit, cadherin 23, ninein, phospholipase, calcium channel, voltage-dependent, gamma subunit 5)*	7	0.045125
Downregulated by Atorvastatin	**#**	p-value
Response to chemical stimulus (solute carrier family 18 (vesicular monoamine) member 1, interleukin 6 receptor (alpha), adipose differentiation related protein, signal transducer and activator of transcription 5B, parkin)	8	0.007404
neurotransmitter transport *(syntaxin 4A, parkin)*	3	0.021786

Discussion

Long-term treatment of mid-aged rats for 9 months with two statins which differ in lipid solubility (simvastatin being more lipophilic than atorvastatin) revealed very distinct effects on the brain *(discussed below).* Statin-specific effects were also observed with short-term statin treatment (1-2 months). These initial studies showed a significant enhancement of LTP only in simvastatin-treated animals. Yet both statins reduced the duration of the AHP (*afterhyperpolarization*). The AHP is associated with cognitive processes and aged animals with impaired memory also have larger AHPs (Landfield, Pitler, 1984; Tombaugh et la., 2005; Gant et al., 2006). The link between hippocampal-dependent memory and the size of the AHP was demonstrated in a series of studies by Disterhoft and colleagues (Disterhoft et al., 1986; Moyer et al., 1990; Power et al., 1997). Typically, a reduction in the AHP would be associated with an increase in excitability and neuronal firing and, thus, would be expected to facilitate LTP. In the present studies, such results were seen only with simvastatin, with atorvastatin only reducing the AHP, suggesting that statins may not have mutual effects on pathways that modulate the AHP and LTP. It is important to note that the AHP represents an electrophysiological response of an individual neuron. LTP, on the other hand, represents a synaptic response of a population of neurons and is dependent on the integration of multiple signaling pathways which control and fine-tune plasticity. Thus, it may not be surprising that occasionally changes in the AHP are not associated with corresponding changes in LTP. These results raise the question of what might be the basis for the statin-specific effects on LTP. One potential mechanism may be found in the different pattern of hippocampal gene expression observed in the animals that were treated with the long-term statins (*see below*). Alternatively, there may be a selective effect of statins on membrane cholesterol.

Long-Term Statins and Reductions in Brain Cholesterol. We found that very long-term treatment (9 months) with simvastatin and atorvastatin reduced brain cholesterol by ~15% and 30%, respectively (Figure 6.9). However, the reduction in brain cholesterol was significant only with atorvastatin. Long-term statin treatment may reduce brain cholesterol by two different mechanisms. A statin (e.g., simvastatin) that crosses the blood brain barrier (BBB) more readily could potentially have a greater effect on inhibiting cholesterol synthesis in the brain than another that is less lipophilic (e.g.,

atorvastatin). Alternatively, even though it may be against conventional thought, brain cholesterol may be affected by peripheral cholesterol levels. Thus, independent of its lipophilicity, any statin could possibly cause cholesterol depletion of the brain, indirectly, by significantly reducing peripheral cholesterol levels. Such a reduction in peripheral levels could create a significant cholesterol concentration gradient across the BBB, thereby, facilitating efflux of cholesterol from the brain. Our microarray results suggest that the two statins have very different effects on hippocampal gene expression and that both of the mechanisms mentioned above may be playing a role in modulating brain cholesterol concentrations. Simvastatin, but not atorvastatin, significantly upregulated genes in the cholesterol biosynthesis pathway, perhaps in an attempt to compensate for the chronic inhibition of HmG-CoA reductase (Figure 6.13). The microarray results, along with measures of brain and serum peripheral cholesterol, would seem to indicate that two statins are depleting cholesterol in different ways. In addition to inhibiting peripheral cholesterol synthesis, the more lipophilic simvastatin crosses the BBB and directly inhibits cholesterol synthesis. Comparatively, brain cholesterol synthesis would be inhibited to a lesser degree with the less lipophilic atorvastatin, perhaps reflected by a lack of upregulation of cholesterol biosynthesis genes. Like simvastatin, atorvastatin lowers serum cholesterol levels (and triglycerides) significantly (Table 6.1 and Figure 6.5), creating a cholesterol sink in the periphery. Together, these results may provide an explanation for the significant decrease in brain cholesterol in the atorvastatin animals (Figure 6.9). In these animals, cholesterol synthesis is not upregulated in the brain as it is with simvastatin and, therefore, the brain is unable to compensate for the cholesterol loss to the periphery. The low levels of triglycerides in the periphery could also be acting to pull triglycerides from the brain as well, reducing available acetyl-CoA precursor needed for cholesterol synthesis.

Effects on LTP. These differences may also help to explain the different effects seen with short-term treatment (1-2 months) on LTP where simvastatin, but not atorvastatin, increased LTP (Figure 6.1). A prior study has shown that isoprenoids, byproducts of cholesterol synthesis via the mevalonate pathway, play an important role in the induction and maintenance of LTP (Kotti et al., 2006). Inhibition of hippocampal LTP, following acute treatment of slices with a statin, was found to be due to a reduction

in levels of geranlygeraniol, an isoprenoid in the mevalonate pathway. In addition to an upregulation of cholesterol synthesis, our microarray results also show that simvastatin, but not atorvastatin, upregulated genes involved in the formation of the isoprenoids essential for LTP (Figure 6.10). Thus, this action of simvastatin, observed with long-term treatment, may be the underlying basis for the robust effect on LTP.

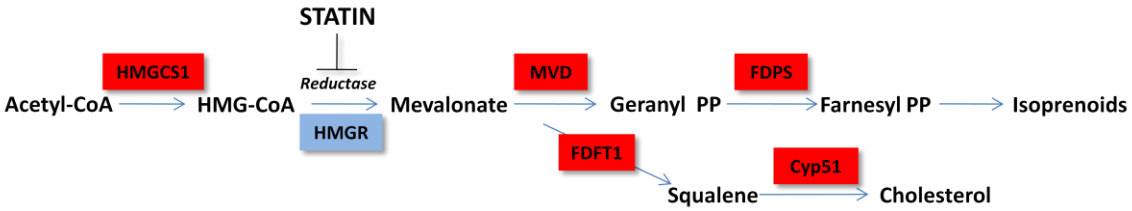

Figure 6.10. Simvastatin induced increase in genes involved in isoprenoid production. Upregulated genes are shown in red.

Effects on Behavior. Yet, these results on LTP after short-term treatment are seemingly at odds with those observed in animals treated with long-term statins. After 9 months of treatment, animals treated chronically with simvastatin performed more poorly on the MWM. As LTP was not measured at 9 months, it is not known whether the positive effects of simvastatin on LTP are still present. If effects on LTP were still maintained at 9 months, then there would appear to be an apparent dissociation between the LTP results and the impaired memory as reflected by behavior in the MWM at 9 months. These results may reflect a competing process induced by chronic cholesterol depletion and the activation of an astrocyte/myelinogenic pathway known to correlate with cognitive impairment in brain aging (Blalock et al., 2003; Rowe et al., 2007; Kadish et al., 2009). This is supported by recently obtained IHC results indicating that simvastatin treated rats had activated, hypertrophic astrocytes in the stratum radiatum of the hippocampus as indicated by significantly greater GFAP staining (Figure 6.11). Furthermore, simvastatin appeared to selectively increase a myelin marker, CNPase, in the same brain region (Figure 6.12). An integrative model taking into consideration the effects on behavior, plasticity and gene expression is shown in Figure 6.14.

Statin Effects in Humans. The compensatory mechanisms seen in the present studies may also be present in humans. A small pilot study in hypercholesterolemic patients at risk for AD showed that treatment with either simvastatin or atorvastatin reduces serum cholesterol and also results in a corresponding decrease in CSF cholesterol levels (reflecting brain cholesterol) during the initial 6 months of treatment. However, after this initial treatment period, the CSF levels return to nearly baseline levels. The same decrease followed by a return to baseline is seen with measures of CSF lathosterol and 24S-hydroxycholesterol, representing markers of cholesterol synthesis and degradation, respectively (Evans et al., 2009). Similar results have been observed in subjects with normal cholesterol levels following statin treatment (Fassbinder et al., 2002). These results are consistent with a turnover rate for brain cholesterol estimated to be ~6 months, the time frame during which a return to baseline levels was seen in the CSF. The parallel drop in 24S-hydroxycholesterol levels suggest that the CNS is compensating for a reduction in synthesis by decreasing cholesterol breakdown, thus allowing it to maintain some level of brain cholesterol. However, as the effects of turnover are gradually experienced by the brain, the brain attempts to compensate by increasing synthesis, thus overriding the effects of chronic statin treatment on the brain. The degree to which such processes occur may depend on duration of treatment as well as the type of statin.

The implications of the results of the present study need to be considered within the context of human brain aging and associated neurodegenerative disorders such as AD. Recent calls urge more aggressive and earlier treatment of hypercholesterolemia with statins in order to reduce age-related cardiovascular risk factors (Steinberg et al., 2008). This approach would appear to have a beneficial effect on the brain as well, given a recent study showing that high serum cholesterol levels at mid-life increases risk for AD as well as vascular dementia (Solomon et al., 2009). However, this aggressive approach must also take into consideration another recent report showing that lower serum cholesterol levels after the age of 65 seem to be predictive of impaired cognitive functioning (van den Kommer et al., 2009). Our results, coupled with those in the literature, would suggest that more caution be exercised when prescribing statins to the elderly and that reports of cognitive impairment on a statin be taken seriously. The

results presented here suggest that chronic use of a lipophilic statin that can more readily penetrate the BBB may be more deleterious to cognition than a less lipophilic statin. There are, undoubtedly, many beneficial effects of statins in the periphery and the present studies also show potentially beneficial effects in the brain (e.g., increased LTP). Reports showing that lower cholesterol levels later in life may increase risk of cognitive decline may indicate that statins should not be given for very long periods (e.g., years) , but rather intermittingly for shorter periods during mid-life. This type of more limited treatment could potentially confer reduced risk of heart attack and stroke and potentially reduce the risk of developing AD later in life.

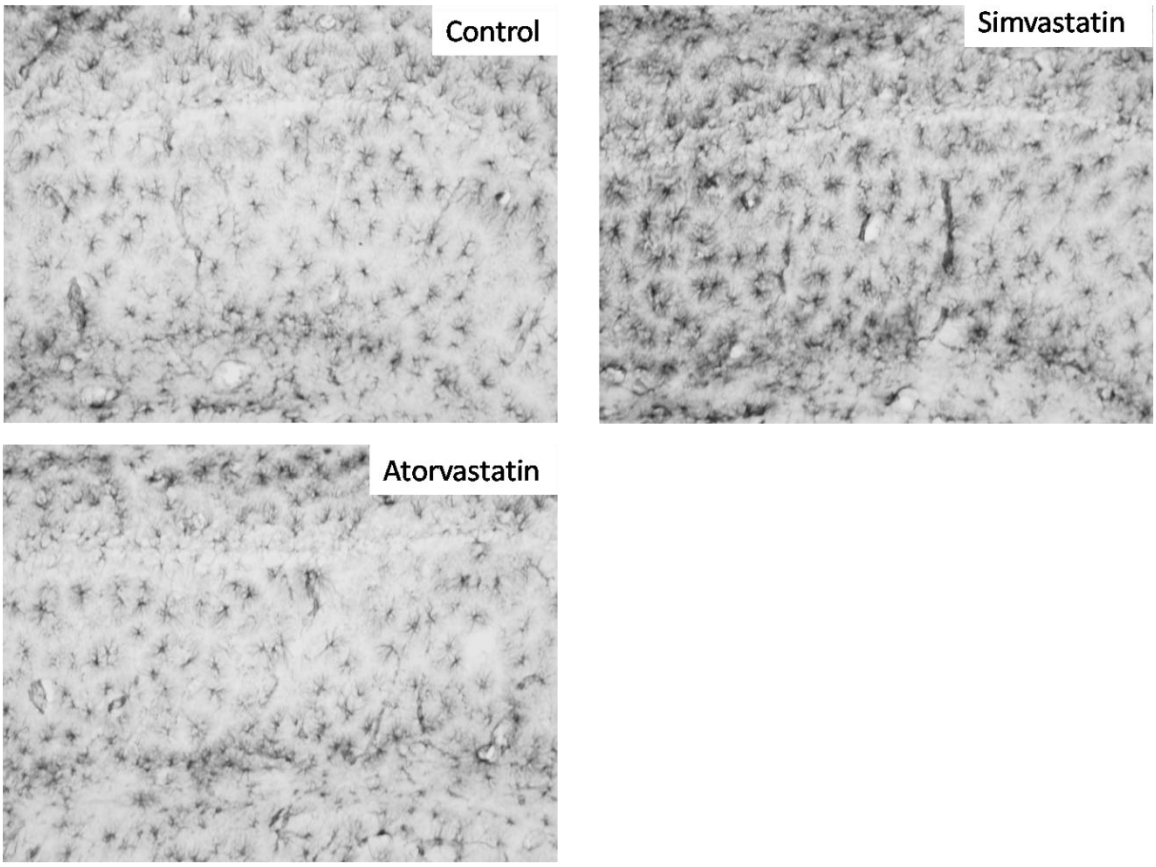

Figure 6.11: GFAP staining in the stratum radiatum of rats treated for nine months with atorvastatin or simvastatin. IHC images reveal activated hypertrophic astrocytes within the stratum radiatum of SIMVA-treated rats. Semiquantitative analysis of the optical density measures within the hippocampi of SIMVA-treated animals revealed significantly higher levels of GFAP (one-way ANOVA, Tukey *post hoc;* $p<0.05$).

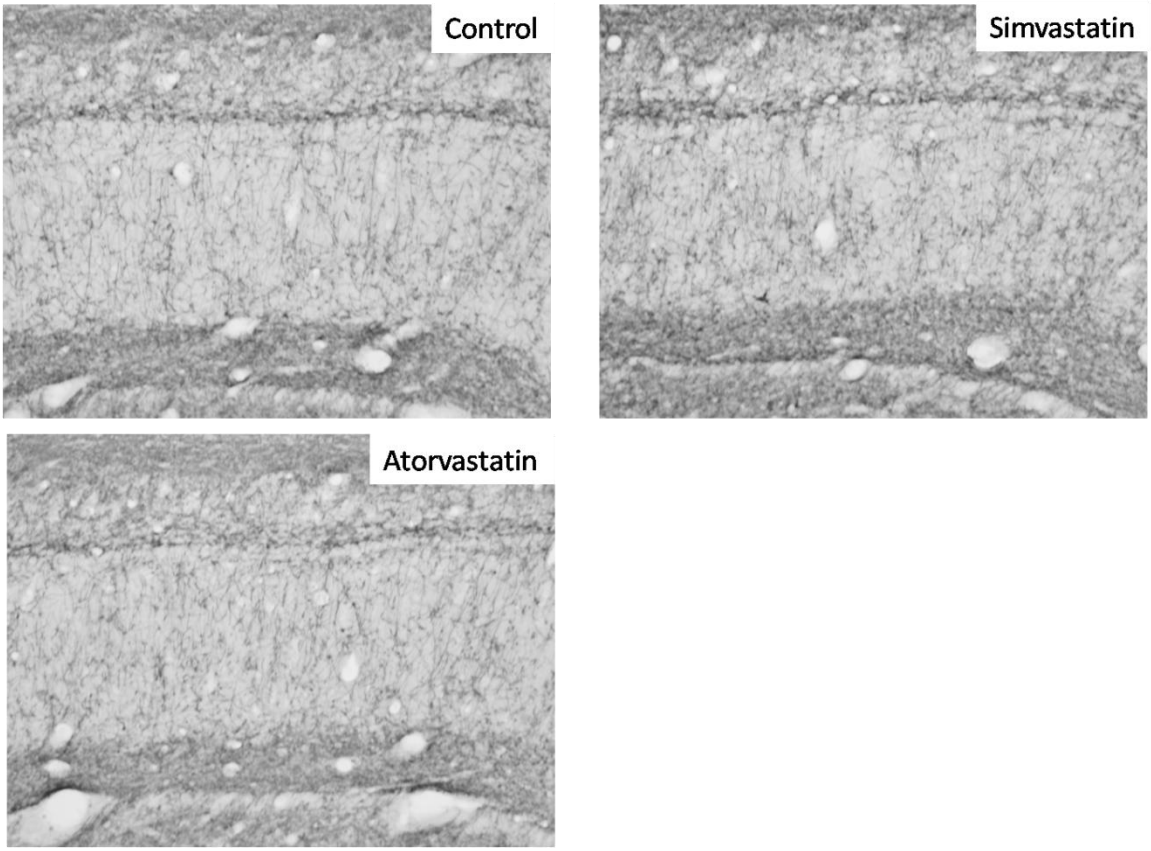

Figure 6.12: CNPase staining in the stratum radiatum of rats treated for nine months with atorvastatin or simvastatin. IHC Semiquantitative analysis of the optical density measures within the hippocampi of SIMVA-treated animals revealed significantly higher levels of CNPase indicative of myelogenesis (one-way ANOVA, Tukey *post hoc;* $p<0.05$).

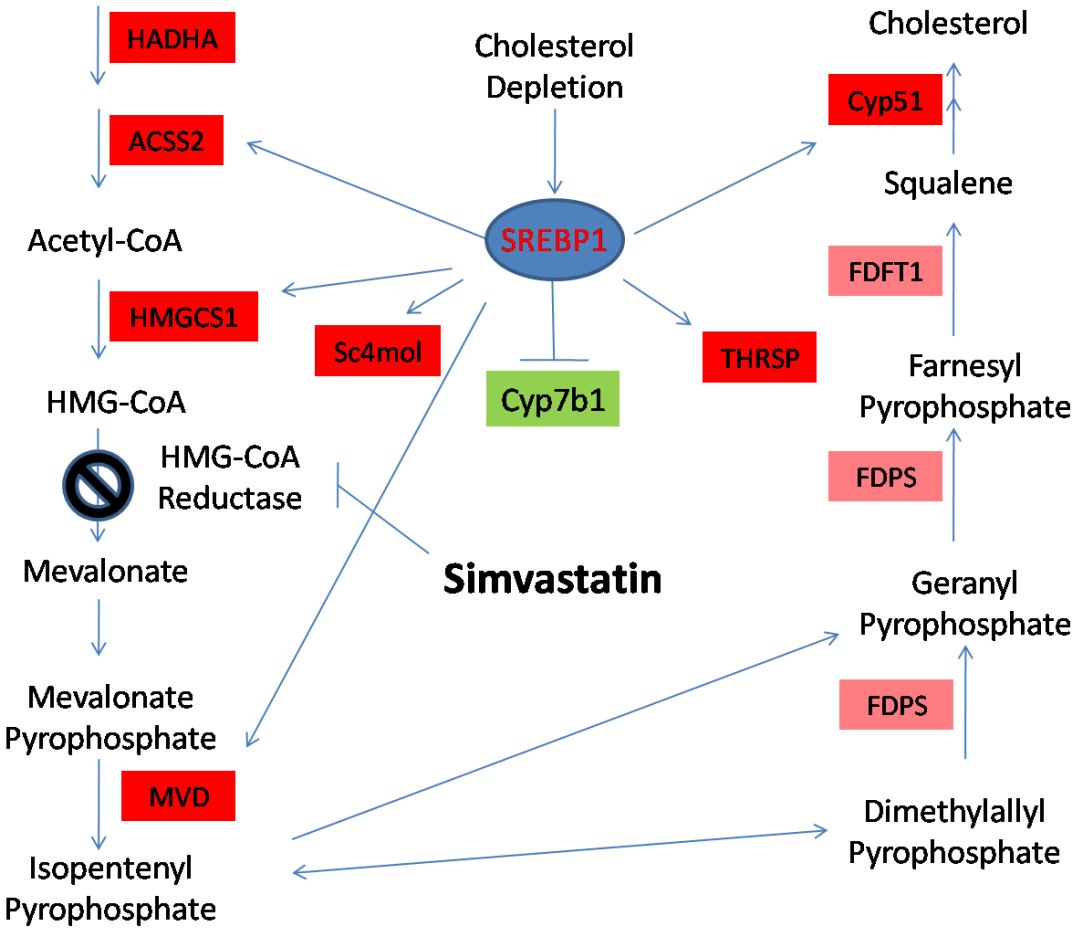

Figure 6.13: Specific effect of simvastatin on genes within the cholesterol biosynthetic pathway. Genes labeled in red and green are significantly upregulated or downregulated respectively at a $p<0.005$ with median FDR of 0.29. Genes shaded in pink were significant at a $p<0.015$, but with a median FDR at 0.34. David functional analysis also indicated a significant modulation in the cholesterol biosynthetic pathway by SIMVA treatment. This indicates perhaps a compensatory upregulation of genes involved in cholesterol synthesis upon inhibition of HmG-CoA reductase both upstream and downstream of the targeted site of drug action.

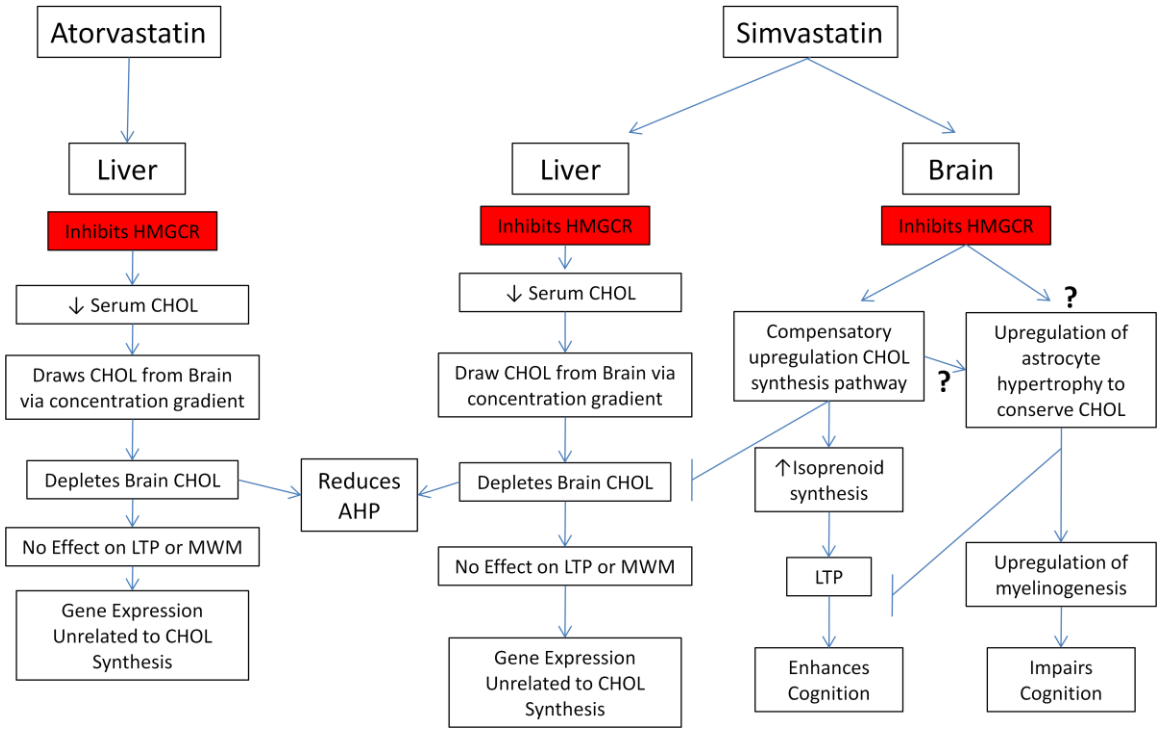

Figure 6.14: Speculative model of the effects of long-term statin treatment on the aging brain. Brain cholesterol depletion leads to the simvastatin-selective increase in cholesterol synthesis pathways in the brain, which can potentially improve early LTP, but also increases astrocytic activation, mimicking processes observed in the normal aging brain, thus acting to increase the rate of cognitive decline.

Overall Conclusions

We originally proposed to elucidate the role lipid metabolism plays in normal and pathological brain aging. The work was driven by two main hypotheses: 1). Chronically activating the liver X receptor (LXR), which in turn drives the expression of genes involved in cholesterol metabolism, transport, and efflux will reduce pathology and cognitive deficits associated with AD as modeled in mice, and 2). Chronically inhibiting cholesterol synthesis in mid-aged rats, at an age when signs of brain aging begin to appear, will attenuate cognitive deficits and electrophysiological correlates in the aging brain.

The studies were, by design, two-pronged in nature. To test the first hypothesis, a potent LXR agonist was administered chronically to two different transgenic AD mouse models, which were then assessed using a battery of measures, including memory paradigms, electrophysiological measures of synaptic plasticity (LTP) and neuronal excitability (AHP), brain pathology assessment, and extensive microarray analysis. To test the second hypothesis, we chronically treated mid-aged Fischer 344 rats with two different HMG-CoA reductase inhibitors (statins) and used similar techniques and outcome measures

Besides providing insight into the role that cholesterol metabolism plays in aging and neurodegenerative disease, the results from these studies, also have far-reaching clinical implications with respect to both interventions. LXR agonists have been considered as a possible therapy for atherosclerosis as well as AD (Repa and Mangelsdorf, 2002; Bruemmer and Law, 2005; Geyeregger et al., 2006; Zelcer et al., 2007), yet, there have been few studies that have treated animal models for the length of time presented here and they typically do not report any peripheral side effects. Statins are among the most widely prescribed drugs in the United States and simvastatin is available over-the-counter in much of Europe. Even with prescriptions in the millions, very few studies, especially long-term intervention studies, as the one described here, have been completed which focus on effects on the brains.

The LXR agonist used in both the 3xTg- and 2xTg-AD models is very potent but has very reliable effects on gene expression which likely underlie decreases in AD-

associated pathologies and apparent improvements in cognition in AD mouse models (Sun et al., 2003; Koldamova et al., 2005; Riddell et al., 2007). Also consistent with some of the gene pathways targeted in the brain (e.g., fatty acid synthase), is the observation of severe peripheral side effects including liver steatosis and cardiac hypertrophy. These effects likely represent actions of the LXR agonist at the same target pathways in the periphery. Despite some potentially beneficial effects in the brain (e.g., the positive effect on behavior), the peripheral side effects raise doubts as to whether this drug could ever be used clinically. Interestingly, much of what LXR agonist treatment does in the brain mirrors many of the molecular changes that occur in the brain at midlife. As stated before, LXR-β is upregulated at midlife in rats along with cholesterol trafficking perhaps as a compensatory mechanism (Rowe et al., 2007; Kadish et al., 2009). Therefore, by chronically activating LXR a situation is created in the brain that mimics many of the molecular alterations seen at midlife. This includes upregulation of Apoe and Srebf as well as genes associated with acyltransferase activity (possessing similar cholesterol storage promoting properties as SOAT1), which were found to be present at higher levels in the brains of aging rats. Normally, the LXR pathway is upregulated in response to higher concentrations of cholesterol, which as noted above, may be the case for the aging brain. In the aging brain, such an upregulation of this pathway may be compensatory, yet the effects of such an upregulation may contribute to age-related deficits; thus chronic activation of this pathway may have the unintended effect of creating a premature aging effect.

Similarly, statins present with their own set of potential problems with long-term use. The study design reflects circumstances in which statins are prescribed in a patient population which are typically initiated at midlife and maintained for a chronic (often indefinite) period. Such a study has not been carried out in rodents, and because of this, several of our findings appear compelling as well as novel. First, unlike prior observations showing no change in serum cholesterol levels with *in vivo* statin treatment, decreases in peripheral cholesterol levels were detected following chronic treatment in aged rats. Secondly, statins were able to reduce brain cholesterol concentrations. Finally, statins with differing lipophilicities had different effects on the brain in relation to both cholesterol levels as well as on cognition. But, where many epidemiological studies have

suggested that a more lipophilic statin, like simvastatin would confer greater benefit on cognition and reduce AD risk, it was found that in fact simvastatin, after very long-term chronic treatment, appeared to be detrimental to the brain. Animals treated with simvastatin performed worse on the memory recall components of the MWM, had greater GFAP staining in the hippocampus indicative of astrocyte reactivity (and a marker of brain aging) and had greater CNPase staining in the hippocampus suggestive of increased myelinogenesis. Simvastatin also had a selective effect on the upregulation of cholesterol synthesis pathways as well. Again, we see similarities between a select drug effect and normal aging. Thus, the effects of simvastatin are similar to those of aging including the associated decrease in memory, increase in astrocyte reactivity, and increase in myelinogenesis. In fact, in some respects, it appeared to produce an accelerated aging phenotype. Neither statin, simvastatin nor atorvastatin conferred any detectable benefit to the aging brain, but atorvastatin failed to exacerbate deficits.

With both the LXR agonist and the statins, two different aspects of cholesterol metabolism were modulated, cholesterol trafficking (transport and efflux) and synthesis. Interestingly, both treatments appeared to potentiate some aspects of brain aging. Perhaps both approaches are affecting cholesterol trafficking and myelinogenesis, suggesting that cognitive deficits first appearing at mid-age may be attributed to the dysregulation of the movement and deposition of cholesterol within the brain, which in turn affects myelinogenic processes. As the brain ages, the degradation of myelin about axons along with remyelination of these axons continues. This can lead to the re-myelination of already myelinated fibers along with changes in nodal size and proximity, both of which can reduce signaling efficiency along the fiber (Peters 2009).

It is possible that as the brain ages, and cholesterol levels become excessive, that some of this brain cholesterol is stored as myelin. This would require the efflux of cholesterol from astrocytes to oligodendrocytes ensheathing axons using mechanisms enabled by activation of the LXR pathway. In the case of chronic simvastatin use, we see a compensatory upregulation of genes involved in cholesterol synthesis which likely takes place in brain astrocytes. This upregulation of cholesterol biosynthesis, in the context of an aging brain, may result in a reactive astrocyte phenotype and upregulated

myelinogenesis, which may potentially occur in response to the presence of excess free cholesterol.

Accordingly, these results do not support the long-term use of either an LXR agonist or a lipophilic statin for brain aging. The risks involved in using the potent LXR agonist TO901317 outweigh any perceived benefit, but the role that the LXR pathway plays in reducing AD-associated pathologies is still interesting and is worthy of further exploration. Perhaps more selective targeting of specific mechanistic components within its target pathways would prove to confer the benefits without the peripheral side effects.

The known benefits of statins in the reduction of cardiovascular disease cannot be ignored or denied. Further, it would be unwise to disregard the potential benefits of an increase in brain perfusion due to reduced atherosclerosis occurring with statin therapy. Improved perfusion may be contributing to the observed statin-associated reduced risk of AD later in life. Nevertheless, our studies do suggest that long-term treatment with a lipophilic statin could be detrimental within the context of normal aging. Perhaps the use of a less lipophilic statin, one that is able to confer lipid-lowering effects in the periphery without promoting some aspects of brain aging, would be preferred.

References

Abildayeva K, Jansen PJ, Hirsch-Reinshagen V, Bloks VW, Bakker AH, Ramaekers FC, de Vente J, Groen AK, Wellington CL, Kuipers F, Mulder M (2006) 24(S)-hydroxycholesterol participates in a liver X receptor-controlled pathway in astrocytes that regulates apolipoprotein E-mediated cholesterol efflux. J Biol Chem 281:12799-12808.

Albers M, Blume B, Schlueter T, Wright MB, Kober I, Kremoser C, Deuschle U, Koegl M (2006) A novel principle for partial agonism of liver X receptor ligands. Competitive recruitment of activators and repressors. J Biol Chem 281:4920-4930.

Allen CL, Bayraktutan U (2008) Risk factors for ischaemic stroke. Int J Stroke 3:105-116.

Anagnostaras SG, Gale GD, Fanselow MS (2001) Hippocampus and contextual fear conditioning: recent controversies and advances. Hippocampus 11:8-17.

Andersson M, Elmberger PG, Edlund C, Kristensson K, Dallner G (1990) Rates of cholesterol, ubiquinone, dolichol and dolichyl-P biosynthesis in rat brain slices. FEBS Lett 269:15-18.

Aoki T, Kataoka H, Ishibashi R, Nakagami H, Nozaki K, Morishita R, Hashimoto N (2009) Pitavastatin suppresses formation and progression of cerebral aneurysms through inhibition of the nuclear factor kappaB pathway. Neurosurgery 64:357-365; discussion 365-356.

Apfel R, Benbrook D, Lernhardt E, Ortiz MA, Salbert G, Pfahl M (1994) A novel orphan receptor specific for a subset of thyroid hormone-responsive elements and its interaction with the retinoid/thyroid hormone receptor subfamily. Mol Cell Biol 14:7025-7035.

Arvanitakis Z, Schneider JA, Wilson RS, Bienias JL, Kelly JF, Evans DA, Bennett DA (2008) Statins, incident Alzheimer disease, change in cognitive function, and neuropathology. Neurology 70:1795-1802.

Bach ME, Barad M, Son H, Zhuo M, Lu YF, Shih R, Mansuy I, Hawkins RD, Kandel ER (1999) Age-related defects in spatial memory are correlated with defects in the late phase of hippocampal long-term potentiation in vitro and are attenuated by drugs that enhance the cAMP signaling pathway. Proc Natl Acad Sci U S A 96:5280-5285.

Bales KR, Liu F, Wu S, Lin S, Koger D, Delong C, Hansen JC, Sullivan PM, Paul SM (2009) Human APOE Isoform-Dependent Effects on Brain {beta}-Amyloid Levels in PDAPP Transgenic Mice. J Neurosci 29:6771-6779.

Barnes CA (1979) Memory deficits associated with senescence: a neurophysiological and behavioral study in the rat. J Comp Physiol Psychol 93:74-104.

Barnes CA (2003) Long-term potentiation and the ageing brain. Philos Trans R Soc Lond B Biol Sci 358:765-772.

Barnes CA, Rao G, McNaughton BL (1987) Increased electrotonic coupling in aged rat hippocampus: a possible mechanism for cellular excitability changes. J Comp Neurol 259:549-558.

Barnes CA, Rao G, Houston FP (2000) LTP induction threshold change in old rats at the perforant path--granule cell synapse. Neurobiol Aging 21:613-620.

Barnes CA, McNaughton BL, Mizumori SJ, Leonard BW, Lin LH (1990) Comparison of spatial and temporal characteristics of neuronal activity in sequential stages of hippocampal processing. Prog Brain Res 83:287-300.

Bartzokis G (2004) Age-related myelin breakdown: a developmental model of cognitive decline and Alzheimer's disease. Neurobiol Aging 25:5-18; author reply 49-62.

Bartzokis G, Lu PH, Mintz J (2007) Human brain myelination and amyloid beta deposition in Alzheimer's disease. Alzheimers Dement 3:122-125.

Bartzokis G, Beckson M, Lu PH, Nuechterlein KH, Edwards N, Mintz J (2001) Age-related changes in frontal and temporal lobe volumes in men: a magnetic resonance imaging study. Arch Gen Psychiatry 58:461-465.

Bartzokis G, Cummings JL, Sultzer D, Henderson VW, Nuechterlein KH, Mintz J (2003) White matter structural integrity in healthy aging adults and patients with Alzheimer disease: a magnetic resonance imaging study. Arch Neurol 60:393-398.

Bartzokis G, Sultzer D, Lu PH, Nuechterlein KH, Mintz J, Cummings JL (2004) Heterogeneous age-related breakdown of white matter structural integrity: implications for cortical "disconnection" in aging and Alzheimer's disease. Neurobiol Aging 25:843-851.

Billings LM, Oddo S, Green KN, McGaugh JL, LaFerla FM (2005) Intraneuronal A[beta] Causes the Onset of Early Alzheimer's Disease-Related Cognitive Deficits in Transgenic Mice. Neuron 45:675-688.

Bizon JL, LaSarge CL, Montgomery KS, McDermott AN, Setlow B, Griffith WH (2009) Spatial reference and working memory across the lifespan of male Fischer 344 rats. Neurobiol Aging 30:646-655.

Bjorkhem I (2006) Crossing the barrier: oxysterols as cholesterol transporters and metabolic modulators in the brain. In, pp 493-508.

Bjorkhem I, Meaney S (2004) Brain cholesterol: long secret life behind a barrier. Arterioscler Thromb Vasc Biol 24:806-815.

Bjorkhem I, Lutjohann D, Breuer O, Sakinis A, Wennmalm A (1997) Importance of a novel oxidative mechanism for elimination of brain cholesterol. Turnover of cholesterol and 24(S)-hydroxycholesterol in rat brain as measured with 18O2 techniques in vivo and in vitro. J Biol Chem 272:30178-30184.

Bjorkhem I, Lutjohann D, Diczfalusy U, Stahle L, Ahlborg G, Wahren J (1998) Cholesterol homeostasis in human brain: turnover of 24S-hydroxycholesterol and evidence for a cerebral origin of most of this oxysterol in the circulation. In, pp 1594-1600.

Blalock EM, Chen KC, Sharrow K, Herman JP, Porter NM, Foster TC, Landfield PW (2003) Gene microarrays in hippocampal aging: statistical profiling identifies novel processes correlated with cognitive impairment. J Neurosci 23:3807-3819.

Blalock EM, Chen KC, Stromberg AJ, Norris CM, Kadish I, Kraner SD, Porter NM, Landfield PW (2005) Harnessing the power of gene microarrays for the study of brain aging and Alzheimer's disease: statistical reliability and functional correlation. Ageing Res Rev 4:481-512.

Bland BH, Andersen P, Ganes T, Sveen O (1980) Automated analysis of rhythmicity of physiologically identified hippocampal formation neurons. Exp Brain Res 38:205-219.

Bodovitz S, Klein WL (1996) Cholesterol modulates alpha-secretase cleavage of amyloid precursor protein. J Biol Chem 271:4436-4440.

Bolles RC (1970) Species-specific defense reactions and avoidance learning. Psychological Review Vol 77:32-48.

Borchelt DR, Ratovitski T, van Lare J, Lee MK, Gonzales V, Jenkins NA, Copeland NG, Price DL, Sisodia SS (1997) Accelerated amyloid deposition in the brains of transgenic mice coexpressing mutant presenilin 1 and amyloid precursor proteins. Neuron 19:939-945.

Borchelt DR, Thinakaran G, Eckman CB, Lee MK, Davenport F, Ratovitsky T, Prada CM, Kim G, Seekins S, Yager D, Slunt HH, Wang R, Seeger M, Levey AI, Gandy SE, Copeland NG, Jenkins NA, Price DL, Younkin SG, Sisodia SS (1996) Familial Alzheimer's disease-linked presenilin 1 variants elevate Abeta1-42/1-40 ratio in vitro and in vivo. Neuron 17:1005-1013.

Boyles JK, Pitas RE, Wilson E, Mahley RW, Taylor JM (1985) Apolipoprotein E associated with astrocytic glia of the central nervous system and with nonmyelinating glia of the peripheral nervous system. J Clin Invest 76:1501-1513.

Brandeis R, Brandys Y, Yehuda S (1989) The use of the Morris Water Maze in the study of memory and learning. Int J Neurosci 48:29-69.

Brewer LD, Dowling AL, Curran-Rauhut MA, Landfield PW, Porter NM, Blalock EM (2009) Estradiol reverses a calcium-related biomarker of brain aging in female rats. J Neurosci 29:6058-6067.

Brito LS, Brito GN (1990) Locomotor activity and one-way active avoidance after intrahippocampal injection of neurotransmitter antagonists. Braz J Med Biol Res 23:1015-1019.

Brooks-Wilson A, Marcil M, Clee SM, Zhang LH, Roomp K, van Dam M, Yu L, Brewer C, Collins JA, Molhuizen HO, Loubser O, Ouelette BF, Fichter K, Ashbourne-Excoffon KJ, Sensen CW, Scherer S, Mott S, Denis M, Martindale D, Frohlich J, Morgan K, Koop B, Pimstone S, Kastelein JJ, Genest J, Jr., Hayden MR (1999) Mutations in ABC1 in Tangier disease and familial high-density lipoprotein deficiency. Nat Genet 22:336-345.

Bruemmer D, Law RE (2005) Liver x receptors: potential novel targets in cardiovascular diseases. Curr Drug Targets Cardiovasc Haematol Disord 5:533-540.

Burns A, Iliffe S (2009) Alzheimer's disease. BMJ 338:b158.

Burns MP, Vardanian L, Pajoohesh-Ganji A, Wang L, Cooper M, Harris DC, Duff K, Rebeck GW (2006) The effects of ABCA1 on cholesterol efflux and Abeta levels in vitro and in vivo. J Neurochem 98:792-800.

Cai XD, Golde TE, Younkin SG (1993) Release of excess amyloid beta protein from a mutant amyloid beta protein precursor. Science 259:514-516.

Campbell LW, Hao SY, Thibault O, Blalock EM, Landfield PW (1996) Aging changes in voltage-gated calcium currents in hippocampal CA1 neurons. J Neurosci 16:6286-6295.

Cao G, Beyer TP, Yang XP, Schmidt RJ, Zhang Y, Bensch WR, Kauffman RF, Gao H, Ryan TP, Liang Y, Eacho PI, Jiang XC (2002) Phospholipid transfer protein is regulated by liver X receptors in vivo. J Biol Chem 277:39561-39565.

Chalmers K, Wilcock G, Love S (2005) Contributors to white matter damage in the frontal lobe in Alzheimer's disease. Neuropathol Appl Neurobiol 31:623-631.

Chen G, Jiang J, Shi J, Ai J, Qi M, Hang C Simvastatin reduces secondary brain injury caused by cortical contusion in rats: Possible involvement of TLR4/NF-[kappa]B pathway. Experimental Neurology In Press, Corrected Proof.

Chia LS, Thompson JE, Moscarello MA (1983) Changes in lipid phase behaviour in human myelin during maturation and aging. Involvement of lipid peroxidation. FEBS Lett 157:155-158.

Chisholm JW, Hong J, Mills SA, Lawn RM (2003) The LXR ligand T0901317 induces severe lipogenesis in the db/db diabetic mouse. J Lipid Res 44:2039-2048.

Cijiang He J, Neves SR, Jordan JD, Iyengar R (2006) Role of the G_{o/i} signaling network in the regulation of neurite outgrowth. Canadian Journal of Physiology & Pharmacology 84:687-694.

Citron M, Oltersdorf T, Haass C, McConlogue L, Hung AY, Seubert P, Vigo-Pelfrey C, Lieberburg I, Selkoe DJ (1992) Mutation of the beta-amyloid precursor protein in familial Alzheimer's disease increases beta-protein production. Nature 360:672-674.

Clarke RM, Lyons A, O'Connell F, Deighan BF, Barry CE, Anyakoha NG, Nicolaou A, Lynch MA (2008) A pivotal role for interleukin-4 in atorvastatin-associated neuroprotection in rat brain. J Biol Chem 283:1808-1817.

Comery TA, Martone RL, Aschmies S, Atchison KP, Diamantidis G, Gong X, Zhou H, Kreft AF, Pangalos MN, Sonnenberg-Reines J, Jacobsen JS, Marquis KL (2005) Acute gamma-secretase inhibition improves contextual fear conditioning in the Tg2576 mouse model of Alzheimer's disease. J Neurosci 25:8898-8902.

Corcoran KA, Lu Y, Turner RS, Maren S (2002) Overexpression of hAPPswe impairs rewarded alternation and contextual fear conditioning in a transgenic mouse model of Alzheimer's disease. Learn Mem 9:243-252.

Corder EH, Saunders AM, Strittmatter WJ, Schmechel DE, Gaskell PC, Small GW, Roses AD, Haines JL, Pericak-Vance MA (1993) Gene dose of apolipoprotein E type 4 allele and the risk of Alzheimer's disease in late onset families. Science 261:921-923.

Corsini A, Maggi FM, Catapano AL (1995) Pharmacology of competitive inhibitors of HMG-CoA reductase. Pharmacol Res 31:9-27.

Corsini A, Bellosta S, Baetta R, Fumagalli R, Paoletti R, Bernini F (1999) New insights into the pharmacodynamic and pharmacokinetic properties of statins. Pharmacol Ther 84:413-428.

D'Hooge R, De Deyn PP (2001) Applications of the Morris water maze in the study of learning and memory. Brain Res Brain Res Rev 36:60-90.

Dalen KT, Ulven SM, Bamberg K, Gustafsson JA, Nebb HI (2003) Expression of the insulin-responsive glucose transporter GLUT4 in adipocytes is dependent on liver X receptor alpha. J Biol Chem 278:48283-48291.

Davis DG, Schmitt FA, Wekstein DR, Markesbery WR (1999) Alzheimer neuropathologic alterations in aged cognitively normal subjects. J Neuropathol Exp Neurol 58:376-388.

de Chaves EI, Rusinol AE, Vance DE, Campenot RB, Vance JE (1997) Role of lipoproteins in the delivery of lipids to axons during axonal regeneration. J Biol Chem 272:30766-30773.

Dean M, Rzhetsky A, Allikmets R (2001) The human ATP-binding cassette (ABC) transporter superfamily. Genome Res 11:1156-1166.

deToledo-Morrell L, Geinisman Y, Morrell F (1988) Age-dependent alterations in hippocampal synaptic plasticity: relation to memory disorders. Neurobiol Aging 9:581-590.

Dickson DW (1997) The pathogenesis of senile plaques. J Neuropathol Exp Neurol 56:321-339.

Dietschy JM (2009) Central nervous system: cholesterol turnover, brain development and neurodegeneration. Biol Chem.

Dietschy JM, Turley SD (2001) Cholesterol metabolism in the brain. Curr Opin Lipidol 12:105-112.

Dietschy JM, Turley SD (2004) Thematic review series: brain Lipids. Cholesterol metabolism in the central nervous system during early development and in the mature animal. J Lipid Res 45:1375-1397.

Dineley KT, Xia X, Bui D, Sweatt JD, Zheng H (2002) Accelerated plaque accumulation, associative learning deficits, and up-regulation of alpha 7 nicotinic receptor protein in transgenic mice co-expressing mutant human presenilin 1 and amyloid precursor proteins. J Biol Chem 277:22768-22780.

Disterhoft JF, Oh MM (2006) Pharmacological and molecular enhancement of learning in aging and Alzheimer's disease. J Physiol Paris 99:180-192.

Disterhoft JF, Coulter DA, Alkon DL (1986) Conditioning-specific membrane changes of rabbit hippocampal neurons measured in vitro. Proc Natl Acad Sci U S A 83:2733-2737.

Edmond J, Korsak RA, Morrow JW, Torok-Both G, Catlin DH (1991) Dietary cholesterol and the origin of cholesterol in the brain of developing rats. J Nutr 121:1323-1330.

Efanov AM, Sewing S, Bokvist K, Gromada J (2004) Liver X receptor activation stimulates insulin secretion via modulation of glucose and lipid metabolism in pancreatic beta-cells. Diabetes 53 Suppl 3:S75-78.

Endo A (1988) Chemistry, biochemistry, and pharmacology of HMG-CoA reductase inhibitors. Klin Wochenschr 66:421-427.

Endo A, Kuroda M, Tanzawa K (1976) Competitive inhibition of 3-hydroxy-3-methylglutaryl coenzyme A reductase by ML-236A and ML-236B fungal metabolites, having hypocholesterolemic activity. FEBS Lett 72:323-326.

Evans BA, Evans JE, Baker SP, Kane K, Swearer J, Hinerfeld D, Caselli R, Rogaeva E, St George-Hyslop P, Moonis M, Pollen DA (2009) Long-Term Statin Therapy and CSF Cholesterol Levels: Implications for Alzheimer's Disease. Dement Geriatr Cogn Disord 27:519-524.

Fabbrini E, Magkos F, Mohammed BS, Pietka T, Abumrad NA, Patterson BW, Okunade A, Klein S (2009) Intrahepatic fat, not visceral fat, is linked with metabolic complications of obesity. Proc Natl Acad Sci U S A.

Fassbender K, Simons M, Bergmann C, Stroick M, Lutjohann D, Keller P, Runz H, Kuhl S, Bertsch T, von Bergmann K, Hennerici M, Beyreuther K, Hartmann T (2001) Simvastatin strongly reduces levels of Alzheimer's disease beta -amyloid peptides Abeta 42 and Abeta 40 in vitro and in vivo. Proc Natl Acad Sci U S A 98:5856-5861.

Fillit H, Hill J (2005) Economics of dementia and pharmacoeconomics of dementia therapy. Am J Geriatr Pharmacother 3:39-49.

Fiorini RN, Kirtz J, Periyasamy B, Evans Z, Haines JK, Cheng G, Polito C, Rodwell D, Shafizadeh SF, Zhou X, Campbell C, Birsner J, Schmidt M, Lewin D, Chavin KD (2004) Development of an unbiased method for the estimation of liver steatosis. Clin Transplant 18:700-706.

Galatti L, Polimeni G, Salvo F, Romani M, Sessa A, Spina E (2006) Short-term memory loss associated with rosuvastatin. Pharmacotherapy 26:1190-1192.

Gallagher M, Nicolle MM (1993) Animal models of normal aging: relationship between cognitive decline and markers in hippocampal circuitry. Behav Brain Res 57:155-162.

Gallagher M, Burwell R, Burchinal M (1993) Severity of spatial learning impairment in aging: development of a learning index for performance in the Morris water maze. Behav Neurosci 107:618-626.

Gant JC, Sama MM, Landfield PW, Thibault O (2006) Early and simultaneous emergence of multiple hippocampal biomarkers of aging is mediated by Ca2+-induced Ca2+ release. J Neurosci 26:3482-3490.

Geinisman Y, Detoledo-Morrell L, Morrell F, Heller RE (1995) Hippocampal markers of age-related memory dysfunction: behavioral, electrophysiological and morphological perspectives. Prog Neurobiol 45:223-252.

Geyeregger R, Zeyda M, Stulnig TM (2006) Liver X receptors in cardiovascular and metabolic disease. Cell Mol Life Sci 63:524-539.

Gibson GE, Karuppagounder SS, Shi Q (2008) Oxidant-induced changes in mitochondria and calcium dynamics in the pathophysiology of Alzheimer's disease. Ann N Y Acad Sci 1147:221-232.

Golde TE (2002) Inflammation takes on Alzheimer disease. Nat Med 8:936-938.

Golde TE, Eckman CB (2001) Cholesterol modulation as an emerging strategy for the treatment of Alzheimer's disease. Drug Discov Today 6:1049-1055.

Goldstein JL, Brown MS (1990) Regulation of the mevalonate pathway. Nature 343:425-430.

Goldstein JL, Brown MS (2009) The LDL receptor. Arterioscler Thromb Vasc Biol 29:431-438.

Gordon MN, Holcomb LA, Jantzen PT, DiCarlo G, Wilcock D, Boyett KW, Connor K, Melachrino J, O'Callaghan JP, Morgan D (2002) Time course of the development of Alzheimer-like pathology in the doubly transgenic PS1+APP mouse. Exp Neurol 173:183-195.

Gotto AM, Jr. (2003) Safety and statin therapy: reconsidering the risks and benefits. Arch Intern Med 163:657-659.

Guttmann CR, Jolesz FA, Kikinis R, Killiany RJ, Moss MB, Sandor T, Albert MS (1998) White matter changes with normal aging. Neurology 50:972-978.

Haag MD, Hofman A, Koudstaal PJ, Stricker BH, Breteler MM (2009) Statins are associated with a reduced risk of Alzheimer disease regardless of lipophilicity. The Rotterdam Study. J Neurol Neurosurg Psychiatry 80:13-17.

Haass C, Hung AY, Selkoe DJ, Teplow DB (1994) Mutations associated with a locus for familial Alzheimer's disease result in alternative processing of amyloid beta-protein precursor. J Biol Chem 269:17741-17748.

Hamelin BA, Turgeon J (1998) Hydrophilicity/lipophilicity: relevance for the pharmacology and clinical effects of HMG-CoA reductase inhibitors. Trends Pharmacol Sci 19:26-37.

Heverin M, Meaney S, Lutjohann D, Diczfalusy U, Wahren J, Bjorkhem I (2005) Crossing the barrier: net flux of 27-hydroxycholesterol into the human brain. J Lipid Res 46:1047-1052.

Higashi Y, Murayama S, Pentchev PG, Suzuki K (1993) Cerebellar degeneration in the Niemann-Pick type C mouse. Acta Neuropathol 85:175-184.

Hirsch-Reinshagen V, Zhou S, Burgess BL, Bernier L, McIsaac SA, Chan JY, Tansley GH, Cohn JS, Hayden MR, Wellington CL (2004) Deficiency of ABCA1 impairs apolipoprotein E metabolism in brain. J Biol Chem 279:41197-41207.

Hirsch-Reinshagen V, Maia LF, Burgess BL, Blain JF, Naus KE, McIsaac SA, Parkinson PF, Chan JY, Tansley GH, Hayden MR, Poirier J, Van Nostrand W, Wellington CL (2005) The absence of ABCA1 decreases soluble ApoE levels but does not diminish amyloid deposition in two murine models of Alzheimer disease. J Biol Chem 280:43243-43256.

Horsburgh K, Graham DI, Stewart J, Nicoll JA (1999) Influence of apolipoprotein E genotype on neuronal damage and apoE immunoreactivity in human hippocampus following global ischemia. J Neuropathol Exp Neurol 58:227-234.

Hu X, Li S, Wu J, Xia C, Lala DS (2003) Liver X receptors interact with corepressors to regulate gene expression. Mol Endocrinol 17:1019-1026.

Huang da W, Sherman BT, Lempicki RA (2009) Systematic and integrative analysis of large gene lists using DAVID bioinformatics resources. Nat Protoc 4:44-57.

Huang Y (2006) Apolipoprotein E and Alzheimer disease. In, pp S79-85.

Hull M, Berger M, Heneka M (2006) Disease-modifying therapies in Alzheimer's disease: how far have we come? Drugs 66:2075-2093.

Igbavboa U, Avdulov NA, Schroeder F, Wood WG (1996) Increasing age alters transbilayer fluidity and cholesterol asymmetry in synaptic plasma membranes of mice. J Neurochem 66:1717-1725.

Igbavboa U, Avdulov NA, Chochina SV, Wood WG (1997) Transbilayer distribution of cholesterol is modified in brain synaptic plasma membranes of knockout mice deficient in the low-density lipoprotein receptor, apolipoprotein E, or both proteins. J Neurochem 69:1661-1667.

Ikonen E, Hölttä-Vuori M (2004) Cellular pathology of Niemann-Pick type C disease. Seminars in Cell & Developmental Biology 15:445-454.

Jankowsky JL, Slunt HH, Ratovitski T, Jenkins NA, Copeland NG, Borchelt DR (2001) Co-expression of multiple transgenes in mouse CNS: a comparison of strategies. Biomol Eng 17:157-165.

Jankowsky JL, Savonenko A, Schilling G, Wang J, Xu G, Borchelt DR (2002) Transgenic mouse models of neurodegenerative disease: opportunities for therapeutic development. Curr Neurol Neurosci Rep 2:457-464.

Jankowsky JL, Fadale DJ, Anderson J, Xu GM, Gonzales V, Jenkins NA, Copeland NG, Lee MK, Younkin LH, Wagner SL, Younkin SG, Borchelt DR (2004) Mutant presenilins specifically elevate the levels of the 42 residue {beta}-amyloid peptide in vivo: evidence for augmentation of a 42-specific {gamma} secretase. In, pp 159-170.

Janowski BA, Willy PJ, Devi TR, Falck JR, Mangelsdorf DJ (1996) An oxysterol signalling pathway mediated by the nuclear receptor LXR alpha. Nature 383:728-731.

Jiang Q, Lee CY, Mandrekar S, Wilkinson B, Cramer P, Zelcer N, Mann K, Lamb B, Willson TM, Collins JL, Richardson JC, Smith JD, Comery TA, Riddell D, Holtzman DM, Tontonoz P, Landreth GE (2008) ApoE promotes the proteolytic degradation of Abeta. Neuron 58:681-693.

Jick H, Zornberg GL, Jick SS, Seshadri S, Drachman DA (2000) Statins and the risk of dementia. Lancet 356:1627-1631.

Joseph SB, Castrillo A, Laffitte BA, Mangelsdorf DJ, Tontonoz P (2003) Reciprocal regulation of inflammation and lipid metabolism by liver X receptors. Nat Med 9:213-219.

Joseph SB, Laffitte BA, Patel PH, Watson MA, Matsukuma KE, Walczak R, Collins JL, Osborne TF, Tontonoz P (2002a) Direct and Indirect Mechanisms for Regulation of Fatty Acid Synthase Gene Expression by Liver X Receptors. In, pp 11019-11025.

Joseph SB, McKilligin E, Pei L, Watson MA, Collins AR, Laffitte BA, Chen M, Noh G, Goodman J, Hagger GN, Tran J, Tippin TK, Wang X, Lusis AJ, Hsueh WA, Law RE, Collins JL, Willson TM, Tontonoz P (2002b) Synthetic LXR ligand inhibits the development of atherosclerosis in mice. Proc Natl Acad Sci U S A 99:7604-7609.

Jurevics H, Morell P (1995) Cholesterol for synthesis of myelin is made locally, not imported into brain. J Neurochem 64:895-901.

Jurevics H, Bouldin TW, Toews AD, Morell P (1998) Regenerating sciatic nerve does not utilize circulating cholesterol. Neurochem Res 23:401-406.

Jurevics HA, Morell P (1994) Sources of cholesterol for kidney and nerve during development. J Lipid Res 35:112-120.

Kadish I, Thibault O, Blalock EM, Chen KC, Gant JC, Porter NM, Landfield PW (2009) Hippocampal and cognitive aging across the lifespan: a bioenergetic shift precedes and increased cholesterol trafficking parallels memory impairment. J Neurosci 29:1805-1816.

Kajikawa S, Harada T, Kawashima A, Imada K, Mizuguchi K (2009a) Highly purified eicosapentaenoic acid prevents the progression of hepatic steatosis by repressing monounsaturated fatty acid synthesis in high-fat/high-sucrose diet-fed mice. Prostaglandins Leukot Essent Fatty Acids 80:229-238.

Kajikawa S, Harada T, Kawashima A, Imada K, Mizuguchi K (2009b) Suppression of hepatic fat accumulation by highly purified eicosapentaenoic acid prevents the

progression of d-galactosamine-induced hepatitis in mice fed with a high-fat/high-sucrose diet. Biochim Biophys Acta 1791:281-288.

Karten B, Campenot RB, Vance DE, Vance JE (2006) Expression of ABCG1, but not ABCA1, correlates with cholesterol release by cerebellar astroglia. J Biol Chem 281:4049-4057.

Kim JJ, Fanselow MS (1992) Modality-specific retrograde amnesia of fear. Science 256:675-677.

Kita T, Brown MS, Goldstein JL (1980) Feedback regulation of 3-hydroxy-3-methylglutaryl coenzyme A reductase in livers of mice treated with mevinolin, a competitive inhibitor of the reductase. J Clin Invest 66:1094-1100.

Klopfleisch S, Merkler D, Schmitz M, Kloppner S, Schedensack M, Jeserich G, Althaus HH, Bruck W (2008) Negative impact of statins on oligodendrocytes and myelin formation in vitro and in vivo. J Neurosci 28:13609-13614.

Kojro E, Gimpl G, Lammich S, Marz W, Fahrenholz F (2001) Low cholesterol stimulates the nonamyloidogenic pathway by its effect on the alpha -secretase ADAM 10. Proc Natl Acad Sci U S A 98:5815-5820.

Koldamova RP, Lefterov IM, Staufenbiel M, Wolfe D, Huang S, Glorioso JC, Walter M, Roth MG, Lazo JS (2005) The liver X receptor ligand T0901317 decreases amyloid beta production in vitro and in a mouse model of Alzheimer's disease. J Biol Chem 280:4079-4088.

Kotti TJ, Ramirez DM, Pfeiffer BE, Huber KM, Russell DW (2006) Brain cholesterol turnover required for geranylgeraniol production and learning in mice. Proc Natl Acad Sci U S A 103:3869-3874.

Krause BR, Newton RS (1995) Lipid-lowering activity of atorvastatin and lovastatin in rodent species: triglyceride-lowering in rats correlates with efficacy in LDL animal models. Atherosclerosis 117:237-244.

Kuo YM, Emmerling MR, Bisgaier CL, Essenburg AD, Lampert HC, Drumm D, Roher AE (1998) Elevated low-density lipoprotein in Alzheimer's disease correlates with brain abeta 1-42 levels. Biochem Biophys Res Commun 252:711-715.

Kwak B, Mulhaupt F, Myit S, Mach F (2000) Statins as a newly recognized type of immunomodulator. Nat Med 6:1399-1402.

LaDu MJ, Falduto MT, Manelli AM, Reardon CA, Getz GS, Frail DE (1994) Isoform-specific binding of apolipoprotein E to beta-amyloid. J Biol Chem 269:23403-23406.

LaDu MJ, Pederson TM, Frail DE, Reardon CA, Getz GS, Falduto MT (1995) Purification of apolipoprotein E attenuates isoform-specific binding to beta-amyloid. J Biol Chem 270:9039-9042.

LaDu MJ, Gilligan SM, Lukens JR, Cabana VG, Reardon CA, Van Eldik LJ, Holtzman DM (1998) Nascent astrocyte particles differ from lipoproteins in CSF. J Neurochem 70:2070-2081.

Lalonde R, Kim HD, Maxwell JA, Fukuchi K (2005) Exploratory activity and spatial learning in 12-month-old APP695SWE/co + PS1/[Delta]E9 mice with amyloid plaques. Neuroscience Letters 390:87-92.

Landfield PW, Lynch G (1977) Impaired monosynaptic potentiation in in vitro hippocampal slices from aged, memory-deficient rats. J Gerontol 32:523-533.

Landfield PW, Pitler TA (1984) Prolonged Ca2+-dependent afterhyperpolarizations in hippocampal neurons of aged rats. Science 226:1089-1092.

Landfield PW, McGaugh JL, Lynch G (1978) Impaired synaptic potentiation processes in the hippocampus of aged, memory-deficient rats. Brain Res 150:85-101.

Landfield PW, Campbell LW, Hao SY, Kerr DS (1989) Aging-related increases in voltage-sensitive, inactivating calcium currents in rat hippocampus. Implications for mechanisms of brain aging and Alzheimer's disease. Ann N Y Acad Sci 568:95-105.

Larson J, Wong D, Lynch G (1986) Patterned stimulation at the theta frequency is optimal for the induction of hippocampal long-term potentiation. Brain Res 368:347-350.

Lawn RM, Wade DP, Garvin MR, Wang X, Schwartz K, Porter JG, Seilhamer JJ, Vaughan AM, Oram JF (1999) The Tangier disease gene product ABC1 controls the cellular apolipoprotein-mediated lipid removal pathway. J Clin Invest 104:R25-31.

Lee YS, Silva AJ (2009) The molecular and cellular biology of enhanced cognition. Nat Rev Neurosci 10:126-140.

Lennernas H (2003) Clinical pharmacokinetics of atorvastatin. Clin Pharmacokinet 42:1141-1160.

Lesser GT, Haroutunian V, Purohit DP, Schnaider Beeri M, Schmeidler J, Honkanen L, Neufeld R, Libow LS (2009) Serum lipids are related to Alzheimer's pathology in nursing home residents. Dement Geriatr Cogn Disord 27:42-49.

Li J, Wang JJ, Chen D, Mott R, Yu Q, Ma JX, Zhang SX (2009) Systemic administration of HMG-CoA reductase inhibitor protects the blood-retinal barrier and ameliorates retinal inflammation in type 2 diabetes. Exp Eye Res.

Liang Y, Lin S, Beyer TP, Zhang Y, Wu X, Bales KR, DeMattos RB, May PC, Li SD, Jiang XC, Eacho PI, Cao G, Paul SM (2004) A liver X receptor and retinoid X receptor heterodimer mediates apolipoprotein E expression, secretion and cholesterol homeostasis in astrocytes. J Neurochem 88:623-634.

Liao JK, Laufs U (2005) Pleiotropic effects of statins. Annu Rev Pharmacol Toxicol 45:89-118.

Lindberg C, Crisby M, Winblad B, Schultzberg M (2005) Effects of statins on microglia. J Neurosci Res 82:10-19.

Liscum L, Luskey KL, Chin DJ, Ho YK, Goldstein JL, Brown MS (1983) Regulation of 3-hydroxy-3-methylglutaryl coenzyme A reductase and its mRNA in rat liver as studied with a monoclonal antibody and a cDNA probe. J Biol Chem 258:8450-8455.

Lu D, Qu C, Goussev A, Jiang H, Lu C, Schallert T, Mahmood A, Chen J, Li Y, Chopp M (2007) Statins increase neurogenesis in the dentate gyrus, reduce delayed neuronal death in the hippocampal CA3 region, and improve spatial learning in rat after traumatic brain injury. J Neurotrauma 24:1132-1146.

Lund EG, Xie C, Kotti T, Turley SD, Dietschy JM, Russell DW (2003) Knockout of the cholesterol 24-hydroxylase gene in mice reveals a brain-specific mechanism of cholesterol turnover. J Biol Chem 278:22980-22988.

Lutjohann D, von Bergmann K (2003) 24S-hydroxycholesterol: a marker of brain cholesterol metabolism. Pharmacopsychiatry 36 Suppl 2:S102-106.

Lutjohann D, Breuer O, Ahlborg G, Nennesmo I, Siden A, Diczfalusy U, Bjorkhem I (1996) Cholesterol homeostasis in human brain: evidence for an age-dependent flux of 24S-hydroxycholesterol from the brain into the circulation. Proc Natl Acad Sci U S A 93:9799-9804.

Lutjohann D, Stroick M, Bertsch T, Kuhl S, Lindenthal B, Thelen K, Andersson U, Bjorkhem I, Bergmann Kv K, Fassbender K (2004) High doses of simvastatin, pravastatin, and cholesterol reduce brain cholesterol synthesis in guinea pigs. Steroids 69:431-438.

Lutjohann D, Papassotiropoulos A, Bjorkhem I, Locatelli S, Bagli M, Oehring RD, Schlegel U, Jessen F, Rao ML, von Bergmann K, Heun R (2000) Plasma 24S-hydroxycholesterol (cerebrosterol) is increased in Alzheimer and vascular demented patients. J Lipid Res 41:195-198.

Lynch G, Rex CS, Gall CM (2006) Synaptic plasticity in early aging. Ageing Res Rev 5:255-280.

Lynch G, Larson J, Kelso S, Barrionuevo G, Schottler F (1983) Intracellular injections of EGTA block induction of hippocampal long-term potentiation. Nature 305:719-721.

Lynch MA (2004) Long-term potentiation and memory. Physiol Rev 84:87-136.

Malenka RC, Nicoll RA (1999) Long-term potentiation--a decade of progress? Science 285:1870-1874.

Mansuy IM, Mayford M, Jacob B, Kandel ER, Bach ME (1998) Restricted and regulated overexpression reveals calcineurin as a key component in the transition from short-term to long-term memory. Cell 92:39-49.

Maren S, Fanselow MS (1997) Electrolytic lesions of the fimbria/fornix, dorsal hippocampus, or entorhinal cortex produce anterograde deficits in contextual fear conditioning in rats. Neurobiol Learn Mem 67:142-149.

Masliah E, Mallory M, Veinbergs I, Miller A, Samuel W (1996) Alterations in apolipoprotein E expression during aging and neurodegeneration. Prog Neurobiol 50:493-503.

Mauch DH, Nagler K, Schumacher S, Goritz C, Muller EC, Otto A, Pfrieger FW (2001) CNS synaptogenesis promoted by glia-derived cholesterol. Science 294:1354-1357.

McColl BW, McGregor AL, Wong A, Harris JD, Amalfitano A, Magnoni S, Baker AH, Dickson G, Horsburgh K (2007) APOE epsilon3 gene transfer attenuates brain damage after experimental stroke. J Cereb Blood Flow Metab 27:477-487.

McGeer PL, McGeer EG (2004) Inflammation and the degenerative diseases of aging. Ann N Y Acad Sci 1035:104-116.

McVean DE, Patrick RL, Witchett CE (1965) An Aqueous Oil Red O Fixative Stain for Histological Preparations. Am J Clin Pathol 43:291-293.

Meaney S, Heverin M, Panzenboeck U, Ekstrom L, Axelsson M, Andersson U, Diczfalusy U, Pikuleva I, Wahren J, Sattler W, Bjorkhem I (2007) Novel route for elimination of brain oxysterols across the blood-brain barrier: conversion into 7{alpha}-hydroxy-3-oxo-4-cholestenoic acid. In, pp 944-951.

Miles LA, Wun KS, Crespi GA, Fodero-Tavoletti MT, Galatis D, Bagley CJ, Beyreuther K, Masters CL, Cappai R, McKinstry WJ, Barnham KJ, Parker MW (2008)

Amyloid-beta-anti-amyloid-beta complex structure reveals an extended conformation in the immunodominant B-cell epitope. J Mol Biol 377:181-192.

Miron VE, Rajasekharan S, Jarjour AA, Zamvil SS, Kennedy TE, Antel JP (2007) Simvastatin regulates oligodendroglial process dynamics and survival. Glia 55:130-143.

Mitro N, Mak PA, Vargas L, Godio C, Hampton E, Molteni V, Kreusch A, Saez E (2007) The nuclear receptor LXR is a glucose sensor. Nature 445:219-223.

Mok SW, Thelen KM, Riemer C, Bamme T, Gultner S, Lutjohann D, Baier M (2006) Simvastatin prolongs survival times in prion infections of the central nervous system. Biochem Biophys Res Commun 348:697-702.

Mori T, Paris D, Town T, Rojiani AM, Sparks DL, Delledonne A, Crawford F, Abdullah LI, Humphrey JA, Dickson DW, Mullan MJ (2001) Cholesterol accumulates in senile plaques of Alzheimer disease patients and in transgenic APP(SW) mice. J Neuropathol Exp Neurol 60:778-785.

Morris RG, Garrud P, Rawlins JN, O'Keefe J (1982) Place navigation impaired in rats with hippocampal lesions. Nature 297:681-683.

Morris RG, Anderson E, Lynch GS, Baudry M (1986) Selective impairment of learning and blockade of long-term potentiation by an N-methyl-D-aspartate receptor antagonist, AP5. Nature 319:774-776.

Morris RGM (1981) Spatial localization does not require the presence of local cues. . Learning and

Motivation 12 239-260

Morrissette DA, Parachikova A, Green KN, LaFerla FM (2009) Relevance of transgenic mouse models to human Alzheimer disease. J Biol Chem 284:6033-6037.

Moyer JR, Jr., Disterhoft JF (1994) Nimodipine decreases calcium action potentials in rabbit hippocampal CA1 neurons in an age-dependent and concentration-dependent manner. Hippocampus 4:11-17.

Moyer JR, Jr., Deyo RA, Disterhoft JF (1990) Hippocampectomy disrupts trace eye-blink conditioning in rabbits. Behav Neurosci 104:243-252.

Moyer JR, Jr., Thompson LT, Black JP, Disterhoft JF (1992) Nimodipine increases excitability of rabbit CA1 pyramidal neurons in an age- and concentration-dependent manner. J Neurophysiol 68:2100-2109.

Munoz C, Grossman SP (1981) Spatial discrimination, reversal and active or passive avoidance learning in rats with KA-induced neuronal depletions in dorsal hippocampus. Brain Res Bull 6:399-406.

Murphy MP, Beckett TL, Ding Q, Patel E, Markesbery WR, St Clair DK, LeVine H, 3rd, Keller JN (2007) Abeta solubility and deposition during AD progression and in APPxPS-1 knock-in mice. Neurobiol Dis 27:301-311.

Naik SU, Wang X, Da Silva JS, Jaye M, Macphee CH, Reilly MP, Billheimer JT, Rothblat GH, Rader DJ (2006) Pharmacological activation of liver X receptors promotes reverse cholesterol transport in vivo. Circulation 113:90-97.

Nelson PT, Braak H, Markesbery WR (2009) Neuropathology and cognitive impairment in Alzheimer disease: a complex but coherent relationship. J Neuropathol Exp Neurol 68:1-14.

Norris CM, Kadish I, Blalock EM, Chen KC, Thibault V, Porter NM, Landfield PW, Kraner SD (2005) Calcineurin triggers reactive/inflammatory processes in astrocytes and is upregulated in aging and Alzheimer's models. J Neurosci 25:4649-4658.

Notkola IL, Sulkava R, Pekkanen J, Erkinjuntti T, Ehnholm C, Kivinen P, Tuomilehto J, Nissinen A (1998) Serum total cholesterol, apolipoprotein E epsilon 4 allele, and Alzheimer's disease. Neuroepidemiology 17:14-20.

Oddo S, Caccamo A, Tran L, Lambert MP, Glabe CG, Klein WL, LaFerla FM (2006) Temporal Profile of Amyloid-beta (Abeta) Oligomerization in an in Vivo Model of Alzheimer Disease: A LINK BETWEEN Abeta AND TAU PATHOLOGY. In, pp 1599-1604.

Oddo S, Caccamo A, Shepherd JD, Murphy MP, Golde TE, Kayed R, Metherate R, Mattson MP, Akbari Y, LaFerla FM (2003) Triple-transgenic model of Alzheimer's disease with plaques and tangles: intracellular Abeta and synaptic dysfunction. Neuron 39:409-421.

Olton DS, Isaacson RL (1968a) Importance of spatial location in active avoidance tasks. J Comp Physiol Psychol 65:535-539.

Olton DS, Isaacson RL (1968b) Hippocampal lesions and active avoidancestar, open. Physiology and Behavior 3:719-724.

Osono Y, Woollett LA, Herz J, Dietschy JM (1995) Role of the low density lipoprotein receptor in the flux of cholesterol through the plasma and across the tissues of the mouse. J Clin Invest 95:1124-1132.

Pakkenberg B, Pelvig D, Marner L, Bundgaard MJ, Gundersen HJ, Nyengaard JR, Regeur L (2003) Aging and the human neocortex. Exp Gerontol 38:95-99.

Papassotiropoulos A, Lutjohann D, Bagli M, Locatelli S, Jessen F, Rao ML, Maier W, Bjorkhem I, von Bergmann K, Heun R (2000) Plasma 24S-hydroxycholesterol: a peripheral indicator of neuronal degeneration and potential state marker for Alzheimer's disease. Neuroreport 11:1959-1962.

Papassotiropoulos A, Streffer JR, Tsolaki M, Schmid S, Thal D, Nicosia F, Iakovidou V, Maddalena A, Lutjohann D, Ghebremedhin E, Hegi T, Pasch T, Traxler M, Bruhl A, Benussi L, Binetti G, Braak H, Nitsch RM, Hock C (2003) Increased brain beta-amyloid load, phosphorylated tau, and risk of Alzheimer disease associated with an intronic CYP46 polymorphism. Arch Neurol 60:29-35.

Pappolla MA, Bryant-Thomas TK, Herbert D, Pacheco J, Fabra Garcia M, Manjon M, Girones X, Henry TL, Matsubara E, Zambon D, Wolozin B, Sano M, Cruz-Sanchez FF, Thal LJ, Petanceska SS, Refolo LM (2003) Mild hypercholesterolemia is an early risk factor for the development of Alzheimer amyloid pathology. Neurology 61:199-205.

Park DC, Lautenschlager G, Hedden T, Davidson NS, Smith AD, Smith PK (2002) Models of visuospatial and verbal memory across the adult life span. Psychol Aging 17:299-320.

Parle M, Singh N (2007) Reversal of memory deficits by Atorvastatin and Simvastatin in rats. Yakugaku Zasshi 127:1125-1137.

Peet DJ, Turley SD, Ma W, Janowski BA, Lobaccaro JM, Hammer RE, Mangelsdorf DJ (1998) Cholesterol and bile acid metabolism are impaired in mice lacking the nuclear oxysterol receptor LXR alpha. Cell 93:693-704.

Pekhletski R, Gerlai R, Overstreet LS, Huang XP, Agopyan N, Slater NT, Abramow-Newerly W, Roder JC, Hampson DR (1996) Impaired cerebellar synaptic plasticity and motor performance in mice lacking the mGluR4 subtype of metabotropic glutamate receptor. J Neurosci 16:6364-6373.

Petanceska SS, DeRosa S, Olm V, Diaz N, Sharma A, Thomas-Bryant T, Duff K, Pappolla M, Refolo LM (2002) Statin therapy for Alzheimer's disease: will it work? J Mol Neurosci 19:155-161.

Peters A (2009) The effects of normal aging on myelinated nerve fibers in monkey central nervous system. Front Neuroanat 3:11.

Pfrieger FW (2003a) Cholesterol homeostasis and function in neurons of the central nervous system. Cell Mol Life Sci 60:1158-1171.

Pfrieger FW (2003b) Outsourcing in the brain: do neurons depend on cholesterol delivery by astrocytes? Bioessays 25:72-78.

Phillips RG, LeDoux JE (1992) Differential contribution of amygdala and hippocampus to cued and contextual fear conditioning. Behav Neurosci 106:274-285.

Pitas RE, Boyles JK, Lee SH, Hui D, Weisgraber KH (1987a) Lipoproteins and their receptors in the central nervous system. Characterization of the lipoproteins in cerebrospinal fluid and identification of apolipoprotein B,E(LDL) receptors in the brain. J Biol Chem 262:14352-14360.

Pitas RE, Boyles JK, Lee SH, Foss D, Mahley RW (1987b) Astrocytes synthesize apolipoprotein E and metabolize apolipoprotein E-containing lipoproteins. Biochim Biophys Acta 917:148-161.

Poirier J (1996) Apolipoprotein E in the brain and its role in Alzheimer's disease. J Psychiatry Neurosci 21:128-134.

Ponce J, de la Ossa NP, Hurtado O, Millan M, Arenillas JF, Davalos A, Gasull T (2008) Simvastatin reduces the association of NMDA receptors to lipid rafts: a cholesterol-mediated effect in neuroprotection. Stroke 39:1269-1275.

Power JM, Thompson LT, Moyer JR, Jr., Disterhoft JF (1997) Enhanced synaptic transmission in CA1 hippocampus after eyeblink conditioning. J Neurophysiol 78:1184-1187.

Quan G, Xie C, Dietschy JM, Turley SD (2003) Ontogenesis and regulation of cholesterol metabolism in the central nervous system of the mouse. Brain Res Dev Brain Res 146:87-98.

Rapp PR, Rosenberg RA, Gallagher M (1987) An evaluation of spatial information processing in aged rats. Behav Neurosci 101:3-12.

Rea TD, Breitner JC, Psaty BM, Fitzpatrick AL, Lopez OL, Newman AB, Hazzard WR, Zandi PP, Burke GL, Lyketsos CG, Bernick C, Kuller LH (2005) Statin use and the risk of incident dementia: the Cardiovascular Health Study. Arch Neurol 62:1047-1051.

Rebeck GW, LaDu MJ, Estus S, Bu G, Weeber EJ (2006) The generation and function of soluble apoE receptors in the CNS. Mol Neurodegener 1:15.

Rebeck GW, Alonzo NC, Berezovska O, Harr SD, Knowles RB, Growdon JH, Hyman BT, Mendez AJ (1998) Structure and functions of human cerebrospinal fluid lipoproteins from individuals of different APOE genotypes. Exp Neurol 149:175-182.

Refolo LM, Malester B, LaFrancois J, Bryant-Thomas T, Wang R, Tint GS, Sambamurti K, Duff K, Pappolla MA (2000) Hypercholesterolemia accelerates the Alzheimer's amyloid pathology in a transgenic mouse model. Neurobiol Dis 7:321-331.

Refolo LM, Pappolla MA, LaFrancois J, Malester B, Schmidt SD, Thomas-Bryant T, Tint GS, Wang R, Mercken M, Petanceska SS, Duff KE (2001) A cholesterol-lowering drug reduces beta-amyloid pathology in a transgenic mouse model of Alzheimer's disease. Neurobiol Dis 8:890-899.

Reiserer RS, Harrison FE, Syverud DC, McDonald MP (2007) Impaired spatial learning in the APPSwe + PSEN1ΔE9 bigenic mouse model of Alzheimer's disease. In, pp 54-65.

Repa JJ, Mangelsdorf DJ (2002) The liver X receptor gene team: potential new players in atherosclerosis. Nat Med 8:1243-1248.

Repa JJ, Berge KE, Pomajzl C, Richardson JA, Hobbs H, Mangelsdorf DJ (2002) Regulation of ATP-binding cassette sterol transporters ABCG5 and ABCG8 by the liver X receptors alpha and beta. J Biol Chem 277:18793-18800.

Riddell DR, Zhou H, Comery TA, Kouranova E, Lo CF, Warwick HK, Ring RH, Kirksey Y, Aschmies S, Xu J, Kubek K, Hirst WD, Gonzales C, Chen Y, Murphy E, Leonard S, Vasylyev D, Oganesian A, Martone RL, Pangalos MN, Reinhart PH, Jacobsen JS (2007) The LXR agonist TO901317 selectively lowers hippocampal Abeta42 and improves memory in the Tg2576 mouse model of Alzheimer's disease. Mol Cell Neurosci 34:621-628.

Rockwood K, Kirkland S, Hogan DB, MacKnight C, Merry H, Verreault R, Wolfson C, McDowell I (2002) Use of lipid-lowering agents, indication bias, and the risk of dementia in community-dwelling elderly people. Arch Neurol 59:223-227.

Rodriguez EG, Dodge HH, Birzescu MA, Stoehr GP, Ganguli M (2002) Use of lipid-lowering drugs in older adults with and without dementia: a community-based epidemiological study. J Am Geriatr Soc 50:1852-1856.

Rogaev EI, Sherrington R, Rogaeva EA, Levesque G, Ikeda M, Liang Y, Chi H, Lin C, Holman K, Tsuda T, et al. (1995) Familial Alzheimer's disease in kindreds with missense mutations in a gene on chromosome 1 related to the Alzheimer's disease type 3 gene. Nature 376:775-778.

Roher AE, Weiss N, Kokjohn TA, Kuo Y-M, Kalback W, Anthony J, Watson D, Luehrs DC, Sue L, Walker D, Emmerling M, Goux W, Beach T (2002) Increased Aβ Peptides and Reduced Cholesterol and Myelin Proteins Characterize White Matter Degeneration in Alzheimer's Disease&#x2020. Biochemistry 41:11080-11090.

Rojo L, Sjoberg MK, Hernandez P, Zambrano C, Maccioni RB (2006) Roles of cholesterol and lipids in the etiopathogenesis of Alzheimer's disease. J Biomed Biotechnol 2006:73976.

Rowe WB, Blalock EM, Chen KC, Kadish I, Wang D, Barrett JE, Thibault O, Porter NM, Rose GM, Landfield PW (2007) Hippocampal expression analyses reveal selective association of immediate-early, neuroenergetic, and myelinogenic pathways with cognitive impairment in aged rats. J Neurosci 27:3098-3110.

Saheki A, Terasaki T, Tamai I, Tsuji A (1994) In vivo and in vitro blood-brain barrier transport of 3-hydroxy-3-methylglutaryl coenzyme A (HMG-CoA) reductase inhibitors. Pharm Res 11:305-311.

Sanders S, Morano C (2008) Alzheimer's disease and related dementias. J Gerontol Soc Work 50 Suppl 1:191-214.

Savonenko A, Xu GM, Melnikova T, Morton JL, Gonzales V, Wong MP, Price DL, Tang F, Markowska AL, Borchelt DR (2005) Episodic-like memory deficits in the APPswe/PS1dE9 mouse model of Alzheimer's disease: relationships to beta-amyloid deposition and neurotransmitter abnormalities. Neurobiol Dis 18:602-617.

Scarpini E, Scheltens P, Feldman H (2003) Treatment of Alzheimer's disease: current status and new perspectives. Lancet Neurol 2:539-547.

Schachter M (2005) Chemical, pharmacokinetic and pharmacodynamic properties of statins: an update. Fundam Clin Pharmacol 19:117-125.

Schneider A, Schulz-Schaeffer W, Hartmann T, Schulz JB, Simons M (2006) Cholesterol depletion reduces aggregation of amyloid-beta peptide in hippocampal neurons. Neurobiology of Disease 23:573-577.

Schultz JR, Tu H, Luk A, Repa JJ, Medina JC, Li L, Schwendner S, Wang S, Thoolen M, Mangelsdorf DJ, Lustig KD, Shan B (2000) Role of LXRs in control of lipogenesis. In, pp 2831-2838.

Scoville WB, Milner B (1957) Loss of recent memory after bilateral hippocampal lesions. J Neurol Neurosurg Psychiatry 20:11-21.

Selkoe DJ (2001) Alzheimer's disease: genes, proteins, and therapy. Physiol Rev 81:741-766.

Selley ML (2005) Simvastatin prevents 1-methyl-4-phenyl-1,2,3,6-tetrahydropyridine-induced striatal dopamine depletion and protein tyrosine nitration in mice. Brain Res 1037:1-6.

Shepherd C, McCann H, Halliday GM (2009) Variations in the neuropathology of familial Alzheimer's disease. Acta Neuropathol 118:37-52.

Sherrington R, Rogaev EI, Liang Y, Rogaeva EA, Levesque G, Ikeda M, Chi H, Lin C, Li G, Holman K, et al. (1995) Cloning of a gene bearing missense mutations in early-onset familial Alzheimer's disease. Nature 375:754-760.

Shukitt-Hale B, Mouzakis G, Joseph JA (1998) Psychomotor and spatial memory performance in aging male Fischer 344 rats. Exp Gerontol 33:615-624.

Simons M, Keller P, De Strooper B, Beyreuther K, Dotti CG, Simons K (1998) Cholesterol depletion inhibits the generation of beta-amyloid in hippocampal neurons. Proc Natl Acad Sci U S A 95:6460-6464.

Smith AD (2002) Imaging the progression of Alzheimer pathology through the brain. Proc Natl Acad Sci U S A 99:4135-4137.

Solomon A, Kivipelto M, Wolozin B, Zhou J, Whitmer RA (2009) Midlife serum cholesterol and increased risk of Alzheimer's and vascular dementia three decades later. Dement Geriatr Cogn Disord 28:75-80.

Solomon A, Kareholt I, Ngandu T, Winblad B, Nissinen A, Tuomilehto J, Soininen H, Kivipelto M (2007) Serum cholesterol changes after midlife and late-life cognition: twenty-one-year follow-up study. Neurology 68:751-756.

Sparks DL, Martins R, Martin T (2002) Cholesterol and cognition: rationale for the AD cholesterol-lowering treatment trial and sex-related Differences in beta-amyloid accumulation in the brains of spontaneously hypercholesterolemic Watanabe rabbits. Ann N Y Acad Sci 977:356-366.

Sparks DL, Kuo YM, Roher A, Martin T, Lukas RJ (2000) Alterations of Alzheimer's disease in the cholesterol-fed rabbit, including vascular inflammation. Preliminary observations. Ann N Y Acad Sci 903:335-344.

Sparks DL, Scheff SW, Hunsaker JC, Liu H, Landers T, Gross DR (1994) Induction of Alzheimer-like [beta]-Amyloid Immunoreactivity in the Brains of Rabbits with Dietary Cholesterol. Experimental Neurology 126:88-94.

Sparks DL, Kryscio RJ, Sabbagh MN, Connor DJ, Sparks LM, Liebsack C (2008) Reduced risk of incident AD with elective statin use in a clinical trial cohort. Curr Alzheimer Res 5:416-421.

Sparks DL, Scheff SW, Liu H, Landers T, Danner F, Coyne CM, Hunsaker JC, 3rd (1996) Increased density of senile plaques (SP), but not neurofibrillary tangles (NFT), in non-demented individuals with the apolipoprotein E4 allele: comparison to confirmed Alzheimer's disease patients. J Neurol Sci 138:97-104.

Sparks DL, Sabbagh M, Connor D, Soares H, Lopez J, Stankovic G, Johnson-Traver S, Ziolkowski C, Browne P (2006) Statin therapy in Alzheimer's disease. Acta Neurol Scand Suppl 185:78-86.

Strittmatter WJ, Saunders AM, Schmechel D, Pericak-Vance M, Enghild J, Salvesen GS, Roses AD (1993) Apolipoprotein E: high-avidity binding to beta-amyloid and increased frequency of type 4 allele in late-onset familial Alzheimer disease. Proc Natl Acad Sci U S A 90:1977-1981.

Sun Y, Yao J, Kim TW, Tall AR (2003) Expression of liver X receptor target genes decreases cellular amyloid beta peptide secretion. J Biol Chem 278:27688-27694.

Sutherland RJ, Whishaw IQ, Kolb B (1983) A behavioural analysis of spatial localization following electrolytic, kainate- or colchicine-induced damage to the hippocampal formation in the rat. Behav Brain Res 7:133-153.

Takikita S, Fukuda T, Mohri I, Yagi T, Suzuki K (2004) Perturbed myelination process of premyelinating oligodendrocyte in Niemann-Pick type C mouse. J Neuropathol Exp Neurol 63:660-673.

Teboul M, Enmark E, Li Q, Wikstrom AC, Pelto-Huikko M, Gustafsson JA (1995) OR-1, a member of the nuclear receptor superfamily that interacts with the 9-cis-retinoic acid receptor. Proc Natl Acad Sci U S A 92:2096-2100.

Thelen KM, Falkai P, Bayer TA, Lutjohann D (2006) Cholesterol synthesis rate in human hippocampus declines with aging. Neurosci Lett 403:15-19.

Thibault O, Mazzanti ML, Blalock EM, Porter NM, Landfield PW (1995) Single-channel and whole-cell studies of calcium currents in young and aged rat hippocampal slice neurons. J Neurosci Methods 59:77-83.

Thomas AJ, Perry R, Barber R, Kalaria RN, O'Brien JT (2002) Pathologies and pathological mechanisms for white matter hyperintensities in depression. Ann N Y Acad Sci 977:333-339.

Tisler A, Pierratos A, Honey JD, Bull SB, Rosivall L, Logan AG (2002) High urinary excretion of uric acid combined with high excretion of calcium links kidney stone disease to familial hypertension. Nephrol Dial Transplant 17:253-259.

Tombaugh GC, Rowe WB, Rose GM (2005) The slow afterhyperpolarization in hippocampal CA1 neurons covaries with spatial learning ability in aged Fisher 344 rats. J Neurosci 25:2609-2616.

Tontonoz P, Mangelsdorf DJ (2003) Liver X receptor signaling pathways in cardiovascular disease. Mol Endocrinol 17:985-993.

Tsuji A, Saheki A, Tamai I, Terasaki T (1993) Transport mechanism of 3-hydroxy-3-methylglutaryl coenzyme A reductase inhibitors at the blood-brain barrier. In, pp 1085-1090.

Tubic-Grozdanis M, Hilfinger JM, Amidon GL, Kim JS, Kijek P, Staubach P, Langguth P (2008) Pharmacokinetics of the CYP 3A substrate simvastatin following administration of delayed versus immediate release oral dosage forms. Pharm Res 25:1591-1600.

Turley SD, Burns DK, Rosenfeld CR, Dietschy JM (1996) Brain does not utilize low density lipoprotein-cholesterol during fetal and neonatal development in the sheep. J Lipid Res 37:1953-1961.

Ulven SM, Dalen KT, Gustafsson JA, Nebb HI (2004) Tissue-specific autoregulation of the LXRalpha gene facilitates induction of apoE in mouse adipose tissue. J Lipid Res 45:2052-2062.

Ulven SM, Dalen KT, Gustafsson JA, Nebb HI (2005) LXR is crucial in lipid metabolism. Prostaglandins Leukot Essent Fatty Acids 73:59-63.

van den Kommer TN, Dik MG, Comijs HC, Fassbender K, Lutjohann D, Jonker C (2009) Total cholesterol and oxysterols: early markers for cognitive decline in elderly? Neurobiol Aging 30:534-545.

van Groen T, Kadish I (2005) Transgenic AD model mice, effects of potential anti-AD treatments on inflammation and pathology. Brain Res Brain Res Rev 48:370-378.

Vance JE, Hayashi H, Karten B (2005) Cholesterol homeostasis in neurons and glial cells. Seminars in Cell & Developmental Biology 16:193-212.

Vance JE, Pan D, Campenot RB, Bussiere M, Vance DE (1994) Evidence that the major membrane lipids, except cholesterol, are made in axons of cultured rat sympathetic neurons. J Neurochem 62:329-337.

Vaya J, Schipper HM (2007) Oxysterols, cholesterol homeostasis, and Alzheimer disease. J Neurochem 102:1727-1737.

Venkateswaran A, Laffitte BA, Joseph SB, Mak PA, Wilpitz DC, Edwards PA, Tontonoz P (2000) Control of cellular cholesterol efflux by the nuclear oxysterol receptor LXR alpha. Proc Natl Acad Sci U S A 97:12097-12102.

Vorhees CV, Williams MT (2006) Morris water maze: procedures for assessing spatial and related forms of learning and memory. Nat Protocols 1:848-858.

Wahrle S, Das P, Nyborg AC, McLendon C, Shoji M, Kawarabayashi T, Younkin LH, Younkin SG, Golde TE (2002) Cholesterol-dependent gamma-secretase activity in buoyant cholesterol-rich membrane microdomains. Neurobiol Dis 9:11-23.

Wahrle SE, Jiang H, Parsadanian M, Hartman RE, Bales KR, Paul SM, Holtzman DM (2005) Deletion of Abca1 increases Abeta deposition in the PDAPP transgenic mouse model of Alzheimer disease. J Biol Chem 280:43236-43242.

Wahrle SE, Jiang H, Parsadanian M, Legleiter J, Han X, Fryer JD, Kowalewski T, Holtzman DM (2004) ABCA1 Is Required for Normal Central Nervous System ApoE Levels and for Lipidation of Astrocyte-secreted apoE. In, pp 40987-40993.

Wang H, Lynch JR, Song P, Yang HJ, Yates RB, Mace B, Warner DS, Guyton JR, Laskowitz DT (2007) Simvastatin and atorvastatin improve behavioral outcome, reduce hippocampal degeneration, and improve cerebral blood flow after experimental traumatic brain injury. Exp Neurol 206:59-69.

Wang J, Tanila H, Puolivali J, Kadish I, van Groen T (2003) Gender differences in the amount and deposition of amyloidbeta in APPswe and PS1 double transgenic mice. Neurobiol Dis 14:318-327.

Wang Q, Zengin A, Deng C, Li Y, Newell KA, Yang G-Y, Lu Y, Wilder-Smith EP, Zhao H, Huang X-F (2009a) High dose of simvastatin induces hyperlocomotive and anxiolytic-like activities: The association with the up-regulation of NMDA receptor binding in the rat brain. Experimental Neurology 216:132-138.

Wang X, Su B, Zheng L, Perry G, Smith MA, Zhu X (2009b) The role of abnormal mitochondrial dynamics in the pathogenesis of Alzheimer's disease. J Neurochem 109 Suppl 1:153-159.

Wang Y, Muneton S, Sjovall J, Jovanovic JN, Griffiths WJ (2008) The effect of 24S-hydroxycholesterol on cholesterol homeostasis in neurons: quantitative changes to the cortical neuron proteome. J Proteome Res 7:1606-1614.

Watanabe Y, Jiang S, Takabe W, Ohashi R, Tanaka T, Uchiyama Y, Katsumi K, Iwanari H, Noguchi N, Naito M, Hamakubo T, Kodama T (2005) Expression of the LXRalpha protein in human atherosclerotic lesions. Arterioscler Thromb Vasc Biol 25:622-627.

Whitney KD, Watson MA, Collins JL, Benson WG, Stone TM, Numerick MJ, Tippin TK, Wilson JG, Winegar DA, Kliewer SA (2002) Regulation of Cholesterol Homeostasis by the Liver X Receptors in the Central Nervous System. In, pp 1378-1385.

Willy PJ, Umesono K, Ong ES, Evans RM, Heyman RA, Mangelsdorf DJ (1995) LXR, a nuclear receptor that defines a distinct retinoid response pathway. Genes Dev 9:1033-1045.

Wolozin B (2001) A fluid connection: cholesterol and Abeta. Proc Natl Acad Sci U S A 98:5371-5373.

Wolozin B (2004) Cholesterol, statins and dementia. Curr Opin Lipidol 15:667-672.

Wolozin B, Brown J, 3rd, Theisler C, Silberman S (2004) The cellular biochemistry of cholesterol and statins: insights into the pathophysiology and therapy of Alzheimer's disease. CNS Drug Rev 10:127-146.

Wolozin B, Kellman W, Ruosseau P, Celesia GG, Siegel G (2000) Decreased prevalence of Alzheimer disease associated with 3-hydroxy-3-methyglutaryl coenzyme A reductase inhibitors. Arch Neurol 57:1439-1443.

Wolozin B, Manger J, Bryant R, Cordy J, Green RC, McKee A (2006) Re-assessing the relationship between cholesterol, statins and Alzheimer's disease. Acta Neurol Scand Suppl 185:63-70.

Wolozin B, Wang SW, Li NC, Lee A, Lee TA, Kazis LE (2007) Simvastatin is associated with a reduced incidence of dementia and Parkinson's disease. BMC Med 5:20.

Wood C (1999) A question of faith: art or science as the new religion? Lancet 353:75-76.

Wood WG, Schroeder F, Igbavboa U, Avdulov NA, Chochina SV (2002) Brain membrane cholesterol domains, aging and amyloid beta-peptides. Neurobiol Aging 23:685-694.

Wu H, Lu D, Jiang H, Xiong Y, Qu C, Li B, Mahmood A, Zhou D, Chopp M (2008) Simvastatin-mediated upregulation of VEGF and BDNF, activation of the PI3K/Akt pathway, and increase of neurogenesis are associated with therapeutic improvement after traumatic brain injury. J Neurotrauma 25:130-139.

Wyss-Coray T (2006) Inflammation in Alzheimer disease: driving force, bystander or beneficial response? Nat Med 12:1005-1015.

Xie C, Lund EG, Turley SD, Russell DW, Dietschy JM (2003) Quantitation of two pathways for cholesterol excretion from the brain in normal mice and mice with neurodegeneration. J Lipid Res 44:1780-1789.

Xiong H, Callaghan D, Jones A, Walker DG, Lue L-F, Beach TG, Sue LI, Woulfe J, Xu H, Stanimirovic DB, Zhang W (2008) Cholesterol retention in Alzheimer's brain is responsible for high [beta]- and [gamma]-secretase activities and A[beta] production. Neurobiology of Disease 29:422-437.

Yaffe K, Barrett-Connor E, Lin F, Grady D (2002) Serum lipoprotein levels, statin use, and cognitive function in older women. Arch Neurol 59:378-384.

Zelcer N, Tontonoz P (2006) Liver X receptors as integrators of metabolic and inflammatory signaling. J Clin Invest 116:607-614.

Zelcer N, Khanlou N, Clare R, Jiang Q, Reed-Geaghan EG, Landreth GE, Vinters HV, Tontonoz P (2007) Attenuation of neuroinflammation and Alzheimer's disease pathology by liver x receptors. Proc Natl Acad Sci U S A 104:10601-10606.

Zhang Y, Repa JJ, Gauthier K, Mangelsdorf DJ (2001) Regulation of lipoprotein lipase by the oxysterol receptors, LXRalpha and LXRbeta. J Biol Chem 276:43018-43024.

Vita

JAMES LUCAS SEARCY
D.O.B. June 6, 1980
Owensboro, KY

EDUCATION

August 2006-Present	Ph.D. Molecular and Biomedical Pharmacology University of Kentucky, Lexington, KY Thesis:
August 2005-2006	Graduate Studies, Integrated Biomedical Sciences (IBS) 1st year curriculum University of Kentucky, Lexington, KY
2003- 2005	**Bachelor of Science**, **Biology** Magna cum laude Concentration: Molecular Biology Brescia University, Owensboro, KY
2001-2002	**Bachelor of Arts, Psychology** Concentration: Neuroscience Lexington, Ky
1999-2001	University of St. Thomas, St. Paul, MN Concentration: Psychology

WORK EXPERIENCE

2002-2005	**Customer Service Representative/Assistant in Accounting Dept./Assistant in Credit/Debit Card Processing/Assistant in HR**, Independence Bank, Owensboro, KY
2001-2002	**Mental Health Associate**, Eastern State Hospital, Geriatric Unit, Lexington, KY

RESEARCH EXPERIENCE

2006-present	**Dissertation Research:** Elucidating the role of lipid metabolism in the context of normal brain aging and Alzheimer disease. **Research Assistant** Molecular and Biomedical Pharmacology University of Kentucky Principal Investigator: Nada Porter, Ph.D.
2005 & 2006 (May-October & March-June)	**Research Assistant** Anatomy and Neurobiology Principal Investigator: Annadora Bruce-Keller, Ph.D.
2005 (October-December)	**Research Assistant** Molecular and Biomedical Pharmacology Principal Investigator: Nada Porter, Ph.D.
2006 (January-March)	**Research Assistant** Molecular Biochemistry Principal Investigator: Becky Dutch, Ph.D.
2004-2005	**Undergraduate Independent Research Student** Biology Brescia University Advisor: Dr. Jennifer Myka,

TRAINING AND RESPONSIBILITIES

August 2006-Present	IBS student recruitment and orientation
August 07-08	Graduate Student Representative, Department of Molecular and Biomedical Pharmacology
November 2007	SFN Short Course: Inhibitory RNAs in Neuroscience. Beverly Davidson, Ph.D., organizer

October 2007	Organized Pharmacology Fall seminar for invited speaker Dr. Barry Sears, Zone Labs, Inc.
January 2007	Colony Management: Principles and Practices sponsored by The Jackson Laboratory, La Jolla, CA
October 2006	Organized Pharmacology Fall Seminar for invited speaker Dr. Guoqing Cao, Lilly Research Laboratories, Eli Lilly & Company

COMMITTEES

Aug.- Oct 2008	Lexington Conference on Translational Neuroscience: Models of Aging Planning Committee, October 2008
Sep.-Nov 2008	Integrated Biomedical Sciences Director Search Committee

CONFERENCES AND MEETINGS

2005	Association of College and University Biology Educator Annual Meeting, Cape Girardeau, MO
2005	Gill Heart Institute Annual Research Day , Lexington, Kentucky
2006	Society for Neuroscience Annual Meeting, Atlanta, Georgia
2006	Molecular and Cellular Cognition Society Annual Meeting, Atlanta, Georgia
2006	Society for Neuroscience, Bluegrass Chapter Spring Neuroscience Day, Lexington, Kentucky
2007	Gill Heart Institute Annual Research Day, Lexington, Kentucky
2007	Society for Neuroscience Annual Meeting, San Diego, California

2007	Society for Neuroscience, Bluegrass Chapter Spring Neuroscience Day, Lexington, Kentucky
2008	International Conference on Alzheimer's Disease Annual Meeting, Chicago, Illinois
2008	Society for Neuroscience Annual Meeting, Washington, DC
2008	Lexington Conference on Translational Neuroscience: Models of Aging, Lexington, Kentucky
2009	International Conference on Alzheimer's Disease Annual Meeting, Vienna, Austria

SEMINAR

May 2008	University of Kentucky, Dept. of Molecular and Biomedical Pharmacology, Graduate Student Seminar, "Lipid Signaling in Brain Aging and Alzheimer's Disease: the role of the liver x receptor"
July 2009	University of Edinburgh, Center for Cognitive and Neural Systems, Recruitment Seminar, "The Liver X Receptor and Alzheimer's Disease: Chronic treatment of AD mouse models with a potent liver x receptor agonist"

TEACHING EXPERIENCE

April 2007	**Group Discussion Facilitator** IBS 602: Biomolecules and Molecular Biology
June-July 2008	**Instructor** Anatomy Area Health Education Center Enrichment Camp

PRESENTED ABSTRACTS

2009	**Long-term effects of simvastatin and atorvastatin on a rat model of normal brain aging** **JL Searcy**, CS Latimer, O Thibault, EM Blalock, K-C Chen, PW Landfield, NM Porter; ICAD 2009.

2008 **Effect of chronic treatment with the LXR agonist, T0901317, in a triple transgenic model of Alzheimer's disease**
JL Searcy, JT Phelps, EM Blalock, ALS Dowling, K-C Chen, PW Landfield, I Kadish, Thibault, NM Porter; ICAD 2008.

2008 **Reversal of age-related electrophysiological biomarkers of aging with statin treatment**
JL Searcy, T Pancani, LD Brewer, O Thibault, PW Landfield, NM Porter; SFN 2008.

2007 **Effect of chronic treatment with the LXR agonist, T0901317, in a triple transgenic model of Alzheimer's disease.**
JL Searcy, JT Phelps, EM Blalock, ALS Dowling, K-C Chen, PW Landfield, I Kadish, Thibault, NM Porter; SFN abstract 2007 & Gill Heart Research Day 2007.

2007 **Modulation of Ca2+-dependent signaling by PPAR-gamma activation in hippocampal neurons and astrocytes.**
T Pancani, JT Phelps, **JL Searcy**, MW Kilgore, NM Porter, O Thibault; SFN 2007.

2007 **Effects of aging and gender on 11-β hydroxysteroid dehydrogenase type I expression in rat brain.**
ALS Dowling, LD Brewer, X Peng, **JL Searcy**, PW Landfield, NM Porter; SFN 2007.

2007 **Effect of chronic treatment with the PPAR-γ agonist, Pioglitazone, in a triple transgenic model of Alzheimer's disease.**
JT Phelps, **JL Searcy**, T Pancani, EM Blalock, K-C Chen, V Thibault, TD Porter, PW Landfield, I Kadish, NM Porter, O. Thibault; SFN 2007.

2006 **Effects of estradiol on cognitive function and synaptic plasticity in middle-aged female rats.**
JT Rogers, JC Gant, **JL Searcy**, ALS Dowling, MT Bridges, LD Brewer, O Thibault, NM Porter; SFN 2006.

PUBLICATIONS

Published

1. **Distinct modulation of voltage and ligand gated Ca2+ currents by PPAR-gamma agonists in cultured hippocampal neurons.**
T Pancani, JT Phelps, **JL Searcy**, Kilgore, MW, Chen, KC, NM Porter, O Thibault. J. Neurochem, 2009.

Manuscripts

1. Effect of chronic treatment with the LXR agonist, T0901317 and PPAR-gamma agonist pioglitazone in a triple transgenic model of Alzheimer's disease. **JL Searcy*,** JT Phelps *, EM Blalock, ALS Dowling, K-C Chen, PW Landfield, I Kadish, O Thibault, NM Porter (In preparation) *Authors contributed equally.

ORGANIZATIONS

2006-Present	Society for Neuroscience
2006-Present	Molecular and Cellular Cognition Society
2005-2008	Association of College and University Biology Educators
2005	Psi Chi –National Honor Society for Psychology

AWARDS

2004-2005	Alpha Chi, Brescia University
2004	Special Recognition in the Biology Area Brescia University
2005	Special Recognition in the Biology Area Brescia Univeristy
2005	John Carlock Travel Award Association of College and University Biology Educators Annual Meeting, Cage Girardeau, MO